Mechanisms underlying the temporal and selective induction of Ptf1a target genes

Doctoral Thesis

Dissertation for the award of the degree
"Doctor rerum naturalium (Dr. rer. nat.)"
in the GGNB program "Genes and Development“
at the Georg August University Göttingen
Faculty of Biology

submitted by
Sven Richts
born in Werl, Germany

Göttingen, December 2017

Members of the Thesis Committee:

Dr. Kristine A. Henningfeld (Supervisor, Reviewer)
Department of Developmental Biochemistry,
University of Göttingen

Prof. Dr. Steven Johnsen (Reviewer)
Clinic for General, Visceral and Pediatric Surgery,
University of Göttingen

Prof. Dr. Thomas Dresbach
Department for Anatomy and Embryology
University of Göttingen

Affidavit

Herewith, I declare that I prepared the PhD thesis "Mechanisms underlying the temporal and selective induction of Ptf1a target genes " on my own and with no other sources and aids than quoted.

Submission date
Göttingen, 31.12.2017

_____

Sven Richts

Table of contents

Acknowledgements

First of all, I would like to express my sincere gratitude to Dr. Kristine Henningfeld for her great supervision and endless support during this thesis. Her guidance inspired me a lot during the time of research and writing.

I would also like to thank Prof. Dr. Pieler for his help and support in many ways including fruitful discussions and suggestions. I am additionally grateful for him being a member of my examination board.

Furthermore, I would like to acknowledge my thesis committee members Prof. Dr. Johnsen, and Prof. Dr. Dresbach for sharing their valuable comments and suggestions. I also would like to thank Prof. Dr. Mansouri and Prof. Dr. Bucher. for being part of my extended thesis committee.

I thank all my lab members, past and present, for your company, support, and fruitful discussions: Especially, I would like to thank Dr. Marie Hedderich, Dr. Patrick Berndt, Dr. Maja Gere, Dr. Juliane Melchert, Dr. Barbara Rust, Esther Essel and Katja Ditter. I also would like to thank the members of the TAL for the extensive help with sequencing.

Finally, I would like to thank my family for the tremendous support. Especially I would like to thank Yehan for her company, encouragement and support during all these years. Without her I would not have made it.

Abstract

The bHLH transcription factor Ptf1a is crucial for the generation of a GABAergic neuronal cell fate over an excitatory glutamatergic fate. Ptf1a is a component of a heterotrimeric transcription factor complex, which in addition to Ptf1a, is comprised of a commonly expressed bHLH E-protein such as E12 and Rbpj. Interaction with Rbpj is essential for the GABAergic cell fate inducing and glutamatergic repressing activities of Ptf1a. In the absence of Rpbj binding, Ptf1a maintains its proneural activity, however, the induced neurons express marker genes indicative of a glutamatergic excitatory neuronal cell fate. In this thesis, the temporal and selective induction of target genes by Ptf1a was further analyzed as well several Ptf1a mutants characterized with respect to the neurotransmitter inducing properties using *X. laevis* as a model system.

A point mutation within the C-terminus of Ptf1a that leads to the induction of a mixed glutamatergic and GABAergic neuronal transmitter phenotype was identified and characterized ($Ptf1^{T243A}$). BiFC analysis revealed that the mixed neuronal transmitter phenotype is not due to an impairment of the interaction with Rbpj or E12, but may be due to enhanced interaction with Prdm13. The global temporal transcriptional program induced Ptf1a was also studied in pluripotent embryonic cells by RNAseq. While some Ptf1a direct target genes such as *prdm13,* are induced within three hours (early genes), others, including *neurog2 and gad1a* are induced only after 12 h (late genes). To gain insight if chromatin accessibility plays a role in the delayed activation, Brg1, which is one of the catalytic subunits of the chromatin remodeling BAF complex, was knocked down. Brg1 was found to be required for Ptf1a-induced neuronal differentiation as shown by the loss of neural-specific tubulin. Only a subset of late induced Ptf1a target genes required Brg1 with most Brg1 dependent target genes being indirect Ptf1a target genes. Furthermore, ATAC-seq suggests that target gene activation by Ptf1a is likely independent of chromatin accessibility. Taken together, these data suggest that Ptf1a acts as a pioneer transcription factor to activate its target genes.

List of figures

List of tables

Abbreviations

%	percent
°C	Celsius degree
aa	amino acid
aIN	ascending premotor interneurons
BCNE center	blastula Chordin- and Noggin-expressing center
bHLH	basic helix-loop-helix
BiFC	Bimolecular Fluorescent Complementation assay
BMP	bone morphogenetic protein
bp	base pairs
Brg1MO	Brg1 morpholino
BSA	bovine serum albumin
CC	noninjected control caps
cdk	cell cycle dependent kinases
cDNA	complementary DNA
CE	noninjected control embryos
CHX	cycloheximide
cIN	commissural premotor interneurons
cMO	control morpholino
dIN	descending premotor interneurons
dINr	descending repetitive excitatory interneurons
dla	dorsolateral ascending sensory interneurons
dlc	dorsolateral commissural sensory interneurons
dll1	Notch ligand delta1
DNA	desoxyribonucleic acid
ecIN	excitatory commissural sensory pathway interneurons
EDTA	ethylenediaminetetraacetic acid
et al.	*et alii*
EtOH	ethanol
FGF	Fibroblast growth factors
for	forward
g	gram
GABA	γ-aminobutyric acid
GR	glucocorticoid receptor

h	hour/hours
hb	hindbrain
kb	kilobase
l	liter
LB	Luria Bertani
µ	micro
m	milli/meter
M	molar
MAB	maleic acid buffer
MAPK	mitogen-activated protein kinase
min	minutes
n	nano
neurog2	neurogenin 2
NICD	intracellular domain of the Notch receptor
p	pico
PBS	phosphate buffered saline
PCR	polymerase chain reaction
pH	negative decade logarithm of hydrogen ion concentration
Ptf1a	Pancreatic transcription factor 1a
rev	reverse
RNA	ribonucleic acid
RNase	ribonuclease
RNAseq	RNA sequencing
rpm	rounds per minute
RT	room temperature
RT-PCR	reverse transcriptase PCR
s	seconds
Shh	Sonic hedgehog
st	stage
TAE	Tris-acetate-EDTA
Tm	melting temperature
tp	trigeminal placodes
U	units
v	volume

WMISH	whole mount *in situ* hybridizations
X-Gal	5-bromo-4-chloro-3-indolyl-β-d-galactopyranoside
X. laevis	*Xenopus laevis*

1. Introduction

1.1 Neurogenesis in *Xenopus laevis*

The African clawed frog *Xenopus laevis* (*X. laevis*) has several advantages that make it a highly suitable model system to study early vertebrate developmental events including the development of the nervous system (Pratt and Khakhalin, 2013; Kofent and Spagnoli, 2016; Borodinsky, 2017; Droz and McLaughlin, 2017; Dubey and Saint-Jeannet, 2017; Lee-Liu *et al.*, 2017). *X. laevis* embryos are quite large (>1mm), undergo an external development, can easily be manipulated by microinjection of mRNA or morpholino antisense oligonucleotides as well as used for CRISPR/Cas9 mutagenesis (Mimoto and Christian, 2011; Wang *et al.*, 2015). Furthermore, pluripotent ectodermal explants can be isolated from the animal half of the embryo at blastula stage and used for in vitro differentiation studies using embryos manipulated with the aforementioned techniques (Borchers and Pieler, 2010).
In *X. laevis,* there are two distinct phases of neurogenesis (Hartenstein, 1989; Roberts, 2000; Thuret *et al.*, 2015). The first phase is termed primary neurogenesis and generates the neurons responsible for the movements and sensation of the tadpole (Hartenstein, 1989; Hartenstein, 1993; Roberts, 2000). This phase of neurogenesis starts at the open neural plate stage and slowly declines until the mid-tadpole stage, where it remains minimally active (Thuret *et al.*, 2015). A second phase of neurogenesis occurs during metamorphosis, in which most early-born neurons are replaced generating the nervous system of the adult frog (Schlosser *et al.*, 2002; Wullimann *et al.*, 2005).

The first primary neurons are born within 24 h after fertilization, in three longitudinal domains (medial, intermediate and lateral) along the dorsal midline and will give rise to neurons of the hindbrain and spinal cord and in the trigeminal placodes (Chitnis and Kintner, 1995). In the anterior neural plate, which gives rise to the forebrain and midbrain, neuronal differentiation starts at the tailbud stage (Papalopulu and Kintner, 1996). After the neual plate rises and folds into the neural tube, the progenitors in the medial domain will reside ventrally and differentiate into motor neurons, those from the intermediate

domain into interneurons, while the progenitors from the lateral domain at the neural plate border will be located most dorsally and differentiate into sensory neurons (Hartenstein, 1989; Chitnis and Kintner, 1995). In the *X. laevis* tadpole there are 10 distinct classes of neurons (Roberts *et al.*, 2012). The first neurons to gain their functionality are the Rohon-beard sensory neurons located adjacent to the roof plate in the dorsal neural tube (Lamborghini, 1980; Rossi *et al.*, 2009). Subsequently, the ventral motor neurons and Kolmer-Agdhur cells (Rossi *et al.*, 2008; Rossi *et al.*, 2009; Groves and LaBonne, 2014) and then seven subpopulations of interneurons are formed (Roberts *et al.*, 2012) (Fig 1.1).

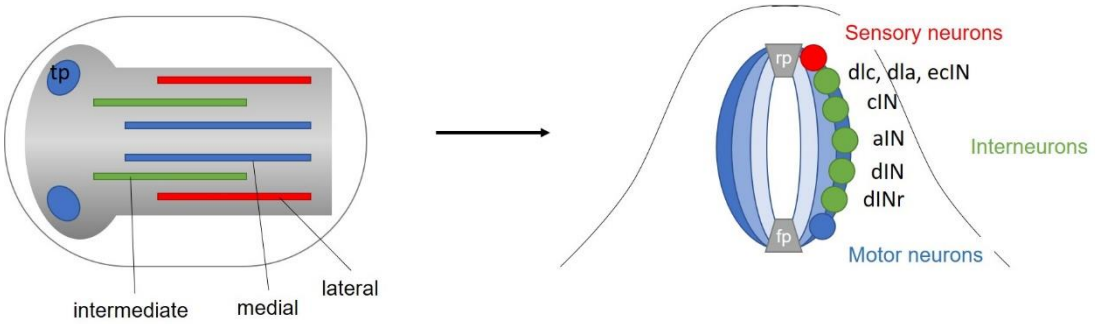

Figure 1.1: Neurogenesis in *X. laevis*

The first primary neurons are born at the open neural plate stage in three longitudinal domains along the dorsal midline. After neural tube closure, the medial domain will give rise to motor neurons in the ventral neural tube, the lateral domain will give rise to sensory neurons in the dorsal neural tube and the intermediate domain will be located medially in the neural tube and give rise to interneurons. *tp*: trigeminal placodes *dla, dlc*: dorsolateral ascending and dorsolateral commissural sensory interneurons; *dIN, cIN, aIN*: descending, commissural, and ascending premotor interneurons; dlNr: descending repetitive excitatory interneurons; *ecIN*: excitatory

1.2 Neural induction

The development of the nervous system is initiated during neural induction where subpopulations of the ectoderm are specified to a neural fate (Rogers *et al.*, 2009). In *X. laevis,* the neural fate is induced during gastrulation (Hamburger, 1969; Sanes *et al.*, 2011) and requires the inhibition of BMP signaling (Hemmati-Brivanlou *et al.*, 1994; Hemmati-Brivanlou and Melton, 1994; De Robertis and Kuroda, 2004). The inhibition of BMP signaling occurs through multiple mechanisms, which includes the secretion of BMP

antagonists from the blastula Chordin- and Noggin-expressing (BCNE) center, which is located in dorsal animal cells at the blastula stage (Kuroda *et al.*, 2004) and during gastrulation from the Spemann Organizer through Chordin (Piccolo *et al.*, 1996; Sasai *et al.*, 1996), Noggin (Zimmerman *et al.*, 1996), Follistatin (Hemmati-Brivanlou *et al.*, 1994) and Cerberus (Bouwmeester *et al.*, 1996; Piccolo *et al.*, 1999). In addition to BMP signaling, a requirement for FGF signaling in the process of neural induction has been established (Launay *et al.*, 1996; Sasai *et al.*, 1996). FGF signaling results in MAPK-induced phosphorylation of Smad1, the intracellular transducer of BMP signaling, resulting in an inhibition of BMP activity (Hardcastle *et al.*, 2000; Pera *et al.*, 2001; Richard-Parpaillon *et al.*, 2002; Pera *et al.*, 2003). In addition to its role in inhibiting BMP, FGF is required for the induction and maintenance of several neural genes (Rogers *et al.*, 2011). Furthermore, Ca^{2+} transients are present in the dorsal ectoderm during neural induction and blocking of calcium release prevents the expression of neuronal markers (Leclerc *et al.*, 1997; Leclerc *et al.*, 2000; Leclerc *et al.*, 2012).

Neural induction leads to the expression of several genes in the forming neural plate including members of the Sox family (*sox2*, *sox3* and *sox15*, formally known as *soxD*), Zic family (*zic1-3)* and Iroquois family (*iro1-3*), as well as the forkhead box protein *foxD5* and *geminin* (Nakata *et al.*, 1997; Bellefroid *et al.*, 1998; Brewster *et al.*, 1998; Gomez-Skarmeta *et al.*, 1998; Kroll *et al.*, 1998; Mizuseki *et al.*, 1998; Mizuseki *et al.*, 1998; Sölter *et al.*, 1999; Uchikawa *et al.*, 1999; Sullivan *et al.*, 2001; Graham *et al.*, 2003; Penzel *et al.*, 2003; Pevny and Placzek, 2005; Pitulescu *et al.*, 2005; Seo and Kroll, 2006; Kroll, 2007; Lefebvre *et al.*, 2007; Houtmeyers *et al.*, 2013).

The genes induced by neural induction regulate multiple processes including progenitor maintenance (*sox2*, *sox3* and *zic2)* (Brewster *et al.*, 1998; Hardcastle *et al.*, 2000; Ellis *et al.*, 2004; Pevny and Placzek, 2005; Rogers *et al.*, 2009), the onset of neuronal differentiation (*zic1*, *zic3, sox15, iro1, iro2* and *iro3*) (Nakata *et al.*, 1997; Mizuseki *et al.*, 1998; Rogers *et al.*, 2009) and control of progenitor proliferation (*geminin, foxD5*) (Kroll *et al.*, 1998; Sullivan *et al.*, 2001; Pitulescu *et al.*, 2005; Seo and Kroll, 2006; Kroll, 2007; Papanayotou *et al.*, 2008).

1.3 bHLH transcription factors and their role during neuronal differentiation and determination

Transcription factors of the basic helix-loop-helix (bHLH) transcription factors are involved in many developmental processes including muscle development (Weintraub, 1993), mesodermal determination (Burgess *et al.*, 1995), skeletal development (Cserjesi *et al.*, 1995) and neural development (Lee, 1997; Bertrand *et al.*, 2002). Members of the bHLH transcription factor family can be categorized into three classes (Murre *et al.*, 1989). Class A bHLH proteins form homo or heterodimers and are ubiquitously expressed genes such as *E12, E47* or *daughterless*. Class B bHLH transcription factors form heterodimers with class A bHLH proteins and show a tissue specific expression pattern, while class C bHLH transcription factors do not interact with either of the class A or class B bHLH transcription factors (Murre *et al.*, 1989). The formed homo- or heterodimers bind to an E-box motif (CANNTG) on the DNA, usually through the basic region, while the HLH domain is involved in the dimerization (Murre *et al.*, 1989). The activity and DNA target choice of bHLH transcription factors can be regulated via the interaction with co-factors (Ma *et al.*, 2008; Mattar *et al.*, 2008; Rodolosse *et al.*, 2009; Li *et al.*, 2011).

Neuronal differentiation is initiated by the expression of proneural genes, which drive the determination and differentiation of progenitor cells to a neuronal cell fate (Bertrand *et al.*, 2002). The proneural genes are mainly class B bHLH transcription factors (Bertrand *et al.*, 2002) belonging to the *drosophila archaete-scute* and *atonal* family. Proneural bHLH transcription factors can be categorized in two distinct subgroups according to their function during neuronal differentiation and based on the timing of their expression: neuronal determination genes and neuronal differentiation genes (Lee, 1997; Farah *et al.*, 2000; Bertrand *et al.*, 2002). Neuronal determination genes such as *neurog2* or *ascl1* are expressed early during neurogenesis in the mitotically active progenitors, which in the neural tube, are found in the inner ventricular zone (Lee, 1997; Bertrand *et al.*, 2002). Neuronal differentiation genes such as *neurod1* are expressed slightly later compared to the determination genes and are positively regulated by the proneural determination genes (Lee, 1997; Bertrand *et al.*, 2002). During neuronal differentiation, bHLH transcription are

involved in the regulation of several processes (Fig.1.3), which in the following will be demonstrated by the multiple activities of the proneural bHLH transcription factor Neurog2.

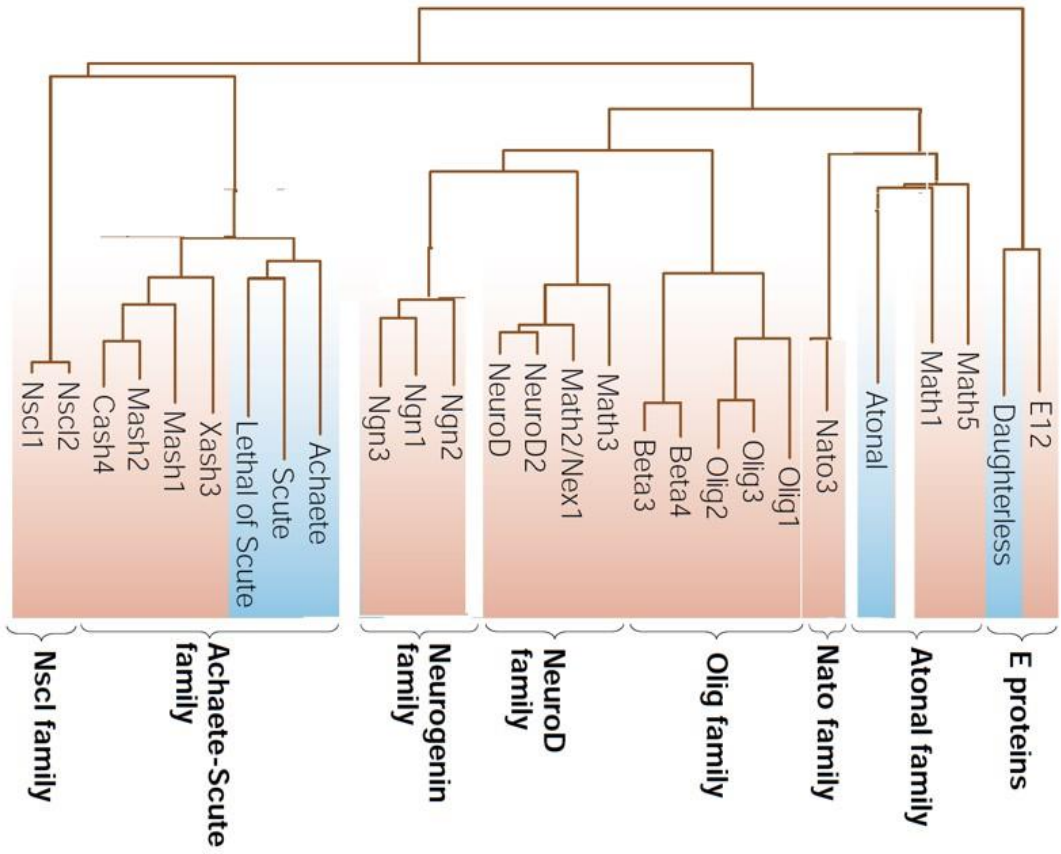

Figure 1.2: Overview over Archaete-Scute and Atonal family members of proneural bHLH transcription factors

Scheme showing the relationship between different families of bHLH proteins involved in neuronal differentiation. bHLH proteins are mainly divided in ubiquitously expressed E-proteins, which are orthologs to *drosophila* Daughterless and the proneural families that are homologue to the *drosophila* Atonal and Achaete-Scute. The Atonal family can be further divided in several subfamilies, which includes the Neurogenin family, the Olig family and the Atonal family. Blue shading highlights the invertebrate family members, while red highlights vertebrate family members. (Modified from Bertrand *et al.* (2002).

Neurog2 is a member Neurogenin family of the *atonal-like* bHLH transcription factors. This family consists of three distinct members (Neurog1, Neurog2 and Neurog3) (Sommer *et al.*, 1996; Nieber *et al.*, 2009), all of which are expressed during gastrulation in *X. laevis.* (Nieber *et al., 2009*). Transcripts of *neurog1* and *neurog2* are present in the three longitudinal domains of primary neurogenesis in open neural plate stages, with the expression of *neurog2*

being broader than *neurog1* (Ma *et al.*, 1996; Nieber *et al.*, 2009). *Neurog3* expression, in comparison, is restricted to the medial domain (Nieber *et al.*, 2009).

Among the members of the Neurogenin family, the function of *neurog2* is best characterized in *X. laevis*. Overexpression of *neurog2* is sufficient to drive neuronal differentiation of the non-neural ectoderm (Ma *et al.*, 1996). Furthermore, Neurog2 induces the expression of other later expressed proneural bHLH transcription factors such as *neurod1,* which on the other hand, is not capable of inducing *neurog2* (Ma *et al.*, 1996). Other early expressed bHLH transcription factors such as Ascl1, which activates *neurod1* expression (Cau *et al.*, 1997), while Neurod1 levels do not affect *ascl1* expression (Gao *et al.*, 2009).

It has been demonstrated that in mammalian cell lines, Neurog2 can act as a pioneer transcription factor, initiating target gene transcription on nucleosome bound regions (Chen and Dent, 2014). Often the binding of a pioneer transcription factor will initiate events that lead to an opening of the chromatin and the recruitment of active histone marks stabilizing target gene transcription (Zaret and Carroll, 2011; Zaret and Mango, 2016). Neurog2, for example, binds to regions of non-accessible chromatin (Smith *et al.*, 2016) and promotes the removal of repressive histone marks and the addition of active histone marks at the *neurod1* and *tubb2b* promoters by interacting with the H3 lysine 9 demethylase Kdm3a (Lin *et al.*, 2017). Several other proneural bHLH transcription factors such as Ascl1 or Neurod1 have been demonstrated to act as pioneer transcription factors in murine ES cells and fibroblasts (Wapinski *et al.*, 2013; Pataskar *et al.*, 2016), indicating a general role of proneural bHLH transcription factors in initiating and stabilizing the onset of neuronal gene expression.

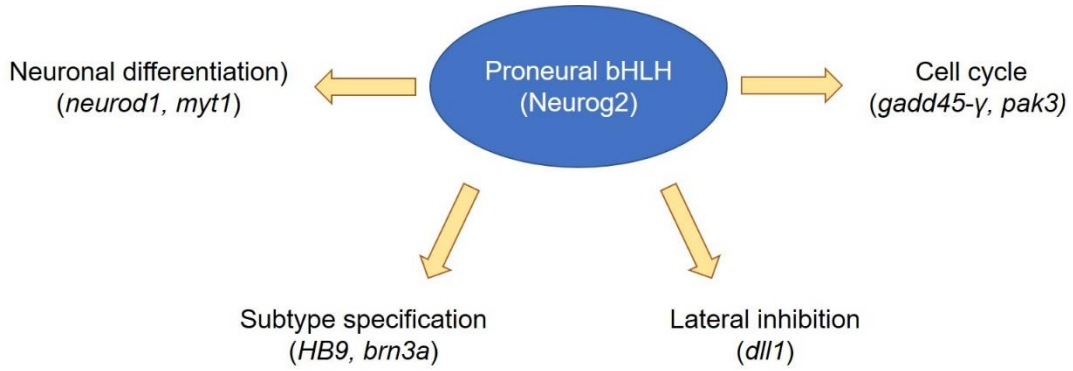

Figure 1.3: Multiple roles of the proneural bHLH transcription factor Neurog2 during neurogenesis. bHLH transcription factors like Neurog2 are involved during many processed in regulating neurogenesis. Neurog2, for example is activating a cascade of proneural genes driving neuronal determination and differentiation (Bellefroid *et al.*, 1996; Ma *et al.*, 1996). It is furthermore involved in activating cell cycle regulators and Notch ligand *dll1* and thereby controls the cell cycle length and lateral inhibition (de la Calle-Mustienes *et al.*, 2002; Kiyota and Kinoshita, 2002; Souopgui *et al.*, 2002; Bray, 2006). In addition, Neurog2 activates genes involved in the specification of distinct neuronal subtypes (Bertrand *et al.*, 2002).

The proneural bHLH proteins lead to the transcription of other bHLH transcription factors that are involved in the differentiation to neuronal cells, such as the HLH transcription factors *ebf2* (Dubois *et al.*, 1998) and *ebf3* (Pozzoli *et al.*, 2001), the atonal family members *atoh1* (Kim *et al.*, 1997) and *atoh7* (Kanekar *et al.*, 1997), as well as the neuronal differentiation factors *neurod1* (Ma *et al.*, 1996) and *neurod4* (Perron *et al.*, 1999). For example, the overexpression of the bHLH transcription factor Atoh1 is sufficient to program ectodermal cells to express neuronal differentiation markers in *X. laevis* without inducing early neuronal differentiation marker genes such as *neurog2* or *neurod1* (Kim *et al.*, 1997).

Besides driving neuronal differentiation, proneural bHLH transcription factors also influence the length of the cell cycle. Neurog2 indirectly represses cyclins D, E1 and E2 involved in G1-phase progression and G/S-phase transit in chick embryos (Lacomme *et al.*, 2012; Pfeuty, 2015). Furthermore, Neurog2 induces the cell cycle inhibitor genes *gadd45-γ* and *pak3* in *X. laevis,* leading to cell cycle withdrawal (de la Calle-Mustienes *et al.*, 2002; Souopgui *et al.*, 2002). The involvement of proneural bHLH proteins in regulating the cell cycle is further supported by studies in mouse, Ascl1 activates several cell cycle regulators that are essential for G1/S transition (*e2f1, cdk1, cdk2*, and *skp2*) or entry into mitosis (*cdk1* and *cdc25b*) (Castro *et al.*, 2006; Castro *et al.*, 2011),

but also other factors associated with cell cycle arrest (*fbxw7*, *gadd45g*, *ccng2h*, and *prmt2*), indicating that Ascl1 has a role in regulating progenitor proliferation as well as in cell cycle exit of progenitor cells (Castro *et al.*, 2011).

Furthermore, many bHLH transcription factors are involved in the regulation of lateral inhibition mediated by the Notch pathway, which controls the number of cells that undergo neuronal differentiation (Lewis, 1998; Bray, 2006; Kageyama *et al.*, 2008; Ahnfelt-Rønne *et al.*, 2012).

1.4 Lateral inhibition

The decision as to which cells will differentiate to functional neurons from an equivalent population of cells is under control of lateral inhibition, which is mediated by the Notch signaling pathway (Beatus and Lendahl, 1998; Bray, 2006; Kageyama *et al.*, 2008) (Fig. 1.4A).

During *X. laevis* neuronal differentiation, the expression of Neurog2 and the *achaete-scute* family member Ascl1 leads to the induction of the Notch-ligands *dll1* and *dll4* and *jagged* (Kiyota and Kinoshita, 2002; Bray, 2006) (Fig. 1.4B). The Notch ligands are transmembrane proteins that recognize and bind to Notch transmembrane receptors on the neighboring cell (Chitnis and Kintner, 1995; Bray, 2006). This leads to several cleavage events on the Notch receptor, which results in the release of intracellular domain of the Notch receptor (NICD) (Schroeter *et al.*, 1998; Selkoe and Kopan, 2003) (Fig 1.4b). The NICD then translocates to the nucleus where it interacts with CSL DNA binding protein Rbpj and induces the expression of bHLH transcription factors of the *hairy and enhancer of split* (*hes*) family (Sasai *et al.*, 1992; Wettstein *et al.*, 1997; Ohtsuka *et al.*, 1999; Davis and Turner, 2001; Bray, 2006). The *hes* genes are transcriptional repressors of proneural genes such as *neurog2*, so that in the end the expression of *dll1* in the neighboring cell is inhibited as well as the activation of downstream differentiation factors (Dawson *et al.*, 1995; Wettstein *et al.*, 1997; Li and Baker, 2001; Schneider *et al.*, 2001; Cau *et al.*, 2002; Louvi and Artavanis-Tsakonas, 2006) (Fig 1.4B). This leads to the differentiation of the *dll1* expressing cell, while the Notch expressing cell will remain

undifferentiated and can differentiate at a later time into a neuron or a glial cell (Sasai *et al.*, 1992; Ohtsuka *et al.*, 1999; Davis and Turner, 2001).

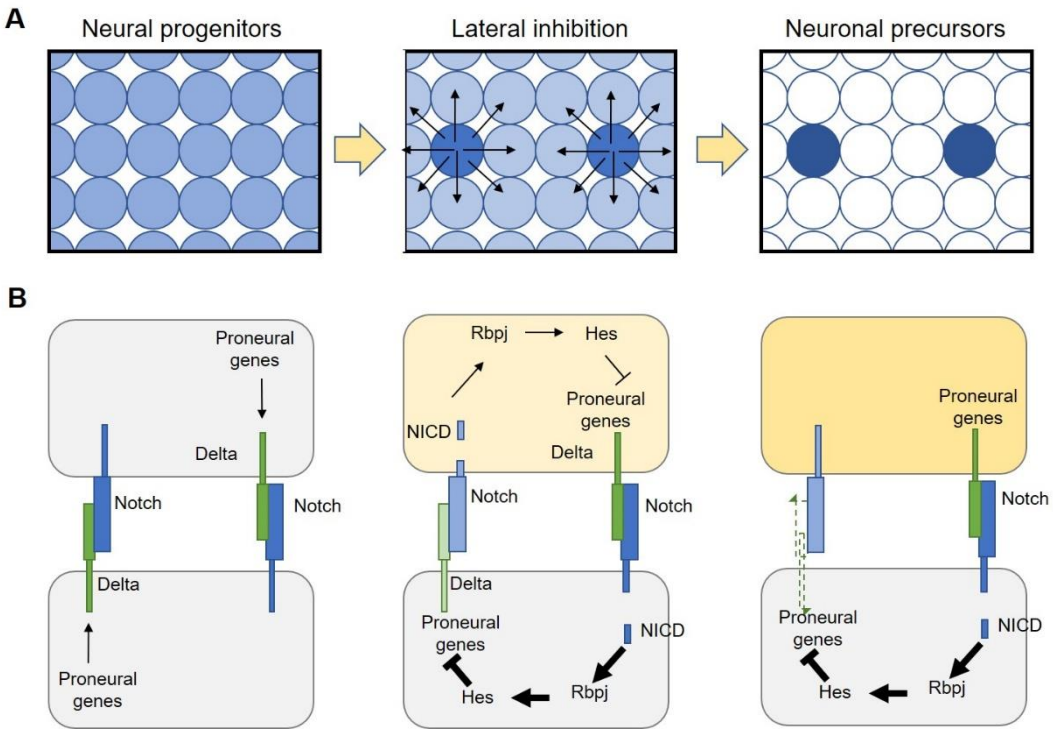

Figure 1.4: Specification of neuronal progenitors via lateral inhibition.

(A) After neural induction, the neural plate consists of equipotent neural progenitor cells. During lateral inhibition, cells get specified by signaling of repressive signals to their neighboring cells, leading signaling cells becoming neuronal progenitor cells, while receiving cells remain undifferentiated and will later give rise to stem cells or glial cells. (B) Overview of the Notch signaling pathway. Expression of proneural genes leads to the expression of the Notch ligands such as *delta*, which binds to the transmembrane Notch receptor on the neighboring cell. The binding of the ligand to the receptor leads to cleavage events at the Notch receptor, so that the notch intracellular domain, NICD, will be released. NICD enters the nucleus and binds to Rbpj activating repressor bHLH proteins such as the *hes* genes. The Hes proteins in turn, suppress the expression of proneural genes and so to a reduction of delta production in the receiving cell. In the end, the cell receiving the smallest amount of repressing signals will differentiate further.

Overexpression of NICD in *X. laevis* embryos leads to an inhibition of neuronal differentiation, while the overexpression of a dominant negative *dll1* increases the number of neurons in the territories of primary neurogenesis (Chitnis and Kintner, 1995). These findings demonstrate the importance of lateral inhibition in the balance between proliferation and differentiation, In *X. laevis*, Neurog2 also activates the zinc finger gene *myt1* (Bellefroid *et al.*, 1996), which allows the cell to escape lateral inhibition (Bellefroid *et al.*, 1996). After neural tube

closure, Notch signaling remains important for preserving a neural progenitor pool in the ventricular zone of mouse and rat embryos (Lindsell *et al.*, 1996; Imayoshi and Kageyama, 2011).

It has been demonstrated in mouse and zebrafish that the expression levels of proneural genes are oscillating within the cell, thereby establishing a dose-dependent regulation of neuronal differentiation mediated by lateral inhibition (Horikawa *et al.*, 2006; Kageyama *et al.*, 2008; Shimojo *et al.*, 2008; Oginuma *et al.*, 2010; Niwa *et al.*, 2011; Okubo *et al.*, 2012; Roese-Koerner *et al.*, 2017). The expression levels of the bHLH repressor *hes1* are inversely oscillating with those of other proneural genes like *neurog2, ascl1* and *dll1* in a 2-3 h period (Ohtsuka *et al.*, 1999; Kageyama *et al.*, 2008; Shimojo *et al.*, 2008; Maurer *et al.*, 2014; Pfeuty, 2015). Hes1 oscillation itself is established by a double negative feedback loop with the miRNA-9 (miR-9), which leads to the degradation of *hes1* mRNA, while the Hes1 protein inhibits miR-9 expression (Bonev *et al.*, 2012; Roese-Koerner *et al.*, 2017). Furthermore, miR-9 also directly binds to the NICD-Rbpj transcription factor complex leading to attenuation of Notch-signaling and promotion of neuronal differentiation (Roese-Koerner *et al.*, 2016; Roese-Koerner *et al.*, 2017). The importance of gene oscillation is supported by the findings that continuous expression of *hes1* and *dll1* lead to defects during neurogenesis (Shimojo *et al.*, 2008; Shimojo *et al.*, 2016).

1.5 Neuronal subtype specification

During neurulation, the identity of the distinct neurons is defined by their positioning in the closing neural tube (Bertrand *et al.*, 2002; Hori and Hoshino, 2012; Roberts *et al.*, 2012). Depending on their position, the differentiating neuronal precursor cell will receive different signals, leading to its development to a certain neuronal subtype identity (Bertrand *et al.*, 2002). In *X. laevis,* ten distinct neuronal subpopulations exist, which are the Rohon-Beard sensory neurons, the ventral motor neurons and Kolmer-Agduhr cells, and seven distinct interneuronal subtypes (Roberts *et al.*, 2012). How the different neuronal subpopulations are defined in *X. laevis* is not well established.

However, the combinatorial of transcription factors for each progenitor domain and post-mitotic neuron has been well characterized in mice and chick embryos, and for those genes studied in *X. laevis*, a conservation of function and expression is preserved.

In contrast to *X. laevis* where the first primary neurons arise already at the open neural plate stage, in mouse and chick, the first neurons are born in the progenitor domains of the closed neural tube (Aaku-Saraste *et al.*, 1996). The neural tube is patterned by the secretion of two morphogens at the dorsal and ventral side (Le Dréau and Martí, 2012). On the dorsal side, the neural ectoderm and the roof plate secrete BMP, while the notochord secretes Sonic hedgehog (Shh), which induces the overlying floor plate to secrete Shh to the ventral neural tube (Jessell and Dodd, 1990; Liem *et al.*, 1997). Through the different dosages of Shh and BMP signaling, the neural tube is patterned to give rise to eleven progenitor domains of neuronal subtypes (Hori and Hoshino, 2012).
The different dosages of Shh and BMP signaling lead to the expression of domain specific combinations of bHLH and homeodomain transcription factors (Briscoe *et al.*, 2000; Briscoe and Ericson, 2001; Helms and Johnson, 2003; Hernandez-Miranda *et al.*, 2017). For example, Ascl1 is expressed in populations that will later develop into dI3-6 and dIL interneurons (Gross *et al.*, 2002; Müller *et al.*, 2002), while cells expression Neurog1 and 2 will give rise to dI2 interneurons (Gowan *et al.*, 2001).

The progenitor domains can all be characterized by giving rise to excitatory or inhibitory neuronal subpopulations. Most excitatory neurons will secrete glutamate as a neurotransmitter, while inhibitory neurons secrete γ-aminobutyric acid (GABA) or glycine and are involved in balancing the excitatory signals (Hori and Hoshino, 2012). In the mouse dorsal neural tube, six progenitor domains are present (Helms and Johnson, 2003), which give rise to six early (dI1-6) and two late (dIL_A and dIL_B) subpopulations of interneurons. The five ventral progenitor domains give rise to five early developing classes of neurons (V0-3 and VMN). The V0 and V2 domain will further develop into two subpopulations expressing different neuronal transmitters (Hori and Hoshino, 2012) (Fig. 1.4).

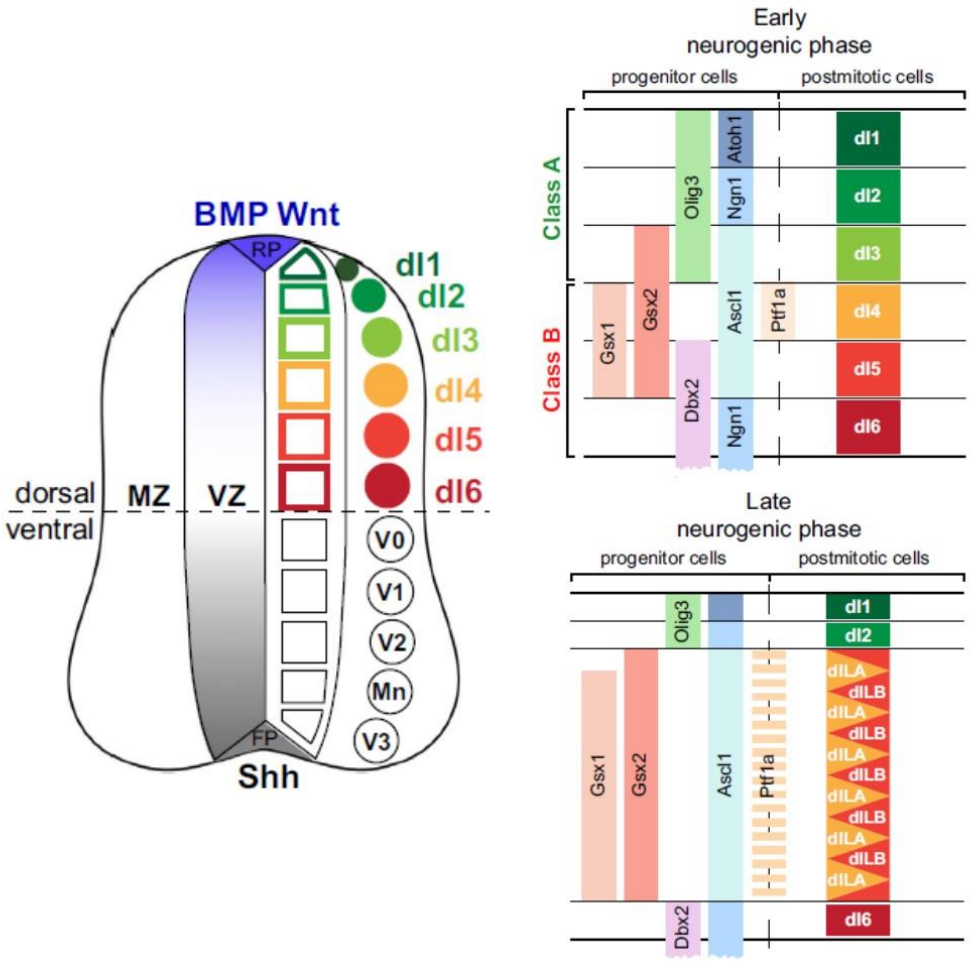

Figure 1.5 Dorsal-ventral patterning of the neural tube

In mice, the neural tube gives rise to six early and two late dorsal population of neurons (dI1-6, $dIL_{A/B}$) and five ventral neurons (V0-V3, MN). The identity of the distinct neuronal progenitor populations is defined by expressing a unique combination of transcription factors, which is established by gradients of Shh and BMP signaling form the dorsal and ventral neural tube (Hernandez-Miranda *et al.*, 2017).

Interestingly, many bHLH transcription factors involved in converting the ectoderm to a general neuronal fate also drive the development of the induced neurons to a distinct neuronal subtype (Bertrand *et al.*, 2002). Moreover, regulation of subtype specification by bHLH transcription factors is highly regulated by co-factor interaction. For instance, in the mouse, Neurog1 and Neurog2, induce the expression of sensory neuronal marker genes (Fode *et al.*, 2000). Overexpression of Neurog2 in chick embryos together with the bHLH transcription factor Olig2, however, induces motor neuron cell fate (Mizuguchi *et al.*, 2001), while overexpression of Neurog2 alone induces the

expression of the glutamatergic sensory marker gene *tlx3* (Patterson and Krieg, 1999; Perron *et al.*, 1999). In contrast, the progenitors with expression of Mash1 undergo a GABAergic cell fate in mice (Fode *et al.*, 2000; Parras *et al.*, 2002), but Mash1 together with Phox2b induces the expression of *phox2a* leading to the development of noradrenergic neurons (Pattyn *et al.*, 2000).

1.6 Role of phosphorylation in regulating neurogenesis

Impairments during neurogenesis are associated with severe diseases including epilepsies, amyotrophic lateral sclerosis or even to agenesis of entire brain areas (Sellick *et al.*, 2004; Allain *et al.*, 2011; Poduri and Lowenstein, 2011). Thus, strict regulation of neurogenesis is essential for the development of a functional nervous system. It is therefore not surprising that most aspects of neurogenesis are under a high degree of regulation ranging from transcriptional, post-transcriptional and to changes on the epigenome (Ubersax and Ferrell, 2006; Yao and Jin, 2014; Hsieh and Zhao, 2016; Yao *et al.*, 2016).

Since cells differentiate after they leave the cell cycle, the timing of cell cycle exit and length of the cell cycle is essential for the balance between neural progenitor cell maintenance and differentiation (Lange *et al.*, 2009; Lange and Calegari, 2010; Miyata *et al.*, 2010; Hardwick *et al.*, 2015). Cell cycle is mainly under the control of cell cycle dependent kinases (Cdk) that transfer a phosphate group to serine or threonine residues of target proteins and in this way regulates their activity (Vernon, 2003; Richard-Parpaillon *et al.*, 2004). Serine or threonine residues, that are modified by Cdk phosphorylation, are often directly followed by a proline residue (SP or TP sites) (Ubersax and Ferrell, 2006).

The importance of cell-cycle-dependent-phosphorylation in neuronal differentiation is supported by the findings that many proneural genes such as Neurog2 or Neurod1 are phosphorylated at several S/T-P residues (Ali *et al.*, 2011; Hardwick and Philpott, 2015). Cell-cycle-dependent-phosphorylation on SP sites in Neurog2 negatively affects its stability and thus decreases its

activity in inducing neuronal differentiation (Vosper *et al.*, 2007; Ali *et al.*, 2011). Furthermore, overexpressing of Neuorg2, where all the serine residues at SP sites were mutated to alanine in *X. laevis* embryos, showed an increase in protein stability (Ali *et al.*, 2011). Corresponding with this increased stability comes an increased activity compared to the wild-type Neurog2 in promoting neuronal differentiation (Ali *et al.*, 2011).

On the other hand, it has been demonstrated that phosphorylation on a conserved serine residue within the HLH domain of Neurog2 and Ascl1 regulates the selectivity of target gene activation during neuronal subtype specification in *drosophila* and mouse (Quan *et al.*, 2016). Furthermore, Neurog2 phosphorylation at the C-terminus (S231and S234) has a direct influence on the interaction with binding partners during neuronal subtype specification as it facilitates the interaction with LIM homeodomain transcription factors Lhx3 and Isl1/2 during murine motor neuron specification (Ma *et al.*, 2008).

1.7 Epigenetic regulation of neurogenesis

The influence of epigenetic regulation of gene expression has drawn increased attention in the last years, as malfunctions in epigenetic regulation have been associated with the development of severe diseases including several types on cancer (Hsieh and Zhao, 2016). Epigenetic mechanisms also play a critical role in neural development and function, with epigenetic dysfunction associated with several neurological disorders (Banik *et al.*, 2017; Delgado-Morales *et al.*, 2017). Gene transcription can be affected through multiple epigenetic events including DNA methylation, regulation via miRNAs or ncRNAs, chromatin remodeling and the modification of histone proteins (Fig. 1.6A) (Hsieh and Zhao, 2016).

Chromatin is a nucleoprotein complex of 147 bp of DNA surrounding a core particle (nucleosomes). One nucleosome core particle consists of DNA wrapped around two copies of the histone proteins H2A, H2B, H3 and H4 (Luger and Richmond, 1998). Depending on the density of the nucleosomes, transcription of a target gene can be facilitated or hindered. Relatively open

accessible chromatin regions are referred to as euchromatin, while those chromatin regions, in which the histone proteins are densely packed and the accessibility of the DNA is reduced is referred to as heterochromatin (Gao, 2017).

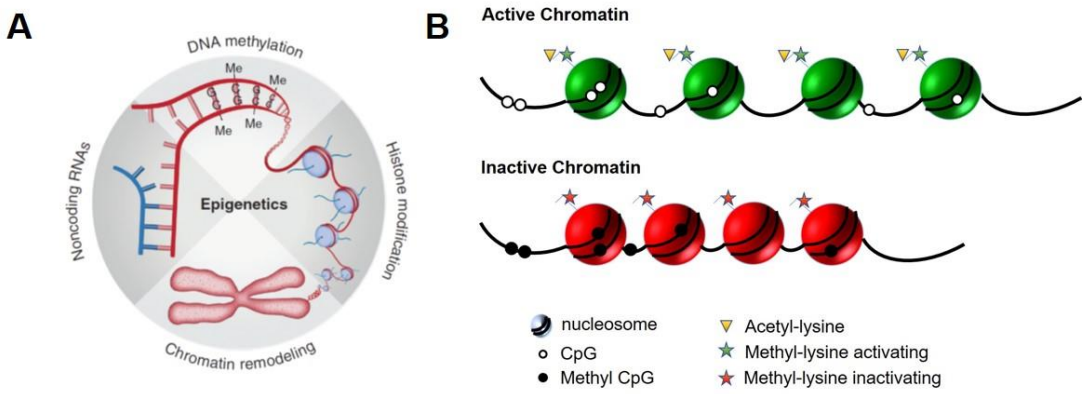

Figure 1.6: Overview of epigenetic mechanisms controlling the transcription of DNA

(A) DNA transcription can be affected by four primary mechanisms: Through ncRNAs, DNA methylation, histone modification and chromatin remodeling (Hsieh and Zhao, 2016) (B) Overview of active and inactive chromatin: Active chromatin is defined by activating histone marks such as acetylation or activating methylation on lysine residues. Inactive chromatin is characterized by repressive histone marks such as inactivating methylation on lysine residues or by methylated DNA.

The tails of histone proteins are target for covalent modifications such as acetylation, methylation, ubiquitination, SUMOylation, ribosylation and phosphorylation (Jenuwein and Allis, 2001; Bernstein *et al.*, 2007). Depending on the type and site of modification, a modification can be referred to as activating or repressing. In general, acetylation and phosphorylation of residues is associated with the activation of transcription (Strahl and Allis, 2000), while for histone methylation, it depends on the modified residue and the number of methyl groups that are transferred to this residue to define if the modification is activating or repressing (Mosammaparast and Shi, 2010) (Fig. 1.6B). Examples for activating histone modifications are the acetylation of the lysine 9 or the lysine 14 of histone H3 (H3K9ac, H3K14ac), the di- or trimethylation of lysine 4 of histone H3 (H3K4me2 H3K4me3) or the phosphorylation of serine 10 of histone H3 (H3S10p) (Hsieh and Zhao, 2016). Examples for repressing marks are the demethylation of lysine 9 of histone H3

(H3K9me2) or di- and trimethylation of lysine27 at histone H3 (H3K27me2, H3K27me3) (Hsieh and Zhao, 2016).

Methylation can also be detected on the DNA itself. Here, methylation occurs at position 5 of cysteine residues (Yao and Jin, 2014). In most cases, these cysteine residues are immediately followed by a guanine residue (CpG islands) (Simmen, 2008). The presence of methylated CpG islands is associated with gene silencing, for example the silencing of the X chromosome (Jaenisch and Bird, 2003) (Fig. 1.6C). Furthermore, during neurogenesis CpG methylation is involved in the silencing of pluripotency genes in neural progenitor cells (Mohn *et al.*, 2008). Gene silencing via DNA methylation can occur by blockage of transcription factor binding, recruitment of methylcytosine binding proteins or induction of other repressive histone modifications (Cedar and Bergman, 2009).

DNA methylation can also occur on cysteine residues that are not adjacent to a guanine residue (CpH) (Mo *et al.*, 2015). The formation of CpH islands, for example, could be detected in mature mouse cortical neurons (Mo *et al.*, 2015). Interestingly, neuronal subtypes can be clearly differentiated by their specific methylation pattern, demonstrating the changes in DNA methylation pattern occurs during differentiation and specification (Hontelez *et al.*, 2015; Mo *et al.*, 2015). CpH methylation levels are low in actively transcribed genes and increase in silenced transcription factor positions on the DNA. So, by comparing the CpH methylation levels over time, the developmental history of cells in the adult embryo can be captured (Mo *et al.*, 2015).

Interestingly, studies in *X. tropicalis* demonstrated that many epigenetic activating or repressing marks like H3K4me3 and H3K27me3 are maternally provided and are located close to the transcriptional start site of genes, while epigenetic marks achieved zygotically are located at a more distant position and are mainly close to enhancer elements (Hontelez *et al.*, 2015).

The state of the chromatin itself can be changed by chromatin remodeling complexes such as the BAF chromatin remodeling complex (also known as the SWI/SNF complex), which is essential for vertebrate neurogenesis (Seo *et al.*, 2005; Bachmann *et al.*, 2016). The BAF complex consists of at least 15 subunits (Ho *et al.*, 2009), with the subunits of the complex differing depending

on the cell type or the time of expression (Lessard *et al.*, 2007; Ho *et al.*, 2009; Kadoch *et al.*, 2013; Ronan *et al.*, 2013; Narayanan and Tuoc, 2014). The BAF complex always contains either Brm or Brg1 as the catalytic subunit, and the three invariant core units BAF47, BAF155 and BAF170 (Lessard *et al.*, 2007; Ronan *et al.*, 2013). The remaining subunits show a high variability, where some subunits are more generally distributed, while many BAF complexes have their unique composition of subunits (Lessard *et al.*, 2007; Ho *et al.*, 2009; Kadoch *et al.*, 2013; Ronan *et al.*, 2013). Nevertheless, it has been demonstrated, that either Brg1 or Brm together with the three core units is sufficient to remodel nucleosomes (Phelan *et al.*, 1999).

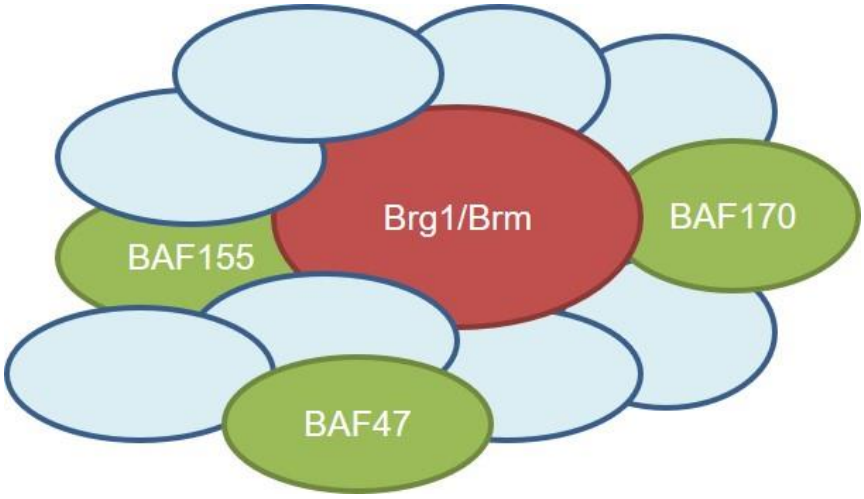

Figure 1.7 Composition of the BAF chromatin remodeling complex

The BAF chromatin remodeling complex consist of one of two catalytic core units (Brg1 or Brm) (red), three invariant core units (BAF47, BAF155 and BAF177) and a various number of context depending variant subunits (blue).

Neurogenesis is impaired in BAF mutants demonstrating the importance of chromatin remodeling via this complex (Matsumoto *et al.*, 2006; Lessard *et al.*, 2007; Narayanan and Tuoc, 2014). A loss of Brg1, for example, leads to severe defects in neurogenesis due to impairments in neuronal differentiation (Bachmann *et al.*, 2016; Sokpor *et al.*, 2017). Specific knock-out of Brg1 in murine neural progenitor cells leads to a reduced size of the brain, due to a lack of the cerebellum and a thinning of the midbrain, which results in a malformed cortex (Matsumoto *et al.*, 2006; Lessard *et al.*, 2007). Mice

heterozygotic for Brg1 suffer from exencephaly, indicating a dosage dependency for Brg1 (Matsumoto *et al.*, 2006; Lessard *et al.*, 2007). Furthermore, a knock-down of Brg1 prevents the induction of neuronal differentiation by proneural genes such as *neurog2* or *neurod1* and leads to developmental arrest of *X. laevis* embryos at gastrula or open neural plate stage (Wagner *et al.*, 2017).

Interestingly, the BAF chromatin remodeling complex can function as a transcriptional activator or as transcriptional repressor by directly binding to different proteins (Zhan *et al.*, 2011; Tuoc *et al.*, 2013). Basal expression of *shh,* for example, is repressed by BAF complex binding to Gli3, while interaction with Gli co-repressor histone deacetylase activates *shh* target genes (Zhan *et al.*, 2011).

In addition to the BAF chromatin remodeling complex, there exist three other families of SWI-like ATPase dependent chromatin remodeling complex families, namely the ISWI complexes, the CHD complexes and the INO80 complex. ISWI complexes have SNF2H or SNF2L as their catalytic subunit and are involved in transcriptional activation and repression as well as the regulation of the chromatin structure, the replication of the DNA through heterochromatin and the segregation of chromosomes (Ho and Crabtree, 2010; Goodwin and Picketts, 2017). CHD complexes are subdivided in in three subfamilies. In mice, subfamily I members (CHD1 and CHD2) are mainly involved in the preservation of pluripotency (Gaspar-Maia *et al.*, 2009), while subfamily II members (CHD3 and CHD4) are members of complexes containing histone deacetylases and function as transcriptional repressors (Zhang *et al.*, 1998). CHD7, the best studied CHD family III member, however, is involved in transcriptional activation of tissue-specific genes during differentiation (Schnetz *et al.*, 2009). Furthermore CHD8 homologue Duplin has been shown to be a negative regulator of canonical Wnt signaling in *X. laevis* (Heasman *et al.,* 2000*;* Sakamoto *et al.,* 2000*)*. For nearly all of the CHD family members, essential regulatory functions during neurogenesis have been reported (Gaspar-Maia *et al.*, 2009; Nieberler, 2012; Egan *et al.*, 2013; Jones *et al.*, 2015; Shen *et al.*, 2015; Durak *et al.*, 2016). A depletion CHD5 in the murine neocortex, for example, leads to an increase of undifferentiated progenitor cells and the expression of genes that normally are repressed

(Egan *et al.*, 2013), while CDH8 promotes the transcription of cell-cycle regulators (Durak *et al.*, 2016). INO80 family members INO80 and SWR1 form large complexes with *in vitro* nucleosome-remodeling activity and are involved in transcriptional regulation (Bao and Shen, 2007).

1.8 Changes in the epigenetic landscape during development

At the time of fertilization, the fertilized oocyte is a totipotent cell, which can develop into cells of all three germ layers (Wobus and Boheler, 2005; Mitalipov and Wolf, 2009). During development, the cells become committed to a certain cell fate and so develop to multipotent progenitor cells, which then give rise to specialized cells (Wobus and Boheler, 2005; Mitalipov and Wolf, 2009). Since limitations in specification of the cells are achieved during development, the chromatin in the early *X. tropicalis* embryo or undifferentiated murine embryonic stem cells is characterized by quite accessible chromatin (Hontelez *et al.*, 2015). In *X tropicalis* embryos, the chromatin itself is relatively unmodified at early stages (Hontelez *et al.*, 2015). While chromatin modifications increase during development, at the tailbud stage, 67% of the total chromatin still remains naïve (Hontelez *et al.*, 2015), The first global changes in the chromatin landscape occurs at the transition from maternal to zygotic transcription, with an increase in histone marks such as H3K4me3 or H3K9ac (Hontelez *et al.*, 2015). Interestingly, most of H3K4me3 or H3K9ac marks are already established without the influence of zygotic factors and can be found even at promoters of late expressed genes, indicating that the presence of active histone marks is not sufficient to drive active transcription (Hontelez *et al.*, 2015). This is supported by the observation that promoters of late expressed genes often are found in hypomethylated regions (Hontelez *et al.*, 2015; Mo *et al.*, 2015). However, after transcription the level of methylation at those genes increases, corresponding with gene silencing (Mo *et al.*, 2015).

High levels of DNA methylation do not necessarily correspond to transcriptional repression, as relatively high DNA methylation upstream and downstream of promoter regions is still compatible with transcriptional activity (Bogdanovic *et al.*, 2012). In addition, DNA methylation does not lead to

transcriptional repression in early embryos, but does so in oocytes and late embryos (Bogdanovic *et al.*, 2012). This is supported by the findings that epigenetic marks achieved by zygotic regulation in *X. tropicalis* were mostly located in regulatory regions of the DNA characterized by large distances from the promoter region and high degree of DNA methylation (Hontelez *et al.*, 2015). Many marks for enhancers could be found in these regions, indicating that regulation via enhancers is not dependent on accessible chromatin (Hontelez *et al.*, 2015).

Interestingly, several bHLH transcription factors involved in neuronal differentiation can work as pioneer transcription factors and do not need accessible chromatin to induce target gene expression. The neuronal differentiation gene Neurod1, for example, can induce target gene activation prior to chromatin opening (Pataskar *et al.*, 2016). Furthermore, Neurod1 itself can alter the state of the chromatin surrounding its target genes (Pataskar *et al.*, 2016). Other bHLH transcription factors like Neurog2 and Ascl1 have also been shown to bind non-accessible regions on the DNA (Smith *et al.*, 2016).

1.9 Ptf1a

Pancreatic transcription factor 1a (Ptf1a) is a bHLH transcription factor that was first identified as a member of a trimeric transcription factor complex involved in the development of the exocrine pancreas (Cockell *et al.*, 1989). In *X. laevis,* Ptf1a expression can first be detected in two longitudinal stripes along the dorsal midline. During subsequent stages of development, *ptf1a* expression becomes restricted to the developing hindbrain, spinal cord, the retina and the early pancreas anlagen (Afelik *et al.*, 2006) (Fig. 1.7A). Transversal sections at tailbud stage indicate that the expression domain of Ptf1a in the neural tube is restricted to the intermediate zone, in which the dorsal inhibitory interneuron population arise (Fig 1.7B).

Ptf1a is best characterized for its role during development of the pancreas, where it is involved in the specification of pancreatic precursor cells (Kawaguchi *et al.*, 2002; Afelik *et al.*, 2006). At later stages, it contributes to

the formation of the exocrine pancreas and the induction of digestive enzymes (Cockell *et al.*, 1989; Krapp *et al.*, 1996; Krapp *et al.*, 1998; Kawaguchi *et al.*, 2002). The importance of Ptf1a in pancreas development can be demonstrated in *ptf1a* knockout-mice, which suffer from a complete loss of the exocrine pancreas and while just a few endocrine cells are present, they are mislocalized to the spleen (Krapp *et al.*, 1998). Correspondingly, a knock-down of *ptf1a* in *X. laevis* and *X. tropicalis* embryos leads to the loss of exocrine marker genes and pancreatic tissue (Afelik *et al.*, 2006; Lei *et al.*, 2012). Furthermore, mutations affecting Ptf1a activity are found in humans who suffer from neonatal diabetes due to pancreatic agenesis (Hoveyda *et al.*, 1999; Sellick *et al.*, 2004; Tutak *et al.*, 2009; Al-Shammari *et al.*, 2011; Weedon *et al.*, 2014).

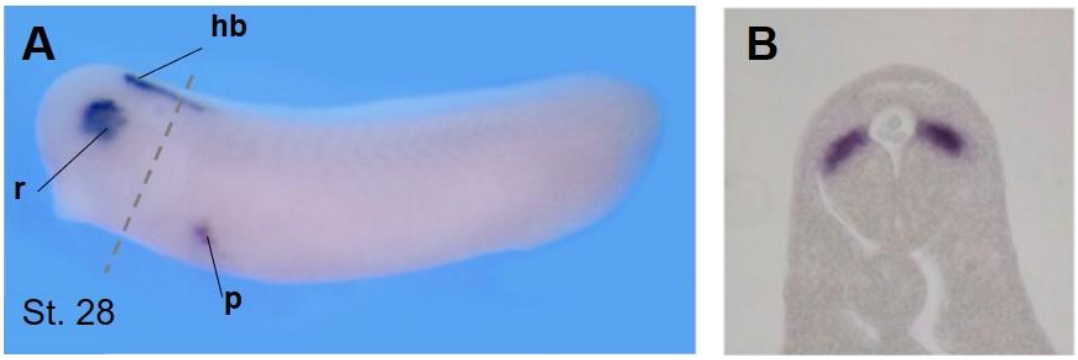

Figure 1.8: Expression pattern of Ptf1a

(A) At tailbud stage *X. laevis* embryos, Ptf1a is expressed in the retina (r), the hindbrain (hb) and the early pancreas anlagen (p). Dashed line indicating the positioning of the cross-section on the right. *r*: retina, *hb*: hindbrain, *p: pancreas* (B) Transversal section of *X. laevis* at the level of the hindbrain. Ptf1a is expressed in the dorsal in the progenitor domain, where the dorsal interneuron populations arise.

In addition to its essential role in pancreas development, Ptf1a is also required during early embryogenesis for the establishment of the nervous system (Sellick *et al.*, 2004; Glasgow *et al.*, 2005; Hoshino *et al.*, 2005; Dullin *et al.*, 2007; Nakhai *et al.*, 2007; Pascual *et al.*, 2007; Hanotel *et al.*, 2014). In this context, Ptf1a is best characterized for its ability to drive the development of GABAergic inhibitory neurons at the expanse of a glutamatergic cell fate in the retina, the hindbrain and the dorsal spinal cord (Glasgow *et al.*, 2005; Hoshino *et al.*, 2005; Fujitani *et al.*, 2006; Dullin *et al.*, 2007; Pascual *et al.*, 2007). In

the mouse hindbrain and dorsal spinal cord, Ptf1a controls the development of dI4 and dIL_A interneuron populations that express the homeodomain transcription factors *pax2* and *lhx1/5* (Glasgow *et al.*, 2005). In Ptf1a null mutant mice, those progenitor domains are completely absent, while the dI5 progenitor population is increased (Glasgow *et al.*, 2005). In the cerebellum, Ptf1a is essential for the formation of all types of GABAergic neurons (Hoshino *et al.*, 2005; Kani *et al.*, 2010; Mizuhara *et al.*, 2010; Nishida *et al.*, 2010), while in the retina, it drives the development of GABAergic amacrine and horizontal cells at the expanse of retinal ganglion and photoreceptor cells (Fujitani *et al.*, 2006; Dullin *et al.*, 2007; Nakhai *et al.*, 2007; Lelievre *et al.*, 2011). However, lineage tracing of Ptf1a positive cells in mice and chick embryos demonstrate that progenitors expressing Ptf1a can also develop into other neuronal subtypes. For example, Ptf1a cooperates with Olig3 in the differentiation of glutamatergic climbing fiber neurons in the inferior olivary nucleus (Yamada *et al.*, 2007; Storm *et al.*, 2009), while subpopulations of Ptf1a expressing cells in the dorsal spinal cord will give rise to glycinergic neurons (Huang *et al.*, 2008; Bessodes *et al.*, 2017). Furthermore, it has been suggested that Ptf1a expressing cells might also be involved in the formation of serotonergic neurons in the zebrafish enteric nervous system (Uribe *et al.*, 2016).

Besides its involvement in driving the development to distinct neuronal subtypes, Ptf1a also promotes neuronal differentiation, with overexpression of Ptf1a in *X. laevis* embryos and ectodermal explants being sufficient to ectopically drive the non-neural ectodermal cells to develop into post-mitotic neurons (Dullin *et al.*, 2007). Interestingly, although Ptf1a and Neurog2 both promote general neuronal differentiation, Neurog2 drives the development of glutamate expressing excitatory neurons (Patterson and Krieg, 1999; Perron *et al.*, 1999), while Ptf1a promotes a GABAergic cell fate (Glasgow *et al.*, 2005; Hoshino *et al.*, 2005; Li *et al.*, 2006; Dullin *et al.*, 2007; Hedderich, 2008). Overexpression of Neurog2 and Ptf1a in *X. laevis* embryos and animal caps demonstrates that Ptf1a can alter the neuronal transmitter phenotype induced by Neurog2 to a GABAergic cell fate (Hedderich, 2012). In a similar way, mis-expression of Ptf1a in *ascl1* expressing cells will also change the induced neuronal transmitter cell fate from glutamatergic to GABAergic (Chang *et al.*, 2013; Borromeo *et al.*, 2014).

1.10 Ptf1a forms a trimeric transcription factor complex

Ptf1a is a bHLH protein that functions as a heterotrimeric transcription complex that recognizes a bipartite binding motif on target genes (Roux *et al.*, 1989; Krapp *et al.*, 1996; Beres *et al.*, 2006; Masui *et al.*, 2007; Hori *et al.*, 2008). Ptf1a binds with a ubiquitously expressed class A bHLH transcription factor, (E2A/p75/HEB/TCF12), which recognizes E-box motifs (CANNTG) on the DNA (Murre *et al.*, 1989; Beres *et al.*, 2006). Furthermore, Ptf1a binds to a CSL family member, which binds to an adjacent TC box motif (TTTCCCA) on the DNA, in a distance of 1-3 helical turns (Beres *et al.*, 2006; Meredith *et al.*, 2013) (Fig. 1.8A). In mammals, two closely related CSL family members are found, Rbpl and Rbpj. While Rbpj is the component of the Ptf1a trimeric complex in the nervous system and pancreatic progenitor cells, the interaction with Rbpl is restricted to the adult pancreatic tissue (Beres *et al.*, 2006; Hori *et al.*, 2008). In contrast to mammals, there are two homeologs of the CSL family in *X. laevis* and both are closely related to Rbpj (Beres *et al.*, 2006). The interaction with mouse Rbpj is mediated by two tryptophan residues within two highly conserved motifs on the Ptf1a C-terminus (C1: HSLSW and C2: VWTPEDPR) (Beres *et al.*, 2006; Hori *et al.*, 2008). This interaction can be disrupted through mutation of the tryptophan residues in the C1 and C2 domain to alanine (Hori *et al.*, 2008). While the C1 domain of the mouse Ptf1a is more important for binding Rbpl, mutation of the C2 domain is sufficient for disruption of binding of Ptf1a to Rbpj (Beres *et al.*, 2006). Complete disruption of Ptf1a with *X. laevis* Rbpj requires mutation at the corresponding tryptophan residues in both the C1 and C2 domains ($Ptf1a^{W224A/W242A}$) (Hanotel *et al.*, 2014).

The binding of Rbpj is thought to be essential for Ptf1a function, since mutations that results in truncation at the Ptf1a C-terminus have been found in children suffering from cerebellar agenesis (Sellick *et al.*, 2004). Furthermore, mutations in the Ptf1a C2 domain in chick embryos result in loss of GABAergic dI4 and dIL_A neurons, a phenotype that is similar to those of Ptf1a knock-out mice (Hori *et al.*, 2008). Interestingly, overexpression of a Ptf1a C1C2 mutant ($Ptf1a^{W224A/242A}$) in *X. laevis* embryos and C-terminal truncation mutants known to cause cerebellar agenesis in humans, still induce neuronal differentiation (Hedderich, 2008; Hedderich, 2012; Richts, 2013). However, the induced

neuronal subtype is changed from a GABAergic to glutamatergic cell fate (Fig 1.8B). Loss of Ptf1a in the mouse brain will not affect the generation of the formerly Ptf1a expressing progenitor populations, but instead, those cells will either migrate to the brainstem or undergo apoptosis (Millen *et al.*, 2014; Iskusnykh *et al.*, 2016).

Rbpj not only binds to Ptf1a, but also binds to the Notch intracellular domain (Nishimura *et al.*, 1998). It has been shown that the interaction of Ptf1a and NICD with Rbpj is mutually exclusive, suggesting that Ptf1a and NICD might compete with each other in binding Rbpj (Beres *et al.*, 2006).

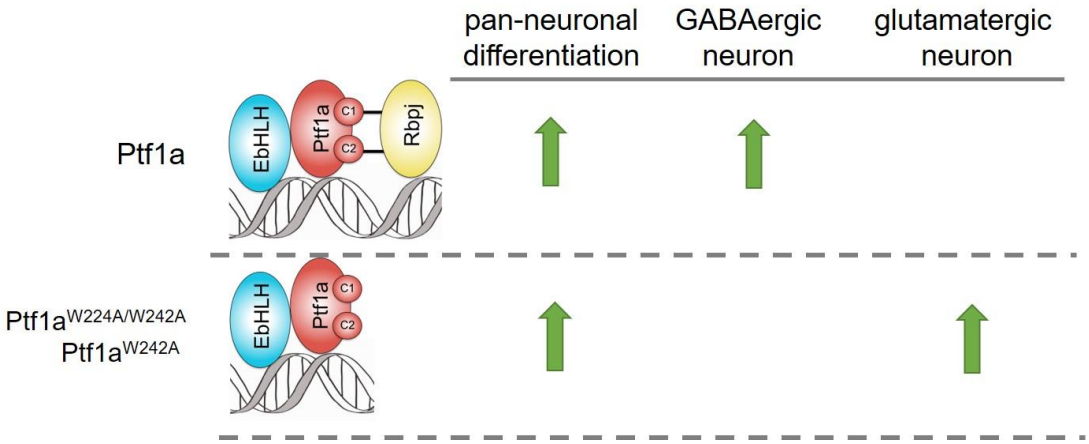

Figure 1.9: Ptf1a forms a heterotrimeric complex

Ptf1a (green) forms a trimeric complex with a class A bHLH protein (blue), binding an E-box motif on the DNA and to Rbpj (orange) binding an adjacent TC-box motif. Interaction with Rbpj is established by two highly conserved motifs (C1 and C2). Interaction with Rbpj can be disrupted by inducing point mutations from tryptophan to alanine within these motifs. While both mutants can promote neuronal differentiation, the wild-type Ptf1a promotes a GABAergic cell fate, while the Ptf1a^{W224A} and Ptf1a$^{W224A/242A}$ mutant induces a glutamatergic cell fate.

1.11 Gene induction and regulation by Ptf1a

In the developing pancreas, Ptf1a directly binds the *pdx1* promoter and drives the development of the early pancreas (Wiebe *et al.*, 2007). Furthermore, Ptf1a is well known for activating genes associated with the maturation of the exocrine pancreas and for the induction of digestive enzymes (Cockell *et al.*, 1989; Krapp *et al.*, 1996; Krapp *et al.*, 1998; Kawaguchi *et al.*, 2002; Masui *et al.*, 2010). Ptf1a is autoregulated by binding to its own promoter in a positive feedback loop (Masui *et al.*, 2008).

In contrast to pancreas development, only a few downstream target genes of Ptf1a are known during neurogenesis. Ptf1a directly activates *neurog2* expression in chick and mouse embryos (Henke *et al.*, 2009). Furthermore, the two immunoglobulin superfamily members, *nephrin* and *neph3* (also known as *kirrel2*) are direct target genes of Ptf1a in mouse (Nishida *et al.*, 2010). As *kirrel2* is expressed in Purkinje progenitor cells, it is suggested that its activation by *Ptf1a* plays a role in GABAergic neuronal subtype specification (Mizuhara *et al.*, 2010). As in pancreas development, it has been shown that Ptf1a expression is under the control of a positive feedback loop, by binding to its own promoter (Meredith *et al.*, 2009). Furthermore, *barhl2* could be shown to act downstream of Ptf1a in the development of amacrine cells in the zebrafish retina (Jusuf *et al.*, 2012). In addition, the zinc finger histone methyltransferase gene Prdm13 has been shown to be a direct Ptf1a target gene in mouse and *X. laevis* and is required to repress a glutamatergic excitatory neuronal cell fate (Chang *et al.*, 2013; Hanotel *et al.*, 2014). Prdm13 inhibits the Neurog2- or Ascl1-induced expression of the glutamatergic selector gene *tlx3* via interaction with its regulatory sequences and direct interaction with Ascl1 (Chang *et al.*, 2013; Hanotel *et al.*, 2014; Mona *et al.*, 2017). In addition, Prdm13 inhibits the expression of its own inducer, Ptf1a, in subpopulations of Ptf1a expressing cells that will develop into glycinergic cell fate (Bessodes *et al.*, 2017; Mona *et al.*, 2017). In *X. laevis* ectodermal explants, activation of direct target genes by Ptf1a underlies a temporal selection (Hedderich, 2012). While some direct target genes like *prdm13* are activated immediately by Ptf1a, other direct target genes like *neurog2* undergo a delayed activation (Hedderich, 2012).

Similar to many bHLH proteins, Ptf1a contains S/T-P residues, which are putative targets of Cdk-mediated phosphorylation (Ubersax and Ferrell, 2006). Preventing phosphorylation at those sites, through mutation of these sites in Neurog2, leads to an increase in activation of the pan-neuronal marker *tubb2b* (Ali *et al.*, 2011). No increase in neuronal inducing activity of Ptf1a was detected upon overexpression of a murine Ptf1a in which all eight S/T-P residues were mutated to alanine (mPtf1a$^{8S/T\rightarrow A}$) in *X. laevis* embryos and animal caps, (Richts, 2013). Surprisingly, additional to its ability to induce markers for a GABAergic cell fate, mPtf1a$^{8S/T\rightarrow A}$ also induced the glutamatergic

marker gene *tlx3,* a gene that is normally repressed by Ptf1a. Mutating the alanine residue at position 299 back to threonine (mPtf1a$^{7S\rightarrow A}$) could prevent the mixed induced neuronal transmitter phenotype back to an induced GABAergic cell fate (Richts, 2013), suggesting that the mutation of the T_{299} was responsible for this activity.

1.12 Aims

The bHLH transcription factor Ptf1a is sufficient to promote neuronal differentiation (Dullin *et al.*, 2007; Hedderich, 2008; Hedderich, 2012) and is able to drive the development of a GABAergic neuronal subtype at the expense of a glutamatergic neuronal subtype in the vertebrate brain, dorsal spinal cord, and retina (Glasgow *et al.*, 2005; Hoshino *et al.*, 2005; Dullin *et al.*, 2007; Pascual *et al.*, 2007). In recent years, Ptf1a mutants were identified that alter the induced neuronal transmitter phenotype (Hedderich, 2008; Hori *et al.*, 2008; Richts, 2013). In this thesis, the selective induction of target genes by Ptf1a will be further analyzed. Therefore, Ptf1a C2 domain mutants inducing various neuronal call fates will be investigated by their activation of target genes and for potential mechanisms causing the alterations in the induced neuronal subtypes by those mutants. Furthermore, the function of chromatin remodeling in controlling the delay in the activation of target genes by Ptf1a will be analyzed. This will be investigated by studying the dependency of Ptf1a target gene activation on chromatin remodeling by the BAF complex and directly studying changes chromatin accessibility over time.

2. Materials and Methods

2.1 Materials

2.1.1 *X. laevis*

X. laevis pigmented males and females were purchased from Nasco (Ft. Atkinson, USA). Developmental stages were defined according to Nieuwkoop and Faber (1967).

2.1.2 Bacteria

The chemical competent *Escherichia coli* strand **XL1-Blue** (recA1, endA1, gyrA96, thi-1, hsdR17, supE44, relA1, lac[FproAB, lacl^{q}ZΔM15, Tn10(Tet^{r})]^{c}) was used for molecular biology standard methods.

2.1.3 Chemicals

Chemicals used were ordered from the following companies: ApplChem, Merck, Roche, Roth, Sigma-Aldrich

2.1.4 Antibiotics and Media

Bacteria culture medium was made by dissolving 32 g Luria Bertani (LB) in 1 l dH_2O. LB Medium was autoclaved at 121 °C and then cooled down on 50 °C. Ampicillin (working concentration: 100 µg/ml, diluted from a 100 mg/ml in dH_2O stock solution) was added and the medium transferred to petri dishes and stored at 4 °C.

2.1.5 Oligonucleotides

Oligonucleotides for cloning and RT-PCR were purchased from Sigma-Aldrich and were dissolved in dH_2O to a 100 µM or 500 µM stock solution. Antisense morpholino oligonucleotides were purchased from Gene Tools and dissolved in RNase-free water to a concentration of 20 ng/nl. The morpholinos were stored at 4 °C and were heated for 5 min at 65 °C before use.

2.1.5.1 RT-PCR oligonucleotides

As *X. laevis* is allotetraploid all chromosomes are present in a large (.L) and a small (.S) copy. The homeolog targeted by the oligonucleotide is indicated behind the gene name.

Oligonucleotide	**Orien-tation**	**Sequence**	**T_A °C**	**Cycles**
odc.L (Heasman *et al.*, 2000)	for	5´-GCCATTGTGAAGACTCTCTCCATTC-3´	57	25
odc.L (Heasman *et al.*, 2000)	rev	5´-TTCGGGTGATTCCTTGCCAC-3´	57	25
n-tubulin.L + S (Stancheva and Meehan, 2000)	for	5´-ACACGGCATTGATCCTACAG-3´	56	32
n-tubulin.L + S (Stancheva and Meehan, 2000)	rev	5´-AGCTCCTTCGGTGTAATGAC-3´	56	32
gad1a.L (Dullin *et al.*, 2007)	for	5´-ATGGGCGTCTTACTCCAATG-3´	60	32
gad1a.L (Dullin *et al.*, 2007)	rev	5´-ATGTCTACATGGCGACCACA-3´	60	32

tlx3.S (Dullin *et al.*, 2007)	for	5´-GCCAACAAGTACAAGTGCACAG-3´	62	27
tlx3.S (Dullin *et al.*, 2007)	rev	5´-CAGGAGCCAGACTCACATTGAC-3´	62	27
prdm13.S (Hanotel *et al.*, 2014)	for	5´-CTGCCGACACATGATGAAAAAGG-3´	63	27
prdm13.S (Hanotel *et al.*, 2014)	rev	5´-AGATTTTGGGGGAGGCAGAAAAG-3´	63	27
neurog2.L	for	5´-TTTGTTAAGGGCGAATGTCA-3´	62	34
neurog2.L	rev	5´-ATCCGGGAAGGTGAAAAAGT-3´	62	34

Table 2.1 List of RT-primers and their PCR parameters

2.1.5.2 Sequencing oligonucleotides

Oligonucleotide	Sequence
T3	5´-TTAACCCTCACTAAAGG-3´
T7	5´-TAATACGACTCACTATAGG-3´
SP6	5´-ATTTAGGTGACACTATAG-3´
Ptf1a rev	5´-CATCAGTCCATGAGAGAG-3´

Table 2.2 List of sequencing oligonucleotides

2.1.5.3 Morpholino oligonucleotides

Morpholino	Sequence
Brg1-MO (Seo *et al.*, 2005)	5´-TCACTGCTAACCTGTCCCCGAATCC-3´
Standard control MO (GeneTools)	5´-CCTCTTACCTCAGTTACAATTTATA-3´

Table 2.3 List of morpholino oligonucleotides

2.1.6 Sense RNA constructs

Construct	Vector	Restriction enzyme	Polymerase	Reference
Ptf1a	pCS2+GR	NotI	SP6	(Afelik et al., 2006)
Ptf1a^{W242A}	pCS2+GR	NotI	SP6	(Hanotel et al., 2014)
Ptf1a$^{W224A/W242A}$	pCS2+GR	NotI	SP6	(Hanotel et al., 2014)
Ptf1a^{T243A}	pCS2+GR	NotI	SP6	This thesis
Ptf1a^{T243E}	pCS2+GR	NotI	SP6	This thesis
Ptf1a-Vn	pCS2+Vn	NotI	SP6	(Hedderich, unpublished data)
Ptf1a$^{W224A/W242A}$-Vn	pCS2+Vn	NotI	SP6	(Hedderich, unpublished data)
Ptf1a^{T243A}-Vn	pCS2+Vn	NotI	SP6	This thesis
Ptf1a^{T243E}-Vn	pCS2+Vn	NotI	SP6	This thesis
Rbpj-Vc	pCS2+Vc	NotI	SP6	(Hedderich, unpublished data)
Prdm13-Vc	pCS2+Vc	NotI	SP6	This thesis
Neurog2-Vn	pCS2+Vn	NotI	SP6	This thesis

E12-Vc	pCS2+Vc	NotI	SP6	(Hedderich, unpublished data)
β-Gal	pCS2+	NotI	SP6	(Chitnis and Kintner, 1995)
mRFP	pCS2+	NotI	SP6	(Saka et al., 2007)

Table 2.4 List of overexpression constructs

Overexpression constructs:

E12-VcpCS2+ (prepared by M. Hedderich and K. Ditter)**:**
E12-VcpCS2+ contains the open reading frame of Rbpj fused at its N-terminus with the C-terminus of Venus YFP (aa 155-238). E12-VcpCS2+, was generated by PCR amplification of the E12 open reading frame using XE12pSP64XBm (obtained from Eric Bellefroid) as a template and the following primers: for, 5´-GTACCGGTGGTGGTGGTGGTGGTAATCAGCAG CAGAGGATG-3´ and rev, 5´-GGGTACGTATCACATGTGTCCCACTGG-3´. The PCR product was inserted into VcpCS2+ (Saka *et al.*, 2007) using AgeI and SnaBI restriction sites. For preparation of sense RNA, the construct was linearized with NotI and transcribed with SP6 polymerase.

Ptf1a-VnpCS2+ (prepared by M. Hedderich and K. Ditter)**:**
Ptf1a-VnpCS2+ contains the open reading frame of Ptf1a fused at its N-terminus with the N-terminus of Venus YFP (aa 1-154). Ptf1a-VnpCS2+, was generated by PCR amplification of the Ptf1a open reading frame using Ptf1a-GRpCS2+ (Afelik *et al.*, 2006) as a template and the following primers: for, 5´-TACCGGTGGTGGTGGTGGTGGTGAAACGGTCCTGGAGC-3´ and rev, 5´-GGGTACGTATCACATATCAAGGCACAAAG-3´. The PCR product was inserted into VnpCS2+ (Saka *et al.*, 2007) using AgeI and SnaBI restriction sites. For preparation of sense RNA, the construct was linearized with NotI and transcribed with SP6 polymerase.

Rbpj-VcpCS2+ (prepared by M. Hedderich and K. Ditter)**:**
Rbpj-VcpCS2+ contains the open reading frame of Rbpj fused at its N-terminus with the C-terminus of Venus YFP (aa 155-238). Rbpj-VcpCS2+, was generated by PCR amplification of the Rbpj open reading frame using Rbpj-GRpCS2+ (Hedderich, 2012) as a template and the following primers: for, 5´-GTACCGGTGGTGGTGGTGG TGGTCAACCTGGCATTCCTAAATAC-3´ and rev, 5´-GGGTACGTATTAGGACACTACTGCTGCAGTG-3´. The PCR product was inserted into VcpCS2+ (Saka *et al.*, 2007) using AgeI and SnaBI restriction sites. For preparation of sense RNA, the construct was linearized with NotI and transcribed with SP6 polymerase.

Ptf1a$^{W224A/W242A}$-VnpCS2+ (prepared by M. Hedderich and K. Ditter)**:**
Ptf1a$^{W224A/W242A}$-VnpCS2+ contains the open reading frame of Ptf1a fused at its N-terminus with the N-terminus of Venus YFP (aa 1-154). Ptf1a$^{W224A/W242A}$-VnpCS2+, was generated by PCR amplification of Ptf1a open reading frame using Ptf1a$^{W224A/W242A}$-GRpCS2+ (Hedderich, 2008) as a template and the following primers: for, 5´-TACCGGTGGTGGTGGTGGTGAAACGGT CCTGGAGC-3´ and rev, 5´-GGGTACGTATCACATATCAAGGCACAAAG-3´. The PCR product was inserted into VnpCS2+ (Saka *et al.*, 2007) using AgeI and SnaBI restriction sites. For preparation of sense RNA, the construct was linearized with NotI and transcribed with SP6 polymerase.

Ptf1a^{T243A}-GRpCS2+ (prepared by M. Hedderich and K. Ditter)**:**
Ptf1a^{T243A}-GRpCS2+ contains the open reading frame of Ptf1a with putative phosphorylation site threonine 243 mutated to alanine. To synthesize Ptf1a^{T243A}-GRpCS2+, the threonine residue in position 243 was mutated using the QuickChange XL Site Directed Mutagenesis Kit (Stratagene) and the following primers (mutations are indicated in red): for, 5´-GGCCAAAGTGTGG GCTCCTGAGGATCCC-3´ and rev, 5´-GGGATCCTCAGGAGCCCACAC TTTGGCC-3´ and Ptf1a-GRpCS2+ as a template. For preparation of sense RNA, the construct was linearized with NotI and transcribed with SP6 polymerase.

Ptf1a^{T243E}-GRpCS2+:

Ptf1a^{T243E}-GRpCS2+ contains the open reading frame of Ptf1a with putative phosphorylation site threonine 243 mutated to glutamate. To synthesize Ptf1a^{T243E}-GRpCS2+, the threonine residue in position 243 was mutated using the QuickChange XL Site Directed Mutagenesis Kit (Stratagene) and the following primers (mutations are indicated in red): for, 5´-CGGC CAAAGTGTGGGAGCCTGAGGATCCCAGG-3´ and rev, 5´-CCTGGGATCC TCAGGCTCCCACACTTTGGCCG-3´ and Ptf1a-GRpCS2+ as a template. For preparation of sense RNA, the construct was linearized with NotI and transcribed with SP6 polymerase.

Ptf1a^{T243A}-VnpCS2+:

Ptf1aT243A-VnpCS2+ contains the open reading frame of Ptf1a^{T243A} fused at its N-terminus with the N-terminus of Venus YFP (aa 1-154). To synthesize Ptf1a^{T243A}-VnpCS2+, the threonine residue in position 243 was mutated using the QuickChange XL Site Directed Mutagenesis Kit (Stratagene) and the following primers (mutations are indicated in red): for, 5´-GGCCAAAGT GTGGGCTCCTGAGGATCCC-3´ and rev, 5´-GGGATCCTCAGGAGCCC ACACTTTGGCC-3´ and Ptf1a-VnpCS2+ as a template. For preparation of sense RNA, the construct was linearized with NotI and transcribed with SP6 polymerase.

Ptf1a^{T243E}-VnpCS2+:

Ptf1a^{T243E}-VnpCS2+ contains the open reading frame of Ptf1a^{T243E} fused at its N-terminus with the N-terminus of Venus YFP (aa 1-154). To synthesize Ptf1a^{T243E}-VnpCS2+, the threonine residue in position 243 was mutated using the QuickChange XL Site Directed Mutagenesis Kit (Stratagene) and the following primers (mutations are indicated in red): for, 5´-CCTGGGATC CTCAGGCTCCCACACTTTGGCCG-3´ and rev, 5´-CGGCCAAAGTGTG GGAGCCTGAGGATCCCAGG-3´ and Ptf1a-VnpCS2+ as a template. For preparation of sense RNA, the construct was linearized with NotI and transcribed with SP6 polymerase.

Neurog2-VnpCS2+:

Neurog2-VnpCS2+ contains the open reading frame of Neurog2 fused at its N-terminus with the N-terminus of Venus YFP (aa 1-154). Neurog2-VnpCS2+, was generated by PCR amplification of the Neurog2 open reading frame using Neurog2-HApCS2+ (Hedderich, unpublished data) as a template and the following primers: for, 5´-GTACCGGTGGTGGTGGTGGTGGTGTGCT GCTCAAGTGCG-3´ and rev, 5´-GGGTACGTATCAAATGAAAGCGCTGCT-3´. The PCR product was inserted into VnpCS2+ (Saka *et al.*, 2007) using the AgeI and SnaBI restriction sites. For preparation of sense RNA, the construct was linearized with NotI and transcribed with SP6 polymerase.

Prdm13-VcpCS2+:

Prdm13-VcpCS2+ contains the open reading frame of Prdm13 fused at its N-terminus with the C-terminus of Venus YFP (aa 155-238). Prdm13-VcpCS2+, was generated by PCR amplification of the Prdm13 open reading frame using cDNA as a template and the following primers: for, 5´-ATGCATTGCAACAGGGCTC-3´ and rev, 5´-TTAGGGTTCCTTGCTG CTTCC-3´. The insert was subcloned into pGemTeasy vector, which was then used as a template for PCR amplification of the Prdm13 open reading frame using the following primers: for, 5´-GTACCGGTGGTGGTGGTGGTGGTC ATTGCAACAGGGCTCTG-3´ and rev, 5´-GGGTACGTATTAGGGTTCC TTGCTGCTTC-3´. The PCR product was inserted into VcpCS2+ (Saka *et al.*, 2007) using the AgeI and SnaBI restriction sites. For preparation of sense RNA, the construct was linearized with NotI and transcribed with SP6 polymerase.

2.1.7 Antisense RNA constructs

Construct	Vector	Restriction enzyme	Polymerase	Reference
tubb2b	pBst KS	BamHI	T3	(Chitnis and Kintner, 1995)
gad1a	pCMV-Sport6ccdB	NotI	SP6	(Dullin *et al.*, 2007)

tlx3	BStEII	Stu1	T3	(Patterson and Krieg, 1999)

Table 2.5 List of RT-primers and their PCR parameters

2.2 Methods

2.2.1 *In vitro* synthesis of capped sense RNA

Capped sense RNA was synthesized using the Ambion SP6 mMessage mMachine Kit according to manufacturer's instructions. For a 20 µl total reaction volume, 1 µg of linearized plasmid DNA was used. The transcription reaction was incubated for 2 h at 37 °C, followed by a 30 min DNA digest using 1 U Turbo DNase I. The synthesized sense RNA was purified using the Illustra RNAspin Mini kit (GE Healthcare) according to the manufacturer's instructions and was eluted in 30 µl RNase free water at 80 °C. The RNA quality was checked on a 1% agarose gel and the RNA concentration was determined by loading 1 µl of purified RNA on a NanoDrop 2000c spectrophotometer (Thermo Scientific). The RNA was stored in 2-4 µl aliquots at -80 °C.

2.2.2 *Xenopus* methods

Unless stated otherwise, standard *X. laevis* methods were done according to Sive *et al.* (2000)

5x MBS 440 mM NaCl, 5 mM KCl, 4.1 mM $MgSO_4$, 12 mM $NaHCO_3$, 2.05 mM $CaCl_2$, 1.65 mM $Ca(NO_3)_2$, 50 mM HEPES, pH 7.8

Cysteine: 2% Cysteine-HCl in 0.1x MBS, pH 8

Injection buffer: 2% Ficoll in 1x MBS

1000x Dexamethasone: 4 mg/ml dexamethasone in 100% EtOH

2.2.2.1 Priming of *X. laevis* frogs

Female frogs were stimulated by injecting 800 U human chorionic gonadotropin (Ovogest, MSD animal health) into the dorsal lymph sac the

evening before egg-laying. Primed frogs were kept overnight at 16 °C. Egg laying started approximately 16 h after hCG priming.

2.2.2.2 Preparation of the testis

Male frogs were anesthetized by putting them for 30 min in narcotic (1g/l tricaine methanesulfonate, 0.1% Na_2HPO_4, pH 7) (Guénette *et al.*, 2013). The testis was isolated and stored at 4 °C in 1x MBS. Prior to usage, a testis lysate was made by macerating a small piece of testis in a small petri dish containing 1.5 ml 1x MBS using a scalpel.

2.2.2.3 *In vitro* fertilization

By applying gentle pressure on the back of female frogs, eggs were collected in a petri-dish and fertilized by the addition of testis lysate 1:10 diluted with H_2O. Typically, between 100 µl and 150 µl of testis lysate were used. After 15-30 min, the eggs were covered with 0.1x MBS and stored at 12.5 °C.

2.2.2.4 Microinjection

Prior to the injection, the embryos were dejellied in a 2% cysteine solution and transferred to injection buffer. Injection needles were made by pulling small glass capillaries (GB100F-8P, Science Products GmbH) in a needle-puller (PN-30, Science Products GmbH). Needles were back-loaded with the desired injection mix and then attached to an microinjector PV 820 (H. Sauer). Using a micrometer scale, the injection drop was adjusted to a final volume of 4 nl. The injection buffer was exchanged 1-2 h after injection with 0.1x MBS and the injected embryos were cultivated at 12.5-18°C until the desired stage.

2.2.2.5 Preparation of ectodermal explants (animal caps)

Blastula staged embryos were transferred to a petri-dish coated with 1% agarose containing 0.8x MBS. The vitelline membrane was removed and explants of the animal cap were made using a gastromaster (Xenotech

Engineering) with a 500 µm yellow tip and “high” intensity. Animal caps were transferred to a fresh agarose-dish containing 0.8x MBS and cultured at 12-18 °C until they reach the desired stage. To fix the caps, the embryos were placed in an Eppendorf tube and the buffer was removed. The embryos were frozen in liquid N_2 and stored at -80 °C.

2.2.2.6 Dexamethasone treatment

At the desired time (stage 10.5 for embryos or after excision of animal caps) dexamethasone in a final concentration of 4 µg/ml (from a 1000x stock solution) was added to the culture medium. The embryos or animal caps were cultured in the dark at 14-18 °C until they reached the desired stage (as determined from sibling control embryos). For collecting stage 14 animal caps or collecting early time points (3, 6 or 9 h incubation time), caps were cultivated at 14 °C. For later time points (12, 15 or 25 h), caps were cultivated at 18 °C. Animal caps were fixed by freezing in liquid N_2 and were stored them at -80 °C.

2.2.2.7 Bimolecular Fluorescent Complementation assay (BiFC)

BiFC (Saka *et al.*, 2007) was used to visualize protein-protein interaction in vivo. Therefore, 500 pg of each sense RNA encoding for the Vc- or Vn-fusion proteins was injected in both animal blastomeres at two cell stage *X. laevis* embryos. To label injected cells, 100 pg *mRFP* sense RNA was co-injected. At blastula stage (stage 8), the cells were dissociated by transferring the embryos to accutase (Sigma Aldrich) and culturing them for 5-6 h. Fluorescence microscopy was done by using an Axioplan2 fluorescent microscope (Zeiss) and pictures were taken using an Intas camera.

2.2.2.8 *In vitro* synthesis of antisense RNA

To prepare antisense RNA for whole mount in situ hybridizations (WMISH), a 25 µl reaction containing 1 ng linearized plasmid, 1x Transcription buffer (Fermentas), 1 mM 1mM rATP (Boehringer), 1 mM rGTP (Boehringer), 1mM rCTP (Boehringer), 0.64 mM rUTPs (Boehringer), 0.34 mM Digoxigenin-rUTP

(Boehringer), 0.03 µM DTT, 40 U Ribolock RNase inhibitor (Fermentas), 30 U T3 or SP6 RNA-Polymerase in RNase-free water was used. The in vitro transcription was incubated at 37 °C for two hours. Afterwards, the template was digested by a 30 min incubation with 1 U TurboDNase I (Ambion) at 37 °C. Purification of the antisense RNA was done using the RNeasy Mini kit (Qiagen) according to manufacturer's instructions. The RNA was eluted two times with 50 µl RNase-free water at 80 °C. The RNA quality was checked on a 1% agarose gel. Afterwards, the antisense RNA was diluted in 1 ml of hybridization buffer (see in situ hybridization) and stored at -20 °C.

2.2.2.9 Whole mount *in-situ* hybridization (WMISH)

10x MEM: 1 M Mops, 20 mM EGTA, 10 mM $MgSO_4$, pH 7.4 (stored in the dark)
10x PBS: 1.75 M NaCl, 1 M KCl, 65 mM Na_2HPO_4, 18 mM KH_2PO_4, pH 7.4
$K_3FE(CN)_6$: 0.5 M in H_2O (stored in the dark)
$K_4FE(CN)_6$: 0.5 M in H_2O (stored in the dark)
MEMFA: 4% (v/v) formaldehyde (37%) in 1x MEM
X-Gal: 40 mg/ml 5-Bromo-4-chloro-3-indolyl-b-D-galactopyranoside in formamide (stored -20 °C in the dark)
X-Gal staining solution: 1 mg/ml X-Gal, 5 mM $K_3FE(CN)_6$, 5 mM $K_4Fe(CN)_6$, 2 mM $MgCl_2$ in 1x PBS
PTw: 0.1% Tween-20 in 1x PBS
Proteinase K: 5 µg/ml proteinase K (Merck) in 0.1x PBS
Triethanolamine: 0.93 g triethanolamine in 50 ml H_2O (0.1 M), pH 7.5
PTw/FA: 4% (v/v) formaldehyde in PTw
Hybridization Mix: 50% formamide, 1 mg/ml Torula RNA, 10 µg/ml Heparin, 1x Denhardt's, 0.1% Tween-20, 0.1% CHAPS, 10 mM EDTA in 5x SSC
20X SSC: 3 M NaCl, 0.3 M NaCitrate, pH 7.2-7.4
100x Denhardts solution: 2% BSA 2% Polyvinylpyrollidone (PVP), 2% Ficoll
RNAse Solution: 10 µg/ml RNAse A, 0.01 U/ml RNAse T1 in 2X SSC
MAB: 100 mM maleic acid, 150 mM NaCl, pH 7.5
MAB/BMB: 2% BMB in 1x MAB
MAB/BMB/HS: 2% BMB, 20% heat-treated horse serum in 1x MAB

APB: 100 mM Tris-HCl, pH 9.0, 50 mM $MgCl_2$, 100 mM NaCl, 0.1% Tween-20, pH 9.0
NBT: 100 mg/ml in 70% dimethylformamide, stored in the dark
BCIP: 50 mg/ml in 100% dimethylformamide, stored in the dark
Staining solution: 80 µg/ml NBT, 175 µg/ml BCIP in APB
Bleaching solution: 5% formamide, 1.5% H_2O_2 in 0.5x SSC

WMISH was used to identify the endogenous temporal and special expression of RNA transcripts. WMISH was performed (Harland, 1991; Hollemann *et al.*, 1996) with minor modifications. For detection, digoxigenin-labeled antisense RNA was used, and visualized using an α-dig antibody coupled to alkaline phosphatase. All steps, if not otherwise indicated, were performed at room temperature with mild shaking.

2.2.2.9.1 Fixation and X-Gal staining

For the identification of the injected side of the embryos and to analyze the distribution of the injected material, embryos were co-injected with 75 pg β-gal mRNA. Embryos were fixed in MEMFA in small glass vials for 20 min, followed by washing three times with 1x PBS for 10 min. To visualize the β-gal distribution, X-Gal staining was performed (Hardcastle *et al.*, 2000). Embryos were incubated in X-Gal staining solution in the dark until the desired staining intensity (approx. between 20-30 min). Afterwards, the staining solution was removed and the embryos were washed three times with 1x PBS for 10 min each washing. Embryos were fixed in MEMFA for 25 min and then washed three times with 100% ethanol for 5 min. Embryos were stored at -20 °C in 100% ethanol.

2.2.2.9.2 Rehydration

The embryos were rehydrated by several washing steps in which ethanol was stepwise replaced by 1x PBS (75%, 50%, 25% ethanol). Following Rehydration, the embryos were washed four times with PTw for 5 min each washing.

2.2.2.9.3 Proteinase K treatment

To make the cells of the embryo accessible for the antisense RNA, the embryos were permeabilized by proteinase K treatment. The duration of the treatment was dependent on the developmental stage of the embryo. Stage 28 embryos were treated for 17 min in 2 ml proteinase K solution. The treatment was stopped by immediately proceeding with the acetylation.

2.2.2.9.4 Acetylation

Embryos were washes two times for 5 min with triethanolamine. To prevent nonspecific antisense RNA interaction, the embryos were acetylated by incubation with 25 µl acetic anhydride in 4 ml triethanolamine. The embryos were then washed two times for 5 min in PTw and refixed with PTw/FA for 20 min. The fixation solution was removed by washing the embryos five times for 5 minutes with PTw.

2.2.2.9.5 Hybridization reaction

Embryos were pre-hybridized in Hybridization mix for 5 h at 65 °C. Afterwards, the embryos were incubated with Hybridization mix containing the antisense RNA overnight at 65 °C.

2.2.2.9.6 Washings

On the next morning, embryos were washed three times with 2x SSC for 15 min at 60 °C. Non-hybridized antisense RNA was removed by RNase treatment for 60 min at 37 °C. The RNases were washed with 2x SSC for 10 min at RT followed by two 30 min washes with 0.2x SSC at 60 °C. For preparation of the AB reaction, the embryos were washed two times with MAB for 15 min at RT.

2.2.2.9.7 Antibody reaction

Before the antibody reaction, several blocking steps were performed by incubating the embryos for 20 min in MAB/BMB, followed by incubation for 40 min of with MAB/BMB/HS. Alkaline phosphatase-coupled anti-Dig antibody (1:5000 in MAB/BMB/HS, Sigma-Aldrich) was used for detection. The AB reaction took place overnight at 4 °C.

2.2.2.9.8 Staining reaction

On the next day, the embryos were washed at least five times for 10 min in MAB, followed by two washes with freshly made APB for 5 min at 4 °C. Afterwards, the embryos were stained in staining solution in the dark at 4 °C. The staining reaction typically took between one and five days.

2.2.2.9.9 Background removal and bleaching

To stop the staining reaction and to reduce the background staining, the embryos were washed in 100% methanol until the wash solution is not stained anymore. The methanol was the stepwise removed by washing in 75%, 50% and 25% methanol. The embryos were fixed in MEMFA for 30 min. To bleach the embryos, they were washed two times in 0.5x SSC and incubated in bleaching solution until the pigmentation was gone (typically between 1 and 4 h). The embryos were washes two times in 0.5x SSC and stored indefinitely in MEMFA.

2.2.3 Agarose gel electrophoresis

TAE (Tris-acetate-EDTA): 40 mM Tris-acetate, 2 mM EDTA, pH 8.5

Analysis of PCR products or DNA fragments was performed by agarose gel electrophoresis (Sharp *et al.*, 1973). Agarose gels were made by melting a final concentration of 1-2% (depending on the expected size of the fragments) agarose powder (Roth) in TAE buffer. TAE buffer was used as running buffer.

To determine the size of the DNA fragments, standard DNA ladders (Fast Ruler DNA ladder, Fermentas) were used. To visualize the DNA fragments, 30 µg (0.5 µg/ml) ethidium bromide was added to the agarose gel. For documentation, a ChemiDoc (Bio-Rad) chamber using an Intas camera and software was used.

2.2.4.1 PCR cloning

For cloning, template DNA was amplified via PCR with the High Fidelity enzyme mix (Thermo Scientific) in a total reaction volume of 50 µl reaction containing 1x High Fidelity Buffer with 15 mM $MgCl_2$, 0.2 mM of each dNTP (Thermo Scientific), 0.2 µM of each primer, 0.02 U High Fidelity PCR enzyme mix (Thermo Scientific) and 100 ng template DNA. PCR was done in a thermocycler using the following settings: 5 min at 95 °C, 45 s at 95 °C, 45 s at T_m of the primer -2 °C, 60 s/kb length 72 °C, 5 min 72 °C. Steps no 2-4 were repeated in a various number of cycles (~30-40 cycles) depending on the primer pairs used.

2.2.4.2 Gel purification of PCR and restriction fragments

PCR fragments from PCR or restriction reactions, were isolated on an agarose gel, the desired fragment was excised and the purified by using the “GFX PCR DNA and Gel Band Purification" kit (GE Healthcare) according to the manufacturer’s instruction.

2.2.4.3 DNA restriction digestion

Restriction digestion was performed using Fermentas Life Science restriction endonucleases according to manufacturer’s instructions.

2.2.4.4 Ligation

Standard ligation reactions were performed using a 20 µl reaction containing 1x T4 DNA Ligase buffer (Fermentas Life Science)., 1U T4 DNA ligases, 100

ng linear vector DNA and insert DNA in a 1:1 to 5:1 ratio. The ligation reaction was incubated overnight at 16 °C.

2.2.4.5 Chemical transformation of bacterial cells

Plasmid DNA was added to 100-200 µl thawed chemical competent cells, and incubated on ice for 30 min. Heat-shock was performed by incubating the cells for 60 s at 42°C for retransformation or 90 s at 42 °C for ligation reactions, followed by immediately cooling on ice for 3 min. Afterwards, 800 µl of LB medium was added to the cells, followed by incubation under constant shaking (300 rpm) for 30 min at 37°C for retransformation or 45 min at 37 °C for cloning. The cells were then centrifuged for 30 s at 10,000 rpm and 800 µl of LB-medium was removed. The cells were resuspended in the remaining medium and plated on a LB agar plate containing the selective antibiotic and incubated overnight at 37 °C.

2.2.4.6 Plasmid DNA preparation

Bacteria were cultured in 4 ml LB media together with the selective antibiotic overnight at 37 °C with shaking at 250 rpm. For mini plasmid preparation, 3 ml of the bacteria suspension was centrifuged for 2 min at 13,000 rpm. Plasmid DNA was isolated using the GeneJET Plasmid Miniprep kit (Fermentas) following manufacturer's instructions. For isolating preparative amounts (1 µg/µl) the NucleoBond Xtra Midi kit (Macherey-Nagel) was used according to the manufacturer's instruction. To quantify the concentration, 1 µl of the DNA was applied on the NanoDrop 2000c spectrophotometer (Thermo Scientific).

2.2.4.7 DNA sequencing

DNA sequencing was performed by "SEQLAB Sequence Laboratories Göttingen GmbH", according to the company's instructions using 1.2 µg of DNA for sequencing.

2.2.5 ATAC sequencing

Lysis buffer 10 mM Tris-HCl, pH 7.4, 10 mM NaCl, 3 mM $MgCl_2$, 0.1% Igepal CA-630, (can be stored at 4 °C for one week)

To identify open chromatin regions on the DNA, ATAC-sequencing was used. ATAC sequencing was performed after (Buenrostro *et al.*, 2013) with modifications. For each sample 40 animal caps previously frozen in liquid N_2 and stored at -80 °C were used.

2.2.5.1 Transposition reaction

Animal caps were carefully lysed in 100 µl fresh ATAC-lysis buffer using a pestle, followed by centrifugation for 5 min at 2000 rpm at 4 °C. The supernatant was removed and the nuclei pellet resuspended on ice in a 50 µl transposition solution containing 2x TD reaction buffer (Nextera DNA Library Prep kit, Illumina), 2.5 µl TDE1 (Nextera DNA Library Prep kit, Illumina) and incubated for 30 min at 37 °C. The transposition reaction was immediately stopped by purifying the DNA using the NucleoSpin GeI and PCR Clean-up kit (Macherey-Nagel) according to the manufacturer's instructions. The DNA was eluted in 10 µl Elution buffer (10 µM Tris-HCl, pH 8).

2.2.5.2 Library preparation

Transposed DNA (10 µl) was added to a total 50 µl reaction mix containing 1.25 µM PCR primer1 (Illumina), 1.25 µM barcoded PCR primer2 (Illumina) and NEBNext High-Fidelity PCR Master mix. The samples were first amplified in the thermocycler using the following program: 5 min at 72 °C, 30 s at 98 °C, followed by 5 cycles of 10 s at 98 °C, 30 s at 63 °C and 1 min at 72 °C. Afterwards, the appropriate number of PCR cycles was determined using qPCR by combining 5 µl of the previously amplified DNA with a 10 µl reaction containing, 1.25 µM PCR primer 1, 1.25 µM PCR primer 2, 1x SYBR Green I and 1x NEBNext High-Fidelity PCR Master Mix. The qPCR was performed using a CFX96^{TM} Real-Time System (Bio-Rad) with the following program (30

s at 98 °C, followed by 20 cycles of 10 s at 98 °C, 30 s at 63 °C and 1 min at 72 °C). Afterwards, the remaining 45 µl PCR reaction was further amplified by 30 s at 98 °C, followed by a custom number of PCR cycles (10 s at 98 °C, 30 s at 63 °C and 1 min at 72 °C), where the number of remaining PCR cycles is the number of cycles that corresponded to one-third of maximum fluorescent intensity in the qPCR. The quality of the library was checked using the Bioanalyzer 2000c (Agilent).

Sample	Number of PCR cycles
CC 3 h replicate 1	10x
Ptf1a 3 h replicate 1	7x
CC 12 h replicate 1	16x
Ptf1a 12 h replicate 1	12x
CC 3h replicate 2	14x
Ptf1a 3 h replicate 2	16x
CC 12 h replicate 2	16x
Ptf1a 12 h replicate 2	12x

Table 2.6 List of PCR cycles for each ATAC sample

2.2.5.3 Sequencing (by TAL)

Sequencing was performed by the University Medical Center Göttingen (UMG) -Transcriptome and Genome Analysis Laboratory (TAL) with the HiSeq 2500 in the 50 bp paired end mode, with a density of 150,000,000 reads. Two biological replicates were used for each reaction. Sequencing quality was analyzed using the FastQ software (http://www.bioinformatics.babraham.ac.uk/projects/fastqc/).

2.2.5.4 Sequencing alignment and processing (performed by TAL)

The sequence reads were aligned to the *X. laevis* genome (J-strain v 9.2) (Bowes *et al.*, 2007). Mapping was performed using Bowtie2 (version 2.5) (Langmead and Salzberg, 2012). For processing and filtering of the data SAMtools (version 1.1) (Li *et al.*, 2009) was used. Picard (version 1.126) was

then used to calculate the number and percentage of duplicates. The filtered BAM file was converted into a tagAlign file containing the genomic coordinates of each read using Bedtools (v2.20.1) (Quinlan and Hall, 2010).

Peaks were called using MACS2 (version 2.1.1.20160309) (Feng *et al.*, 2012) using smoothing window 150 and p-value threshold of 0.01 for calling peaks. Peaks were merged a differential peak analysis was done using the DESeq2 package (version 1.16.1) (Love *et al.*, 2014) within the R/Bioconductor environment (www.bioconductor.org). Peaks determined as significantly enriched were those with adjusted p-value < 0.1.

2.2.6 Gene expression analysis by semiquantitative RT-PCR or quantitative Nanostring analysis

2.2.6.1 Total RNA isolation from ectodermal explants and whole embryos

X. laevis embryos (5) or ectodermal explants (50) were fixed in liquid nitrogen and stored at 80 °C. The animal caps or embryos were then lysed in 400 µl preqGOLD TriFast reagent (Preqlab) using a 29-gauge syringe and incubated at room temperature for 10 min. During that time, they were vortexed for 30 s. Afterwards, 80 µl of chloroform (Roth) was added followed by vortexing for 30 s and 10 min centrifugation at 13,000 rpm at 4 °C. The upper phase (200 µl) was transferred into a new eppendorf tube and then mixed with 1 volume (200 µl) chloroform by vortexing for 30 s. After centrifugation for 5 min at 13,000 rpm and 4 °C, the upper phase (200 µl) was transferred into a new eppendorf tube and 1 volume of 2-propanol was added. After mixing, precipitation took place at -20 °C for at least 2 h. Afterwards, the precipitated RNA was centrifuged for 30 min at 4 °C. The supernatant was removed and the pellet was washed with 400 µl 75% ethanol. The air-dried pellet was dissolved in 12.5 µl RNase-free water and DNase digest using 0,75 U DNase I (Thermo Scientific) was performed for 1.5 h at 37 °C. DNase activity was stopped by incubation at 70 °C for 10 min. The RNA concentration was determined on the NanoDrop 2000c spectrophotometer (Thermo Scientific). To check for genomic DNA contamination, a control PCR with 100 ng RNA using primer for

the housekeeping gene *ornithine decarboxylase* (*odc*) was performed and analyzed on a 2% agarose gel.

2.2.6.2.1 Reverse transcription

To synthesize 10 µl cDNA, 100 ng of total RNA was used in a reaction mix containing 1x Go Taq flexi buffer (Promega), 5 mM $MgCl_2$ (Fermentas), 2.5 mM random hexamer (Invitrogen), 1 mM dNTP mix (Thermo Scientific), 0,16 U Ribolock RNase inhibitor (Thermo Scientific), and 0,8 U MulV reverse transcriptase (Roche). The reaction took place in a thermocycler (Biometra) using the following program: 20 min at 20 °C, 1 h at 42 °C, 5 min at 95 °C.

2.2.6.2.2 Reverse transcription-PCR (RT-PCR)

Semiquantitative RT-PCR was performed using a total volume of 12.5 µl containing 1x GoTaq green reaction buffer (Promega), 0.2 µM of both forward and reverse primer and 0.5 units GoTaq DNA polymerase (Promega). For each reaction 2.5 µl cDNA was used as a template for PCR. Amplification took place in a thermocycler (Biometra) using the following program: 2 min at 95 °C, 45 s at 95 °C, 45 s at T_m of the primer -2 °C, 45 s at 72 °C, 5 min at 72 °C. Steps no 2-4 were repeated in a various number of cycles (~25-35 cycles), which is dependent on the specific primer pairs, before proceeding with step 5. RT-PCR reactions were analyzed on a 2% agarose gel as described above.

2.2.6.3 Quantitative Nanostring analysis

Quantitative analysis was performed using 700 ng of total RNA on the Nanostring digital multiplexed expression analysis system. The analyzed genes as well as the target region are shown in the appendix. Data analysis was performed by using the nSolver software (version 2.5). For normalization, the counts were first normalized to the mean of the positive control counts. Afterwards, the counts were normalized for the geometric mean of the housekeeping genes *odc*, *rplp0* and *ppi1l*. If several developmental stages were analyzed at the same time, normalization was performed to the geometric

mean of the housekeeping gene *ppi1l* only. Background subtraction was performed by subtracting the mean value and two times the standard deviation of the eight negative control counts for each lane. Negative values were set to 1. Data from three independent experiments (A, B and C) were analyzed.

2.2.7 RNA sequencing

2.2.7.1 RNA isolation

RNA isolation for RNA sequencing was performed similar to isolating RNA for RT-PCR with the following adjustments to the protocol:

RNA from 50 animal caps was extracted as described above until the first step of precipitation with isopropanol. Afterwards, the precipitated RNA was centrifuged for 30 min at 4 °C. The supernatant was removed and the pellet was washed with 400 µl 75% ethanol. The air-dried pellet was dissolved in 47 µl RNase-free water. DNA digest was performed by incubating the isolated RNA for 1 h at 37 °C in a 50 µl total reaction volume containing 1x DNase I reaction buffer (Thermo Scientific), 1 U DNase I (Thermo Scientific) and 0.4 U RNase inhibitor (Thermo Scientific). DNA digest was stopped by the addition of 150 µl RNase-free water. Phenol-chloroform-isoamylalcohol (Roth) (200 µl) was added and the samples were vortexed for 30 s, followed by 10 min centrifugation at 13,000 rpm at 4 °C. To the upper phase (200 µl), 1 volume (200 µl) of chloroform-isoamylalcohol (ratio 24:1) was added. After vortexing for 30 s, the samples were centrifuged for 5 min at 13,000 rpm and 4 °C. 1/10 volume (20 µl) ammonium acetate and 1 volume (200 µl) 2-propanol were added and incubated for at least 2 h at -20 °C. The precipitate was centrifuged for 30 min at 13,000 rpm at 4 °C and then washed by 400 µl of 75% ethanol. The RNA pellet was then dissolved in 20 µl RNase-free water. To check for genomic DNA contamination, a control PCR with 100 ng RNA using oligonucleotides for housekeeping gene *ornithine decarboxylase* (*odc*) was performed and analyzed on a 2% agarose gel. RNA quality was checked by use of the 2100 Bioanalyzer (Aglient).

2.2.7.2 Sample preparation and sequencing

Library preparation and sequencing was performed by the University Medical Center Göttingen (UMG) - Transcriptome and Genome Analysis Laboratory (TAL). Libraries were prepared with the TruSeq RNA Sample Prep Kit v2 (Illumina) following the manufacturer's instructions. Sequencing was performed with the HiSeq 2500 in the 50 bp single end mode. Two or three biological replicates were used for each reaction. Sequencing quality was analyzed using the FastQ software (http://www.bioinformatics.babraham.ac.uk/projects/fastqc/).

2.2.7.3 Sequencing alignment (performed by TAL)

The sequence reads were aligned to the *X. laevis* genome (J-strain v 9.2) (Bowes *et al.*, 2007). Mapping was performed using the software the STAR alignment software (ver. 2.5) (Dobin *et al.*, 2013).

2.2.7.4 Statistical analysis (performed by TAL)

Normalization of the library samples and the differential gene analysis was performed using the DESeq2 package (version 1.16.1) (Love *et al.*, 2014) within the R/Bioconductor environment (www.bioconductor.org). Candidate genes had a two-fold change induction compared to control samples and a FDR-corrected p-value of <0.05.

3. Results

3.1 Mutation of a single threonine residue in the Ptf1a C2 domain is sufficient to induce a mixed induced neuronal transmitter phenotype

Similar to many bHLH proteins, Ptf1a contains multiple S/T-P residues, which are putative targets of cdk-dependent phosphorylation (Ubersax and Ferrell, 2006; Richts, 2013). Preventing of phosphorylation at those sites through mutation in Neurog2 leads to an increase in activation of the pan-neuronal marker *tubb2b* (Ali *et al.*, 2011). To evaluate the role of such phosphorylation sites in Ptf1a activity, a mutant of the mouse Ptf1a in which all eight serine and threonine residues were mutated to alanine (mPtf1a$^{8S/T\rightarrow A}$) was evaluated in gain of function studies using pluripotent *X. laevis* embryonic cells (animal cap explants) in comparison to the wild-type Ptf1a. In contrast to Neurog2, no increase in neuronal-inducing activity of by the Ptf1a$^{8S/T\rightarrow A}$ mutant was observed. However, in addition to its ability to induce markers for a GABAergic cell fate, the Ptf1a$^{8S/T\rightarrow A}$ mutant also induced the glutamatergic marker gene *tlx3*, a gene that is normally repressed by Ptf1a (Richts, 2013). Mutating the alanine residue at position 299 back to threonine (mPtf1a$^{7S\rightarrow A}$) abolished the *tlx3* induction (Richts, 2013), suggesting that the mutation of the T_{299} was responsible for this mixed neuronal transmitter phenotype activity (Richts, 2013).

To investigate if the mixed neuronal subtypes activity of the Ptf1a threonine mutant is conserved and is indeed sufficient to induce a mixed neuronal phenotype, the *X. laevis* variant (Ptf1a^{T243A}) of the mouse Ptf1a^{T299A} was created (Fig. 3.1A and B). The activity of this construct was compared with the wild-type Ptf1a, which promotes GABAergic markers and represses glutamatergic markers, as well as with the Rbpj-binding deficient mutant (Ptf1a$^{W224A/W242A}$), which promotes a glutamatergic fate (Fig. 3.1A and B) (Hedderich, 2008; Hori *et al.*, 2008; Hedderich, 2012; Hanotel *et al.*, 2014) as the mutated threonine residue in the Ptf1a^{T243A} mutant is directly adjacent to the Rbpj binding tryptophan residue within the Ptf1a C2 domain (Fig. 3.1B) The wild-type and mutated versions of Ptf1a were fused to the ligand binding

domain of the glucocorticoid receptor (GR) (Gammill and Sive, 1997) to allow control over protein activity. In one blastomere at the two-cell, 20 pg mRNA encoding the Ptf1a-fusion proteins was injected together with 75 pg of *β-galactosidase* mRNA to allow identification of the injected side of the embryo. The protein activity was induced via dexamethasone treatment at gastrula stage (stage 10.5) and at tailbud stage (stage 28), embryos were collected and whole mount in-situ hybridization against the pan-neuronal marker *tubb2b*, the GABAergic marker *gad1a*, and the glutamatergic marker *tlx3* performed.

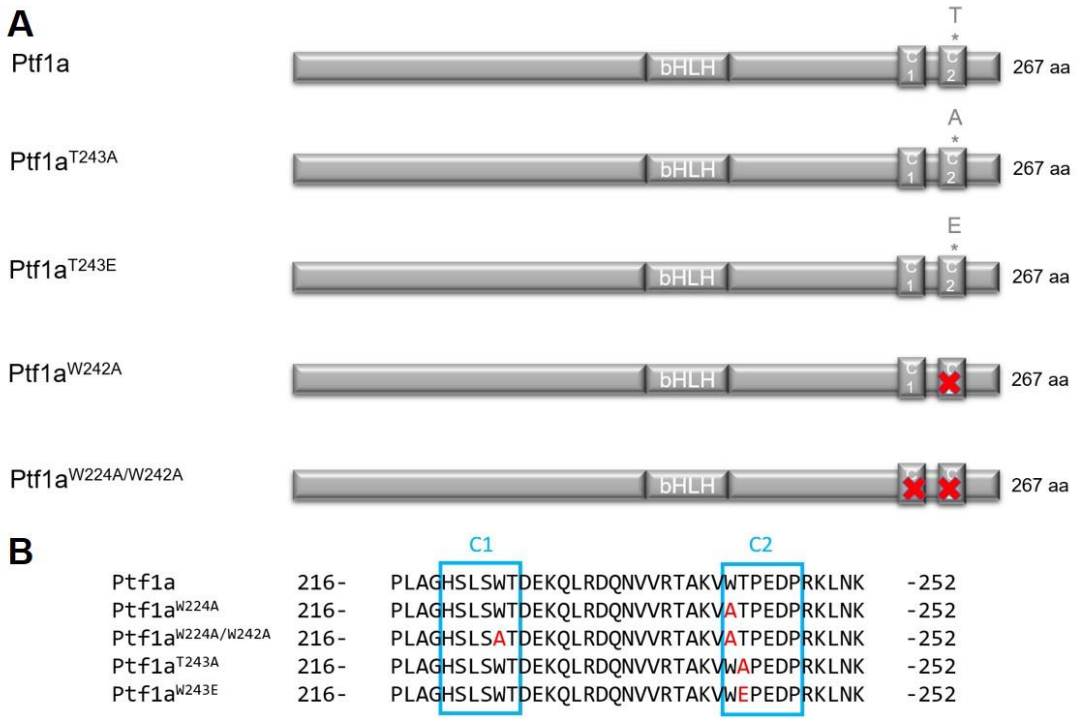

Figure 3.1: Overview *X. laevis* Ptf1a mutants

(A) Schematic overview over the Ptf1a constructs used for overexpression studies. Grey asterisks highlight the position of a mutated T-P site in the Ptf1a C2 domain. Red crosses indicate a mutation in a conserved Rbpj binding site. (B) Alignment of the highly conserved Ptf1a C1 and C2 domains of all Ptf1a constructs. The C1 and C2 domain are highlighted in blue, mutated residues are highlighted in red.

As shown in Figure 3.2B and consistent with previous reports, overexpression of wild-type Ptf1a promotes ectopic expression of *tubb2b* and *gad1a*, while *tlx3* expression was suppressed. Ptf1a$^{W224A/W242A}$ also induces ectopic expression of *tubb2b*, but these ectopic neurons express *tlx3* (Hedderich, 2008; Hedderich, 2012).

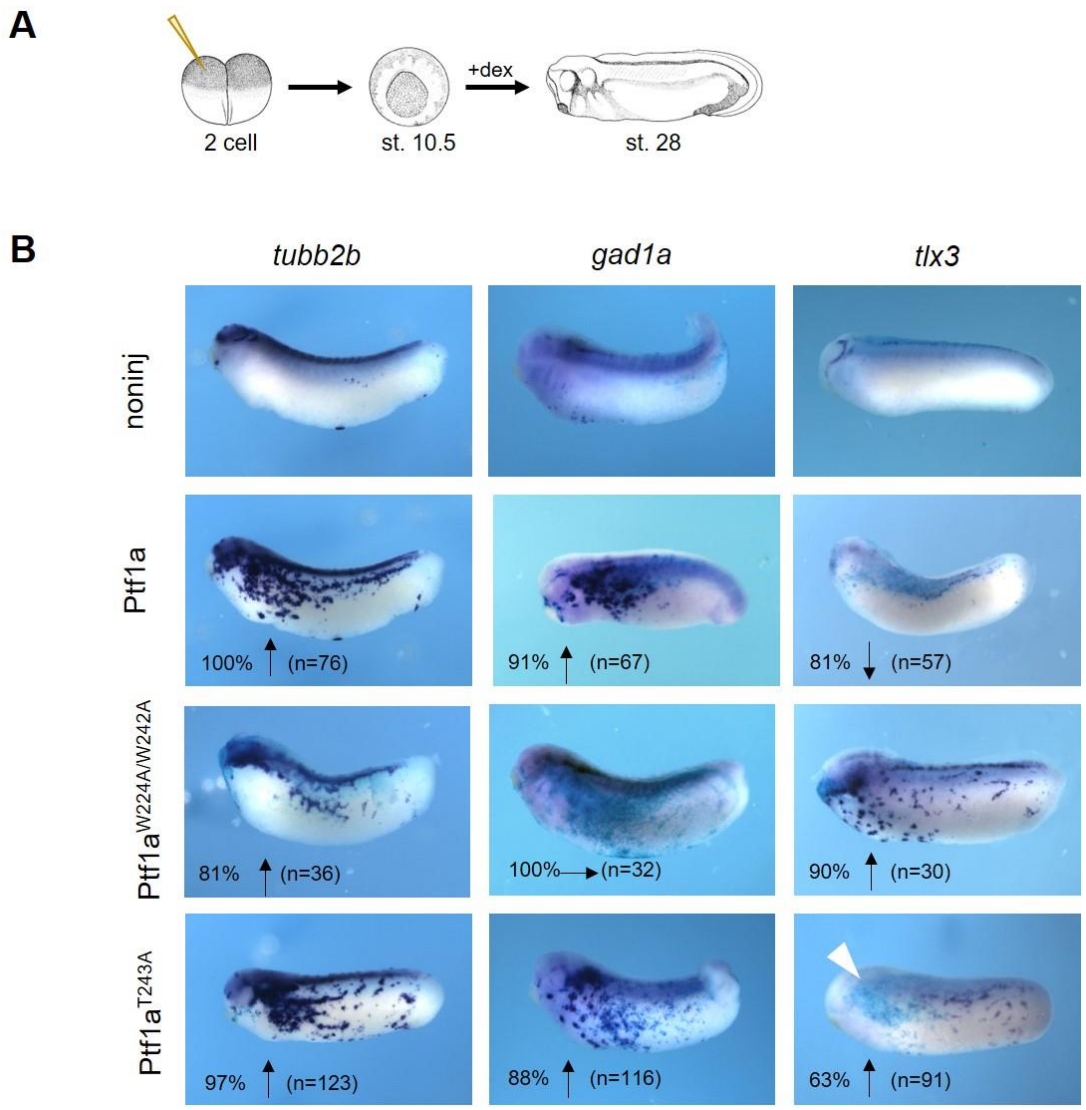

Figure 3.2: Ptf1a^{T243A} mutant induces a mixed neuronal transmitter phenotype in embryos

(A) Experimental procedure: 20 pg of *ptf1a-GR*, *ptf1a*$^{W224A/W242A}$-GR or *ptf1a*^{T243A}*-GR* mRNA were injected in one animal blastomere at two-cell stage. For recognition of the injected side *β-galactosidase* RNA was co-injected. Protein activity was induced by addition of dexamethasone at stage 10.5. Embryos were collected for WMISH at stage 28. (B) Overview of WMISH for neuronal differentiation (*tubb2b*), GABAergic (*gad1a)* or glutamatergic (*tlx3*) cell fate of embryos overexpressing Ptf1a-GR, Ptf1a$^{W224A/W242A}$-GR or Ptf1a^{T243A}-GR. Shown is the injected side of the embryo. For comparison non-injected embryos were shown at the top. Percentages refer to the total number of embryos showing the shown phenotype in relation to the total numbers of embryos showing β-gal expression (n). Black arrows refer to the induced phenotype (upregulation, downregulation or not affected). White arrowhead highlights the area of downregulation of endogenous *tlx3* expression by the Ptf1a^{T243A} mutant.

In contrast, overexpression of Ptf1a^{T243A} leads to an activation of all three markers, supporting our previous observations with the mouse Ptf1a^{T299A} mutant. Interestingly, overexpression of Ptf1a^{T243A} still results in a repression

of the endogenous *tlx3* expression on the injected side of the embryo. However, ectopic *tlx3* expression is now observed (Fig3.2B).

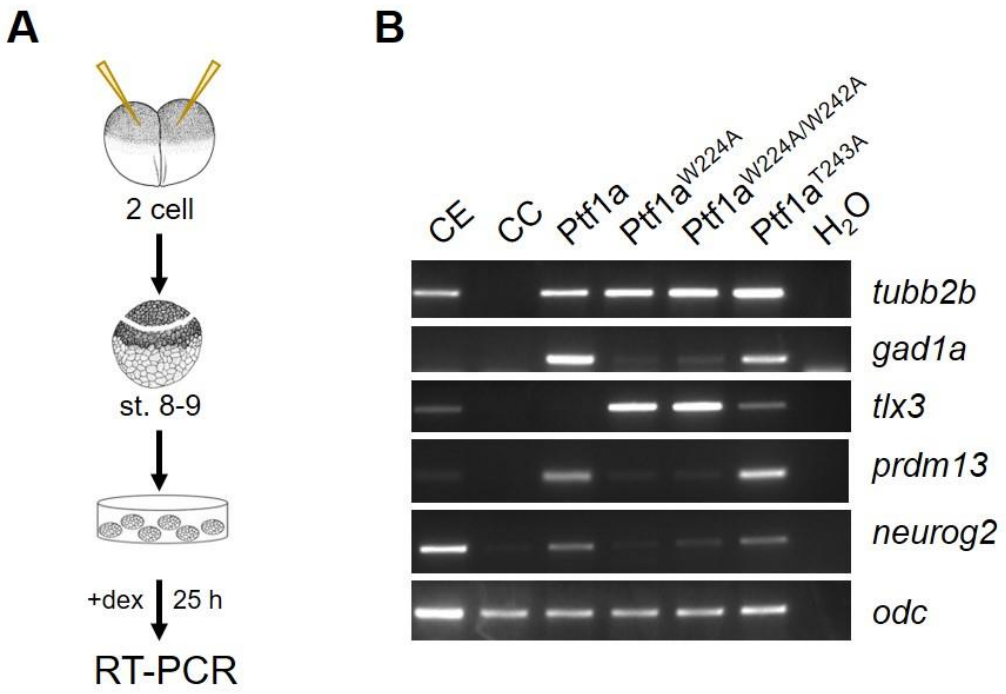

Figure 3.3 Ptf1a^{T243A} mutant induces a mixed neuronal transmitter phenotype in ectopic explants

(A) Experimental procedure: 20 pg of *ptf1a-GR*, *ptf1a^{W42A}-GR*, *ptf1a$^{W224A/W242A}$-GR* or *ptf1a^{T243A}-GR* mRNA were injected in animally in both blastomeres of two-cell stage embryos. At blastula stage, animal caps were excised and protein activity induced by dexamethasone treatment for 25 h. (B) RT-PCR analysis against markers for neuronal differentiation (*tubb2b*), GABAergic (*gad1a)* or glutamatergic (*tlx3*) cell fate, as well as two target genes for the trimeric Ptf1a complex (*prdm13, neurog2*). The housekeeping gene *odc* was used as a loading control. As additional controls, cDNA from total RNA isolations of noninjected control caps (CC) and non-injected control embryos (of the same developmental stage) were analyzed.

As the mutated threonine residue in the Ptf1a^{T243A} mutant is located adjacent to a known Rbpj binding site (Beres *et al.*, 2006) in the Ptf1a C2 domain (Fig. 3.1B), a comparison of the overexpression phenotype between the Ptf1a^{T243A} and the Ptf1a^{W242A} mutants was performed by injection 20 pg of *ptf1a-GR*, *ptf1a^{W242A}-GR ptf1a$^{W224A/W242A}$-GR* or *ptf1a^{T243A}-GR* mRNA in the animal hemisphere of both blastomeres at two-cell stage. At blastula stage, the animal caps were excised and cultured for 25 h in the presence of dexamethasone to induce protein activity. Afterwards, RNA was isolated and semi-quantitative

RT-PCR was performed against *tubb2b*, *tlx3* and *gad1a* expression (Fig. 3.3A). As expected, overexpression of all four constructs promotes neuronal differentiation as shown by the increase in *tubb2b* expression (Fig. 3.3B). While the wild-type Ptf1a leads to an induction of *gad1a*, but not *tlx3*, the Ptf1a$^{W224A/W242A}$ and Ptf1a^{W242A} mutants strongly induce *tlx3* but not *gad1a*. In contrast, overexpression of Ptf1a^{T243A} induces both *gad1a* and *tlx3* (Fig. 3.3B), indicating that the phenotype is specific for the mutation in the T_{243} residue.

To better understand the differential gene induction by the wild-type Ptf1a and Ptf1a mutants, either *ptf1a-GR*, *ptf1a$^{W224A/W242A}$-GR*, or *ptf1a^{T243A}-GR* mRNA (20 pg) were injected in the animal hemispheres of both blastomeres of two-cell stage *X. laevis* embryos. At blastula stage, the animal caps were excised and cultured in the presence of dexamethasone for 25 h to induce the protein activity. Afterwards, RNA was isolated and quantitative Nanostring analysis was performed using a codeset containing known Ptf1a dimeric and trimeric target genes, as well as markers of neuronal differentiation and subtype specification (Fig. 3.4A).

All three Ptf1a constructs were able to upregulate markers for pan-neuronal differentiation such as *tubb2b, myt1, ebf2* or *dll1.* (Fig. 3.4C-E; Table S1). Consistent with previous observations, the wild-type Ptf1a but not Rbpj-binding deficient mutant (Ptf1a$^{W224A/W242A}$), upregulated genes associated with the development of a GABAergic cell fate such as *gad1a* and *prdm13*, while Ptf1a$^{W224A/W242A}$ strongly upregulated *tlx3* expression, which was not activated by the wild-type Ptf1a (Fig. 3.4F-H). As previously demonstrated, the Ptf1a^{T243A} mutant upregulated markers associated with a GABAergic cell fate such as *gad1a, prdm13, slc32a1* and *pax2* as well as *tlx3* expression (Fig. 3.4F-H; TableS1). Comparing the expression levels induced by the different Ptf1a constructs showed that the strength of induction by the Ptf1a^{T243A} mutant of GABAergic marker genes such as *prdm13* and *gad1a* was lower than for the wild-type Ptf1a (Fig. 3.4G, H). Moreover, the induction of *tlx3* expression was weaker than that induced by Ptf1a$^{W224A/W242A}$ (Fig. 3.4F), highlighting the mixed identity of the Ptf1a^{T243A} mutant. Interestingly, the levels of activation of genes (e.g. *tubb2b, ebf2, myt1, dll1*) induced by Ptf1a and Ptf1a$^{W224A/W242A}$ differed (Fig. 3.4C-E, Table S1). Those markers showed a weaker induction by the

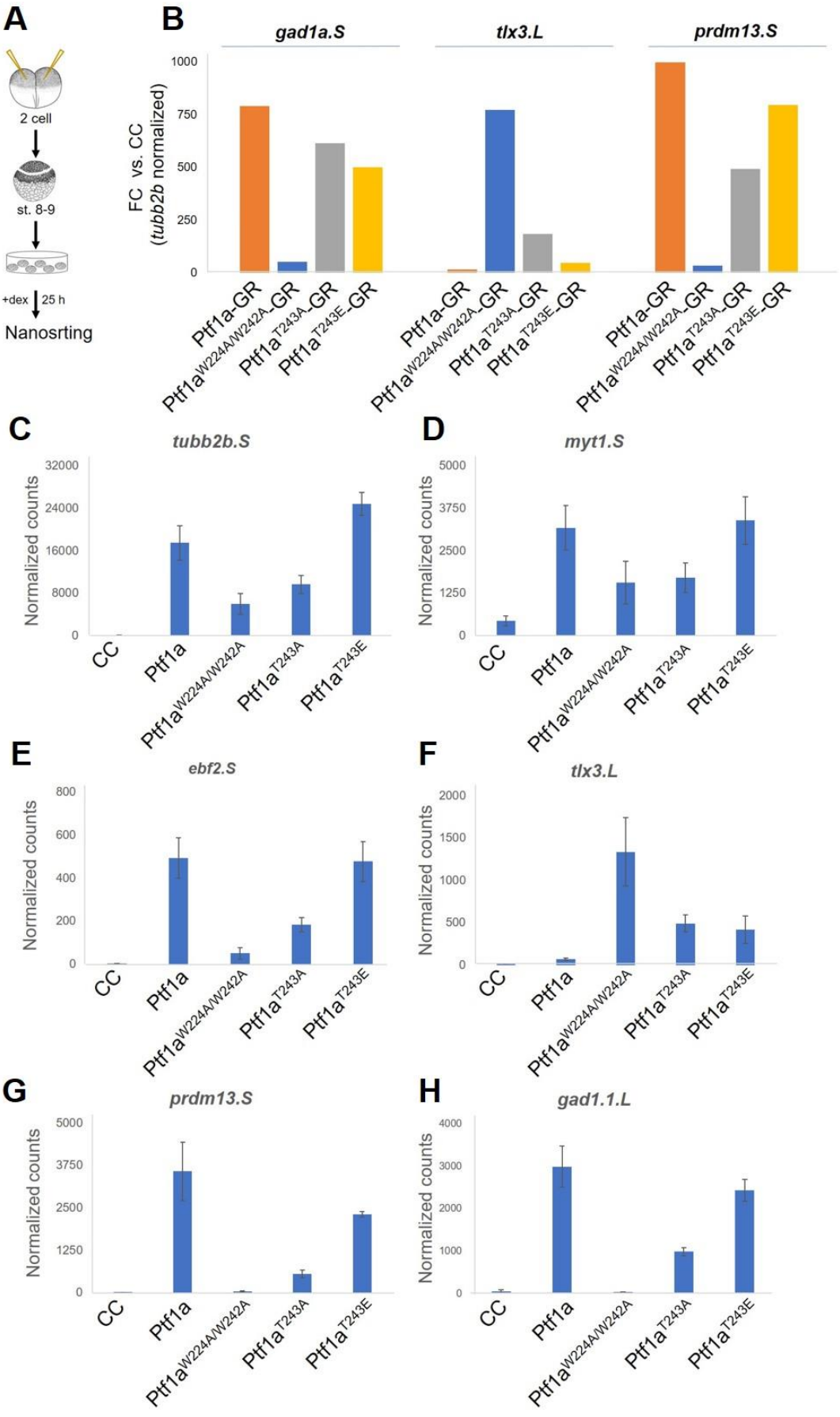
A
2 cell
st. 8-9
+dex
25 h
Nanosrting
B
gad1a.S
tlx3.L
prdm13.S
FC vs. CC (tubb2b normalized)
1000
750
500
250
0
Ptf1a-GR
Ptf1a W224A/W242A-GR
Ptf1a T243A-GR
Ptf1a T243E-GR
C
tubb2b.S
Normalized counts
32000
24000
16000
8000
0
CC
Ptf1a
Ptf1a W224A/W242A
Ptf1a T243A
Ptf1a T243E
D
myt1.S
5000
3750
2500
1250
E
ebf2.S
800
600
400
200
F
tlx3.L
2000
1500
1000
500
G
prdm13.S
H
gad1.1.L
4000
3000
2000
1000

Figure 3.4: Activities of distinct Ptf1aT$_{243}$ mutants

(A) Experimental procedure: 20 pg of *ptf1a-GR*, *ptf1a*^{T243E}*-GR*, *ptf1a*$^{W224A/W242A}$*-GR* or *ptf1a*^{T243A}*-GR* mRNA were injected in both animal blastomeres of two-cell stage. At blastula stage, animal caps were excised. Protein activity was induced by dexamethasone treatment for 25 h. (B) Shown is the average fold-change induction over non-injected control caps from three individual replicates. Data were normalized for the induction of *tubb2b*. The gene analyzed can be found on the x-axis (C-H) Results of the quantitative Nanostring analysis. Shown are the average expression levels of marker genes from three biological replicates. Error bars refer to the standard error of the mean. Data were normalized for the three housekeeping genes *odc, ppi1l* and *rplp0*. .S and .L refer to the corresponding *X. laevis* homeolog targeted by the Nanostring probe. Note the different scales in each diagram.

Ptf1a$^{W224A/W242A}$ and the Ptf1a^{T243A} mutants, compared to the wild-type Ptf1a. These differences between versions of Ptf1a constructs were detected consistently in all three replicates (Table S2). To exclude that the differences in the induction of subtype specific marker genes *gad1a* and *tlx3* had their cause in a different efficiency of neuronal differentiation, the Nanostring data were normalized for *tubb2b* and the fold-change induction by wild-type and mutant Ptf1a compared to non-injected control caps. Considering the *tubb2b* levels, the differences in the induction of *gad1a* between Ptf1a and Ptf1a^{T243A} was lower, but still significant. Moreover, normalization to *tubb2b* did not alter the observed gene induction by the different Ptf1a constructs, as *gad1a* was still induced by Ptf1a and Ptf1a^{T243A} but not by Ptf1a$^{W224A/W242A}$, while *tlx3* expression was only induced by Ptf1a$^{W224A/W242A}$ and Ptf1a^{T243A} (Fig. 3.4B).

3.2 Introducing a negative charge at the Ptf1aT$_{243}$ residue induces a more wildtype Ptf1a like phenotype

As the mutated threonine residue in the Ptf1a^{T243A} is a putative target of cell cycle dependent phosphorylation, a phosphomimic mutant was created in which threonine 243 was exchanged for glutamate (Ptf1a^{T243E}-GR) and analyzed in analogous gain of function assays (Fig. 3.1).

Similar to the wild-type Ptf1a and the Ptf1a mutants, the Ptf1a^{T243E} mutant induced pan-neuronal differentiation markers (*myt1, zc3h12c, tubb2b, ebf2, dll1*), but the strength of induction was similar to the wild-type Ptf1a with the

other mutants inducing a much lower induction (Fig. 3.4, Table S1). In addition, the strength of the GABAergic markers genes (*gad1a* and *prdm13)* upregulation was much stronger for the phosphomimetic Ptf1a^{T243E}, compared to the phosphorylation-null mutant (Ptf1a^{T243A}), further indicating this mutant behaved more like the wild-type Ptf1a (Fig. 3.4G, H). However, both Ptf1a^{T243E} and Ptf1a^{T243A} induced similar levels of the glutamatergic selector gene *tlx3* (Fig. 3.4F). To identify if the more wild-type like activity of Ptf1a^{T243E} is only the result of its stronger neuronal differentiation promoting activity compared to Ptf1a^{T243A}, *gad1a* and *tlx3* activation by those two constructs was investigated after normalization to *tubb2b* expression. Although the expression levels of *gad1a* were very similar after *tubb2b* normalization, expression of other markers for a GABAergic lineage such as *prdm13* (Fig3.4B; Table S1) were stronger activated by Ptf1a^{T243E} than by Ptf1a^{T243A}, while the glutamatergic markers *tlx3* and *slc17a7* induction was stronger by Ptf1a^{T243A} (Fig. 3.4B; Table S1). Altogether these results indicate that although Ptf1a^{T243E}-GR is still inducing a mixed neuronal transmitter phenotype, this mutant behaved more like the wild-type Ptf1a.

3.3 The mixed neuronal transmitter phenotype induced by Ptf1a^{T243A} is not the result of an impaired interaction with Rbpj

As the interaction with Rbpj is essential for promoting a GABAergic cell fate and suppression of a glutamatergic cell fate, the mixed neuronal transmitter phenotype by Ptf1a^{T243A} might be the result of an impairment of Rbpj interaction (Hori *et al.*, 2008; Hanotel *et al.*, 2014). Therefore, to study the binding of Rbpj and Ptf1a in vivo, a biomolecular fluorescence complementation assay (BiFC) was performed (Fig. 3.5A). Towards this end, constructs were created in which Ptf1a, Ptf1a$^{W224A/242A}$ or Ptf1a^{T243A} were fused to the N-terminus of Venus EYFP (Ptf1a-Vn, Ptf1a$^{W224A/W242A}$-Vn, Ptf1a^{T243A}-Vn) as well as a construct in which the C-terminal fragment of Venus EYFP was fused to Rbpj. As a positive control, the C-terminal fragment of Venus EYFP was fused to the ubiquitously expressed class A bHLH protein E12. For BiFC, 500 pg of *ptf1a-Vn*, *ptf1a$^{W224A/W242A}$-Vn* or *ptf1a^{T243A}-Vn* mRNA was co-

injected together with 500 pg *rbpj-Vc* or *e12-Vc* mRNA animally in both blastomeres of two-cell stage *X. laevis* embryos. To identify injected cells, 100 pg *mRFP* mRNA was also co-injected. At blastula stage, the embryos were dissociated to single cells and imaged (Fig. 3.5B).

All three Ptf1a-Vn constructs, when co-injected with E12-Vc, showed a strong nuclear BIFC signal, demonstrating their universal ability to form heterodimers with E12 (Fig. 3.5C and D). A nuclear BiFC signal could be detected in 49% of RFP positive cells expressing Rbpj-Vc together with Ptf1a-Vn but not with Ptf1a$^{W224A/W242A}$-Vn (Fig. 3.5 C, D). This recapitulates previous results indicating the importance of these two tryptophan residues in the C-terminus of Ptf1a for the interaction with Rbpj and demonstrates the functionality of the BiFC assay (Beres *et al.*, 2006; Hori *et al.*, 2008). In contrast to Ptf1a$^{W224A/W242A}$-Vn, a strong nuclear BiFC signal was observed between Rbpj-Vc and Ptf1a^{T243A}-Vn (Fig. 3.5C and D), demonstrating that the mutation in the threonine does not significantly alter binding to Rbpj.

Altogether, those data show that the induced mixed neuronal transmitter phenotype by Ptf1a^{T243A} is not the result of an impaired interaction with Rbpj, suggesting that another mechanism is responsible for the induced neuronal transmitter phenotype.

3.4 Ptf1aT$_{243}$ mutants strongly bind to Prdm13

Ptf1a suppressed a glutamatergic cell fate through the direct activation of Prdm13, which in turn inhibits the expression of the glutamatergic selector gene *tlx3* (Chang *et al.*, 2013; Borromeo *et al.*, 2014; Hanotel *et al.*, 2014). Furthermore, it has been shown that Prdm13 directly binds to the *tlx3* regulatory regions and suppress *tlx3* expression in mouse in a mechanism that involves direct binding to the DNA by Prdm13, as well as recruitment to the promoter of *tlx3* by the bHLH transcription factor Ascl1 (Chang *et al.*, 2013). Interestingly, overexpression of Ptf1a^{T243A} in *X. laevis* ectodermal explants induces *prdm13* expression as well as the expression of *tlx3*, which would somehow contradict the previous studies demonstrating that in the presence

of Prdm13, *tlx3* expression is inhibited. In subpopulations of *prdm13*-expressing cells, Prdm13 represses its own activator, Ptf1a, through directly

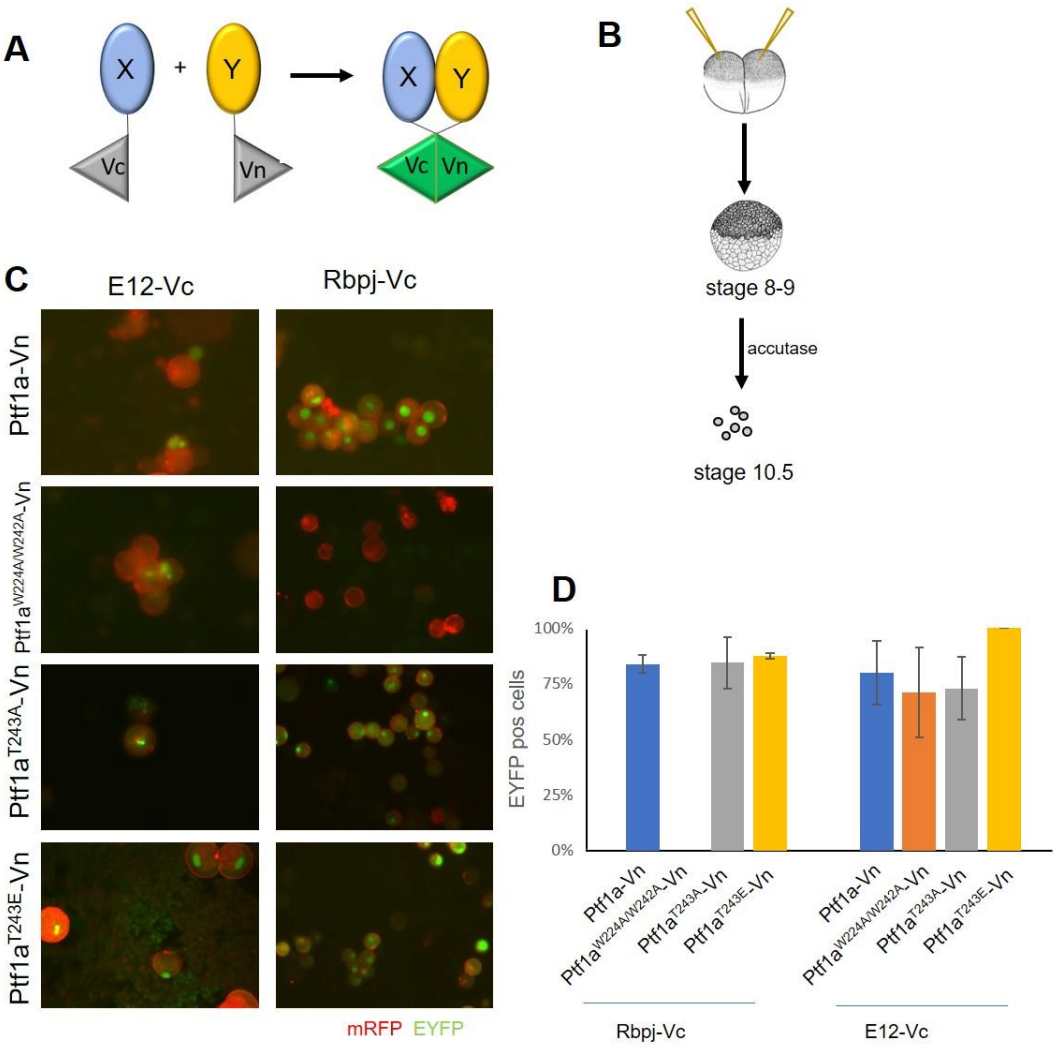

Figure 3.5: Ptf1a^{T243A} mutation does not affect its ability to bind Rbpj

(A) Overview bimolecular fluorescence complementation assay (BiFC). Proteins were fused to the N- or C-terminus of Venus-EYFP. Interaction of proteins of X and Y will lead to the formation of a complete EYFP, which can be detected by its fluorescence. (B) Experimental procedure: 500 pg of *ptf1a-Vn*, *ptf1a^{T243E}-Vn*, *ptf1a$^{W224A/W242A}$-Vn* or *ptf1a^{T243A}-Vn* mRNA were co-injected with 500 pg of either *rbpj-Vc* or *e12-Vc* mRNA and with 100 pg of *mRFP* mRNA in both animal blastomeres of two-cell stage. At blastula stage, cells were dissociated by the use of accutase and analyzed for fluorescence. (C) Results of the BiFC analysis. On the top, the injected construct carrying the c-terminal Venus EYFP is shown. The corresponding N-terminal Venus EYFP construct is shown on the left. Red fluorescence indicated injected cells due to the expression of mRFP, green fluorescence is the corresponding YFP signal. (D) Quantification of the BiFC analysis. The given numbers and ratios all refer to the total amount of mRFP positive cells that have been analyzed. Error bars refer to the standard error of the mean.

binding Ptf1a and inhibiting its positive autoregulation (Bessodes *et al.*, 2017; Mona *et al.*, 2017). Interestingly, in the *X. laevis* retina, those cells where Prdm13 inhibits *ptf1a* will later gain a glycinergic instead of GABAergic cell fate (Bessodes *et al.*, 2017). Considering the outcome of Ptf1a^{T243A} overexpression in inducing *prdm13* as well as GABAergic and glutamatergic marker genes, it might be that Prdm13 needs to interact with Ptf1a to actively suppress glutamatergic markers such as *tlx3*.

To test this hypothesis, Prdm13 was fused to the C-terminal half of Venus EYFP and BiFC was performed by co-injecting *prdm13-Vc and mRFP* mRNA together with *ptf1a-Vn*, *ptf1a$^{W224A/W242A}$-Vn*, *ptf1a^{T243A}-Vn* or *ptf1a^{T243E}-Vn* mRNA in both blastomeres of two-cell stage *X. laevis* embryos. At blastula stage, the embryos were dissociated and fluorescence microscopy performed to visualize BiFC (Fig. 3.6A).

Interestingly, a BiFC signal could be observed in a very low number of cells (<1%) when Ptf1a-Vn or Ptf1a$^{W224A/W242A}$-Vn was co-injected with Prdm13 (Fig. 3.6B and C). Surprisingly, a quite strong BiFC signal could be detected in approximately half of the Ptf1a^{T243A}-Vn and Prdm13-Vc injected cells (Fig. 3.6B and C). Interestingly, in some of the cells showing EYFP fluorescence, the BiFC signal was not restricted to the nucleus, but additionally scattered in several aggregations throughout the cytoplasm (Fig. 3.6D). Surprisingly, a strong BiFC signal could be detected when Ptf1a^{T243E}-Vn was co-expressed with Prdm13-Vc (Fig. 3.7B). Here too, aggregates of EYFP signal could be detected in several cells. Quantification showed that the number of cells showing interaction with Prdm13 resembled those of Ptf1a^{T243A}-Vn (Fig. 3.6C).

Altogether, the data show that the Ptf1a^{T243} play an essential role in the neuronal cell fate inducing activity and mutations in it, lead to a strong interaction of Prdm13, but do not alter its association with Rbpj or E12.

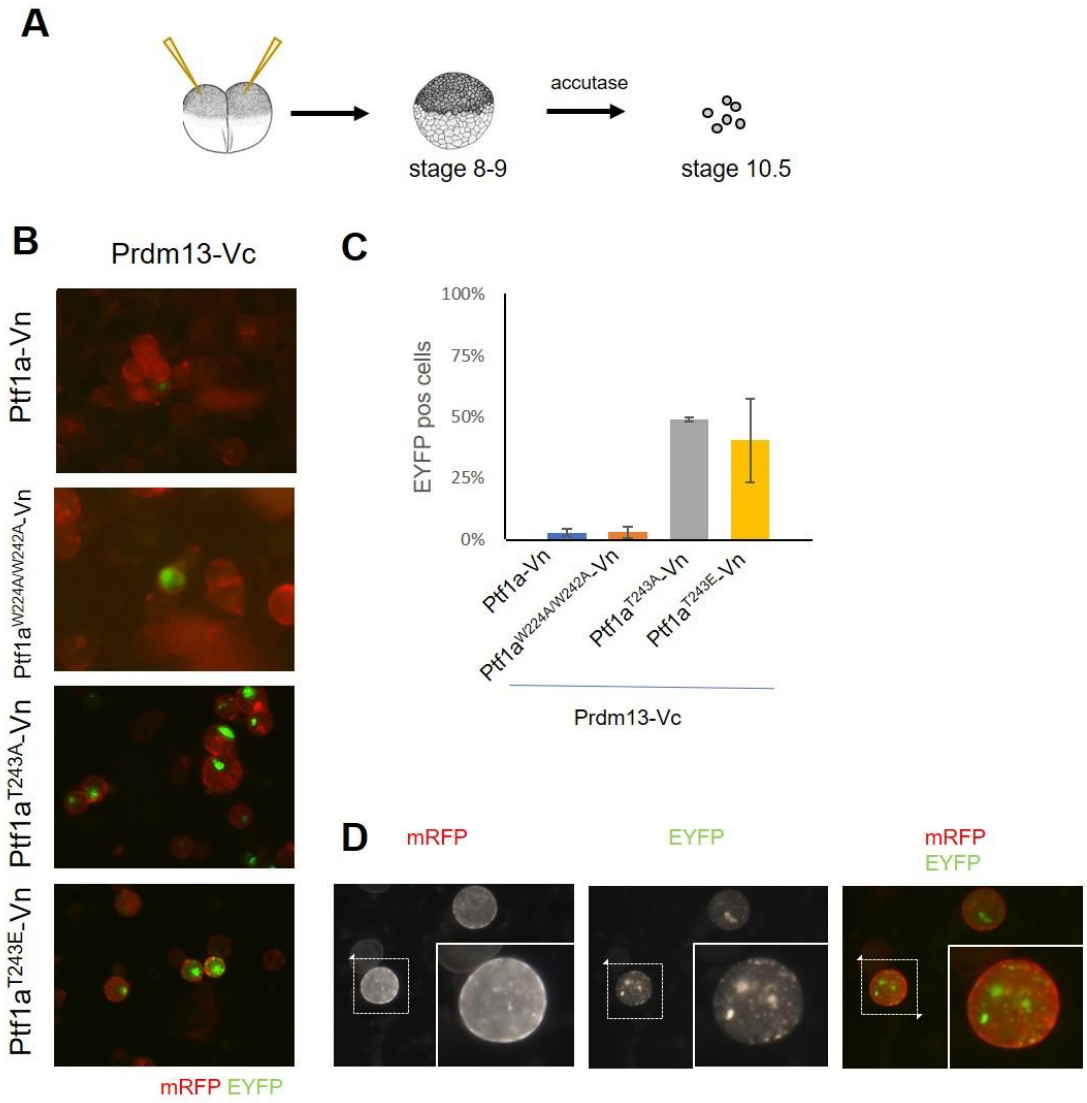

Figure 3.6: Ptf1a^{T243A} and Ptf1a^{T243E} mutants strongly interact with Prdm13.

(A) Experimental procedure: 500 pg of *ptf1a-Vn*, *ptf1a^{T243E}-Vn*, *ptf1a$^{W224A/W242A}$-Vn* or *ptf1a^{T243A}-Vn* mRNA were co-injected with 500 pg of *prdm13-Vc* mRNA and with 100 pg of *mRFP* mRNA in animally both blastomeres of two-cell stage embryos. At blastula stage, cells were dissociated by the use of accutase and analyzed for fluorescence. (B) BiFC analysis. Indicated on the top are the injected constructs carrying the C-terminal Venus-EYFP. The corresponding N-terminal Venus-EYFP construct is shown left. Injected cells are stained red due to their expression of mRFP, while green is the corresponding EYFP signal indicating BiFC. C) Quantification of the BiFC analysis. The given numbers and ratios all refer to the total amount of mRFP positive cells that have been analyzed. Error bars refer to the standard error of the mean. D) Example for a “scattered” distribution of the EYFP signal within a cell. Given are the channels for mRFP (left) and EYFP (middle) alone and merged (right).

3.5 Ptf1a induces direct target genes at different time points

For a better understanding of the mechanisms driving the development to a distinct neuronal subtype induced by Ptf1a, it is important to understand which genes were induced by Ptf1a. Previous studies investigating the transcriptional program induced by Ptf1a after 6 and 25 h in *X. laevis* ectodermal explants, afforded insight into the temporal control of Ptf1a gene induction (Hedderich, 2012). In another analysis, Ptf1a was overexpressed in animal caps in the presence of the translational inhibitor cycloheximide (CHX) to identify direct target genes of Ptf1a. Through comparison of both analysis, it could be shown that several Ptf1a direct target genes were not activated in an immediate early fashion, but were delayed in their activation (Hedderich, 2012). Direct target genes showing an immediate activation by Ptf1a consist mostly of genes involved in neuronal differentiation such as the Notch ligand *delta1* (*dll1*) or the neuronal differentiation genes *ebf2* or *myt1*, as well as *prdm13.* Among the delayed direct target genes were genes like *gad1a, barhl2, kirrel2* or *neurog2.*

To get a better understanding in the mechanics for the delayed target gene induction, the exact onset of Ptf1a target gene induction needs to be defined. Therefore, 20 pg of *ptf1a-GR* mRNA was injected into the animal hemispheres of both blastomeres at the two-cell stage. At blastula stage, the animal cap was excised and protein activity was induced for 3, 6, 9, 12, 15 and 25 h. The RNA was isolated and analyzed by quantitative Nanostring analysis using a codeset consisting of known early and late Ptf1a target genes and neuronal marker genes (Fig. 3.7A, Table S7).

To ensure that constructs indeed behaved as expected, the late time point at the 25 h was first analyzed for known Ptf1a-downstream genes. Compared to the non-injected control explants, Ptf1a-injected animal caps strongly expressed the pan-neuronal marker *tubb2b*, the direct target genes of Ptf1a, *prdm13* and *kirrel2* as well as the GABAergic marker *gad1a*, *slc32a1* and *pax2,* but not the glutamatergic selector gene *tlx3* and the vesicular glutamate transporter *slc17a7* (Fig. 3.7B, Table S3). This expression reflects the activities of Ptf1a in promoting neuronal differentiation, inducing a GABAergic cell fate and inhibiting a glutamatergic cell fate (Glasgow *et al.*, 2005; Hoshino *et al.*,

2005; Dullin *et al.*, 2007; Pascual *et al.*, 2007). (Fig. 3.7B). The Ptf1a-induced genes analyzed can be classified into groups based on their timing of activation (Fig. 3.7 C-H, Table S3). The first group of genes has the onset of their activation already at 3 h (*dll1, ebf2, myt1, prdm13, prdm14, zc3h12c*), the second at 6 h (*barhl2, kirrel2, lhx1, nr5a2, onecut1.2, tlx3, aldh1b1*), the third group between 9 and 12 h, with a strong tendency towards 12 h (*pax2, tubb2b, gad1a, neurog2, pdia2*) and one gene at 25 h (*slc32a2*). Under those genes activated at the earliest stages (3 h, 6 h) were direct Ptf1a target genes (*prdm13*, *kirrel2*) (Nishida *et al.*, 2010; Chang *et al.*, 2013) as well as many genes predicted to be direct Ptf1a target genes by their activation in presence of the translational inhibitor cycloheximide (CHX) (Schneider-Poetsch *et al.*, 2010) could be found (*dll1, ebf2, myt1, zc3h12c*) (Hedderich, 2012), but known and predicted direct target genes were also present under those genes activated at the 12 h time point (*neurog2, gad1a, pdia2*) (Henke *et al.*, 2009; Hedderich, 2012) (Fig. 3.7C-H, Table S4). Interestingly, the activation of delayed Ptf1a target genes followed the activation of the post-mitotic neuronal marker *tubb2b*, which indicates that the expression of those genes may be connected with cell cycle exit.

Interestingly, a significant induction of *tlx3* expression by Ptf1a could be detected in early stages, which is increasing up to the 9 h time point, but afterwards is declines and is no longer detected after 25 h (Fig. 3.7H), indicating that during the onset of neuronal differentiation Ptf1a induces *tlx3* expression, which is subsequently suppressed during subtype specification. Altogether the data suggest that the delayed activation of Ptf1a direct target genes begins their onset of expression 12 h following Ptf1a induction. As only a limited number of genes were analyzed, it is unclear if all the delayed target genes behave in such a manner.

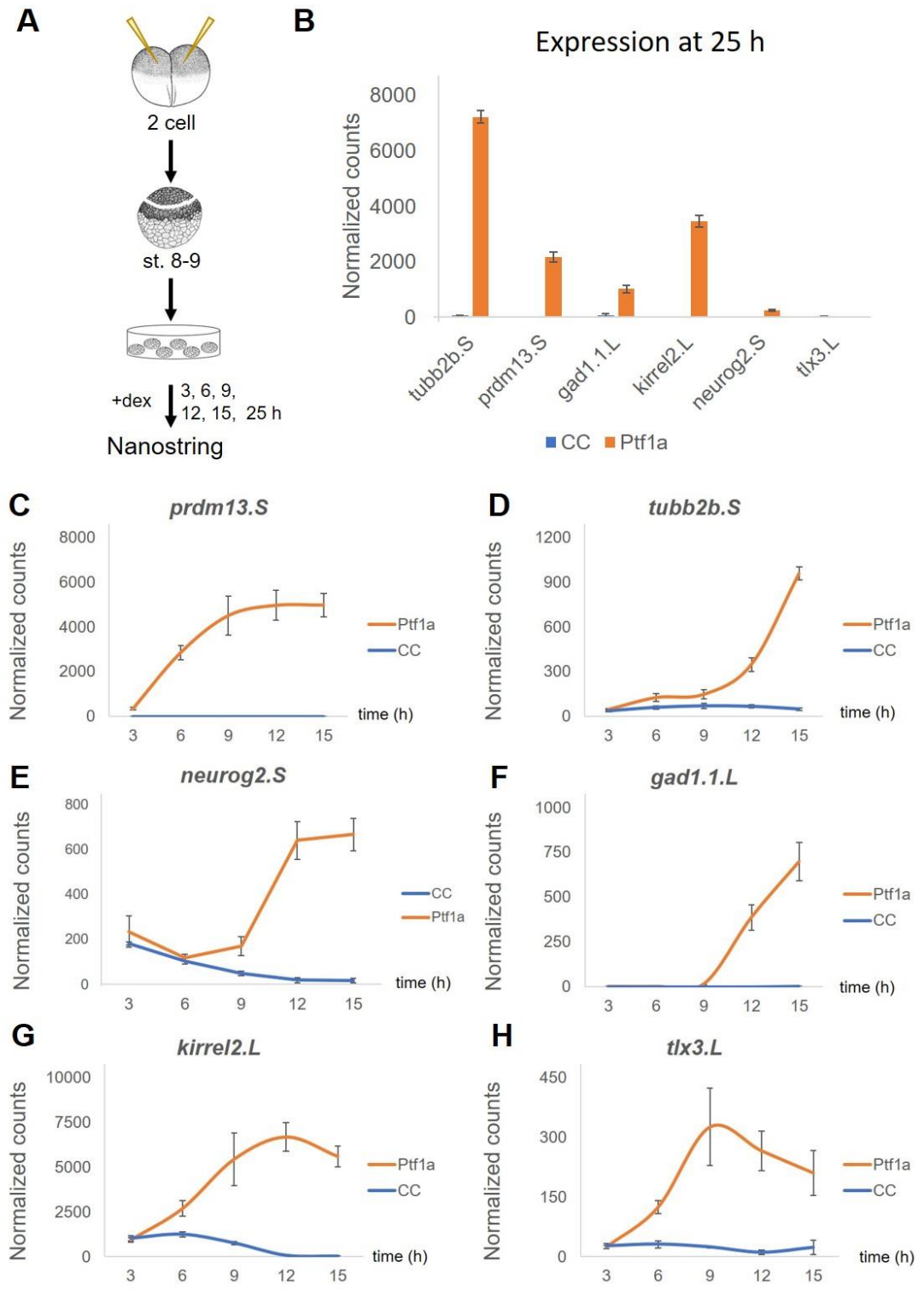

Figure 3.7: Ptf1a is activating its target genes in a temporal manner

(A) Experimental procedure: 20 pg of *ptf1a-GR*, mRNA was injected animally in both blastomeres of two-cell stage embryos. At blastula stage, animal caps were excised. Protein activity was induced by dexamethasone treatment for 3, 6, 9, 12, 15 and 25 h. Animal caps were collected for RNA isolation at the indicated times and gene expression quantified by Nanostring analysis. (B) Results of the quantitative Nanostring analysis. Shown are the average expression levels of marker genes from three biological replicates. Error bars refer to the standard error of the mean. Data →

were normalized for the expression levels of the housekeeping gene *ppi1l.* (C-H) Results of the quantitative Nanostring analysis. Shown are the average expression levels of marker genes from three biological replicates. Error bars refer to the standard error of the mean. Data were normalized for the three housekeeping gene *ppi1l*. .S and .L refer to the corresponding *X. laevis* homeolog targeted by the Nanostring probe. Note the different scales in each diagram. *CC,* control cap.

3.6 Temporal expression of Ptf1a target genes by RNA sequencing

To understand the temporal induction of Ptf1a target genes on a global level, RNA sequencing was performed by injecting 20 pg of *ptf1a-GR* mRNA animally in both blastomeres of the two-cell stage blastomeres. At blastula stage, animal caps were excised and protein activity was induced by the addition of dexamethasone to the culture medium. After 3, 6 or 12 h, the RNA was isolated and analyzed by RNA-seq (Fig. 3.8A).

To get an insight in the similarity between the different replicates, the distinct samples were clustered according to their similarity using the R/Bioconductor environment (www.bioconductor.org). Analysis clearly showed a high similarity in the 3 h and 6 h groups, which much higher similarity than any of these groups to the 12 h time point samples, supporting the argumentation that a major change at the 12 h time point has occurred (Fig. 3.8B)

Applying a cutoff of at least a $\log_2$ fold-change of two over non-injected control caps, 133 genes were upregulated by Ptf1a after 3 h of protein induction, while after 6 h and 12 h of protein induction, 241 and 468 genes were upregulated (Fig. 3.8B). In contrast, only 15 genes were downregulated after 3 h of protein induction, while after 6 h and 12 h, 3 and 20 genes were downregulated. From these, 140 and 353 genes also had their onset of induction after 6 h and 12 h. Under the genes being upregulated, known Ptf1a target genes like *prdm13* (Hedderich, 2012; Chang *et al.*, 2013) or *kirrel2* (Nishida *et al.*, 2010) could be found (Table S14-16).

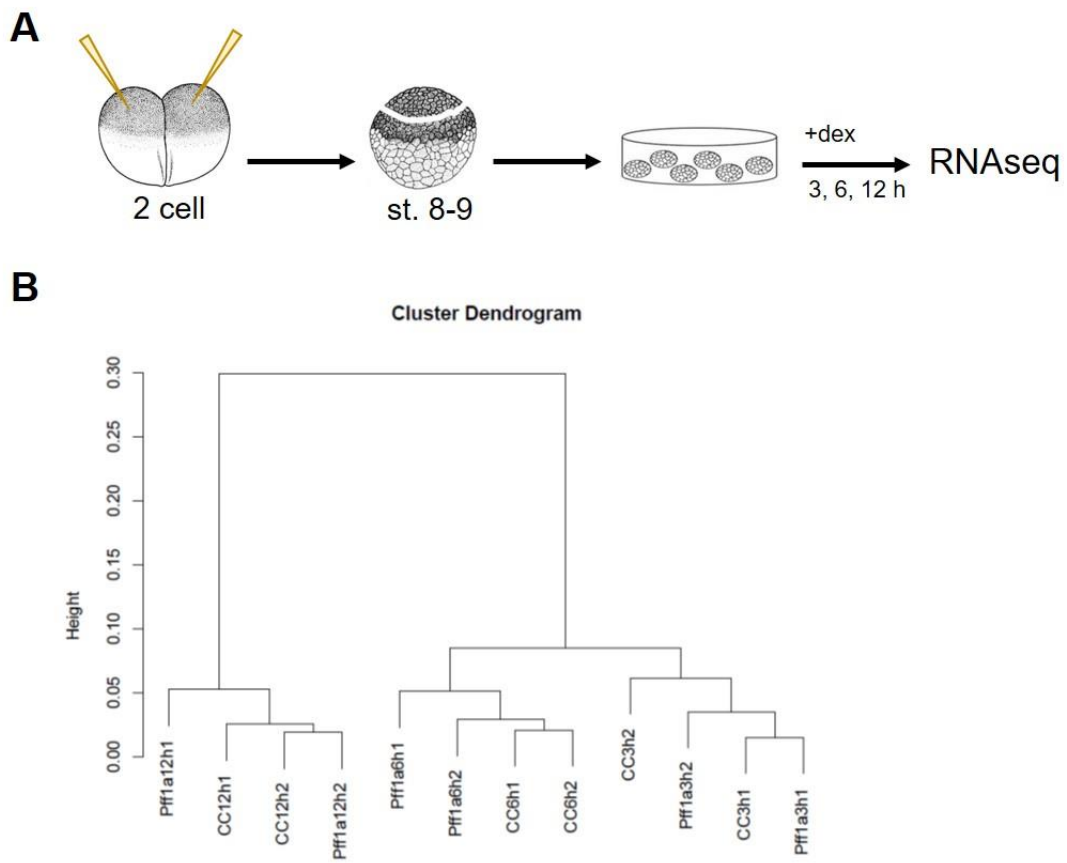

Figure 3.8: Summary of the RNAseq

(A) Experimental procedure: 20 pg of *ptf1a-GR*, mRNA was injected in both animal blastomeres of two-cell stage. At blastula stage, animal cap is excised. Protein activity is induced by dexamethasone treatment for 3, 6, and 12 h. Afterwards, the animal caps were collected for RNA isolation. RNA expression was analyzed by RNAseq. (B) Cluster Dendrogram showing the similarity of the different samples.

To identify the direct target genes being upregulated at the distinct time points, the list of upregulated genes from the RNA-seq was compared to a list of genes induced by Ptf1a in the presence of the translational inhibitor cycloheximide (CHX) (Hedderich, 2012). From the 133 genes upregulated at least four-fold after 3 h, 59 genes could be identified as direct target genes (Fig. 3.9C). Of the genes upregulated after 6 h, 90 were direct target genes. From those, 41% (37 genes) had their onset at 6 h. After 12 h, 99 direct target genes could be found. Interestingly, approximately half of the direct target genes (45 genes) activated after 12 h of protein induction had their onset at this time point, indicating a greater change in the activated target genes occurring at this time point

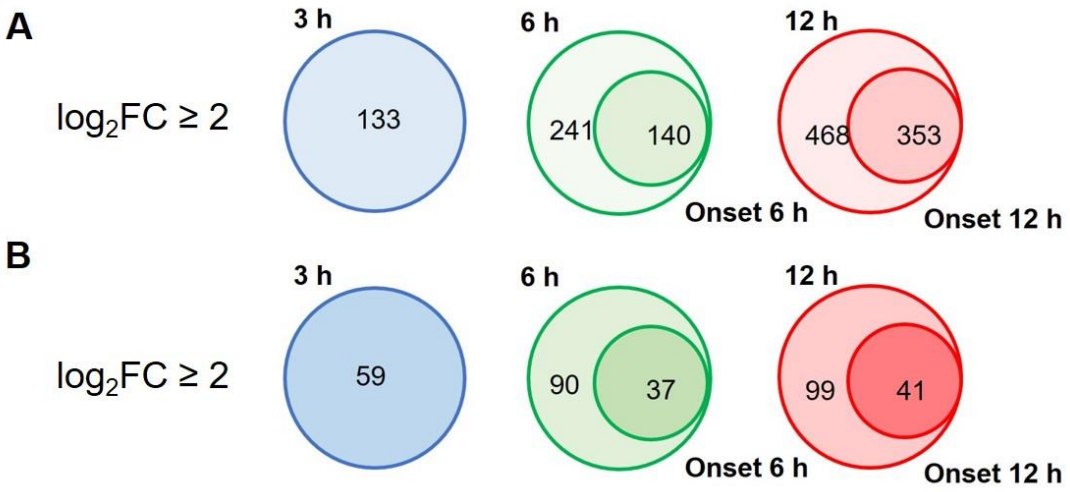

Figure 3.9 Comparison of target gene activation by Ptf1a after 3, 6 and 12 h

Venn diagrams indicating number of upregulated genes at 3, 6 and 12 h by the given threshold in general (A) and for direct target genes only (B). Given is the number of genes with a $\log_2$ fold change higher or equal than 2 compared to non-injected control caps.

3.7 Ptf1a target genes are highly enriched for playing roles during transcription and neurogenesis

To identify the function of the upregulated genes at the different time points, gene ontology analysis was performed using DAVID (Database for Annotation, Visualization and Integrated Discovery, http://david,abcc.ncifcrf.gov/). GO analysis revealed an enrichment of the genes upregulated after 3 h involved in the positive or negative regulation of transcription (e.g. *myt1, dll1, ebf2, prdm13*), the development of the nervous system (e.g. *dll1, olig2, lhx1*) or neuron fate commitment (e.g. *notch1, id2, olig2*) (Fig. 3.10A). Gene ontology analysis for the genes upregulated after 12 h of protein induction also showed a significant enrichment in processes for positive or negative regulation of transcription (*barlh2, lhx1, neurog1, neuro2, myt1, olig2*) and the development of the nervous system (*lbx1, olig2, barlh2, myT1, lhx1, neurog1, neurog2, neurod4*) (Fig. 3.10B). At both time points, a high overlap in the genes listed in the different GO terms could be detected, as for example *dll1*, *olig2* or *myt1*

were involved in transcriptional regulation as well as in the development of the neural system after 3 h. Similarly, *neurog1*, *neurog2, myt1* or *barlh2* were involved in transcriptional regulation as well as in the development of the neural system after 12 h. Nevertheless, no strong differences between the gene function between the 3 and 12 h time point could be detected.

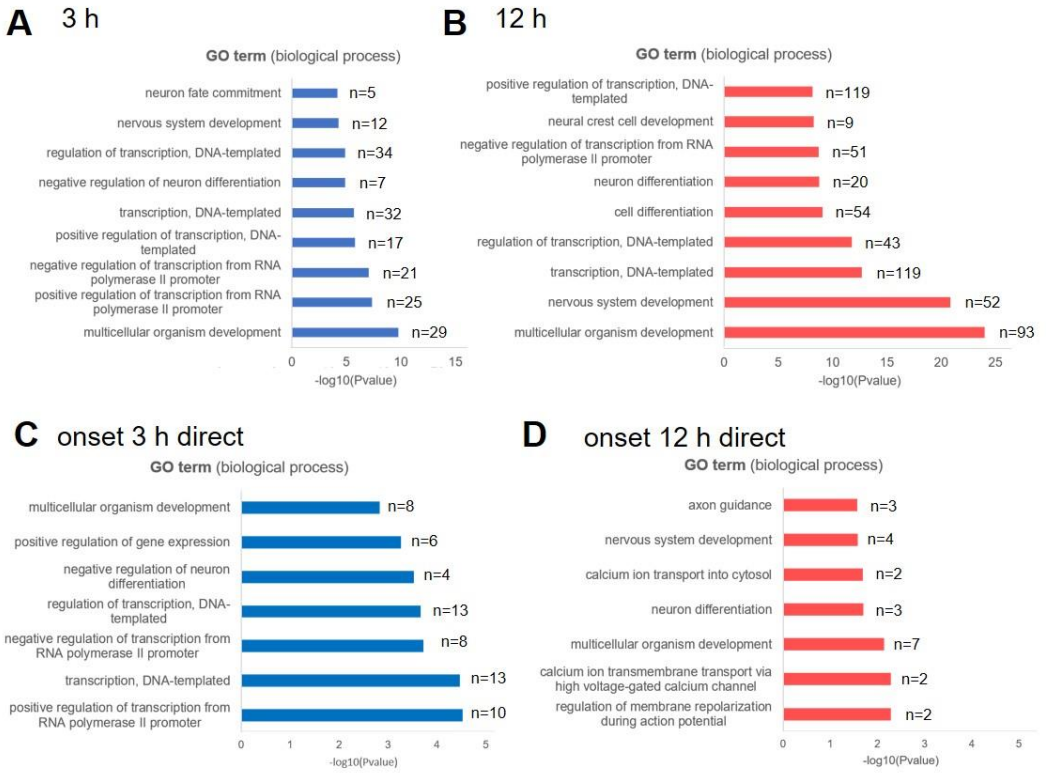

Figure 3.10: Genes involved in processes involved in neurogenesis are enriched in all three time points

Gene Ontology (GO) analysis was performed using DAVID (http://david.abcc.nclfcrf.gov) (Dennis et al. 2003). The number of genes in each category is shown as well as the -log10 P-value of false discovery rate. Shown are the top listed terms of each category ranked by their P-value. The different diagrams refer to genes activated after 3 h (blue) and 12h (red) in general (A) and for direct target genes having their onset at the given time point (B)

When considering only those direct target genes that were upregulated at the particular time point, however, differences could be found (Fig. 3.10C and D). While direct target genes induced after 3 h still were strongest enriched for positive or negative regulation of transcription (e.g. *ebf2, myt1, prdm13 or dll1*) (Fig. 3.10C), direct target genes having their onset of expression after 12 h,

were involved in axon guidance (e.g. *neurog2, tubb3)* regulation of membrane repolarization during action potential or calcium transport (*cacna2d1, cacnb3*), or neuron differentiation (*neurog2, tubb3, unc5a*) (Fig. 3.10D) indicating that genes expressed after 12 h play a role in function and maturation of neurons, while early induced genes are more likely involved early neuronal differentiation.

3.8 A knock-down of Brg1 affects the induction of indirect Ptf1a target genes

Chromatin remodeling mediated by the BAF chromatin remodeling complex plays an essential role during vertebrate neurogenesis (Bachmann *et al.*, 2016). It had been shown that a knock-down of Brg1, one of the two catalytic subunits of the BAF complex lead to an impairment in the induction of neuronal differentiation by proneuronal transcription factors like Neurog2 (Seo *et al.*, 2007). As induction of delayed Ptf1a target genes was connected with the induction of the post-mitotic neuronal marker *tubb2b*, the delayed activation of direct target genes might be dependent on chromatin remodeling via the BAF chromatin remodeling complex. To investigate which genes are affected by a Brg1 knock-down in Ptf1a overexpressing animal caps, RNA sequencing was performed using stage 14 ectodermal explants from embryos injected with 20 pg of *ptf1a-GR* mRNA together with 20 ng of either control morpholino (cMO) or Brg1 morpholino (Brg1-MO) previously shown to be effective in knockdown of Brg1 by inhibiting translation (Seo *et al.*, 2007) (Fig 3.11A).

In total, Ptf1a together with the control MO upregulated more than 819 genes by applying a threshold of $\log_2$ fold-change of two compared to non-injected control caps and an FDR value <0.05, while 668 genes were upregulated by Ptf1a in the presence of the Brg1-MO. From these upregulated genes, in total, 527 genes were shared by both samples, while 236 genes were exclusively induced by Ptf1a-GR and the cMO (Fig3.11B)

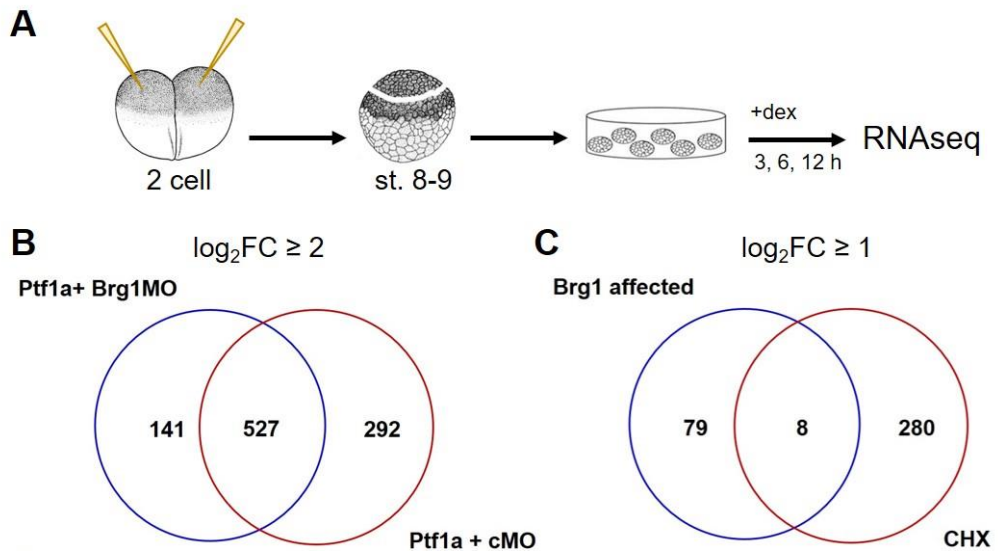

Figure 3.11: Brg1 dependent genes are mostly indirect Ptf1a target genes

(A) Experimental procedure: 20 pg of *ptf1a-GR* mRNA was injected individually or together with either a control morpholino or a Brg1 morpholino in both animal blastomeres of two-cell stage. At blastula stage, animal cap is excised. Protein activity was induced by dexamethasone treatment. At stage 14, the animal caps were collected for RNA isolation. RNA expression was analyzed by RNA sequencing. (B) Venn Diagram showing the number of unique and shared genes being at least four-fold (left) or 16-fold upregulated by Ptf1a in presence of cMO (blue) or Brg1-MO (red) (C) Venn Diagram showing the number of unique and shared genes being at least four-fold (left) or two-fold (right) upregulated by Ptf1a and cMO over Ptf1a together with the Brg1-MO (blue) and by a list of genes induced by Ptf1a in the presence of CHX (Hedderich, 2012) (red).

To identify, which genes were most strongly affected by a Brg1 knock-down, the gene expression levels were compared between Ptf1a in the presence of the Brg1-MO versus the presence of the control MO. In the presence of the Brg1-MO, 56 genes were upregulated and one of these genes were induced by Ptf1a in presence of CHX (Hedderich, 2012) and 87 genes were significantly reduced by more than two-fold (Fig. 3.11C). As only a limited number of genes were altered, the influence of the Brg1 knock-down on target gene induction by Ptf1a is specific for selected genes. *Tubb2b* could be found under those genes showing a strong impairment in Ptf1a induction upon Brg1 knock-down. From the 87 genes negatively affected by the Brg1-MO, only eight genes (*flnc.S, nr5a2.S, tubb3.S, six3.L, traf4.S, LOC100496628-like.S, emilin1.L, st18.L*) were identified as direct target genes by Ptf1a based on their ability to activated in the presence of CHX (Hedderich, 2012). (Fig. 3.11C)

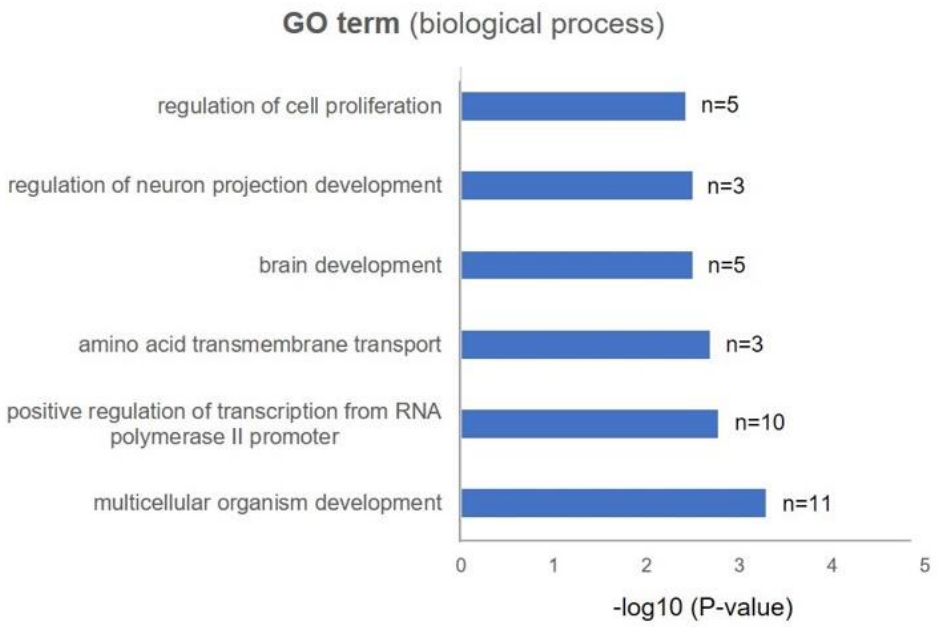

Figure 3.12: Genes affected by an Brg1 knock-down have activities during neurogenesis

GO analysis of genes being at least four-fold downregulated in the presence of the Ptf1a together with Brg1-MO versus the control MO. Analysis was performed using DAVID (http://david.abcc.nclfcrf.gov) (Dennis *et al.,* 2003). Shown are the top listed terms of each category ranked by their P-value. The number of genes in each category is shown to the right of the bar diagram.

For identification, which gene functions were affected by a Brg1 knockdown, Gene Ontology analysis was performed on the strongest Brg1-MO affected genes using DAVID. Corresponding to the Ptf1a gene function, genes affected by a Brg1 knock-down were enriched in terms having a function during neurogenesis, including “brain development” (*nes, bcr, six3*), or regulation of neuron projection development” (*pak3, sfrp2*), but also “regulation of cell proliferation” (*ppp1r9b, nr5a2*) (Fig. 3.12).

Altogether, these data suggest that most Ptf1a direct target genes do not require chromatin remodeling by the Brg1 containing BAF complex.

3.9 Induction of selected Ptf1a downstream genes requires Brg1

For verification of the RNA sequencing results, 20 pg of *ptf1a-GR* mRNA was injected alone or in combination with 20 ng of a control MO or the Brg1-MO, in

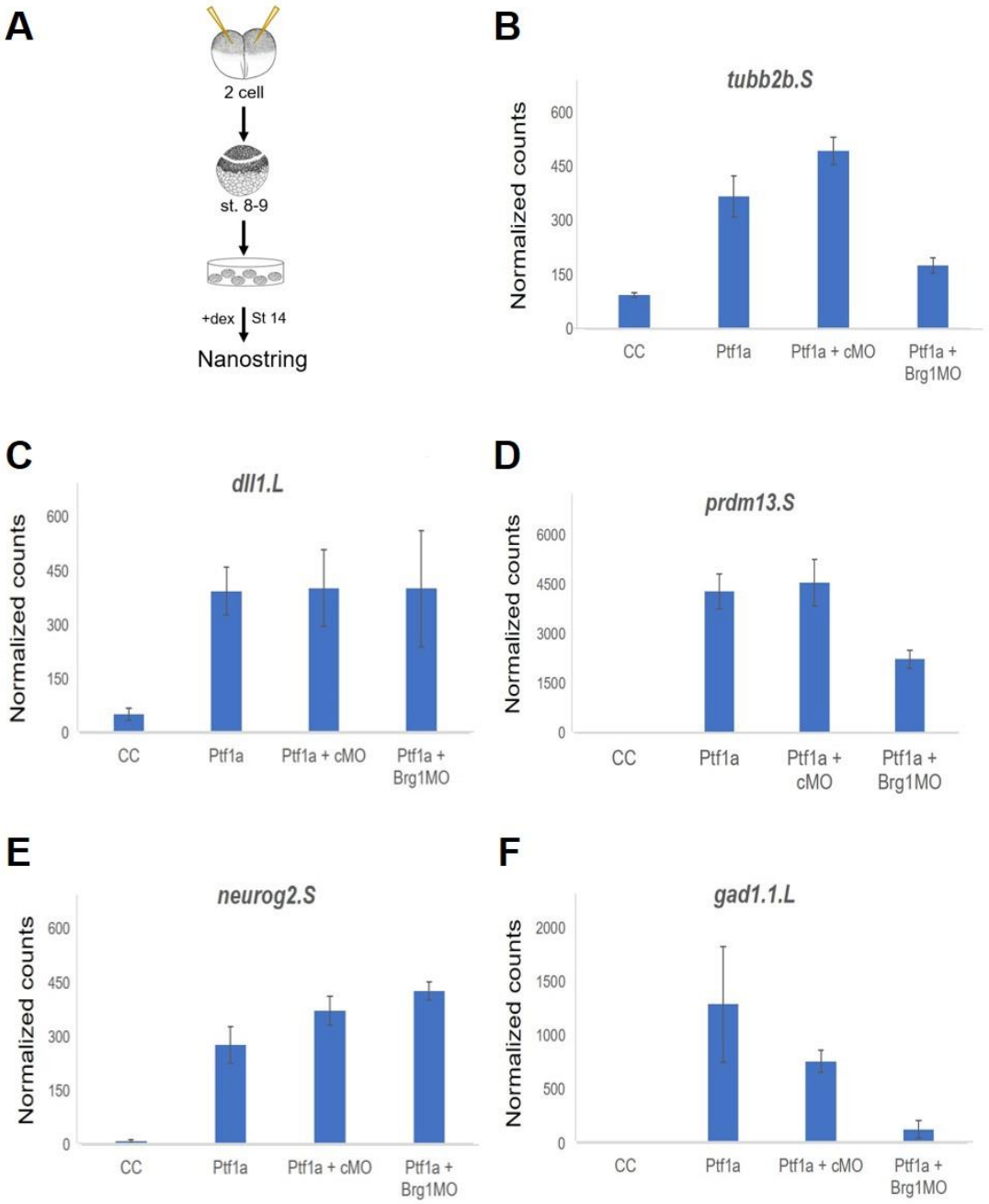

Figure 3.13: Induction of some delayed Ptf1a target genes is depended on Brg1

(A) Experimental procedure: 20 pg of *ptf1a-GR* mRNA was injected individually or together with either a control morpholino (cMO) or a Brg1 morpholino (Brg1MO) in both animal blastomeres of two-cell stage. At blastula stage, animal cap is excised. Protein activity was induced by dexamethasone treatment. At stage 14, the animal caps were collected for RNA isolation. RNA expression was analyzed by quantitative Nanostring analysis. B-F) Examples of Brg1 dependent or independent target genes. Shown are the average expression levels of marker genes from three biological replicates. Error bars refer to the standard error of the mean. Data were normalized for the three housekeeping genes *odc*, *ppi1l* and *rplp0*. Note the different scales in each diagram.

both blastomeres at the two-cell stage. At blastula stage, animal caps were excised and protein activity was induced by the addition of dexamethasone to the culture medium. At the equivalent of stage 14, the RNA of the explants was isolated and gene expression was analyzed by quantitative Nanostring analysis using a codeset containing Ptf1a direct and indirect early and late target genes, as well as selected markers of neuronal differentiation and subtype specification (in total 96 genes were analyzed) (Fig. 3.13A, Table S7).

Overexpression of Ptf1a upregulated almost all investigated target genes previously shown to be upregulated by Ptf1a in the RNA-seq (Fig. 3.14, Fig. 3.15). As it was previously shown for other proneural transcription factors like Neurog2 (Seo *et al.*, 2007) and the Ptf1a-Brg1-MO RNAseq analysis, the

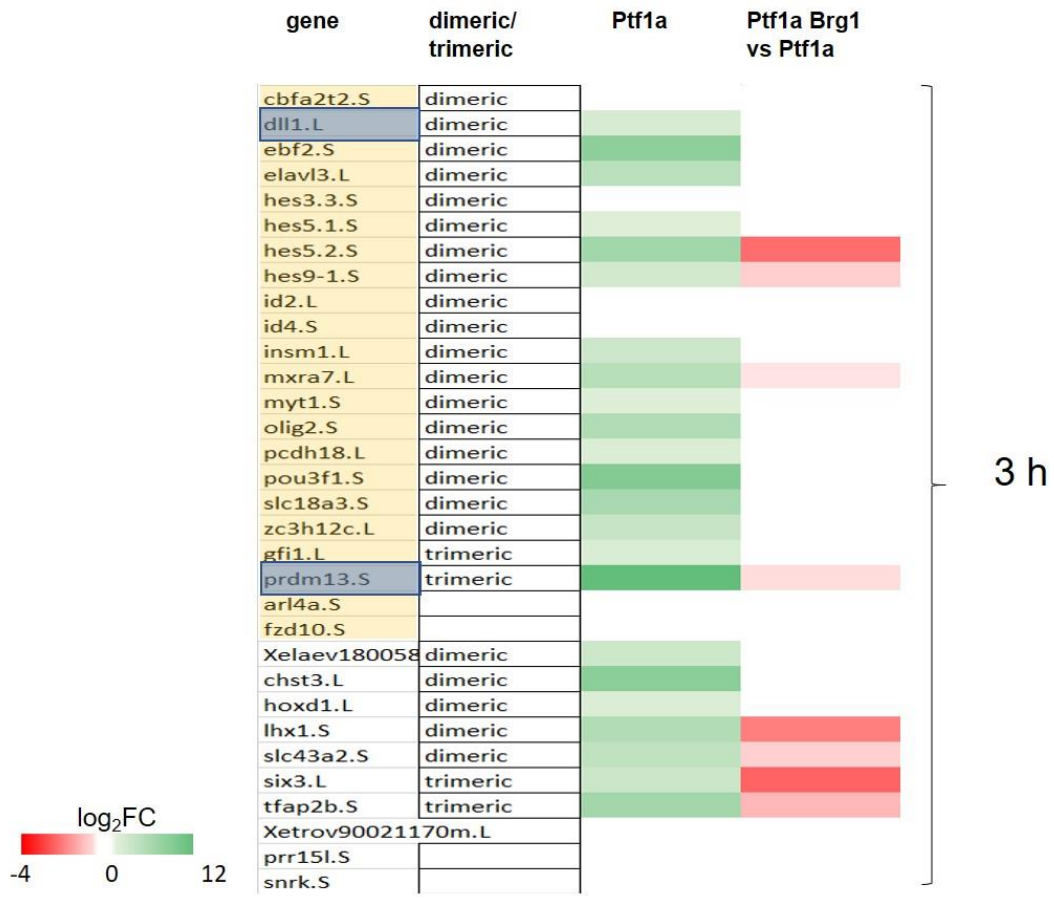

Figure 3.14 Summary of the Nanostring analysis for genes induced after 3 h

Shown is a heatmap showing the log2 fold-change activation of target genes by Ptf1a (green) or the fold-change reduction when Co-injected with Brg1 morpholino compared to the Co-injection with a control morpholino (red). Genes activated by Ptf1a in presence of CHX are highlighted in yellow.

upregulation of *tubb2b* expression by Ptf1a was significantly attenuated in the presence of the Brg1-MO compared to the control MO (Fig. 3.13B), indicating the importance of Brg1 for neuronal differentiation. Ptf1a direct target genes such as the early upregulated *dll1* or the late upregulated *neurog2,* were not affected by a Brg1 knockdown (Fig. 3.13C, E). Interestingly, with respect to the timing of target gene induction, most of the observed genes activated within 3 h of Ptf1a induction were not affected by a Brg1 knock-down. From those early induced target genes being affected by a Brg1 knock-down, four were direct target genes (out of 22 direct Ptf1a target genes present for this time point), while four were indirect Ptf1a target genes (out of 10 indirect Ptf1a target genes present for this time point). In general, in the target genes analyzed, the number of indirect target genes affected by the Brg1 knock-down was higher than the number of direct target genes (Fig. 3.17G). For later activated genes, including both direct (e.g. *neurod4* and *gad1a*) and indirect (e.g. *pou3f2* or *lbx1*), the number of Brg1 dependent genes increases. All genes being affected the Brg1 knock-down in the RNA-seq that were analyzed, were also affected in the Nanostring analysis (Fig. 3.17G). Furthermore, the finding from the RNA-seq that many affected genes were indirect Ptf1a target genes could be demonstrated in the Nanostring analysis. However, many genes like *gad1a* or *prdm13* that showed no significant reduction in the RNA-seq analysis, showed a reduction in the induction by Ptf1a in the presence of the Brg1-MO (Fig. 3.13D, Fig. 3.14) Altogether, the data suggest that the induction of most early target genes by Ptf1a is not dependent of chromatin remodeling via the BAF chromatin remodeling complex, while this mechanism becomes more important for the induction of selected late target genes. However, BAF-mediated chromatin remodeling cannot be the only mechanism responsible for the delayed target gene activation as even at the 12 h time point, induction of several direct Ptf1a target genes is not affected by a Brg1 knock-down.

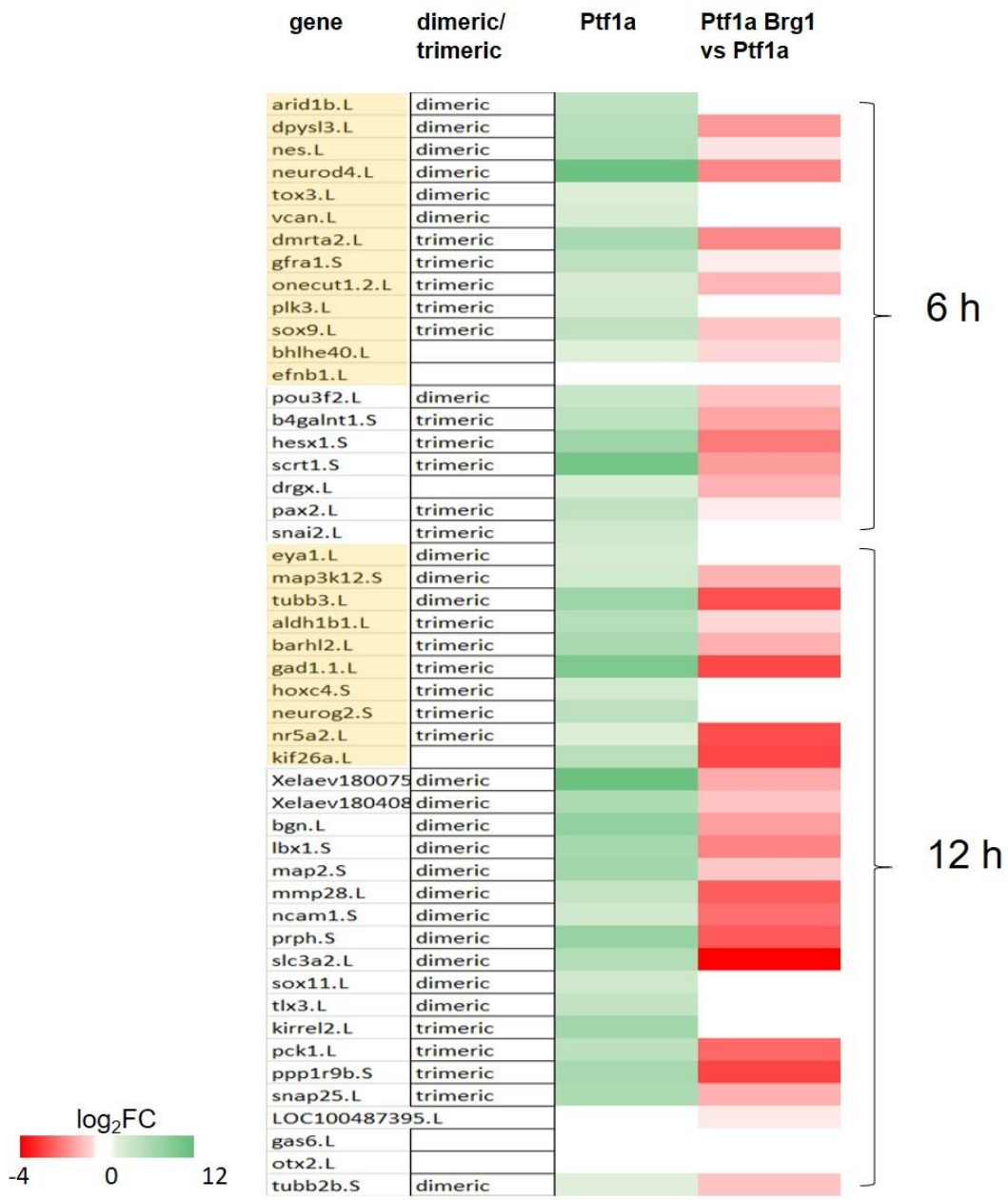

Figure 3.15 Summary of the Nanostring analysis for genes induced after 3 h

Shown is a heatmap showing the log2 fold-change activation of target genes by Ptf1a (green) or the fold-change reduction when Co-injected with Brg1 morpholino compared to the Co-injection with a control morpholino (red). Genes activated by Ptf1a in presence of CHX are highlighted in yellow.

3.10 Ptf1a can alter the chromatin state of its target genes

Since other chromatin remodeling complexes exist that are Brg1 independent it cannot be ruled out that that the delayed activation of Ptf1a is due to chromatin accessibility. Therefore, analysis of the chromatin landscape of

Ptf1a direct target genes were analyzed by using ATAC-seq (Assay for Transposase Accessible Chromatin). Therefore, 20 pg of *ptf1a-GR* was injected in both blastomeres at the two-cell stage of *X. laevis* embryos. At blastula stage, the animal caps were excised and protein activity induced by dexamethasone treatment for 3 (when the earliest target genes are activated) or 12 h (the timing when late target genes were activated). Afterwards, ATAC sequencing was performed (Fig. 3.16A, B). The results of the ATAC sequencing were compared to the expression levels of the genes obtained from the RNA-seq to determine the correlation between the chromatin levels with the target gene expression.

In total between 100,000,000 and 200,000,000 reads could be mapped for each sample. However, many duplicate reads could be found in the samples, so that after removal of those duplicates only between 2,000,000 and 12,000,000 reads remained, so that the amounts of reads that remained was quite low indicating restriction in the analysis due to a non-sufficient quality of the samples.

Nevertheless, genes strongly expressed in the naïve animal cap (3 h, equivalent stage 10 or 12 h, equivalent stage 12.5) like *odc* (data not shown), *pou5f3.2* or *fcgbp* could be located in areas of quite open chromatin in the presence and absence of Ptf1a (Fig 3.16C). Time dependent changes in the loci of genes could be detected, with *pou5f3.2* at early stages, for example, was located in a quite open area. At later stages, however, the chromatin at the *pou5f3.2* locus becomes much more closed, which correlated with a decrease in *pou5f3.2* expression levels (Fig. 3.16C, D). The opposite effect could be identified for example on the expression of *fcgbp*. Here, the *fcgbp* gene locus is located in closed chromatin regions at the 3 h time point. At the 12 h time point, however, the chromatin at the *fcgbp* locus is quite accessible, matching with a strong increase of *fcgbp* expression levels (Fig. 3.16E, F). These results highlight the correlation between chromatin remodeling and gene expression and demonstrate the validity of the analysis.

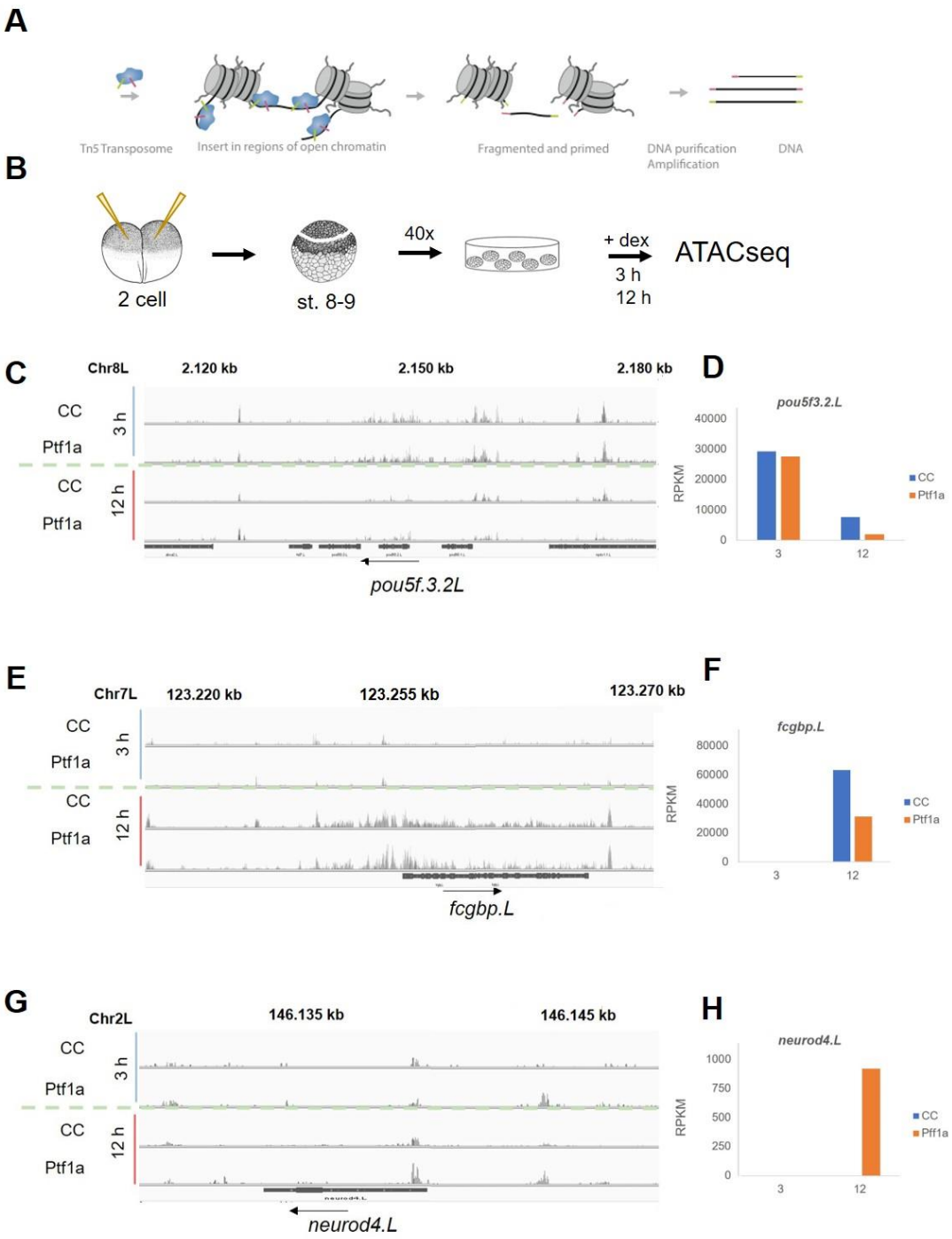

Figure 3.16: Ptf1a overexpression can change the chromatin state of its target genes

(A) Overview ATAC-seq (Scheme modified from (Buenrostro *et al.*, 2013)). Intact nuclei were treated with a highly reactive Tn5 transposase. The transposase binds at accessible chromatin regions introducing signaling sequences. Accessible regions were amplified via PCR against the introduced sequences. PCR library is then sequenced with 50 bp paired-end reads. (B) Experimental procedure: 20 pg of *ptf1a-GR*, mRNA was injected in both animal blastomeres of two-cell stage. At blastula stage, animal cap is excised. Protein activity is induced by dexamethasone treatment for 3 and 12 h. Afterwards, the animal caps were collected for ATAC sequencing. (C, E, G) ATAC tracks from read coverage files mapped to the *X. laevis* genome. The corresponding sample control Cap (CC) or Ptf1a injected (Ptf1a) and the →

corresponding time point is given on the left. The transcriptional direction of the investigated gene is indicated with a black arrow. The grey bars represent the total numbers of reads at the corresponding position of the genome. (D, G, H) The corresponding target gene's expression level from the RNAseq is shown on the right side. Note the different scales.

When looking at the loci of Ptf1a direct target genes (in total 44 genes, from those, 6 genes were activated after 3 h, 10 after 6 h and 24 genes after 12 h). Ptf1a dependent changes in the chromatin states could be found. At the locus of the Ptf1a direct target gene *neurod4*, for example, a region of open chromatin could be detected approximately 5 kb upstream of the transcription start site in the Ptf1a injected explants, but not in non-injected control explants (Fig. 3.16G). *Neurod4* expression levels, however, could not be detected at the 3 h time point, even though the open chromatin region appeared at this time point in the Ptf1a expressing explants (Fig 3.16H). However, in the RNA-seq analysis expression of *neurod4* becomes detectable at the 6 h time point (Table S15), indicating that even though the chromatin at this position is accessible, some time is needed until transcription can start. Together, these results indicate that overexpression of Ptf1a can lead to changes in the chromatin state of selected genes target genes.

3.11 Ptf1a target genes lay in closed chromatin regions

To identify if chromatin remodeling is responsible for the delayed activation of target genes, the chromatin state of Ptf1a target gene loci have been investigated and compared with their onset of expression. Interestingly most of the investigated early and late target genes were located in regions of rather closed chromatin, which was even the case for early induced genes like *prdm13* (Fig 3.17A).

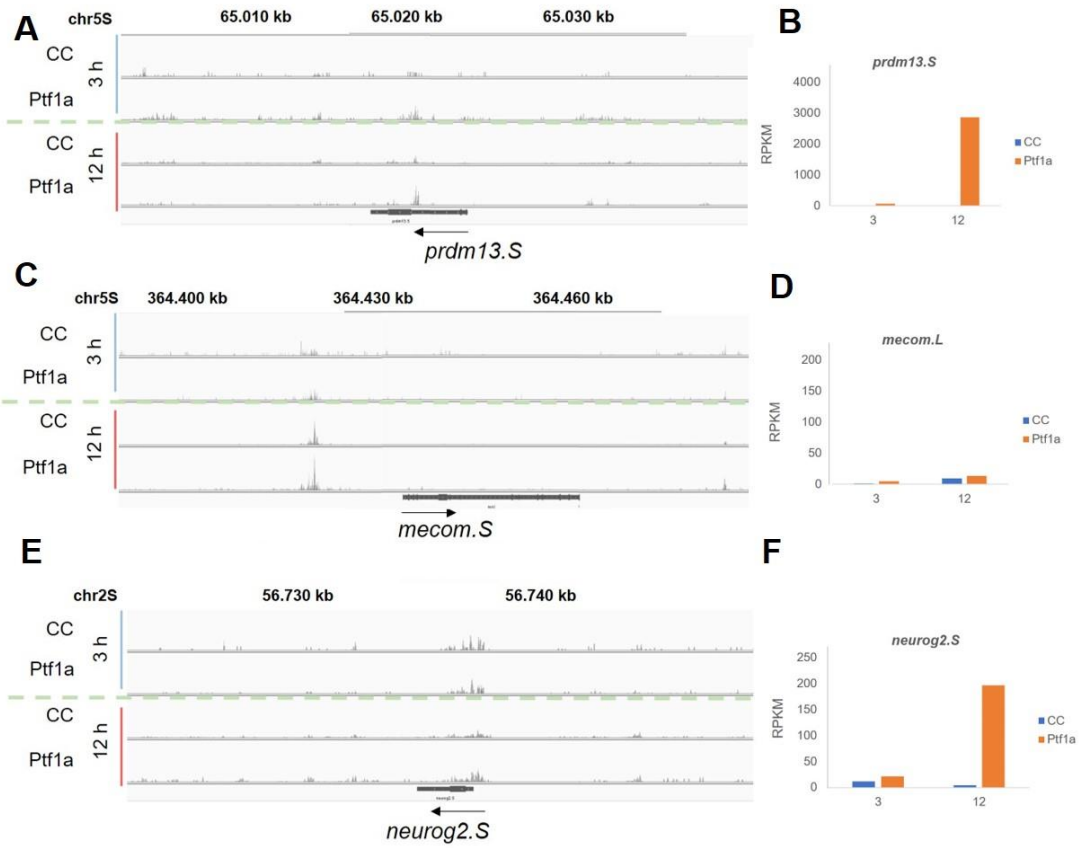

Figure 3.17: Chromatin remodeling plays a minor role in the delayed induction of Ptf1a target genes

(A, C, E) ATAC tracks from read coverage files mapped to the *X. laevis* genome. The corresponding sample (control Cap (CC) or Ptf1a injected (Ptf1a) and the corresponding time point is given on the left. The transcriptional direction of the investigated gene is indicated with a black arrow. The grey bars represent the total numbers of reads at the corresponding position of the genome. (B, D, F) The corresponding target gene's expression level from the RNAseq is shown on the right side. Note the different scales.

Even though the transcriptional start site was accessible for most genes, no significant changes in chromatin accessibility at the loci of those direct target genes could be found at the time points analyzed (Fig. 3.17A, C, E). This finding was the case for time dependent changes, as well as for Ptf1a dependent changes in the chromatin accessibility. Even late induced target genes, such as *mecom* (Fig 3.17E) or *neurog2* (Fig 3.17C) showed no significant differences in their chromatin levels over time or a change due to Ptf1a expression, indicating that Ptf1a indeed does not need chromatin remodeling to activate the investigated direct target genes.

4. Discussion

4.1 The Ptf1a C-terminus is essential for the induced neuronal transmitter phenotype

The bHLH transcription factor Ptf1a not only plays a critical role during neuronal subtype specification where it promotes an inhibitory GABAergic cell fate and suppresses an excitatory glutamatergic cell fate, it also possesses proneural activity (Glasgow *et al.*, 2005; Hoshino *et al.*, 2005; Fujitani *et al.*, 2006; Dullin *et al.*, 2007; Nakhai *et al.*, 2007; Pascual *et al.*, 2007; Hedderich, 2008; Lelievre *et al.*, 2011; Hedderich, 2012). The neuronal subtype specificity of Ptf1a depends on its interaction with Rbpj via two highly conserved motifs in the Ptf1a C-terminus. Ptf1a mutants where the Rbpj binding sites are disrupted through mutation of the tryptophan residues in the C1 and C2 domains to alanine maintain proneural activity, but the induced neurons express glutamatergic marker genes rather than GABAergic markers (Dullin *et al.*, 2007; Hedderich, 2008; Hedderich, 2012; Hanotel *et al.*, 2014).

In this work, a new Ptf1a mutant ($Ptf1a^{T243A}$) was identified, in which the threonine residue within the Ptf1a C2 domain was mutated to alanine. Overexpression of $Ptf1a^{T243A}$ induces a mixed neuronal transmitter phenotype, by activating GABAergic markers like *gad1a* as well as glutamatergic markers like *tlx3.* This mixed neuronal transmitter phenotype, however, is not due to an inhibition of Rbpj binding as demonstrated by the interaction of Rbpj and $Ptf1a^{T243A}$ through BiFC as well the upregulation of Ptf1a early (*prdm13*) and late (*aldh1b1, barhl2, kirrel2*) trimeric target genes. Albeit the induction of these genes was lower than that obtained with the wild-type Ptf1a, mutants where Rbpj interaction is impaired ($Ptf1a^{W242A}$, $Ptf1a^{W224A/W242A}$) do not interact in the BiFC assay and these mutants fail to induce the trimeric target genes.

Studies in mouse and *X. laevis* embryos demonstrated that overexpression of Prdm13 together with Ascl1 or Neurog2 overrides the glutamatergic promoting activity of these factors and promotes a GABAergic cell fate (Chang *et al.*, 2013; Hanotel *et al.*, 2014). However, overexpression of $Ptf1a^{T243A}$ in *X. laevis*

animal caps results in both *prdm13* and *tlx3* expression. Ptf1a^{T243A} is not as effective as the wild-type Ptf1a with regards to *prdm13* upregulation (11-fold less), thus the amount of Prdm13 may be limiting to suppress a glutamatergic fate. However, Ptf1a^{T243E} is only slightly less effective (1.5-fold less) in the induction of *prdm13* compared to the wild-type Ptf1a, but still induces *tlx3* indicating the possibility that an unknown mechanism induced by Ptf1a^{T243A} impairs the ability of *Prdm13* to repress *tlx3.*

Interestingly, a strong BiFC signal was observed between Ptf1a^{T243A} and Prdm13, while only a very week signal and in few cells was observed for Ptf1a or Ptf1a$^{W224A/W242A}$ and Prdm13. In subpopulation of Ptf1a-expressing cells in the *X. laevis* retina that will give rise to glycinergic neurons, Prdm13 negatively regulates *ptf1a* (Bessodes *et al.*, 2017). The molecular basis for Prdm13-repression of ptf1a was shown in the mouse dorsal neural tube, where Prdm13 is recruited to the Ptf1a autoregulatory enhancer through direct interaction with Ptf1a (Mona *et al.*, 2017). Thus, in the Ptf1a^{T243A} mutant, the ability of Prdm13 to interact with Ptf1a and to suppress its activity may be increased. This would lead to a reduced induction of *prdm13* by Ptf1a, so that the inhibition of *tlx3* is not as effective. This hypothesis is supported by the finding that *tlx3* is induced under CHX by Ptf1a (Hedderich, 2012) and that Ptf1a induced expression of *tlx3* at early time points (6-9 h) but at later developmental stages *tlx3* expression is silenced.

Interestingly, overexpressing Ptf1a^{T243A} in *X. laevis* embryos still affects the endogenous *tlx3* expression, so that only ectopically induced neurons become glutamatergic. This would indicate the presence of a second co-factor, that is induced by the wild-type Ptf1a but not by the Ptf1a^{T243A} mutant or co-factor present in the neural tube, and needed for Prdm13 to down-regulates *tlx3* expression. So, it would be interesting to identify the transcription factor complex controlling the target gene induction by Ptf1a or Ptf1a^{T243A} to prove this hypothesis. Furthermore, these data indicate that the induced neuronal transmitter phenotype might be the result of a mixed population of cells within the ectodermal explants, so that it would be also of interest to investigate the target gene induction by the Ptf1a^{T243A} at the single cellular level. This might give a better insight in the induced activity of this mutant.

4.2 Role of phosphorylation on Ptf1a on its activity

Phosphorylation by Cdks on S/T-P sites in proneural bHLH transcription factors like Neurod4, Ascl1 and Neurog2 regulates their activity in inducing neuronal differentiation (Ali *et al.*, 2011; Ali *et al.*, 2014; Hardwick and Philpott, 2015). Although Ptf1a also contains multiple S/T-P sites, an increase in the induction of pan-neuronal marker genes could be detected when overexpressing murine Ptf1a$^{8S/T\rightarrow A}$ in animal caps compared to overexpression of the wild-type murine Ptf1a (Richts, 2013), indicating that strength of Ptf1a activity might not be regulated by Cdk dependent phosphorylation. However, as previously reported (Richts, 2013), the murine Ptf1a constructs in general tend to have a stronger neuronal inducing activity compared to the *X. laevis* Ptf1a when overexpressed in *X. laevis* embryos. This would mean that potential differences in the strength of induction of neuronal differentiation may be masked by the general increase in activity of the murine Ptf1a constructs.

Mutation of a threonine residue to alanine in the Ptf1a C2 domain resulted in the up-regulation of marker genes for both GABAergic and glutamatergic cell fates. This change in the neuronal transmitter phenotype was conserved between the murine and the *X. laevis* Ptf1a, indicating this residue is required and sufficient in the regulation of the induced neuronal subtype. Mutations in a single serine residue in the second helix domain for bHLH transcription factors such as Ascl1 and Neurog2 disrupts their activity during neuronal subtype specification by affecting their binding to certain promoter regions (Ali *et al.*, 2011; Hindley *et al.*, 2012; Ali *et al.*, 2014; Quan *et al.*, 2016). However, as the C2 domain in Ptf1a is well characterized for the interaction with Rbpj (Beres *et al.*, 2006; Hori *et al.*, 2008), such a mechanism is rather unlikely as being responsible for the mixed induced neuronal transmitter phenotype. Interestingly, the neuronal differentiation promoting activity of Ptf1a^{T243A} was reduced compared to the wild-type Ptf1a, a phenotype similar to those of the Ptf1a$^{W2424A/W224A}$ mutant. However, the decreased ability to induce neuronal differentiation is unlikely the reason for the switch in the induced neuronal subtype, as the mixed neuronal subtype induced by Ptf1a^{T243A} can still be observed even when normalized for the various strength of neuronal differentiation inducing activity. The differences in the ability of the different

Ptf1a mutants to promote neuronal differentiation might occur due to differences in the protein stability of those mutants. Protein stability was not directly measured and would be of interest to determine, but the similar BiFC signal observed for all mutants with E12 is not indicative of dramatically differences in stability. However, it should be noted that the concentration used for the BiFC studies was more than 10-fold higher than used in the ectodermal explant assays.

Direct evidence that Ptf1a is indeed phosphorylated on the T_{243} position is still missing. However, overexpression of the phosphomimic mutant (Ptf1^{T243E}) also induces a mixed neuronal transmitter phenotype. The activity of Ptf1^{T243E} was more similar to the activity of wild-type Ptf1a indicating that the presence of a negative charge at this position may influence the correct neuronal subtype inducing activity, supporting a role for phosphorylation at this residue. Interestingly, similar to the Ptf1^{T243A} mutant, the Ptf1^{T243E} still strongly interacts with Prdm13 in BiFC assays. This may explain why the induced neuronal transmitter phenotype by Ptf1^{T243E} is still mixed, even if it resembles more the wild-type Ptf1a than Ptf1^{T243A} in GABAergic gene induction. On the other hand, the negative charge introduced by a single phosphomimic mutation is less strong than a phosphorylated residue (Strickfaden *et al.*, 2007; Pearlman *et al.*, 2011). So, a complete rescue might not be possible by introducing just a single glutamate residue and the introduction of two adjacent phosphomimic mutations may be a more suitable construct (Strickfaden *et al.*, 2007; Pearlman *et al.*, 2011). In future, it would be interesting to provide evidence that the phosphorylation on the T_{243} residue occurs during neurogenesis on Ptf1a to gain a better understanding if phosphorylation indeed regulates Ptf1a activity.

4.3 BAF complex mediated chromatin remodeling is important for the activation of delayed target gene expression by Ptf1a

The BAF chromatin remodeling complex has been demonstrated to be essential for vertebrate neurogenesis (Seo *et al.*, 2005; Narayanan *et al.*, 2015; Bachmann *et al.*, 2016). A knock-down of the BAF catalytic core unit Brg1

impairs neuronal differentiation induced by proneural transcription factors like Neurog2 and Neurod1 (Seo *et al.*, 2005). Further supporting the importance of a functional BAF complex for neurogenesis, Ptf1a-induced neuronal differentiation is also impaired by a knock-down of Brg1 in *X. laevis* ectodermal explants. Considering the temporal induction of target genes by Ptf1a, only a few direct Ptf1a target genes were affected after 3 h (4 out of 22 genes), while the amount of affected direct target genes increases for delayed direct target genes (12 h, 7 out of 10 genes). Even if this tendency might be the result of a bias in the selection of target genes studied by Nanostring analysis, indications exist that a functional Brg1 is required for the induction of at least a subset of delayed Ptf1a target genes. A similar effect has been shown during myogenesis, where BAF complex dependent chromatin remodeling is required for the activation of only a subset of target genes involved in muscle differentiation (de la Serna *et al.*, 2001; Roy *et al.*, 2002; Berkes *et al.*, 2004). However, the general effect of a Brg1 knock-down on the activation of target genes by Ptf1a was quite low (53 out of 819 genes). Nevertheless, the finding that the most strongly affected genes were indirect Ptf1a target genes indicates that additional mechanism are responsible for the delayed activation of target genes by Ptf1a. Furthermore, besides of its role in remodeling chromatin, the subunits of BAF complex can directly interact with other proteins like transcription factors and so activate or inhibit their function (Zhan *et al.*, 2011; Ninkovic *et al.*, 2013). It would be of interest for future studies to compare Ptf1a overexpressing ectopic explants in presence of a Brg1 morpholino by ATAC-seq to demonstrate that the effects Brg1 knockdown on the upregulations of the identified genes is indeed due to chromatin remodeling. However, since it has been reported that a knock-down of Brg1 cannot completely abolish Brg1 activity due to putative maternal expression (Li *et al.*, 2013) and the fact that a down-regulation of Brg1 is associated with cell-cycle arrest and so lethal for the cells (Li *et al.*, 2013), meaning that a complete Brg1 activity cannot be degraded without killing the cells, suggesting that a higher number of genes dependent on Brg1 might exist. Furthermore, the BAF chromatin remodeling complex can also contain Brm instead of Brg1 as catalytic subunit, so that activation of several target genes might not be

dependent on Brg1 but on Brm instead. Performing a double-knock-down of Brg1 and Brm would give new insights in this matter.

4.4 Ptf1a does not need open chromatin to induce its targets

Active transcription of target genes has been associated with accessible chromatin at target genes regulatory regions. It has been reported that chromatin regions of many proneural genes become accessible before their transcription starts (Chen and Dent, 2014; Hontelez *et al.*, 2015; Mo *et al.*, 2015). Here, it has been demonstrated that Ptf1a is able to cause changes in the state of chromatin of some of its direct targets, although it has not been shown if this is a direct or indirect effect. However, most of investigated direct Ptf1a target genes lay in quite closed chromatin regions, whose pattern did not change over time or in dependency of Ptf1a. Since the quality of the ATAC sequencing library was impaired due to redundancy of sequences, these results should be viewed caution. Additional open chromatin regions in those target genes might be detected in samples with more unique reads. Nevertheless, the results indicate that Ptf1a does not need open chromatin to drive the activation of its target genes. This is supported by the fact, that other proneural bHLH transcription factors like Neurod1, Ascl1 and Neurog2 can bind to closed chromatin regions to induce the expression of their target genes (Soufi *et al.*, 2015; Pataskar *et al.*, 2016; Smith *et al.*, 2016). In parallel to the onset of gene expression, the proneural genes induce changes in the chromatin pattern, which then lead to a stabilization of transcription. Studies investigating the distribution of maternally provided epigenetic marks in *X. tropicalis* indicate that many marks for enhancer elements are zygotically provided and are located in regions characterized by repressive histone marks and high levels of methylated DNA (Hontelez *et al.*, 2015), further supporting the idea that Ptf1a is a pioneer transcription factor, which does not need open chromatin region to activate transcription of their target genes. On the other hand, it was reported that the promoter regions of late transcribed genes are already poised with activating histone marks and often are hypomethylated at a very early stage of the embryo (Hontelez *et al.*, 2015) and that the presence of active marks is not sufficient to drive target gene transcription (Hontelez *et*

al., 2015). A similar effect could also be detected in the ATAC sequencing since for most of the Ptf1a target genes, open chromatin regions could be found at the transcriptional start site of the genes, while the remaining regions were in general not accessible, supporting the idea that open chromatin is not sufficient for the onset of target gene transcription by Ptf1a. However, whether Ptf1a also opens the chromatin of most of its target genes like Neurod1 (Pataskar *et al.*, 2016) remains unclear. After 12 h of Ptf1a induction, such a phenomenon could not be detected. But as also early expressed Ptf1a target genes were mostly located in closed chromatin regions, which did not change at the later stage, it might be that Ptf1a activates its target genes without opening the chromatin. However, at this time point, the expression of delayed target genes has just started, so that a change in the chromatin might not be detectable at this stage. Performing ATAC sequencing at a later stage after Ptf1a induction would give more insights in this question.

4.5 Mechanisms driving the delayed activation of target genes

Nanostring and RNA-seq data from Ptf1a overexpressing animal caps indicate that Ptf1a activates its direct target genes at different time points. Interestingly, by comparing the induced target genes with a list of genes being activated by Ptf1a in the presence of the translational inhibitor CHX (Schneider-Poetsch *et al.*, 2010), the time of late target gene induction could be detected at a 12 h timepoint after gene induction. This indicates that certain events have to take place leading to the activation of first delayed target genes.

Interestingly, delayed target gene activation correlates with the timing of *tubb2b* activation. As *tubb2b* is a marker for post-mitotic neurons (Oschwald *et al.*, 1991), indicating that the timing of delayed target gene activation may correlate with the exit of the cell cycle. Considering that direct target genes having their onset after 12 h of Ptf1a induction and are highly enriched for functions in neuronal specification, while early activated genes are more associated with regulation of transcription and the regulation of the cell cycle, would support such a mechanism. Together this would mean that cell cycle escape triggers the events leading to the activation of late target genes.

However, how cell cycle escape can be associated with the delayed expression of Ptf1a late target genes need to be further analyzed. It has been reported that the length of the cell cycle plays an essential role in neuronal differentiation, as an elongation of the cell cycle is required for inducing the onset of differentiation by proneural bHLH transcription factors (Lange *et al.*, 2009; Lange and Calegari, 2010). Furthermore, the activity of many bHLH transcription factors involved in promoting neuronal differentiation including Neurog2 or Neurod4, are highly regulated by the cell cycle through Cdk-mediated phosphorylation (Ali *et al.*, 2011; Hindley *et al.*, 2012; Hardwick and Philpott, 2015). As Ptf1a also contains residues that would make it a candidate for Cdk-dependent phosphorylation, a cell cycle dependent regulation of Ptf1a activity cannot be excluded.

Chromatin remodeling has been reported to regulate transcription during development since actively transcribed genes are associated with accessible chromatin as well as activating histone marks and demethylated DNA (Yao and Jin, 2014; Hsieh and Zhao, 2016; Yao *et al.*, 2016). However, the findings in ATAC-seq that Ptf1a target genes are located within rather closed chromatin regions suggests that chromatin remodeling plays a minor role in the delayed activation of Ptf1a target genes. This is further supported by the fact that the presence of open chromatin marks is not sufficient for inducing transcription (Hontelez *et al.*, 2015) and that high levels of DNA methylation, which is associated with transcriptional silencing, does not affect the transcription of target genes in the early embryo (Bogdanovic *et al.*, 2012). Considering that especially late Ptf1a target genes need Brg1 to be expressed, while induction of most direct early Ptf1a target genes is not affected, BAF complex mediated chromatin remodeling still has an influence on late target gene activation. The finding that Brg1 is required for the activation of several of the late Ptf1a direct target genes would support an implement of cell cycle regulation in Ptf1a late target gene activation. This is further supported by Brg1 has been reported to be involved in the regulation of cell cycle exit via interaction with Geminin (Seo *et al.*, 2005). This could also explain that early Ptf1a target genes are mostly unaffected by a Brg1 knockdown, because as those genes are mostly involved in transcriptional and cell cycle regulation, their activity is required before cell cycle exit, which is regulated by Brg1. Nevertheless, chromatin remodeling

alone cannot explain the delayed activation of late target genes, indicating that several mechanisms drive the delate activation of target genes. A potential mechanism might be the presence or absence of a certain Co-factor or repressor regulating the transcription of those genes. Such a possibility would be supported by findings that the onset of late Ptf1a target gene activation is preponed in presence of CHX (Hedderich, 2012).

Together, these indications lead to a model that Ptf1a induces at least two waves of target gene activation. The first one is activated nearly immediately and mostly controls the transcription of genes controlling the differentiation of the cell to a neuronal cell fate, which leads to a cell cycle escape. An exception is Prdm13, which allows for an early bias of the progenitor cell to a GABAergic cell fate. At the time of cell cycle arrest, a second wave of target genes are activated, which further regulate the subtype specification and function of the induced neuron. Activation of these genes is regulated by several mechanisms. BAF complex mediated chromatin remodeling is required for the activation of a subset of those genes, while another unknown mechanism like the presence an unknown Co-factor or repressor controls the expression of the other late target genes. This would mean that investigating the Ptf1a transcription factor complex at the early and the late time point would be interesting to identify which differences occur in the composition of these complexes between those two time points.

5. Bibliography

Aaku-Saraste, E., et al. (1996). "Loss of occludin and functional tight junctions, but not ZO-1, during neural tube closure—remodeling of the neuroepithelium prior to neurogenesis." Dev Biol **180**(2): 664-679.
Afelik, S., et al. (2006). "Combined ectopic expression of Pdx1 and Ptf1a/p48 results in the stable conversion of posterior endoderm into endocrine and exocrine pancreatic tissue." Genes Dev **20**(11): 1441-1446.
Ahnfelt-Rønne, J., et al. (2012). "Ptf1a control of Dll1 reveals an alternative to the lateral inhibition mechanism." Development **139**: 33-45.
Al-Shammari, M., et al. (2011). "A novel PTF1A mutation in a patient with severe pancreatic and cerebellar involvement." Clin Genet **80**(2): 196-198.
Ali, F., et al. (2011). "Cell cycle-regulated multi-site phosphorylation of Neurogenin 2 coordinates cell cycling with differentiation during neurogenesis." Development **138**(19): 4267-4277.
Ali, F. R., et al. (2014). "The phosphorylation status of Ascl1 is a key determinant of neuronal differentiation and maturation in vivo and in vitro." Development **141**(11): 2216-2224.
Allain, A. E., et al. (2011). "Maturation of the GABAergic transmission in normal and pathologic motoneurons." Neural Plast **2011**: 905624.
Bachmann, C., et al. (2016). "mSWI/SNF (BAF) Complexes Are Indispensable for the Neurogenesis and Development of Embryonic Olfactory Epithelium." PLoS Genet **12**(9): e1006274.
Banik, A., et al. (2017). "Maternal Factors that Induce Epigenetic Changes Contribute to Neurological Disorders in Offspring." Genes **8**(6): 150.
Bao, Y. and X. Shen (2007). "INO80 subfamily of chromatin remodeling complexes." Mutation Research/Fundamental and Molecular Mechanisms of Mutagenesis **618**(1): 18-29.
Beatus, P. and U. Lendahl (1998). "Notch and neurogenesis." Journal of neuroscience research **54**(2): 125-136.
Bellefroid, E. J., et al. (1996). "X-MyT1, a Xenopus C2HC-type zinc finger protein with a regulatory function in neuronal differentiation." Cell **87**: 1191-1202.
Bellefroid, E. J., et al. (1998). "Xiro3 encodes a Xenopus homolog of the Drosophila Iroquois genes and functions in neural specification." EMBO J. **17**(1): 191-203.
Beres, T. M., et al. (2006). "PTF1 is an organ-specific and Notch-independent basic helix-loop-helix complex containing the mammalian Suppressor of Hairless (RBP-J) or its paralogue, RBP-L." Mol Cell Biol **26**(1): 117-130.
Berkes, C. A., et al. (2004). "Pbx marks genes for activation by MyoD indicating a role for a homeodomain protein in establishing myogenic potential." Molecular cell **14**(4): 465-477.
Bernstein, B. E., et al. (2007). "The mammalian epigenome." Cell **128**(4): 669-681.
Bertrand, N., et al. (2002). "Proneural genes and the specification of neural cell types." Nat Rev Neurosci **3**(7): 517-530.
Bessodes, N., et al. (2017). "Prdm13 forms a feedback loop with Ptf1a and is required for glycinergic amacrine cell genesis in the Xenopus Retina." Neural Dev **12**(1): 16.

Bogdanovic, O., et al. (2012). "The epigenome in early vertebrate development." Genesis **50**(3): 192-206.
Bonev, B., et al. (2012). "MicroRNA-9 modulates Hes1 ultradian oscillations by forming a double-negative feedback loop." Cell reports **2**(1): 10-18.
Borchers, A. and T. Pieler (2010). "Programming pluripotent precursor cells derived from Xenopus embryos to generate specific tissues and organs." Genes **1**(3): 413-426.
Borodinsky, L. N. (2017). "Xenopus laevis as a Model Organism for the Study of Spinal Cord Formation, Development, Function and Regeneration." Frontiers in Neural Circuits **11**(90).
Borromeo, M. D., et al. (2014). "A transcription factor network specifying inhibitory versus excitatory neurons in the dorsal spinal cord." Development **141**(14): 2803-2812.
Bouwmeester, T., et al. (1996). "Cerberus is a head-inducing secreted factor expressed in the anterior endoderm of Spemann's organizer." Nature **382**(6592): 595-601.
Bowes, J. B., et al. (2007). "Xenbase: a Xenopus biology and genomics resource." Nucleic Acids Res **36**(suppl_1): D761-D767.
Bray, S. J. (2006). "Notch signalling: a simple pathway becomes complex." Nature reviews Molecular cell biology **7**(9): 678-689.
Brewster, R., et al. (1998). "Gli/Zic factors pattern the neural plate by defining domains of cell differentiation." Nature **393**(6685): 579-583.
Briscoe, J. and J. Ericson (2001). "Specification of neuronal fates in the ventral neural tube." Current Opinion in Neurobiology **11**: 43-49.
Briscoe, J., et al. (2000). "A Homeodomain Protein Code Specifies Progenitor Cell Identity and Neuronal Fate in the Ventral Neural Tube." Cell **101**: 435-445.
Buenrostro, J. D., et al. (2013). "Transposition of native chromatin for fast and sensitive epigenomic profiling of open chromatin, DNA-binding proteins and nucleosome position." Nat Methods **10**(12): 1213-1218.
Burgess, R., et al. (1995). "Paraxis: a basic helix-loop-helix protein expressed in paraxial mesoderm and developing somites." Dev Biol **168**(2).
Castro, D. S., et al. (2011). "A novel function of the proneural factor Ascl1 in progenitor proliferation identified by genome-wide characterization of its targets." Genes Dev **25**(9): 930-945.
Castro, D. S., et al. (2006). "Proneural bHLH and Brn proteins coregulate a neurogenic program through cooperative binding to a conserved DNA motif." Dev Cell **11**(6): 831-844.
Cau, E., et al. (2002). "Mash1 and Ngn1 control distinct steps of determination and differentiation in the olfactory sensory neuron lineage." Development **129**(8): 1871-1880.
Cau, E., et al. (1997). "Mash1 activates a cascade of bHLH regulators in olfactory neuron progenitors." Development **124**(8): 1611-1621.
Cedar, H. and Y. Bergman (2009). "Linking DNA methylation and histone modification: patterns and paradigms." Nature Reviews Genetics **10**(5): 295-304.
Chang, J. C., et al. (2013). "Prdm13 mediates the balance of inhibitory and excitatory neurons in somatosensory circuits." Dev Cell **25**(2): 182-195.
Chen, T. and S. Y. Dent (2014). "Chromatin modifiers and remodellers: regulators of cellular differentiation." Nat Rev Genet **15**(2): 93-106.

Chitnis, A. and C. Kintner (1995). "Neural induction and neurogenesis in amphibian embryos. ." Perspect Dev Neurobiol **3**(1): 3-15.
Cockell, M., et al. (1989). "Identification of a cell-specific DNA-binding activity that interacts with a transcriptional activator of genes expressed in the acinar pancreas." Mol Cell Biol **9**(6): 2464-2476.
Cserjesi, P., et al. (1995). "Scleraxis: a basic helix-loop-helix protein that prefigures skeletal formation during mouse embryogenesis." Development **121**(4): 1099-1110.
Davis, R. L. and D. L. Turner (2001). "Vertebrate hairy and Enhancer of split related proteins: transcriptional repressors regulating cellular differentiation and embryonic patterning." Oncogene **20**(58): 8342-8357.
Dawson, S. R., et al. (1995). "Specificity for the hairy/enhancer of split basic helix-loop-helix (bHLH) proteins maps outside the bHLH domain and suggests two separable modes of transcriptional repression." Mol Cell Biol **15**(12): 6923-6931.
de la Calle-Mustienes, E., et al. (2002). "Xiro homeoproteins coordinate cell cycle exit and primary neuron formation by upregulating neuronal-fate repressors and downregulating the cell-cycle inhibitor XGadd45-γ." Mech Dev **119**(1): 69-80.
de la Serna, I. L., et al. (2001). "MyoD Can Induce Cell Cycle Arrest but Not Muscle Differentiation in the Presence of Dominant Negative SWI/SNF Chromatin Remodeling Enzymes." Journal of Biological Chemistry **276**(44): 41486-41491.
De Robertis, E. M. and H. Kuroda (2004). "Dorsal-Ventral Patterning and Neural Induction in Xenopus Embryos." Annu Rev Cell Dev Biol **20**: 285-308.
Delgado-Morales, R., et al. (2017). "Epigenetic mechanisms during ageing and neurogenesis as novel therapeutic avenues in human brain disorders." Clinical epigenetics **9**(1): 67.
Dobin, A., et al. (2013). "STAR: ultrafast universal RNA-seq aligner." Bioinformatics **29**(1): 15-21.
Droz, S. T. and K. A. McLaughlin (2017). Use of Xenopus Frogs to Study Renal Development/Repair. Kidney Development and Disease. R. K. Miller. Cham, Springer International Publishing**:** 77-107.
Dubey, A. and J.-P. Saint-Jeannet (2017). "Modeling Human Craniofacial Disorders in Xenopus." Current Pathobiology Reports **5**(1): 79-92.
Dubois, L., et al. (1998). "XCoe2, a transcription factor of the Col/Olf-1/EBF family involved in the specification of primary neurons in Xenopus." Curr Biol **8**(4): 199-209.
Dullin, J. P., et al. (2007). "Ptf1a triggers GABAergic neuronal cell fates in the retina." BMC Dev Biol **7**: 110.
Durak, O., et al. (2016). "Chd8 mediates cortical neurogenesis via transcriptional regulation of cell cycle and Wnt signaling." Nat Neurosci.
Egan, C. M., et al. (2013). "CHD5 is required for neurogenesis and has a dual role in facilitating gene expression and polycomb gene repression." Dev Cell **26**(3): 223-236.
Ellis, P., et al. (2004). "SOX2, a persistent marker for multipotential neural stem cells derived from embryonic stem cells, the embryo or the adult." Developmental neuroscience **26**(2-4): 148-165.
Farah, M. H., et al. (2000). "Generation of neurons by transient expression of neural bHLH proteins in mammalian cells." Development **127**: 693-702.

Feng, J., et al. (2012). "Identifying ChIP-seq enrichment using MACS." Nat Protoc **7**(9): 1728-1740.
Fode, C., et al. (2000). "A role for neural determination genes in specifying the dorsoventral identity of telencephalic neurons." Genes and Development **14**: 67-80.
Fujitani, Y., et al. (2006). "Ptf1a determines horizontal and amacrine cell fates during mouse retinal development." Development **133**(22): 4439-4450.
Gammill, L. S. and H. Sive (1997). "Identification of otx2 target genes and restrictions in ectodermal competence during Xenopus cement gland formation." Development **124**(2): 471-481.
Gao, S. (2017). "Epigenetic regulation of somatic cell reprogramming Yixuan Wang, Yan Bi and Shaorong Gao." Current opinion in genetics & development **46**: 156-163.
Gao, Z., et al. (2009). "Neurod1 is essential for the survival and maturation of adult-born neurons." Nat Neurosci **12**(9): 1090.
Gaspar-Maia, A., et al. (2009). "Chd1 regulates open chromatin and pluripotency of embryonic stem cells." Nature **460**(7257): 863-868.
Glasgow, S. M., et al. (2005). "Ptf1a determines GABAergic over glutamatergic neuronal cell fate in the spinal cord dorsal horn." Development **132**(24): 5461-5469.
Gomez-Skarmeta, J. L., et al. (1998). "Xiro, a Xenopus homolog of the Drosophila Iroquois complex genes, controls development at the neural plate." EMBO J. **17**(1): 181-190.
Goodwin, L. R. and D. J. Picketts (2017). "The role of ISWI chromatin remodeling complexes in brain development and neurodevelopmental disorders." Molecular and Cellular Neuroscience.
Gowan, K., et al. (2001). "Crossinhibitory Activities of Ngn1 and Math1 Allow Specification of Distinct Dorsal Interneurons." Neuron **31**(2): 219-232.
Graham, V., et al. (2003). "SOX2 functions to maintain neural progenitor identity." Neuron **39**(5): 749-765.
Gross, M. K., et al. (2002). "Lbx1 Specifies Somatosensory Association Interneurons in the Dorsal Spinal Cord." Neuron **34**: 535-549.
Groves, A. K. and C. LaBonne (2014). "Setting appropriate boundaries: fate, patterning and competence at the neural plate border." Dev Biol **389**(1): 2-12.
Guénette, S. A., et al. (2013). "Pain Perception and Anaesthesia in Research Frogs." Experimental Animals **62**(2): 87-92.
Hamburger, V. (1969). "Hans Spemann and the organizer concept." Cellular and Molecular Life Sciences **25**(11): 1121-1125.
Hanotel, J., et al. (2014). "The Prdm13 histone methyltransferase encoding gene is a Ptf1a-Rbpj downstream target that suppresses glutamatergic and promotes GABAergic neuronal fate in the dorsal neural tube." Dev Biol **386**(2): 340-357.
Hardcastle, Z., et al. (2000). "FGF-8 stimulates neuronal differentiation through FGFR-4a and interferes with mesoderm induction in Xenopus embryos." Current Biology **10**(23): 1511-1514.
Hardwick, L. J., et al. (2015). "Cell cycle regulation of proliferation versus differentiation in the central nervous system." Cell Tissue Res **359**(1): 187-200.

Hardwick, L. J. and A. Philpott (2015). "Multi-site phosphorylation regulates NeuroD4 activity during primary neurogenesis: a conserved mechanism amongst proneural proteins." Neural Dev **10**: 15.
Harland, R. M. (1991). "In situ hybridization: an improved whole-mount method for Xenopus embryos." Methods Cell Biol **36**: 685-695.
Hartenstein, V. (1989). "Early neurogenesis in Xenopus: the spatio-temporal pattern of proliferation and cell lineages in the embryonic spinal cord." Neuron. **3**(4): 399-411.
Hartenstein, V. (1993). "Early pattern of neuronal differentiation in the Xenopus embryonic brainstem and spinal cord." Journal of Comparative Neurology **328**(2): 213-231.
Heasman, J., et al. (2000). "βCatenin Signaling Activity Dissected in the Early Xenopus Embryo: A Novel Antisense Approach." Dev Biol **222**(1): 124-134.
Hedderich, M. (2008) Diploma Thesis: Charakterisierung der proneuralen Aktivität von Ptf1a/p48 in Xenopus University Medical Center Göttingen, Department of Developmental Biochemistry, University of Göttingen
Hedderich, M. (2012). "Doctoral Thesis: Molecular characterization of Ptf1a activity during *Xenopus* embryogenesis."
Helms, A. W. and J. E. Johnson (2003). "Specification of dorsal spinal cord interneurons." Curr Opin Neurobiol **13**(1): 42-49.
Hemmati-Brivanlou, A., et al. (1994). "Follistatin, an Antagonist of Activin, Is Expressed in the Spemann Organizer and Displays Direct Neuralizing Activity." Cell **77**: 283-295.
Hemmati-Brivanlou, A. and D. A. Melton (1994). "Inhibition of Activin Receptor Signaling Promotes Neuralization in Xenopus." Cell **77**: 273-281.
Henke, R. M., et al. (2009). "Neurog2 is a direct downstream target of the Ptf1a-Rbpj transcription complex in dorsal spinal cord." Development **136**(17): 2945-2954.
Hernandez-Miranda, L. R., et al. (2017). "The dorsal spinal cord and hindbrain: From developmental mechanisms to functional circuits." Dev Biol **432**(1): 34-42.
Hindley, C., et al. (2012). "Post-translational modification of Ngn2 differentially affects transcription of distinct targets to regulate the balance between progenitor maintenance and differentiation." Development **139**(10): 1718-1723.
Ho, L. and G. R. Crabtree (2010). "Chromatin remodelling during development." Nature **463**(7280): 474-484.
Ho, L., et al. (2009). "An embryonic stem cell chromatin remodeling complex, esBAF, is essential for embryonic stem cell self-renewal and pluripotency." Proceedings of the National Academy of Sciences **106**(13): 5181-5186.
Hollemann, T., et al. (1996). "Xenopus Xsal-1, a vertebrate homolog of the region specific homeotic gene spalt of Drosophila." Mech Dev **55**(1): 19-32.
Hontelez, S., et al. (2015). "Embryonic transcription is controlled by maternally defined chromatin state." Nat Commun **6**: 10148.
Hori, K., et al. (2008). "A nonclassical bHLH Rbpj transcription factor complex is required for specification of GABAergic neurons independent of Notch signaling." Genes Dev **22**(2): 166-178.
Hori, K. and M. Hoshino (2012). "GABAergic neuron specification in the spinal cord, the cerebellum, and the cochlear nucleus." Neural Plast **2012**: 921732.

Horikawa, K., et al. (2006). "Noise-resistant and synchronized oscillation of the segmentation clock." Nature **441**(7094): 719-723.
Hoshino, M., et al. (2005). "Ptf1a, a bHLH transcriptional gene, defines GABAergic neuronal fates in cerebellum." Neuron **47**(2): 201-213.
Houtmeyers, R., et al. (2013). "The ZIC gene family encodes multi-functional proteins essential for patterning and morphogenesis." Cellular and Molecular Life Sciences **70**(20): 3791-3811.
Hoveyda, N., et al. (1999). "Neonatal diabetes mellitus and cerebellar hypoplasia/agenesis: report of a new recessive syndrome." J Med Genet **36**: 700-704.
Hsieh, J. and X. Zhao (2016). "Genetics and Epigenetics in Adult Neurogenesis." Cold Spring Harb Perspect Biol **8**(6).
Huang, M., et al. (2008). "Ptf1a, Lbx1 and Pax2 coordinate glycinergic and peptidergic transmitter phenotypes in dorsal spinal inhibitory neurons." Dev Biol **322**(2): 394-405.
Imayoshi, I. and R. Kageyama (2011). "The role of Notch signaling in adult neurogenesis." Molecular neurobiology **44**(1): 7-12.
Iskusnykh, I. Y., et al. (2016). "Loss of Ptf1a Leads to a Widespread Cell-Fate Misspecification in the Brainstem, Affecting the Development of Somatosensory and Viscerosensory Nuclei." J Neurosci **36**(9): 2691-2710.
Jaenisch, R. and A. Bird (2003). "Epigenetic regulation of gene expression: how the genome integrates intrinsic and environmental signals." Nature genetics **33**: 245-254.
Jenuwein, T. and C. D. Allis (2001). "Translating the Histone Code." Science **293**(5532): 1074-1080.
Jessell, T. M. and J. Dodd (1990). "Floor plate-derived signals and the control of neural cell pattern in vertebrates." Harvey Lect **86**: 87-128.
Jones, K. M., et al. (2015). "CHD7 maintains neural stem cell quiescence and prevents premature stem cell depletion in the adult hippocampus." Stem Cells **33**(1): 196-210.
Jusuf, P. R., et al. (2012). "Biasing amacrine subtypes in the Atoh7 lineage through expression of Barhl2." Journal of Neuroscience **32**(40): 13929-13944.
Kadoch, C., et al. (2013). "Proteomic and bioinformatic analysis of mammalian SWI/SNF complexes identifies extensive roles in human malignancy." Nature genetics **45**(6): 592-601.
Kageyama, R., et al. (2008). "Dynamic Notch signaling in neural progenitor cells and a revised view of lateral inhibition." Nat Neurosci **11**(11): 1247-1251.
Kanekar, S., et al. (1997). "Xath5 participates in a network of bHLH genes in the developing Xenopus retina." Neuron **19**(5): 981-994.
Kani, S., et al. (2010). "Proneural gene-linked neurogenesis in zebrafish cerebellum." Dev Biol **343**(1-2): 1-17.
Kawaguchi, Y., et al. (2002). "The role of the transcriptional regulator Ptf1a in converting intestinal to pancreatic progenitors." Nat Genet **32**(1): 128-134.
Kim, P., et al. (1997). "XATH-1, a Vertebrate Homolog of Drosophila atonal, Induces Neuronal Differentiation within Ectodermal Progenitors." Dev Biol **187**: 1-12.
Kiyota, T. and T. Kinoshita (2002). "Cysteine-rich region of X-Serrate-1 is required for activation of Notch signaling in Xenopus primary neurogenesis." International Journal of Developmental Biology **46**(8): 1057-1060.

Kofent, J. and F. M. Spagnoli (2016). "Xenopus as a model system for studying pancreatic development and diabetes." Seminars in Cell & Developmental Biology **51**: 106-116.
Krapp, A., et al. (1996). "The p48 DNA-binding subunit of transcription factor PTF1 is a new exocrine pancreas-specific basic helix-loop-helix protein." EMBO J. **15**(16): 4317-4329.
Krapp, A., et al. (1998). "The bHLH protein PTF1-p48 is essential for the formation of the exocrine and the correct spatial organization of the endocrine pancreas." Genes Dev **12**(23): 3752-3763.
Kroll, K. L. (2007). "Geminin in embryonic development: coordinating transcription and the cell cycle during differentiation." Front Biosci **12**(1395): 409.
Kroll, K. L., et al. (1998). "Geminin, a neuralizing molecule that demarcates the future neural plate at the onset of gastrulation." Development **125**(16): 3247-3258.
Kuroda, H., et al. (2004). "Neural induction in Xenopus: requirement for ectodermal and endomesodermal signals via Chordin, Noggin, β-Catenin, and Cerberus." PLoS biology **2**(5): e92.
Lacomme, M., et al. (2012). "NEUROG2 drives cell cycle exit of neuronal precursors by specifically repressing a subset of cyclins acting at the G1 and S phases of the cell cycle." Mol Cell Biol **32**(13): 2596-2607.
Lamborghini, J. E. (1980). "Rohon-beard cells and other large neurons in Xenopus embryos originate during gastrulation." Journal of Comparative Neurology **189**(2): 323-333.
Lange, C. and F. Calegari (2010). "Cdks and cyclins link G1 length and differentiation of embryonic, neural and hematopoietic stem cells." Cell Cycle **9**(10): 1893-1900.
Lange, C., et al. (2009). "Cdk4/cyclinD1 overexpression in neural stem cells shortens G1, delays neurogenesis, and promotes the generation and expansion of basal progenitors." Cell stem cell **5**(3): 320-331.
Langmead, B. and S. L. Salzberg (2012). "Fast gapped-read alignment with Bowtie 2." Nat Methods **9**(4): 357-359.
Launay, C., et al. (1996). "A truncated FGF receptor blocks neural induction by endogenous Xenopus inducers." Development **122**(3): 869-880.
Le Dréau, G. and E. Martí (2012). "Dorsal–ventral patterning of the neural tube: a tale of three signals." Dev Neurobiol **72**(12): 1471-1481.
Leclerc, C., et al. (1997). "L-type calcium channel activation controls the in vivo transduction of the neuralizing signal in the amphibian embryos." Mech Dev **64**(1-2): 105-110.
Leclerc, C., et al. (2012). "The calcium: an early signal that initiates the formation of the nervous system during embryogenesis." Frontiers in molecular neuroscience **5**: 64.
Leclerc, C., et al. (2000). "Imaging patterns of calcium transients during neural induction in Xenopus laevis embryos." Journal of cell science **113**(19): 3519-3529.
Lee-Liu, D., et al. (2017). "The African clawed frog Xenopus laevis: A model organism to study regeneration of the central nervous system." Neuroscience Letters **652**: 82-93.
Lee, J. E. (1997). "Basic helix-loop-helix genes in neural development." Curr Opin Neurobiol **7**(1): 13-20.

Lefebvre, V., et al. (2007). "Control of cell fate and differentiation by Sry-related high-mobility-group box (Sox) transcription factors." The international journal of biochemistry & cell biology **39**(12): 2195-2214.
Lei, Y., et al. (2012). "Efficient targeted gene disruption in Xenopus embryos using engineered transcription activator-like effector nucleases (TALENs)." PNAS **109**(43): 17484-17489.
Lelievre, E. C., et al. (2011). "Ptf1a/Rbpj complex inhibits ganglion cell fate and drives the specification of all horizontal cell subtypes in the chick retina." Dev Biol **358**(2): 296-308.
Lessard, J., et al. (2007). "An essential switch in subunit composition of a chromatin remodeling complex

during neural development. Neuron. 2007; 55:201–21." Neuron. **55**: 201-221.
Lewis, J. (1998). Notch signalling and the control of cell fate choices in vertebrates. Seminars in Cell & Developmental Biology, Elsevier.
Li, H., et al. (2011). "Phosphorylation regulates OLIG2 cofactor choice and the motor neuron-oligodendrocyte fate switch." Neuron **69**(5): 918-929.
Li, H., et al. (2009). "The sequence alignment/map format and SAMtools." Bioinformatics **25**(16): 2078-2079.
Li, M., et al. (2006). "The role of early lineage in GABAergic and glutamatergic cell fate determination in Xenopus laevis." J Comp Neurol **495**(6): 645-657.
Li, W., et al. (2013). "Brg1 governs distinct pathways to direct multiple aspects of mammalian neural crest cell development." Proceedings of the National Academy of Sciences **110**(5): 1738-1743.
Li, Y. and N. E. Baker (2001). "Proneural enhancement by Notch overcomes Suppressor-of-Hairless repressor function in the developing Drosophila eye." Current Biology **11**(5): 330-338.
Liem, K. F., Jr.,, et al. (1997). "A role for the roof plate and its resident TGFbeta-related proteins in neuronal patterning in the dorsal spinal cord." Cell **91**(1): 127-138.
Lin, H., et al. (2017). "KDM3A-mediated demethylation of histone H3 lysine 9 facilitates the chromatin binding of Neurog2 during neurogenesis." Development **144**(20): 3674-3685.
Lindsell, C. E., et al. (1996). "Expression Patterns ofJagged, Delta1, Notch1, Notch2, andNotch3Genes Identify Ligand–Receptor Pairs That May Function in Neural Development." Molecular and Cellular Neuroscience **8**(1): 14-27.
Louvi, A. and S. Artavanis-Tsakonas (2006). "Notch signalling in vertebrate neural development." Nature Reviews Neuroscience **7**(2): 93-102.
Love, M. I., et al. (2014). "Moderated estimation of fold change and dispersion for RNA-seq data with DESeq2." Genome Biology **15**(12): 550.
Luger, K. and T. J. Richmond (1998). "The histone tails of the nucleosome." Current opinion in genetics & development **8**(2): 140-146.
Ma, Q., et al. (1996). "Identification of neurogenin, a Vertebrate Neuronal Determination Gene." Cell **87**.
Ma, Y. C., et al. (2008). "Regulation of motor neuron specification by phosphorylation of neurogenin 2." Neuron **58**(1): 65-77.
Masui, T., et al. (2007). "Early pancreatic development requires the vertebrate Suppressor of Hairless (RBPJ) in the PTF1 bHLH complex." Genes Dev **21**(20): 2629-2643.

Masui, T., et al. (2010). "Replacement of Rbpj with Rbpjl in the PTF1 complex controls the final maturation of pancreatic acinar cells." Gastroenterology **139**(1): 270-280.
Masui, T., et al. (2008). "Transcriptional autoregulation controls pancreatic Ptf1a expression during development and adulthood." Mol Cell Biol **28**(17): 5458-5468.
Matsumoto, S., et al. (2006). "Brg1 is required for murine neural stem cell maintenance and gliogenesis." Dev Biol **289**(2): 372-383.
Mattar, P., et al. (2008). "Basic helix-loop-helix transcription factors cooperate to specify a cortical projection neuron identity." Mol Cell Biol **28**(5): 1456-1469.
Maurer, K. A., et al. (2014). "Notch signaling differentially regulates Atoh7 and Neurog2 in the distal mouse retina." Development **141**(16): 3243-3254.
Meredith, D. M., et al. (2013). "Program Specificyty for Ptf1a in Pancreas versus Neural Tube Development Correlates with Distinct Collaborating Cofactors and Chromatin Accessability

" Mol Cell Biol **33**(16): 3166-3179.
Meredith, D. M., et al. (2009). "Multiple transcriptional mechanisms control Ptf1a levels during neural development including autoregulation by the PTF1-J complex." J Neurosci **29**(36): 11139-11148.
Millen, K. J., et al. (2014). "Transformation of the cerebellum into more ventral brainstem fates causes cerebellar agenesis in the absence of Ptf1a function." Proc Natl Acad Sci U S A **111**(17): E1777-1786.
Mimoto, M. S. and J. L. Christian (2011). "Manipulation of gene function in Xenopus laevis." Vertebrate Embryogenesis: Embryological, Cellular, and Genetic Methods: 55-75.
Mitalipov, S. and D. Wolf (2009). Totipotency, pluripotency and nuclear reprogramming. Engineering of stem cells, Springer**:** 185-199.
Miyata, Y., et al. (2010). "Cyclin C regulates human hematopoietic stem/progenitor cell quiescence." Stem Cells **28**(2): 308-317.
Mizuguchi, R., et al. (2001). "Combinatorial roles of olig2 and neurogenin2 in the coordinated induction of pan-neuronal and subtype-specific properties of motoneurons." Neuron **31**(5): 757-771.
Mizuhara, E., et al. (2010). "Purkinje cells originate from cerebellar ventricular zone progenitors positive for Neph3 and E-cadherin." Dev Biol **338**(2): 202-214.
Mizuseki, K., et al. (1998). "Xenopus Zic-related-1 and Sox-2, two factors induced by chordin, have distinct activities in the initiation of neural induction." Development **125**(4): 579-587.
Mizuseki, K., et al. (1998). "SoxD:an essential mediator of induction of anterior neural tissues in Xenopus embryos." Neuron **21**(1): 77-85.
Mo, A., et al. (2015). "Epigenomic Signatures of Neuronal Diversity in the Mammalian Brain." Neuron **86**(6): 1369-1384.
Mohn, F., et al. (2008). "Lineage-specific polycomb targets and de novo DNA methylation define restriction and potential of neuronal progenitors." Molecular cell **30**(6): 755-766.
Mona, B., et al. (2017). "Repression by PRDM13 is critical for generating precision in neuronal identity." Elife **6**.
Mosammaparast, N. and Y. Shi (2010). "Reversal of histone methylation: biochemical and molecular mechanisms of histone demethylases." Annual review of biochemistry **79**: 155-179.

Müller, T., et al. (2002). "The Homeodomain Factor Lbx1 Distinguishes Two Major Programs of Neuronal Differentiation in the Dorsal Spinal Cord." Neuron **34**: 551-562.
Murre, C., et al. (1989). "Interactions between heterologous helix-loop-helix proteins generate complexes that bind specifically to a common DNA sequence." Cell **58**(3): 537-544.
Nakata, K., et al. (1997). "Xenopus Zic3, a primary regulator both in neural and neural crest development." Proc Natl Acad Sci U S A **1997**(94): 22.
Nakhai, H., et al. (2007). "Ptf1a is essential for the differentiation of GABAergic and glycinergic amacrine cells and horizontal cells in the mouse retina." Development **134**(6): 1151-1160.
Narayanan, R., et al. (2015). "Loss of BAF (mSWI/SNF) complexes causes global transcriptional and chromatin state changes in forebrain development." Cell reports **13**(9): 1842-1854.
Narayanan, R. and T. C. Tuoc (2014). "Roles of chromatin remodeling BAF complex in neural differentiation and reprogramming." Cell Tissue Res **356**(3): 575-584.
Nieber, F., et al. (2009). "Comparative expression analysis of the neurogenins in Xenopus tropicalis and Xenopus laevis." Dev Dyn **238**(2): 451-458.
Nieberler, M. (2012) Function of the CHD4/Mi-2ß chromatin remodelling ATPase during neural development of Xenopus laevis
Nieuwkoop, P. D. and J. Faber (1967). "Normal Table of Xenopus laevis(Daudln)." 2nd ed. North Holland Publ. Co.. Amsterdam.
Ninkovic, J., et al. (2013). "The BAF complex interacts with Pax6 in adult neural progenitors to establish a neurogenic cross-regulatory transcriptional network." Cell stem cell **13**(4): 403-418.
Nishida, K., et al. (2010). "Ptf1a directly controls expression of immunoglobulin superfamily molecules Nephrin and Neph3 in the developing central nervous system." J Biol Chem **285**(1): 373-380.
Nishimura, M., et al. (1998). "Structure, Chromosomal Locus, and Promoter of MouseHes2Gene, a Homologue ofDrosophila hairyandEnhancer of split." Genomics **49**(1): 69-75.
Niwa, Y., et al. (2011). "Different types of oscillations in Notch and Fgf signaling regulate the spatiotemporal periodicity of somitogenesis." Genes Dev **25**(11): 1115-1120.
Oginuma, M., et al. (2010). "The oscillation of Notch activation, but not its boundary, is required for somite border formation and rostral-caudal patterning within a somite." Development **137**(9): 1515-1522.
Ohtsuka, T., et al. (1999). "Hes1 and Hes5 as notch effectors in mammalian neuronal differentiation." EMBO J **18**(8): 2196-2207.
Okubo, Y., et al. (2012). "Lfng regulates the synchronized oscillation of the mouse segmentation clock via trans-repression of Notch signalling." Nat Commun **3**: 1141.
Oschwald, R., et al. (1991). "Localization of a nervous system-specific class II beta-tubulin gene in Xenopus laevis embryos by whole-mount in situ hybridization." Int J Dev Biol **35**: 399-405.
Papalopulu, N. and C. Kintner (1996). "A posteriorising factor, retinoic acid, reveals that anteroposterior patterning controls the timing of neuronal differentiation in Xenopus neuroectoderm." Development **122**(11): 3409-3418.

Papanayotou, C., et al. (2008). "A mechanism regulating the onset of Sox2 expression in the embryonic neural plate." PLoS biology **6**(1): e2.
Parras, C. M., et al. (2002). "Divergent functions of the proneural genes Mash1 and Ngn2 in the specification of neuronal subtype identity." Genes Dev **16**(3): 324-338.
Pascual, M., et al. (2007). "Cerebellar GABAergic progenitors adopt an external granule cell-like phenotype in the absence of Ptf1a transcription factor expression." Proc Natl Acad Sci U S A **104**(12): 5193-5198.
Pataskar, A., et al. (2016). "NeuroD1 reprograms chromatin and transcription factor landscapes to induce the neuronal program." EMBO J **35**(1): 24-45.
Patterson, K. D. and P. A. Krieg (1999). "Hox11-family genes XHox11 and XHox11L2 in xenopus: XHox11L2 expression is restricted to a subset of the primary sensory neurons." Dev Dyn **214**(1): 34-43.
Pattyn, A., et al. (2000). "Control of hindbrain motor neuron differentiation by the homeobox gene Phox2b." Development **127**(7): 1349-1358.
Pearlman, S. M., et al. (2011). "A Mechanism for the Evolution of Phosphorylation Sites." Cell **147**(4): 934-946.
Penzel, R., et al. (2003). "Characterization and early embryonic expression of a neural specific transcription factor xSOX3 in Xenopus laevis." International Journal of Developmental Biology **41**(5): 667-677.
Pera, E. M., et al. (2003). "Integration of IGF, FGF, and anti-BMP signals via Smad1 phosphorylation in neural induction." Genes Dev **17**(24): 3023-3028.
Pera, E. M., et al. (2001). "Neural and head induction by insulin-like growth factor signals." Dev Cell **1**(5): 655-665.
Perron, M., et al. (1999). "X-ngnr-1 and Xath3 promote ectopic expression of sensory neuron markers in the neurula ectoderm and have distinct inducing properties in the retina." Proc Natl Acad Sci U S A **96**(26): 14996-15001.
Pevny, L. and M. Placzek (2005). "SOX genes and neural progenitor identity." Current Opinion in Neurobiology **15**(1): 7-13.
Pfeuty, B. (2015). "Neuronal specification exploits the inherent flexibility of cell-cycle gap phases." Neurogenesis (Austin) **2**(1): e1095694.
Phelan, M. L., et al. (1999). "Reconstitution of a core chromatin remodeling complex from SWI/SNF subunits." Molecular cell **3**(2): 247-253.
Piccolo, S., et al. (1999). "The head inducer Cerberus is a multifunctional antagonist of Nodal, BMP and Wnt signals." Nature **397**(6721): 707-710.
Piccolo, S., et al. (1996). "Dorsoventral Patterning in Xenopus: Inhibition of Ventral Signals by Direct Binding of Chordin to BMP-4." Cell **86**(4): 589-598.
Pitulescu, M., et al. (2005). "The regulation of embryonic patterning and DNA replication by geminin." Cellular and Molecular Life Sciences CMLS **62**(13): 1425-1433.
Poduri, A. and D. Lowenstein (2011). "Epilepsy genetics--past, present, and future." Curr Opin Genet Dev **21**(3): 325-332.
Pozzoli, O., et al. (2001). "Xebf3 is a regulator of neuronal differentiation during primary neurogenesis in Xenopus." Dev Biol **233**(2): 495-512.
Pratt, K. G. and A. S. Khakhalin (2013). "Modeling human neurodevelopmental disorders in the Xenopus tadpole: from mechanisms to therapeutic targets." Disease Models & Mechanisms.
Quan, X.-J., et al. (2016). "Post-translational control of the temporal dynamics of transcription factor activity regulates neurogenesis." Cell **164**(3): 460-475.

Quinlan, A. R. and I. M. Hall (2010). "BEDTools: a flexible suite of utilities for comparing genomic features." Bioinformatics **26**(6): 841-842.
Richard-Parpaillon, L., et al. (2004). "G1/S phase cyclin-dependent kinase overexpression perturbs early development and delays tissue-specific differentiation in Xenopus." Development **131**(11): 2577-2586.
Richard-Parpaillon, L., et al. (2002). "The IGF pathway regulates head formation by inhibiting Wnt signaling in Xenopus." Dev Biol **244**(2): 407-417.
Richts, S. (2013) Master's Thesis: Characterization of Ptf1a protein domains during neurogenesis University Medical Center Göttingen, Department of Developmental Biochemistry, University of Göttingen
Roberts, A. (2000). "Early functional organization of spinal neurons in developing lower vertebrates." Brain research bulletin **53**(5): 585-593.
Roberts, A., et al. (2012). "A functional scaffold of CNS neurons for the vertebrates: the developing Xenopus laevis spinal cord." Dev Neurobiol **72**(4): 575-584.
Rodolosse, A., et al. (2009). "p/CAF modulates the activity of the transcription factor p48/Ptf1a involved in pancreatic acinar differentiation." Biochem J **418**(2): 463-473.
Roese-Koerner, B., et al. (2016). "Reciprocal Regulation between Bifunctional miR-9/9∗ and its Transcriptional Modulator Notch in Human Neural Stem Cell Self-Renewal and Differentiation." Stem Cell Reports **7**(2): 207-219.
Roese-Koerner, B., et al. (2017). "Notch/Hes signaling and miR-9 engage in complex feedback interactions controlling neural progenitor cell proliferation and differentiation." Neurogenesis (Austin) **4**(1): e1313647.
Rogers, C. D., et al. (2011). "The response of early neural genes to FGF signaling or inhibition of BMP indicate the absence of a conserved neural induction module." BMC Dev Biol **11**(1): 74.
Rogers, C. D., et al. (2009). "Xenopus Sox3 activates sox2 and geminin and indirectly represses Xvent2 expression to induce neural progenitor formation at the expense of non-neural ectodermal derivatives." Mech Dev **126**(1-2): 42-55.
Ronan, J. L., et al. (2013). "From neural development to cognition: unexpected roles for chromatin." Nat Rev Genet **14**(5): 347--359.
Rossi, C. C., et al. (2008). "Rohon-Beard sensory neurons are induced by BMP4 expressing non-neural ectoderm in Xenopus laevis." Dev Biol **314**(2): 351-361.
Rossi, C. C., et al. (2009). "Transcriptional control of Rohon-Beard sensory neuron development at the neural plate border." Developmental Dynamics **238**(4): 931-943.
Roux, E., et al. (1989). "The cell-specific transcription factor PTF1 contains two different subunits that interact with the DNA." Genes Dev **3**(10): 1613-1624.
Roy, K., et al. (2002). "The myogenic basic helix-loop-helix family of transcription factors shows similar requirements for SWI/SNF chromatin remodeling enzymes during muscle differentiation in culture." Journal of Biological Chemistry **277**(37): 33818-33824.
Saka, Y., et al. (2007). "Nuclear accumulation of Smad complexes occurs only after the midblastula transition in Xenopus." Development **134**(23): 4209-4218.

Sakamoto, I., et al. (2000). "A novel β-catenin-binding protein inhibits β-catenin-dependent Tcf activation and axis formation." Journal of Biological Chemistry **275**(42): 32871-32878.
Sanes, D. H., et al. (2011). Development of the nervous system, Academic Press.
Sasai, Y., et al. (1992). "Two mammalian helix-loop-helix factors structurally related to Drosophila hairy and Enhancer of split." Genes Dev **6**(12b): 2620-2634.
Sasai, Y., et al. (1996). "Endoderm induction by the organizer-secreted factors chordin and noggin in Xenopus animal caps." EMBO J. **15**(17): 4547-4555.
Schlosser, G., et al. (2002). "Thyroid hormone promotes neurogenesis in the Xenopus spinal cord." Dev Dyn **225**(4): 485-498.
Schneider-Poetsch, T., et al. (2010). "Inhibition of eukaryotic translation elongation by cycloheximide and lactimidomycin." Nature chemical biology **6**(3): 209-217.
Schneider, M. L., et al. (2001). "Notch signaling can inhibit Xath5 function in the neural plate and developing retina." Molecular and Cellular Neuroscience **18**(5): 458-472.
Schnetz, M. P., et al. (2009). "Genomic distribution of CHD7 on chromatin tracks H3K4 methylation patterns." Genome Res **19**(4): 590-601.
Schroeter, E. H., et al. (1998). "Notch-1 signalling requires ligand-induced proteolytic release of intracellular domain." Nature **393**(6683): 382-386.
Selkoe, D. and R. Kopan (2003). "Notch and Presenilin: regulated intramembrane proteolysis links development and degeneration." Annual review of neuroscience **26**(1): 565-597.
Sellick, G. S., et al. (2004). "Mutations in PTF1A cause pancreatic and cerebellar agenesis." Nat Genet **36**(12): 1301-1305.
Seo, S. and K. L. Kroll (2006). "Geminin's double life: chromatin connections that regulate transcription at the transition from proliferation to differentiation." Cell Cycle **5**(4): 374-379.
Seo, S., et al. (2007). "Neurogenin and NeuroD direct transcriptional targets and their regulatory enhancers." EMBO J **26**: 5093-5108.
Seo, S., et al. (2005). "The SWI/SNF chromatin remodeling protein Brg1 is required for vertebrate neurogenesis and mediates transactivation of Ngn and NeuroD." Development **132**(1): 105-115.
Sharp, P. A., et al. (1973). "Detection of two restriction endonuclease activities in Haemophilus parainfluenzae using analytical agarose--ethidium bromide electrophoresis." Biochemistry **12**(16): 3055-3063.
Shen, T., et al. (2015). "CHD2 is required for embryonic neurogenesis in the developing cerebral cortex." Stem Cells **33**(6): 1794-1806.
Shimojo, H., et al. (2016). "Oscillatory control of Delta-like1 in cell interactions regulates dynamic gene expression and tissue morphogenesis." Genes and Development **30**(1): 102-116.
Shimojo, H., et al. (2008). "Oscillations in notch signaling regulate maintenance of neural progenitors." Neuron **58**(1): 52-64.
Simmen, M. W. (2008). "Genome-scale relationships between cytosine methylation and dinucleotide abundances in animals." Genomics **92**(1): 33-40.
Sive, H. L., et al. (2000). "Early Development of Xenopus laevis - A Laboratory Manual." Cold Spring Harb Laboratory Press **London**.

Smith, D. K., et al. (2016). "Small Molecules Modulate Chromatin Accessibility to Promote NEUROG2-Mediated Fibroblast-to-Neuron Reprogramming." Stem Cell Reports **7**(5): 955-969.
Sokpor, G., et al. (2017). "Chromatin Remodeling BAF (SWI/SNF) Complexes in Neural Development and Disorders." Frontiers in molecular neuroscience **10**: 243.
Sölter, M., et al. (1999). "Characterization of a subfamily of related winged helix genes, XFD-12/12′/12 ″(XFLIP), during Xenopus embryogenesis." Mech Dev **89**(1): 161-165.
Sommer, L., et al. (1996). "neurogenins, a novel family of atonal-related bHLH transcription factors, are Putative mammalian neuronal determination genes that reveal progenitor cell heterogeneity in the developing CNS and PNS." Molecular and Cellular Neuroscince **8**: 221-241.
Soufi, A., et al. (2015). "Pioneer transcription factors target partial DNA motifs on nucleosomes to initiate reprogramming." Cell **161**(3): 555-568.
Souopgui, J., et al. (2002). "Xebf3 is a regulator of neuronal differentiation during primary neurogenesis in Xenopus." Dev Biol **233**(2): 495-512.
Stancheva, I. and R. R. Meehan (2000). "Transient depletion of xDnmt1 leads to premature gene activation in Xenopus embryos." Genes Dev **14**(3): 313-327.
Storm, R., et al. (2009). "The bHLH transcription factor Olig3 marks the dorsal neuroepithelium of the hindbrain and is essential for the development of brainstem nuclei." Development **136**(2): 295-305.
Strahl, B. D. and C. D. Allis (2000). "The language of covalent histone modifications." Nature **403**(6765): 41-45.
Strickfaden, S. C., et al. (2007). "A Mechanism for Cell Cycle Regulation of MAP Kinase Signaling in a Yeast Differentiation Pathway." Cell **128**(3): 519-531.
Sullivan, S. A., et al. (2001). "foxD5a, a Xenopus winged helix gene, maintains an immature neural ectoderm via transcriptional repression that is dependent on the C-terminal domain." Dev Biol **232**(2): 439-457.
Thuret, R., et al. (2015). "Analysis of neural progenitors from embryogenesis to juvenile adult in Xenopus laevis reveals biphasic neurogenesis and continuous lengthening of the cell cycle." Biol Open **4**(12): 1772-1781.
Tuoc, T. C., et al. (2013). "Chromatin regulation by BAF170 controls cerebral cortical size and thickness." Dev Cell **25**(3): 256-269.
Tutak, E., et al. (2009). "A Turkish newborn infant with cerebellar agenesis/neonatal diabetes mellitus and PTF1A mutation." Genet Couns. **20**(0): 147-152.
Ubersax, J. A. and J. E. Ferrell, Jr. (2006). "A noisy 'Start' to the cell cycle." Mol Syst Biol **2**: 2006 0014.
Uchikawa, M., et al. (1999). "Two distinct subgroups of Group B Sox genes for transcriptional activators and repressors: their expression during embryonic organogenesis of the chicken." Mech Dev **84**(1): 103-120.
Uribe, R. A., et al. (2016). "A novel subset of enteric neurons revealed by ptf1a:GFP in the developing zebrafish enteric nervous system." Genesis **54**(3): 123-128.
Vernon, A. E. (2003). "The cdk inhibitor p27Xic1 is required for differentiation of primary neurones in Xenopus." Development **130**(1): 85-92.
Vosper, J. M., et al. (2007). "Regulation of neurogenin stability by ubiquitin-mediated proteolysis." Biochem J **407**(2): 277-284.

Wagner, G., et al. (2017). "Brg1 chromatin remodeling ATPase balances germ layer patterning by amplifying the transcriptional burst at midblastula transition." PLoS Genet **13**(5): e1006757.
Wang, F., et al. (2015). "Targeted gene disruption in Xenopus laevis using CRISPR/Cas9." Cell & bioscience **5**(1): 15.
Wapinski, O. L., et al. (2013). "Hierarchical mechanisms for direct reprogramming of fibroblasts to neurons." Cell **155**(3): 621-635.
Weedon, M. N., et al. (2014). "Recessive mutations in a distal PTF1A enhancer cause isolated pancreatic agenesis." Nat Genet **46**(1): 61-64.
Weintraub, H. (1993). "The MyoD Family and Myogenesis: Redundancy, Networks, and Thresholds." Cell **75**(7): 1241-1244.
Wettstein, D. A., et al. (1997). "The Xenopus homolog of Drosophila Suppressor of Hairless mediates Notch signaling during primary neurogenesis." Development **124**(3): 693-702.
Wiebe, P. O., et al. (2007). "Ptf1a binds to and activates area III, a highly conserved region of the Pdx1 promoter that mediates early pancreas-wide Pdx1 expression." Mol Cell Biol **27**(11): 4093-4104.
Wobus, A. M. and K. R. Boheler (2005). "Embryonic stem cells: prospects for developmental biology and cell therapy." Physiological reviews **85**(2): 635-678.
Wullimann, M. F., et al. (2005). "Secondary neurogenesis in the brain of the African clawed frog, Xenopus laevis, as revealed by PCNA, Delta-1, Neurogenin-related-1, and NeuroD expression." J Comp Neurol **489**(3): 387-402.
Yamada, M., et al. (2007). "Origin of climbing fiber neurons and their developmental dependence on Ptf1a." J Neurosci **27**(41): 10924-10934.
Yao, B., et al. (2016). "Epigenetic mechanisms in neurogenesis." Nat Rev Neurosci **17**(9): 537-549.
Yao, B. and P. Jin (2014). "Unlocking epigenetic codes in neurogenesis." Genes Dev **28**(12): 1253-1271.
Zaret, K. S. and J. S. Carroll (2011). "Pioneer transcription factors: establishing competence for gene expression." Genes Dev **25**(21): 2227-2241.
Zaret, K. S. and S. E. Mango (2016). "Pioneer transcription factors, chromatin dynamics, and cell fate control." Curr Opin Genet Dev **37**: 76-81.
Zhan, X., et al. (2011). "Dual role of Brg chromatin remodeling factor in Sonic hedgehog signaling during neural development." Proceedings of the National Academy of Sciences **108**(31): 12758-12763.
Zhang, Y., et al. (1998). "The dermatomyositis-specific autoantigen Mi2 is a component of a complex containing histone deacetylase and nucleosome remodeling activities." Cell **95**(2): 279-289.
Zimmerman, L. B., et al. (1996). "The Spemann Organizer Signal noggin Binds and Inactivates Bone Morphogenetic Protein 4." Cell **86**: 599-606.

6. Appendix

6.1 Summary of Nanostring data

Given are the average counts after normalization and background subtraction of three independent experiments for each sample and gene, respectively. In a second table, the calculated standard error of the mean (SEM) is given for each sample and gene, respectively. Data were processed as described in Material and Methods.

6.1.1 Ptf1a threonine mutants

Table S1: Summary of average normalized counts of three independent Nanostring experiments for each sample and gene

Gene Name	CC	Ptf1a	Ptf1a$^{W224A/W242A}$	Ptf1a^{T243A}	Ptf1a^{T243E}
odc1.L	15504	20639	18332	17622	20778
ppi1.l	2825	3110	2921	2912	3073
rplp0.S	33879	23110	27623	28940	23618
t.S	81	23	55	47	34
pax2.L	12	524	11	104	299
prdm14.L	17	562	789	889	1603
tubb2b.S	100	17477	5978	9622	24822
dll1.L	14	168	26	49	134
ebf2.S	1	493	50	184	476
lhx1.S	3	779	6	146	904
myt1.S	430	3173	1560	1697	3389
prdm13.S	4	3572	33	547	2303
zc3h12c.L	432	1528	1302	1017	1613
onecut1.2.L	22	9630	944	4628	9215
aldh1b1.L	9	235	7	31	148
barhl2.L	38	238	21	31	169
gad1.1.L	52	2989	32	981	2435
kirrel2.L	11	4356	19	406	1494
neurog2.S	3	244	9	40	129

nr5a2.L	9	737	184	507	1082
tlx3.L	11	70	1336	492	418
pdia2.L	18	62	13	12	35
slc17a7.L	2	219	372	377	648
slc32a1.S	14	583	58	176	773

Table S2: Summary of the calculated SEM of the normalized counts shown in Table S1 for each sample and gene

Gene Name	CC	Ptf1a	Ptf1a$^{W224A/W242A}$	Ptf1a^{T243A}	Ptf1a^{T243E}
odc1.L	3578	4765	4568	4501	4749
ppi1.l	407	479	448	367	307
rplp0.S	7747	5206	5543	6417	6601
t.S	29	8	15	20	16
pax2.L	3	146	5	18	33
prdm14.L	5	159	203	179	80
tubb2b.S	22	3230	1981	1686	2168
dll1.L	4	44	13	9	22
ebf2.S	1	94	26	33	93
lhx1.S	1	156	3	31	172
myt1.S	144	651	625	435	700
prdm13.S	2	858	16	111	83
zc3h12c.L	123	275	401	195	324
onecut1.2.L	5	1484	325	797	1383
aldh1b1.L	2	54	3	9	14
barhl2.L	13	38	7	10	10
gad1.1.L	33	483	8	99	259
kirrel2.L	2	1082	8	88	217
neurog2.S	1	85	3	20	33
nr5a2.L	3	117	61	134	229
tlx3.L	7	13	400	101	159
pdia2.L	9	5	0	3	4

slc17a7.L	1	75	93	82	77
slc32a1.S	4	100	19	50	218

6.1.2 Time course analysis

Table S3: Summary of average normalized counts of three independent Nanostring experiments for each sample and gene

	3 h		6 h		9 h		12 h		15 h		25 h	
Gene name	**CC**	**Ptf1a**	**CC**	**Ptf1a**	**CC**	**Ptf1a**	**CC**	**Ptf1a**	**CC**	**Ptf1a**	**CC**	**Ptf1a**
odc1.L	33893	33078	40930	42484	43118	41525	31637	35136	26616	29026	13869	14788
ppi1.l	2092	2094	2092	2094	2090	2093	2093	2090	2091	2088	2090	2086
rplp0.S	8787	8936	8803	9148	8850	9127	9872	10422	11934	10118	28671	20126
t.S	38	169	67	58	57	67	81	45	41	31	140	17
pax2.L	4	8	5	16	4	24	9	116	11	255	28	403
prdm14.L	392	705	536	794	349	377	265	365	212	308	7	101
tubb2b.S	36	46	59	126	69	147	66	348	48	958	59	7236
dll1.L	61	264	127	672	214	841	72	537	36	530	16	181
ebf2.S	1	151	1	682	1	451	1	342	1	424	1	234
lhx1.S	56	77	37	99	2	82	1	93	1	139	1	305
myt1.S	149	1512	279	9508	590	10047	1099	7541	1400	6967	358	2421
prdm13.S	1	348	1	2845	1	4498	1	4960	1	4970	1	2172
zc3h12c.L	118	1845	270	6817	351	5820	157	3947	123	3283	528	1038
onecut1.2.L	21	18	101	422	508	1966	777	5344	544	6221	10	5517
aldh1b1.L	2	47	2	169	4	523	1	824	1	786	3	159
barhl2.L	18	37	15	115	22	476	14	974	9	686	9	118
gad1.1.L	1	1	1	1	1	14	1	385	1	697	72	1027
kirrel2.L	1028	938	1251	2695	761	5455	71	6693	26	5610	13	3474
neurog2.S	182	235	104	120	49	171	20	641	17	667	2	252
nr5a2.L	2	12	2	146	7	330	83	543	65	538	1	365
tlx3.L	27	24	31	125	24	326	11	266	23	211	21	11
pdia2.L	2	19	1	36	1	110	1	162	1	160	12	74
slc17a7.L	3	2	1	1	1	2	2	1	1	1	1	17
slc32a1.S	21	21	16	21	7	15	2	44	2	39	2	248

Table S4: Summary of the calculated SEM of the normalized counts shown in Table S3 for each sample and gene

	3 h		6 h		9 h		12 h		15 h		25 h	
Gene Name	**CC**	**Ptf1a**	**CC**	**Ptf1a**	**CC**	**Ptf1a**	**CC**	**Ptf1a**	**CC**	**Ptf1a**	**CC**	**Ptf1a**
odc1.L	2289	3005	4585	5388	5548	3565	4115	2821	3236	2935	1943	2463
ppi1.l	37	36	36	37	36	37	37	37	37	39	36	36
rplp0.S	817	885	956	1333	496	351	794	687	1016	772	2715	2286
t.S	4	56	32	10	3	35	41	22	17	5	23	3
pax2.L	2	2	1	6	2	3	2	16	5	27	13	29
prdm14.L	93	113	58	223	90	57	188	58	157	105	4	17
tubb2b.S	7	8	10	26	16	29	10	46	7	43	7	237
dll1.L	30	24	37	70	71	134	17	108	11	98	3	22
ebf2.S	0	24	0	35	0	54	0	36	0	20	0	15
lhx1.S	6	4	12	7	1	5	0	17	0	12	0	23
myt1.S	37	120	63	645	171	1555	138	1048	272	915	51	180
prdm13.S	0	62	0	323	0	866	0	667	0	527	0	176
zc3h12c.L	59	286	86	321	106	226	65	380	54	277	97	110
onecut1.2.L	14	5	35	116	203	830	126	766	60	617	2	349
aldh1b1.L	1	20	1	65	1	154	0	306	0	245	1	38
barhl2.L	4	12	5	23	8	194	3	236	3	123	3	12
gad1.1.L	0	0	0	0	0	0	0	70	0	107	53	134
kirrel2.L	147	130	150	427	90	1471	17	797	4	582	6	213
neurog2.S	7	69	13	14	9	42	11	83	11	72	1	30
nr5a2.L	1	4	1	40	2	103	11	94	15	71	0	46
tlx3.L	7	4	9	16	2	97	5	50	18	56	11	4
pdia2.L	1	3	0	11	0	19	0	30	0	14	5	7
slc17a7.L	1	1	0	0	0	1	0	0	0	0	0	4
slc32a1.S	3	8	4	4	3	3	1	10	1	12	1	56

6.1.2 Brg1 knock-down

Table S5: Summary of average normalized counts of three independent Nanostring experiments for each sample and gene

Gene Name	**CC**	**Ptf1a**	**Ptf1a + cMO**	**Ptf1a + Brg1MO**
LOC100487395.L	0	0	3	0

Xelaev18005831m.g	20	247	280	177
Xelaev18007508m.g	1	2650	2653	857
Xelaev18040877m.g	12	877	1020	386
Xetrov90021170m.L	43	45	37	77
adamts20.L	1	0	4	5
aldh1b1.L	1	38	59	24
arid1b.L	71	1961	2065	1368
arl4a.S	7406	8582	8358	11119
b4galnt1.S	9	300	260	86
barhl2.L	6	484	619	187
bgn.L	2	771	585	195
bhlhe40.L	53	244	233	115
cacna2d2.L	2	69	79	32
cbfa2t2.S	360	7883	8720	9569
chst3.L	1	641	762	466
dll1.L	52	395	403	402
dmbx1.S	12	71	109	54
dmrta2.L	6	576	628	141
dpysl3.L	7	291	311	82
drgx.L	21	161	177	59
ebf2.S	1	371	435	261
efnb1.L	17	19	22	25
elavl3.L	298	9329	11480	7174
eya1.L	882	6855	7133	4627
fam102b.L	85	48	47	96
fzd10.S	1513	1227	1248	1785
gad1.1.L	1	1293	764	133
gas6.L	1146	2812	2280	2107
gfi1.L	56	345	405	653
gfra1.S	56	1575	1800	907
hes3.3.S	1752	3874	4086	4770
hes5.1.S	819	3827	4457	4893
hes5.2.S	0	132	143	25
hes9-1.S	54	524	547	243
hesx1.S	21	3694	3490	740
hoxc4.S	3	24	30	22
hoxd1.L	16	103	95	299
id2.L	11345	20374	19866	25793

id4.S	3645	7030	6969	5193
insm1.L	258	3388	3753	2799
kif26a.L	0	31	49	5
kirrel2.L	30	3798	4499	3343
klhl14.L	0	0	1	0
lbx1.S	1	92	122	24
lhx1.S	2	89	126	23
map2.S	6	709	741	307
map3k12.S	13	120	152	48
mmp28.L	30	653	648	102
mxra7.L	33	1324	1579	755
myt1.S	1589	7720	8590	6062
ncam1.S	76	822	880	159
nes.L	22	1019	1488	651
neurod4.L	2	5382	5844	1307
neurog2.S	10	277	373	428
nr5a2.L	6	29	37	4
olig2.S	30	1645	2079	1253
onecut1.2.L	661	4637	4972	1747
otx2.L	367	776	1116	663
pax2.L	2	55	69	33
pcdh18.L	1	3	9	25
pck1.L	27	930	715	142
pdia2.L	1	37	37	38
plk3.L	177	1473	1625	960
pou3f1.S	2	1510	2069	1137
pou3f2.L	37	494	680	238
ppp1r9b.S	4	418	428	53
prdm13.S	1	4303	4560	2242
prdm14.L	337	434	698	680
prph.S	10	2106	2578	352
prr15l.S	0	1	1	2
rapgef5.L	1149	812	690	565
runx1t1.L	12	482	489	181
scrt1.S	1	1523	1930	489
six3.L	75	1025	1181	183
slc17a7.L	2	0	4	4
slc18a3.S	9	843	924	751

slc32a1.S	2	6	11	2
slc3a2.L	45	2599	2543	170
slc43a2.S	29	692	841	351
snai2.L	85	885	1121	1004
snap25.L	14	1227	992	377
snrk.S	179	190	189	405
sox11.L	906	9292	12047	6872
sox9.L	15	385	420	166
t.S	7	8	12	20
tfap2b.S	21	2824	2672	999
tlx3.L	22	434	526	428
tox3.L	543	2779	3087	2363
tubb2b.S	94	369	494	176
tubb3.L	1	130	221	24
vcan.L	9	58	80	86
zc3h12c.L	222	3702	4360	3906
odc1.L	25972	27916	29603	24441
ppi1.l	2249	2365	2324	2117
rplp0.S	6807	5917	5697	7544

TableS6: Summary of the calculated SEM of the normalized counts shown in TableS5 for each sample and gene

Gene Name	CC	Ptf1a	Ptf1a + cMO	Ptf1a + Brg1MO
LOC100487395.L	0.3	0.3	1.4	0.3
Xelaev18005831m.g	12.0	91.9	73.6	55.1
Xelaev18007508m.g	0.4	266.0	669.2	53.5
Xelaev18040877m.g	4.0	125.1	72.8	154.7
Xetrov90021170m.L	11.4	2.8	8.7	22.0
adamts20.L	1.2	0.3	1.8	1.4
aldh1b1.L	0.4	11.9	28.5	4.2
arid1b.L	6.6	309.4	337.5	162.3
arl4a.S	1032.3	1162.4	853.1	1197.2
b4galnt1.S	4.8	86.9	72.1	23.6
barhl2.L	2.5	67.4	105.4	77.3
bgn.L	1.9	290.7	129.7	60.9
bhlhe40.L	6.5	39.2	26.4	11.8

cacna2d2.L	0.8	18.6	17.9	11.0
cbfa2t2.S	122.8	1600.8	1785.0	1799.8
chst3.L	1.2	120.1	146.5	92.7
dll1.L	16.8	66.4	106.8	160.9
dmbx1.S	8.3	4.2	22.9	16.1
dmrta2.L	4.8	145.0	186.9	58.3
dpysl3.L	2.5	79.4	84.2	27.8
drgx.L	4.7	35.7	32.2	1.9
ebf2.S	0.4	47.0	94.9	38.3
efnb1.L	6.3	5.0	0.6	2.5
elavl3.L	20.9	1184.4	1339.5	1441.1
eya1.L	297.7	1517.1	1473.2	1064.7
fam102b.L	10.2	13.1	7.0	24.5
fzd10.S	283.5	294.1	330.8	321.9
gad1.1.L	0.4	536.2	101.1	78.2
gas6.L	442.4	971.7	474.5	392.7
gfi1.L	11.6	74.3	67.4	190.4
gfra1.S	11.5	77.3	58.4	235.7
hes3.3.S	561.9	1095.9	1239.8	1551.3
hes5.1.S	187.4	554.1	541.7	1153.2
hes5.2.S	0.3	33.1	15.6	6.9
hes9-1.S	11.2	71.5	51.3	46.0
hesx1.S	10.9	797.8	641.8	197.8
hoxc4.S	1.7	7.4	6.0	6.5
hoxd1.L	6.9	28.7	40.9	81.6
id2.L	3042.5	6611.5	5984.5	8745.8
id4.S	835.0	1936.9	1406.9	1060.0
insm1.L	101.7	844.6	914.4	276.8
kif26a.L	0.3	13.7	14.7	3.5
kirrel2.L	7.6	226.6	587.5	105.0
klhl14.L	0.3	0.3	0.4	0.3
lbx1.S	0.4	11.5	21.8	12.4
lhx1.S	0.7	37.5	20.9	6.3
map2.S	0.9	132.5	130.9	46.9
map3k12.S	5.7	33.3	5.8	14.9
mmp28.L	11.0	199.2	179.1	17.9
mxra7.L	10.2	380.8	369.8	134.4
myt1.S	726.4	1958.6	2241.6	1004.7

ncam1.S	6.9	131.2	120.8	34.5
nes.L	2.0	70.8	106.6	128.9
neurod4.L	1.2	760.6	1314.2	120.2
neurog2.S	4.0	50.5	39.7	26.2
nr5a2.L	2.1	8.4	8.2	3.2
olig2.S	8.9	518.4	542.8	63.8
onecut1.2.L	191.8	1040.7	672.5	436.2
otx2.L	69.5	14.6	74.1	224.8
pax2.L	0.5	8.5	12.0	14.7
pcdh18.L	0.1	1.0	0.5	3.7
pck1.L	15.8	222.2	177.1	27.5
pdia2.L	0.4	7.0	9.7	11.7
plk3.L	38.6	118.7	165.0	81.0
pou3f1.S	1.9	480.6	740.8	304.0
pou3f2.L	11.0	96.0	189.0	42.7
ppp1r9b.S	3.3	69.0	27.5	31.6
prdm13.S	0.2	531.2	705.8	272.9
prdm14.L	128.7	27.3	86.6	147.4
prph.S	3.0	345.1	393.2	154.0
prr15l.S	0.3	0.4	0.4	1.6
rapgef5.L	332.6	220.2	131.5	89.0
runx1t1.L	5.8	82.0	90.8	7.4
scrt1.S	0.4	122.9	340.8	115.4
six3.L	29.2	134.9	143.9	53.6
slc17a7.L	1.3	0.2	1.6	2.1
slc18a3.S	5.9	235.1	255.6	129.1
slc32a1.S	1.1	1.4	1.6	0.6
slc3a2.L	10.9	640.0	571.7	86.7
slc43a2.S	3.9	134.9	91.4	63.4
snai2.L	30.1	126.7	170.1	228.2
snap25.L	6.2	232.0	121.8	55.4
snrk.S	21.9	11.9	16.9	100.3
sox11.L	302.1	734.5	1214.8	729.2
sox9.L	3.5	25.1	33.0	41.7
t.S	5.7	0.7	2.1	7.4
tfap2b.S	1.1	179.5	247.8	347.4
tlx3.L	12.3	141.6	149.1	109.3
tox3.L	189.7	534.0	504.7	419.6

tubb2b.S	5.9	57.4	37.5	20.8
tubb3.L	0.1	14.1	14.5	10.3
vcan.L	3.0	6.2	8.8	15.3
zc3h12c.L	107.2	944.4	1209.4	1032.3
odc1.L	5393.4	5003.5	5961.8	4832.0
ppi1.l	183.5	231.2	273.2	243.0
rplp0.S	1306.4	1089.4	825.9	1179.1

6.2 Summary of the genes analyzed with the Nanostring

Table S7: Summary of the geneses analyzed with Nanostring. Given is the gene symbol, its accession number as well as the target region and the target sequence. Grey marks the genes analyzed on the 24 gene codeset used for analysis of the time course and threonine mutants experiments

Gene	Accession	Target region	Target Sequence
odc1.L	NM_001086698.1	856-955	GGATATAATTGGTGTGAGTTTCCATGTTGGCAGTGGCTGCACTGATCCACAGACTTATGTACAAGCTGTCTCAGATGCACGATGTGTCTTTGACATGGGG
ppi1.l	NM_001193402.1	430-529	AAACAGACTTGGAATGGTGGAAACAGATTCTCAGGACCGACCACTTGATGAAGTTCAAGTATTGCGGGCTTATCCATCTGGCTAAATGGAGGCAGATAAA
rplp0.S	NM_001086665.1	127-226	TCAATTGCTCGATGATTATCCAAAATGCTTCATTGTGGGGGCGGACAATGTTGGTTCAAAACAAATGCAGCAGATCCGTATGTCCCTGCGTGGAAAAGCT
t.S	NM_001090578.1	1530-1629	TGTAGGCCTCCAAAACAACTTAAAGATGTGCTTAGGCAAGTTATATCAGTGTTTACCTGCTTCTAAAGACTTCATGGGCCCAACCAGGTGTGGGTGGTCT
tubb2b.S	NM_001086064.1	901-1000	TGCACTTTTTTATGCCAGGCTTTGCCCCATTAACAAGTCGTGGCAGCCAACAATACCGAGCCCTGACAGTGCCAGAACTAACACAGCAAATGTTTGATTC
neurog2.S	NM_001088335.1	1173-1272	CATCGTTAGCTATGTGTATTAGGAAACTGTCTATCCCTCATCTGCACCTGTTAGACTACAGCTACCAACTTCCTGTTACCAGGGGGCTACTGGGTAATGT
ebf2.S	NM_001085678.1	1765-1864	CTCCAATGGTTTCCGAGAAAATCTGTTGAAGGACAGTCCTGCCATGAGGCAAGGTCAATACTTCGCCCAGTGCAGCAATCCCTCAGTGGGTTTCTGGTAG
tlx3.L	XM_018252115.1	340-439	ACCTTCATGGATGTGCTGTGAGGAAGACGAAGCGTTTAGAGGGGAGAGTTCTCATTTGAGACAATAAATCTATCGACGGAGGATGGATCAGCCAACAACT
gad1.1.L	NM_001085801.1	795-894	GGCAGCAGTCCCCAGATTGGTCCTGTTTACTTCAGAACACAGCCACTATTCCATAAAGAAAACTGGCGCGGCATTAGGATTTGGAAGTGAAAATGTGATC
slc32a1.S	NM_001086492.1	1078-1177	TTAATGTACAACAGCTTTCCAAACCTGCCCATATCCCAGAAGTCTTGGTCCATCATGGCCACTGCTGTGCTCCTGCCCTGTGCATTTCTCAAGAACCTTA

slc17a7.L	NM_001089635.1	2178-2277	AGTGAATTGAGTTAGATGTACACATTACTGCGTGATTCCCAGGGATACGGTGTAGAAAATATCCATGAGGATGGGGCATGATCAATTCTACATCACTTGG
prdm14.L	Xelaev18032099m.1	586-685	ATCTCCCATAGTCCCCAAAAAGTGCAAAAATGTGTCCCTGAGTGTCCCCAGCCTACAGGTGAGACCCACTCGCACTTACCACTTTACAGAAGAAGACTTA
prdm13.S	XM_018265418.1	33-132	ATTGGATTTTTAGGAATGAGAAGGTCGCCTGGACCATTGTCTGGTTACCATTCATGGGAGCTGATTATGCAGGAGGCTTAGGGAAAGTCTCCATGTGACC
zc3h12c.L	XM_018247762.1	86-185	GTGTCTGAGGCGGGCAGCTTGCTCCCTAATGACTTGGCCTCTCACTGAGCAGCTGCCTGCTGCCTCCTTTGTGTTGGCCTATTGTTGCCGCACACCCCTC
myt1.S	NM_001088192.1	685-784	GAGCTAAACAATGAAAAGCCAACTTCAGTAAAGTCGGGTCAAGCGGAAATAGAACAACTTATGGTAGAAGAGGCGTGTGAGAAAGAAATCATCATCCAGA
dll1.L	XM_018263063.1	3628-3727	CCCATGTAACTTCAACAGTATTTCTGGTGGGGGTTCACTGTGATTGGCAGAGGAGTGGGTGTAGTATCTCTGGCGTCAACCCCTGCATGCTTTTGGTCCCT
kirrel2.L	NM_001086488.1	691-790	CCCAGTCGCCAATGTCCTGCTTGATGTACCCTACAATCTCACCTGTCTTGCTTCCGTCGCTAAGCCTGCTGCAGAGATTACCTGGTTCCGTGATGGAAAG
pax2.L	NM_001086361.1	1495-1594	GAGTGGCCTACTCTGCTTTCCCTACTGACGTTTCTCAGCTGTAATAAGCTGCTCTTACCTCTGCTGCAAGCCTCTTTGTTGTTATTGTGCACGGTAGCTA
lhx1.S	NM_001090659.1	22-121	TCTATTCTCCTAATCCGCCCATTCCTCTAAAATCCCAAATAACCAAAGGCAATGGTTCACTGTGCTGGATGCGAAAGGCCCATTCTGGACCGTTTCTTGT
onecut1.2.L	XM_002935458.4	4346-4445	ATGCTCATTATAACAAGGAGAGTCTGGGGTGAGGTCCCCAATTTGTGTGGGGGATTCAACTGAGGAACCACAGGAAATGCAGGCAAGAAGGGATCTTTTC
barhl2.L	NM_001161386.1	860-959	ATTGGAGTTACTAGCCGAAGCTGGCAATTATTCAGCCCTGCAGAGAATGTTCCCATCACCCTATTTCTATCATCCGAGTCTGCTGAGCAGTATGGACAGT
nr5a2.L	NM_001087716.1	152-251	CCACTTACTCCCTAGCTCATGCTCCCTACGGAACTTGCTTTATCCGATGACTGTAATTCCAATTCTGCCACAGGACAACCGACTGATTCACCTCCAAATC
aldh1b1.L	XM_018257027.1	967-1066	AGAACAAGCCGTGGAACAATGTCACGAGGCTTTGTTTTTTAACATGGGACAGTGTTGTGCTGCAGGTTCCAGGACTTTTGTGGAGGAAACGATCTACCGT
pdia2.L	NM_001090179.1	882-981	TGCTGCCCAGATCCCAAACCACTTGTTGCTGTTTATCAATAAGAGTGACGATTCCCAACTGGTGCTGCTGGAACATTTCCGCAAAGCAGCTCCTGACTTT
arl4a.S	NM_001090805.1	893-992	AAACACCAGGAAACCTAATGTACGTCAGAGGCTGAAACGCAATCTAGTCATTGTGAGTGTAAACTGTGAATGTGTGCAGGGTGTTGAAACAGCTGAGGGT
elavl3.L	NM_001090611.1	919-1018	ACATCCCGTATCCTGGTGGATCAAGTGACAGGTGTTTCTCGAGGTGTGGGCTTTATCCGGTTTGATAAGAGAATAGAGGCAGAAGAGGCTATTAAAGGCC
fzd10.S	NM_001087457.1	2470-2569	AGCAGTCATGGAAATAGTAGTTAGTTCAGTAGGATCTGGATTGCTGCAACAGGGCAGTGCCCACCTAAGTTCTTAGCATGCGTAGGGTTTGCTTGGCTCT
gfi1.L	XM_018258576.1	735-834	CCTGCTCTGCACGCGGCTGCTAATCAACAACGGCTCATACAAATGCCTTAAATGCAGCAAGGTTTTCTCCACACCCCATGGGCTTGAAGTCCATGTACGT

hes3.3.S	XM_018227971.1	974-1073	ACCCTAGGCTGAACGCAGGCAGGCCGGACTTGCAGCCCTCTGGCAATTTTGCCCTGAGGAAAACTTGCAAATTCTGCAATGGTTTATCCATGGCACTTAA
hes5.1.S	NM_001095627.1	327-426	CAGAAAATGGAGAAACCCAGATGAAACTGCTTAATCACCTGCAAGCACCCCAAAGGCTCTCAGTTGCCCCTCACACCTATATCCCCAGTGTTTCTGACTC
hes5.2.S	NM_001095626.2	339-438	AAGCAGCCAGAAGCAGAAGCCAAGCTAATCAGTCATTTCCATTCAAATGCGGCAGCCAGCAGCATGTCGTCTTTTCCTATGAGATACAATCAATCCAAGC
hes9-1.S	NM_001095628.1	352-451	GCTTCTGCAAAATTTCCATGATGATGTGACAGCGTGTCCTTCTGTGTCACCTTTTTACCAGAATCCTGCCAAGTGCACAACCCCTGAGGCCAACAAAGTT
slc18a3.S	XM_018239458.1	329-428	CCAAAATGAGGGAGTCCCGCTCCTATCTGTGATGCTACTGGAGTCACCATGTGAGAGGGGAGGTTCGCTCACCGGCAATTGGTTAATGTTCCTCCATGTG
mxra7.L	NM_001094445.1	663-762	ACACATCACCTAGTGGTAGTGGGTGATACTGCAGCGCAAGATGCTTAAAGACACAGAAACGGTGACCGGCCAATAGAGTTCTGCAATAACGTGGCAGTGT
olig2.S	XM_018248885.1	1734-1833	TTCGGTTCTGTGTCCCAGACACTGACAATGAACTATCAGCCTGTAAGTCTTAACTACTTCTACCACAGTCAGGTGCAGATCACTTTAAATGCCACCAACA
pcdh18.L	XM_018231826.1	590-689	TTGTGGCAGCTATATTTATCACTTGGTGGCTGTGTACTTGGACATGACCAGCCTGCTGCCCTCCAGATGTAGTGGATTGAAGTGTCAGCAGAGTTTCAAT
pou3f1.S	NM_001103185.1	424-523	ATCTACTCGCAGTCCTCCTACACCAACCTGAATGGCATGCTGGGACCTCAGGCTTCCTCTTTGCACCACAGCATGAGAGACCCCTTGCACGATGACCCCG
id2.L	NM_001088433.1	868-967	CGACTTTTTGGGCGATAAAAGGAGCGAAGAAGATCGGGAAACTTATTTCAGTTTTTGCTCGAAGTGTAAAACCAGAAAACCTTGAAACCTTCCCATCCCG
id4.S	NM_001171975.1	149-248	ATGATATGAATGACTGTTACAGCCGGCTCAAGAGGCTCGTGCCCACCATTCCACCCAACAAGAAAGTCAGCAAAGTGGAAATCCTGCAGCATGTTATTGA
insm1.L	NM_001110719.1	2178-2277	CAAATGACTGTGTCCGCCCATGAGTCGCTTCTACAATGAGATAAATGTATATTGCCCAGTTGCCATCCACTCACTGTTACAGCATTTGTGATGCCCTGAC
cbfa2t2.S	NM_001086475.1	2327-2426	TCATTTGGTTGCTATCAGCTTGCTACAGCCTTCAAATATGGCCTCAAAGTGCTATCCCAATTATAGACTGCTTACTGGACTAAGCCATGTCTGTATTTGG
chst3.L	XM_018225491.1	4782-4881	GGTCATCATTGTATCTATCCAGTAAAAGGTATCACCCAATCCACAGGATCCACACTTGTGCCCTTACACATACCTATGCTAAAAGCAGGTATTTTCCAGA
prr15l.S	XM_018238024.1	249-348	CGTTCCTTTTGTCGTCCATACCCACCAGCTAGAAAAGGTTGTAGGTCGGGAAGTCTCAGTTGTACATACAGTTTGCCTCAAGCAAATCTGAAGGGGCTAT
six3.L	NM_001085702.1	777-876	ACAGAGCGGCCGCCGCTAAAAACAGGCTTCAGCACCAATCTATCGGACAGAGTGGCATGAGGTCGTTGGCAGATCCCGGCTGCCCCACACACAGCTCGGC
snrk.S	XM_018269314.1	2348-2447	TCGCCCAGAAGTGCTGGAGAGTTGGTGGAAAGTTTAAAACTAATGAGCCTCTGTTTGGGCACGCAGCTACATAACGGGGCTAAGTATATAATTGACTCTC
tfap2b.S	NM_001094232.1	1243-1342	CTTTGTAAAGAGTTCACAGATCTTTTGGCCCAAGACAGGACACCCATAGGCAACAGTAGGCCCAGTCCAATTTTGGAACCTGGAATCCAGAGCTGCTTGA

slc43a2.S	NM_001097830.1	3239-3338	GGTGACCTACTGTCAGTCTTTTGTGTGATCAGAGGTGAATCTGGGAAAATGAATGTTTTGGGAAGCAAAACTCAACTCAGATACATCTGGCATCAGGACA
Xetrov90021170m.L	XM_018232445.1	1120-1219	TGCCTCTGGCACAGGCTCACCAGACAATTGCTCTTCGTTTCAAGAGGATGAGGACTTAGATATGGAAAACCTTGGCTGGCCTGTTAGTAGTTTCACCATC
Xelaev18005831m.g	XM_018252463.1	379-478	TGGATCCCTCAGCACCATGGGTTCAAGGGATTATCAAGAAAAATTCTCTACAAGCAGGCAACAGAGATAAGTAAGACAAAGAAGAAGAGCAAGTCTTCGA
hoxd1.L	XM_018235932.1	961-1060	ACGCTTGACTACAGACTCTCAGCTAGAAACCAAATATATGGGATTGTCTCGTAACACAATGCATACTGCTGCACCCCAAGCAGCCATAAACTAAGGGGAC
arid1b.L	XM_018263082.1	193-292	GCTGAGCACTCTACCAAATGATATGCTTATTGCCAGACTGTGTCCAAAGTAGGAAAGGGCACCATACATCCTTGGATTCTTCTTGCTAGAAATCACCTTG
bhlhe40.L	XM_018259016.1	386-485	CTCACTAGCCCTGGACGAGCCCATTCGCTCCGTCAGGTTCATGCCACTGACTGGAATACACACACCCACCCGCTCCATTCCCAAACAGCTGCCACTCGGG
dmrta2.L	XM_018258408.1	629-728	ATAGGGCAGTGAGTGCAGTTATTGGCGCTTTACTGTAGCGCATAGAGTGTGTATAGAGTTGTACCAGTCAGGGGAGTTTGTGCCCTTTCCAGTCCCGTGT
dpysl3.L	NM_001086642.1	80-179	AAAAAATACATTGCCTGTATCTGATCAGCTGTAAATCAGTCAGGGGAAGCAGAAGCAGCGGGCTCGGAGGCAAAACATGTCTTACCAGGGGAAGAAGAAC
efnb1.L	NM_001087479.2	110-209	TTATATCTGGAAAGGGCCTGGTTCTATACCCTGAAATTGGCGACCGCTTGGACATTATCTGCCCCAAGGGGGACTCTTCCCAGCCTTATGAATACTATAA
gfra1.S	XM_018227240.1	1934-2033	ACAAGATCGAGAACAACCAATTCGACTCTAACAGAGGAAAAATAAAATAAAGACTGCTCTCTGGTATTTAGGGGGTGTTGTAATTTATCACTGAGGTGCC
nes.L	XM_018231440.1	6793-6892	GTACTGTAAGGCTACAGGGTCTTTACAGGCTTGGGATATTGAGGGTTTAAAATGTTAGCTGTATGGAAATGGGTTGATTCTTAGGAATGGCAGCTGAGTG
neurod4.L	NM_001087744.1	666-765	AGTAATGGATCCTTCTGTGGTAACCCATACACTTAACTGTACCACTCCACCATATGAAGGAGCTCTAACACCTCCACTCAGCATCGGTGGTAATTTTTCT
plk3.L	XM_018258343.1	2967-3066	GACTGTTTTTGACGGAACACAAAGCAGACCAGCAATATGCAACACTTTGTGTAAGAGTAGAGAAAACACTACAGTTGTGGATCACTTCAATCAGCAGACC
snai2.L	NM_001086282.1	554-653	CTCTACTTTCTCTGGGTTGGCTAAGCACAAGCAGCTGCATTGCGACGCCCAGTCTCGGAAATCATTTAGCTGCAAGTACTGTGAAAAGGAGTATGTGAGC
sox9.L	NM_001094473.1	163-262	CTGACTTGGCCACTTCCATTGTTCTCGGTTAAGTTGCGCAAAGACGCGGCTCTGCGCAAACAGTGCCACCCGCAGCCGACGAACTCGCTTTTCCAACATT
tox3.L	XM_018257839.1	557-656	ACAAACCGAACAGCTAGCTCCTACCACAGAGACTCCTCTCTAGATTTTTGTGCGATTGTAAATGCCGAGTAACTGGAAGATCTGCCACCAGCCTTTACGC
vcan.L	NM_001110715.1	433-532	TCTTTGGATGTTTCAGGAGTCGTGTTTCACTACCGAGCCTCTACAGACAAGTACTCTTTGGACTTTGAGGCTGCTCAGAAAGCTTGTATAGACAGCGGTG
pou3f2.L	NM_001096751.1	29-128	GCTCAGCATCCCGCAGGTTGGAAAAGGGTGGGCGGGACTGTTTGGATCATCATCCAATGGCTACGGCGGAAAGTCTCCGGTTGCTAGAGGTATCCACGTA

scrt1.S	XM_018238286.1	4316-4415	TAGGCAGGGACTACATATTAGCCGTGTGCTCTTTCTCCACCCTATAGTATTTCTTTGGAACAGTTGGAAGGGGCTACTTATGAGACTCACGCTCTTCCAT
hesx1.S	NM_001085795.1	169-268	TTGAGTGCAGCAGCAAGGTTGACGGCACCTTTTGGCAAATCCCATTGATCAGCTATGACCTTCCCGTACAAGTTGACGCCATGCGCCGATCCGCAGAAGA
drgx.L	XM_018225618.1	12-111	ACATGGGACTAGGCAGACAGCGCTAATTCTGACCCGAAGGGAAGACAAGACTTCCCCTCGAGGATCAAGTCAGCGATCATGAGCATGACCATAGCTCCCC
b4galnt1.S	XM_018250090.1	2683-2782	TCTGAAGCGCAACTTAGTAAGAGCAAGTAAGAGCCTAGGATGCTAGAAAAGAAAGACCTCAACTCCTCCAACCTACATAATCACCAAAGCTCCTACCCAT
map3k12.S	NM_001100941.1	1870-1969	AGAGGAATGTACCTCAGAAATTATCCCCACATGGGAAAAGGCCAGACATTTTGAAATCTGAAGTCCTGCTGCCAAAGGTAGACTCTGTCTTGTCACCCTC
tubb3.L	NM_001094986.1	1642-1741	AGGTACTGCACCTTAATAACCCTTTTAACGCTTGCCAGTTTCAGCAGCAGAGCAATGTTCAGCATTCAACAACATATCATTGCAGGCTCCAGTGAACAGA
hoxc4.S	XM_018250129.1	483-582	TTGGAATGAGCCTCTGGTTCCTTATCCGGGGACCTGAGCGCACGTTGTGATTGGCTGCCGGAGTCACATGGTGAAAGTAACTTTACGGGGTCGCCAGCTA
kif26a.L	XM_018230605.1	118-217	TTATAAGTATTGATTGATACCCACCTGCCTCTTATTGCACGGGCTGCACTTCCATTACCACGTGATTGACTACACGACTAAGTGCTTTCCTTGTAGCTGT
eya1.L	NM_001090419.1	820-919	ACAGCCGAATACAGCACTATCCACAGTCCATCAACGCCTATTAAAGATTCAGATTCAGATCGATTGCGGCGCAGTTCGGATGGAAAGTCACGGGGACGAG
bgn.L	NM_001090709.1	1208-1307	GTTGGCGTCAATGACTTCTGCCCTATAGGATTCGGAGTGAAACGCGCCTACTACAACGGAATTAGTCTATTTAACAACCCCGTGCCCTACTGGGAAGTGC
Xelaev18040877m.g	NM_001086467.1	1086-1185	CAACCCCAACGGGATCATTGCCACACCCATCACCCAAATTAACCCAATCACTTCTTCTTCAGGTACCAGTACTCCACCAACACTCACTGCCACTCAAGTA
LOC100487395.L	XM_004911907.2	5272-5371	GCCTTACCACTGACTTCCTCTACTTTGGCCATTTTCTGATAGGTTACACCCATCTCCGGCCAAGTCCAGAGTCTCTGTAGTTGTGCTGTGACCTAACAGG
gas6.L	NM_001089688.1	1811-1910	TCCTTTGATGGGACCCTCGGACTAAAAGAACTGCCTGATTCACAGATGCAGATGACTTTGCTTCTGCTAAATGACCACTTAGGAAAGGGTGTAAAGACAT
lbx1.S	XM_018227455.1	272-371	TTCTTTTACCTTCTCCCTGGCCAAAGGATGAATTTAGCTGGGAGTAGGCTGAATTCTGTTTGAAGGGAAGGAGCCTGAGATTGCACAAGAAACATCCAGC
Xelaev18007508m.g	XR_001935594.1	572-671	CTTCAACAGGATGTGCAGAAGTGAGCACCAAGCACTGGTAAGATTGCATACACAGAGCTGCAAGAGAGTCCTGGTACTTATCCATACAAGACCTCCAGAG
map2.S	NM_001086770.1	1188-1287	CCACAAACCAGGTGGTGGACATGTGAGGATTGAAAGTGTAAAACTTGATTTCAAGGAGAAAGCACAGGCTAAAATTGGCTCTTTAGACAATGCCAGTCAT
mmp28.L	NM_001172229.2	14-113	GGTGAGCAGCTACAGGTCTCAATCCAAGGACTATACCATGCCTGGCTGAGAAGAACAGCAGAAGTCTCTGATAACTCTGCCAAACTCTACACTTGGGAAG
ncam1.S	NM_001087827.1	45-144	CATCTGGACTTTATATTTCATAGGAACTGCAGTGGCGTTGGAAGTGAACATTGTTCCAGATCAAGGAGAAATAAGCCTTGGGGAGTCCAAATTCTTCCTG

otx2.L	NM_001090691.1	43-142	TCCACTTGTAGAAAATTGTGCGCAAAAAAAAATAAGAAAAAACGCCCAACGGATCCAGCAAACACTGATCGCCCGACTTTGTCGCTGCAACGATTTCTTC
pck1.L	NM_001086683.1	2306-2405	TGTAGGGTGGATGTACAAAGCAAAGGCGGTATAGTTTGTGCCTCTTCTTTATTAGAGGTGGGTCAGTCTAGTGAAATAAGACTCAATCCAGATTGTCACT
ppp1r9b.S	XM_018238072.1	3927-4026	TCCGGCTGCCCCAGATATCCTAGCACCTCTCATGACCCTCCCGTTGTGTTAAAATTCCACTGTAAGAATGCAGAGGAGGTTCGCTGTTTGGGGGTGACAT
snap25.L	NM_001090411.1	495-594	TAGAGAAACAGAAATGGATGAGAACCTTGAGCAAGTCGGTGGCATTATTGGAAATCTTCGTCACATGGCCCTCGATATGGGCAATGAGATTGACACACAA
sox11.L	NM_001142362.1	593-692	AGCGGCAGCGGCTCCAAGTCGCTCAGTATCAAGTCCGAGTACAGCGGCGGCAGCGACGAGTATGTGTTCGGCAGCCCCAAAGCGTCCGGCAAAGCTGCGG
prph.S	NM_001086386.1	227-326	AAGGTCCAGTACCCCTGTCCGAGTCTCATTGGACCGAGTGGACTTCTCTGCGGCTGAGGCTGTTAACCAAGAATTCCTGACCACCCGCAGTAATGAGAAA
slc3a2.L	NM_001085977.1	855-954	AGAGTCCTGTTGTTATCCACAAGTAGTGCTCAAAACAACCTTACTGGTGGCTTCAATGAGACAATAGATGGCACGCTCTTCTACCGCTTCCTGGGTGCTG
runx1t1.L	NM_001095596.1	650-749	ACCTTCATCCTCTTCGTCATCGTCGCTGGCCAATCAGCAGTTGCCTCCGGCTTGTGGCGCACGGCAGCTCAGTAAGCTCAAGCGATTCCTCACTACATTG
dmbx1.S	XM_018260870.1	2128-2227	TGCGAAAAGGAAATGCTTTAGCTGTAGGGAAGAAAACACTTTTGGTGTGGACTGTGTTCCGCAGAGACTAGATGCCATACTTTTCCTCTGACTGAATGCC
cacna2d2.L	XM_018258986.1	5458-5557	ACCTCCCTGTCATACAGTACGGTACCAAAGAAGCAGGTTTTGACTAAACGTGTTGCATCTCTTCGGCGTAACGTGTCACATCTGAACAGGAAGCAATGGC
rapgef5.L	XM_018267363.1	1998-2097	CTGCGGGGAAAAACATGAGCTTCTACCAAATGAATTGGTCCTCTCCAAAACCCTGGAGCCCTCCAACCGTATTTATACTTACAGGAAGAGTGACACATTG
klhl14.L	XM_018267966.1	524-623	CATTATTGCTACTCGCACATTCCTGCTCTCCCTCGGCGGCTCATTCACTACTAGGAGCACCATGTTGATGATATACGGACAAATACACTGTGAGGAGTGA
fam102b.L	XM_018258650.1	3715-3814	GTGCTGCTGATTCACTATAAGAGCAAGTATATTGGCAGTAGTTCAAAGGGCAGAGGCCAAAACAATTAAAATCGGTGCCATTCAGTTGTATGGCAGATAC
adamts20.L	XM_018251404.1	3770-3869	CAGCTTCTTGTGGGAGGGGTAATCGTGCTCGATATGTGAGTTGTAGGGATGCGTTTGGTGGAGTTGCTGAAGAACTGTTTTTGCGCCCATTTTCCACGACC

6.3 GO tables RNA sequencing experiments

6.3.1 RNA sequencing experiment onset of target gene activation by Ptf1a

Gene Ontology (GO) analysis was performed using DAVID (http://david.abcc.ncifcrf.gov) as previously described (Dennis *et al.,* 2003). Analyzed were genes which were upregulated after 3, 6 and 12 h, respectively.

6.3.1.1 GO analysis of candidate genes upregulated after 3, 6 or 12 h.

Given is the biological process, the number of genes and the P-value. Biological processes were sorted according to the P-value from lowest to highest.

Table S8: Summary of GO analysis of genes upregulated after 3 h. Shown is the top 20 enriched categories in Biological Processes

Term	Count	PValue
GO:0007275~multicellular organism development	29	1.67E-10
GO:0045944~positive regulation of transcription from RNA polymerase II promoter	25	4.33E-08
GO:0000122~negative regulation of transcription from RNA polymerase II promoter	21	8.74E-08
GO:0045893~positive regulation of transcription, DNA-templated	17	1.65E-06
GO:0006351~transcription, DNA-templated	32	1.93E-06
GO:0045665~negative regulation of neuron differentiation	7	1.24E-05
GO:0006355~regulation of transcription, DNA-templated	34	1.30E-05
GO:0007399~nervous system development	12	4.97E-05
GO:0048663~neuron fate commitment	5	6.13E-05
GO:0042472~inner ear morphogenesis	6	1.26E-04
GO:0045892~negative regulation of transcription, DNA-templated	14	1.47E-04
GO:0007386~compartment pattern specification	3	2.69E-04
GO:0001657~ureteric bud development	5	3.05E-04
GO:0090090~negative regulation of canonical Wnt signaling pathway	6	6.36E-04
GO:0008045~motor neuron axon guidance	4	8.68E-04
GO:0014807~regulation of somitogenesis	3	1.23E-03
GO:0060612~adipose tissue development	4	1.54E-03
GO:0001822~kidney development	6	1.88E-03
GO:0045747~positive regulation of Notch signaling pathway	4	1.97E-03
GO:0043507~positive regulation of JUN kinase activity	4	2.47E-03

Table S9: Summary of GO analysis of genes upregulated after 6 h. Shown is the top 20 enriched categories in Biological Processes

Term	Count	PValue
GO:0007275~multicellular organism development	57	1.15E-20
GO:0006351~transcription, DNA-templated	62	8.09E-12
GO:0045944~positive regulation of transcription from RNA polymerase II promoter	42	3.68E-11
GO:0006355~regulation of transcription, DNA-templated	67	1.17E-10
GO:0007399~nervous system development	25	1.40E-10
GO:0000122~negative regulation of transcription from RNA polymerase II promoter	34	3.61E-10
GO:0045893~positive regulation of transcription, DNA-templated	29	1.84E-09
GO:0045665~negative regulation of neuron differentiation	11	4.92E-08
GO:0001822~kidney development	13	1.25E-07
GO:0048665~neuron fate specification	6	9.40E-07
GO:0045892~negative regulation of transcription, DNA-templated	24	1.95E-06
GO:0007219~Notch signaling pathway	11	5.26E-06
GO:0030182~neuron differentiation	10	4.12E-05
GO:0010628~positive regulation of gene expression	17	6.68E-05
GO:0071599~otic vesicle development	4	7.21E-05
GO:0030154~cell differentiation	25	7.94E-05
GO:0061314~Notch signaling involved in heart development	4	1.14E-04
GO:0014807~regulation of somitogenesis	4	1.14E-04
GO:0010977~negative regulation of neuron projection development	7	1.76E-04
GO:0010629~negative regulation of gene expression	13	1.82E-04

Table S10: Summary of GO analysis of genes upregulated after 12 h. Shown is the top 20 enriched categories in Biological Processes

Term	Count	PValue
GO:0007275~multicellular organism development	93	9.40E-25
GO:0007399~nervous system development	52	1.45E-21
GO:0006351~transcription, DNA-templated	107	1.89E-13
GO:0006355~regulation of transcription, DNA-templated	119	1.64E-12
GO:0030154~cell differentiation	54	8.26E-10
GO:0030182~neuron differentiation	20	1.59E-09
GO:0000122~negative regulation of transcription from RNA polymerase II promoter	51	1.88E-09
GO:0014032~neural crest cell development	9	5.56E-09
GO:0045893~positive regulation of transcription, DNA-templated	43	6.98E-09
GO:0045944~positive regulation of transcription from RNA polymerase II promoter	59	3.46E-08
GO:0001822~kidney development	18	8.94E-08
GO:0007411~axon guidance	18	6.53E-07
GO:0009952~anterior/posterior pattern specification	15	2.13E-06

GO:0045165~cell fate commitment	12	3.66E-06
GO:0001501~skeletal system development	14	6.74E-06
GO:0045892~negative regulation of transcription, DNA-templated	36	9.39E-06
GO:0001756~somitogenesis	10	1.85E-05
GO:0007507~heart development	21	3.31E-05
GO:0010977~negative regulation of neuron projection development	10	5.54E-05
GO:0001649~osteoblast differentiation	13	5.90E-05

6.3.1.2 GO analysis of direct target genes having their onset at 3, 6 or 12 h.

Given is the biological process, the number of genes and the P-value. Biological processes were sorted according to the P-value from lowest to highest

Table S11: Summary of GO analysis of direct target genes having their onset at 3 h. Shown is the top 20 enriched categories in Biological Processes

Term	Count	PValue
GO:0045944~positive regulation of transcription from RNA polymerase II promoter	10	2.99E-05
GO:0006351~transcription, DNA-templated	13	3.37E-05
GO:0000122~negative regulation of transcription from RNA polymerase II promoter	8	1.90E-04
GO:0006355~regulation of transcription, DNA-templated	13	2.17E-04
GO:0045665~negative regulation of neuron differentiation	4	2.95E-04
GO:0010628~positive regulation of gene expression	6	5.40E-04
GO:0007275~multicellular organism development	8	0.001492903
GO:0043507~positive regulation of JUN kinase activity	3	0.002130504
GO:0061074~regulation of neural retina development	2	0.005134707
GO:0007420~brain development	4	0.005905572
GO:0051302~regulation of cell division	2	0.010243896
GO:0001701~in utero embryonic development	4	0.014292421
GO:0032308~positive regulation of prostaglandin secretion	2	0.015327688
GO:0045893~positive regulation of transcription, DNA-templated	5	0.016211328
GO:0045892~negative regulation of transcription, DNA-templated	5	0.016493689
GO:0007399~nervous system development	4	0.026252205
GO:0042491~auditory receptor cell differentiation	2	0.02709179
GO:0060042~retina morphogenesis in camera-type eye	2	0.02709179
GO:0014032~neural crest cell development	2	0.028761233
GO:0050880~regulation of blood vessel size	2	0.032091806

Table S12: Summary of GO analysis of direct target genes having their onset at 6 h. Shown is the top 20 enriched categories in Biological Processes

Term	Count	PValue
GO:0006351~transcription, DNA-templated	21	4.03E-07
GO:0045944~positive regulation of transcription from RNA polymerase II promoter	15	1.41E-06
GO:0000122~negative regulation of transcription from RNA polymerase II promoter	13	1.84E-06
GO:0006355~regulation of transcription, DNA-templated	21	7.97E-06
GO:0010628~positive regulation of gene expression	9	2.95E-05
GO:0051302~regulation of cell division	3	1.40E-04
GO:0007399~nervous system development	8	1.56E-04
GO:0007219~Notch signaling pathway	5	6.05E-04
GO:0048666~neuron development	4	7.69E-04
GO:0010977~negative regulation of neuron projection development	4	0.001025439
GO:0007275~multicellular organism development	11	0.001109445
GO:0007405~neuroblast proliferation	3	0.001557353
GO:0001701~in utero embryonic development	6	0.002292675
GO:0045840~positive regulation of mitotic nuclear division	3	0.003624933
GO:0043507~positive regulation of JUN kinase activity	3	0.00681414
GO:0031018~endocrine pancreas development	3	0.007149433
GO:0045893~positive regulation of transcription, DNA-templated	7	0.008573353
GO:0045892~negative regulation of transcription, DNA-templated	7	0.008783602
GO:0060741~prostate gland stromal morphogenesis	2	0.009262774
GO:0001660~fever generation	2	0.015391087

Table S13: Summary of GO analysis of direct target genes having their onset at 12 h.

Term	Count	PValue
GO:0098903~regulation of membrane repolarization during action potential	2	0.005135
GO:0061577~calcium ion transmembrane transport via high voltage-gated calcium channel	2	0.005135
GO:0007275~multicellular organism development	7	0.007235
GO:0030182~neuron differentiation	3	0.019926
GO:0060402~calcium ion transport into cytosol	2	0.020386
GO:0007399~nervous system development	4	0.026252
GO:0007411~axon guidance	3	0.026829
GO:0006351~transcription, DNA-templated	8	0.037116
GO:0009755~hormone-mediated signaling pathway	2	0.042017
GO:0042127~regulation of cell proliferation	3	0.057504
GO:0016358~dendrite development	2	0.059959
GO:0007017~microtubule-based process	2	0.068006

GO:0006355~regulation of transcription, DNA-templated	8	0.086822

6.3.2 RNA sequencing experiment Brg1 knock-down

Gene Ontology (GO) analysis was performed using DAVID (http://david.abcc.ncifcrf.gov) as previously described (Dennis *et al.,* 2003). Analyzed were genes which were affected by a Brg1 knock-down at stage 14

Table S14: Summary of GO analysis Brg1 affected candidate genes. Shown is the top 20 enriched categories in Biological Processes

Term	Count	PValue
GO:0007275~multicellular organism development	11	5.15E-04
GO:0045944~positive regulation of transcription from RNA polymerase II promoter	10	0.001680363
GO:0003333~amino acid transmembrane transport	3	0.002068881
GO:0007420~brain development	5	0.003190223
GO:0010975~regulation of neuron projection development	3	0.003225707
GO:0042127~regulation of cell proliferation	5	0.003809389
GO:0007017~microtubule-based process	3	0.00596161
GO:0006865~amino acid transport	3	0.006248464
GO:0009953~dorsal/ventral pattern formation	3	0.008427991
GO:0006351~transcription, DNA-templated	12	0.014441686
GO:0015807~L-amino acid transport	2	0.016806335
GO:0050680~negative regulation of epithelial cell proliferation	3	0.017579689
GO:0021766~hippocampus development	3	0.018042667
GO:0045665~negative regulation of neuron differentiation	3	0.019462391
GO:0021798~forebrain dorsal/ventral pattern formation	2	0.019580338
GO:0007399~nervous system development	5	0.02153236
GO:0030154~cell differentiation	7	0.021850607
GO:0021978~telencephalon regionalization	2	0.022346667
GO:0001843~neural tube closure	3	0.03062912
GO:0030336~negative regulation of cell migration	3	0.036028973

6.4 RNA-seq data

6.4.1 Candidate gene list for the RNA sequencing analysis of Ptf1a-GR time course

Given are the genes which are differentially expressed between Ptf1a-GR overexpressing animal caps over non-injected control caps after 3, 6 and 12 h in two individual replicates. Given are the gene ID, the log_2FC activation over CC and the p-value.

Table S15: Summary of differentially expressed genes activates after 3 h

ID	log2FC	P-value
ptf1a.L	7.97	1.39E-44
zc3h12c.L	6.21	8.02E-38
hes5.1.L	6.19	1.55E-28
prdm13.S	5.62	8.35E-17
zc3h12c.S	5.40	3.36E-23
hes5.1.S	5.13	9.48E-43
hes5_X2.S	5.12	7.14E-11
ebf2.L	4.93	3.11E-16
prr15l.S	4.77	4.79E-07
grb14.L	4.75	3.79E-11
slc18a3.S	4.73	1.75E-12
nkx2-1.L	4.71	3.29E-05
cbfa2t2.S	4.57	1.62E-31
hes5.2.S	4.55	1.67E-11
dlc.L	4.50	2.01E-13
il1b.S	4.48	4.19E-07
myt1.L	4.47	2.50E-24
hes5.3.S	4.35	1.02E-14
mxra7.L	4.24	3.29E-10
hes9-1.L	4.13	8.82E-08
fzd10.S	4.12	1.34E-19
rbm24.L	4.08	4.59E-28
LOC100494099.S	4.00	5.02E-04
thbs1.L	3.99	2.46E-24
pcdh18.L	3.97	5.08E-14
foxc1.L	3.87	8.53E-08
nhsl2.L	3.81	5.66E-08

hes5.2.L	3.76	6.74E-11
LOC100495335.L	3.72	2.78E-05
hepacam2.L	3.69	2.30E-10
dll1.L	3.67	7.75E-21
Xelaev18037602m.g	3.64	1.65E-10
hoxd1.L	3.61	5.49E-06
gpr63.S	3.52	1.78E-14
hes9-2.L	3.52	2.55E-05
lrrn1-like.1.S	3.51	2.48E-13
arl4a.S	3.50	1.23E-29
prdm13.L	3.49	3.34E-05
LOC101733706-like.L	3.48	6.55E-06
post.L	3.45	7.62E-12
hes10.L	3.44	3.01E-07
Xetrov90021170m.L	3.41	7.76E-25
sp5.L	3.38	3.16E-07
adam33.S	3.37	5.14E-05
aldh1b1.L	3.35	1.43E-03
gfi1.L	3.28	5.02E-04
post.S	3.25	3.21E-10
lrrn1-like.1.L	3.23	1.31E-25
id4.S	3.21	7.30E-15
pzp.L	3.21	6.20E-05
dll1.S	3.20	1.76E-10
hes3.3.S	3.19	3.61E-06
cd247.S	3.17	8.11E-04
lrrc36.L	3.16	5.17E-08
fstl1.S	3.15	7.74E-04
hes5_X1.L	3.14	5.54E-08
tfap2b.S	3.14	1.86E-03
pou3f1.L	3.08	7.70E-06
dlk2.L	3.07	4.47E-05
hes6.2.L	3.03	2.12E-02
hes9-1.S	3.03	1.02E-09
LOC101733157.L	3.03	2.52E-04
ebf2.S	3.02	9.24E-06
insm1.S	3.02	7.99E-06
elavl3.S	3.01	3.63E-08

kcnn1.S	3.01	8.87E-04
mmp11.S	3.00	3.40E-02
olig2.S	2.99	2.43E-02
c8orf46.S	2.98	1.53E-02
sybu.L	2.98	1.01E-09
Xelaev18035340m.g	2.98	4.48E-07
myt1.S	2.92	2.25E-06
zbtb18.S	2.92	1.01E-09
cdc25b.L	2.89	1.17E-10
lmcd1.L	2.86	2.34E-02
id4.L	2.82	2.55E-03
LOC100487224.L	2.81	1.34E-08
numbl.L	2.81	1.00E-10
LOC100127750.S	2.80	1.12E-04
cbfa2t2.L	2.72	1.71E-11
fgf16.L	2.72	6.54E-03
npnt.S	2.70	2.39E-04
LOC100489305.S	2.67	9.28E-03
spo11.L	2.67	7.50E-03
tril.S	2.65	2.90E-07
Xelaev18032619m.g	2.63	9.71E-04
six3.L	2.62	7.74E-04
hes8.L	2.61	2.74E-02
tiparp.L	2.61	1.72E-20
tsc22d3.L	2.56	4.11E-06
prr7.L	2.53	8.16E-04
myb.S	2.52	1.17E-06
lhx4.S	2.51	4.05E-02
pou3f1.S	2.51	7.32E-08
ankrd65.L	2.50	4.79E-03
Xelaev18007001m.g	2.49	4.41E-07
slc43a2.S	2.47	3.01E-07
ca2.L	2.44	1.57E-02
Xelaev18000619m.g	2.44	2.21E-02
amotl2.L	2.41	3.17E-16
hes5_X2.L	2.39	3.00E-05
lhx1.S	2.36	4.47E-05
atp6v1c2.L	2.35	4.65E-04

mmp17.L	2.35	4.90E-02
nek2.L	2.35	1.32E-03
egr4.L	2.33	6.54E-03
manea.L	2.33	1.25E-02
sec24d-like.1.L	2.32	4.19E-04
kitlg.S	2.25	3.81E-03
Xelaev18005831m.g	2.23	1.16E-03
edn1.L	2.22	1.46E-02
fam198b.L	2.21	2.73E-06
ampd2.S	2.17	4.05E-02
rbl2.L	2.17	1.64E-02
dkk2.L	2.16	4.05E-02
znf534.L	2.14	2.44E-03
aplnr.L	2.13	4.52E-03
axin2.L	2.13	3.93E-02
foxi1.L	2.12	1.86E-03
gjc2.L	2.12	6.77E-03
insm1.L	2.12	1.96E-03
lancl3.S	2.12	4.51E-02
tp73.S	2.10	2.03E-02
rab15.L	2.09	5.19E-04
LOC101731452.L	2.07	5.12E-05
stard4.L	2.07	7.74E-04
fam101b.L	2.06	2.44E-03
mxi1.L	2.05	1.16E-04
myb.L	2.05	5.17E-04
vash2.S	2.05	1.28E-05
fzd10.L	2.03	3.57E-03
prickle1.S	2.03	4.02E-08
cdknx.L	2.02	1.35E-07

Table S16: Summary of differentially expressed genes activates after 6 h

ID	log2FC	P-value
ptf1a.L	8.52	3,81E-43
prdm13.S	7.86	3,91E-34
prdm13.L	7.36	7,60E-23

ebf2.L	7.08	9,35E-33
gfi1.L	6.31	9,57E-13
pou3f1.L	6.27	2,34E-20
mxra7.L	6.03	6,25E-17
pou3f1.S	5.88	1,21E-33
cbfa2t2.S	5.78	2,21E-50
LOC100127750.S	5.69	3,79E-11
zc3h12c.L	5.62	2,98E-38
hes5.2.L	5.6	7,18E-13
prr15l.S	5.57	2,06E-09
hes8.L	5.55	4,89E-14
ebf2.S	5.48	2,28E-17
hes5.1.L	5.46	2,69E-27
neurod4.L	5.36	2,16E-09
grb14.L	5.26	1,29E-08
LOC100494099.S	5.22	1,99E-07
fzd10.S	5.11	4,26E-33
hes8.S	5.11	3,17E-12
zc3h12c.S	5.09	5,61E-23
id4.S	4.99	2,69E-46
gpr63.S	4.96	5,62E-18
dmrt2.L	4.93	6,25E-17
hepacam2.L	4.91	1,55E-17
elavl3.S	4.88	1,32E-17
hes3.3.S	4.84	6,69E-19
Xelaev18007001m.g	4.84	9,10E-25
cd247.S	4.82	4,15E-08
slc18a3.S	4.78	3,58E-09
thbs1.L	4.69	2,19E-26
chst3.L	4.6	2,63E-15
olig2.S	4.58	4,78E-06
hes5.1.S	4.56	2,92E-35
pzp.L	4.54	4,14E-09
b4galnt1.S	4.53	6,59E-10
hes9-1.L	4.47	9,16E-09
fam101b.L	4.45	8,32E-14
lhx1.S	4.45	5,62E-18
hoxd1.L	4.44	2,51E-08

hes5_X2.S	4.42	5,18E-10
runx1t1.L	4.39	1,85E-09
igf2.L	4.36	3,14E-07
ptger3.L	4.35	1,26E-06
hes5_X1.L	4.34	1,81E-13
hes5.3.S	4.29	5,26E-13
c8orf46.S	4.27	2,17E-06
foxc1.L	4.26	1,55E-07
tcf15.L	4.19	1,33E-06
myt1.S	4.17	7,72E-14
c8orf46.L	4.16	6,26E-04
zbtb18.S	4.13	2,29E-17
myt1.L	4.1	4,67E-21
tlx3.S	4.03	1,58E-07
nhsl2.L	4.02	2,52E-07
six1.L	4.02	9,30E-05
lhx4.S	3.98	2,77E-06
hes10.L	3.97	1,59E-09
mamdc2.L	3.96	5,76E-06
dlk2.L	3.93	4,14E-09
numbl.L	3.93	1,06E-22
drgx.L	3.85	1,75E-04
scrt1.S	3.84	7,49E-07
Xelaev18036651m.g	3.84	9,19E-04
cbfa2t2.L	3.78	3,44E-23
Xelaev18036200m.g	3.78	9,23E-06
hes6.2.L	3.77	2,81E-04
fstl1.S	3.72	1,16E-04
bmp3.L	3.71	2,15E-05
Xelaev18037602m.g	3.71	7,13E-11
cdc25b.L	3.7	4,76E-18
il1b.S	3.67	2,87E-04
sybu.L	3.65	5,63E-13
mmp17.L	3.63	1,12E-04
kitlg.S	3.59	2,90E-07
egr4.L	3.58	7,11E-06
zc3h12a.L	3.55	6,53E-03
plk3.L	3.51	3,72E-13

drgx.S	3.48	4,14E-05
Xelaev18028850m.g	3.48	7,23E-11
hnf1b.S	3.44	3,31E-03
hes6.2.S	3.43	6,91E-03
myos-like.S	3.41	6,38E-03
Xetrov90021170m.L	3.38	9,93E-25
hes9-1.S	3.37	2,09E-11
adam33.S	3.36	5,10E-05
gfra1.S	3.36	9,67E-04
twist1.L	3.36	9,70E-04
edn1.L	3.35	2,10E-05
gfra3.S	3.35	1,42E-02
relt.S	3.35	2,04E-05
Xelaev18005831m.g	3.31	1,58E-07
arl4a.S	3.3	2,08E-26
LOC100036671.L	3.29	3,67E-04
dpysl3.L	3.28	3,88E-04
lrrn1-like.1.S	3.28	7,50E-17
pou3f3.L	3.27	4,64E-03
slc43a2.S	3.27	2,10E-11
tril.S	3.26	2,71E-10
dmrta2.S	3.24	8,19E-06
fzd10.L	3.23	1,56E-08
LOC101733706-like.L	3.23	2,44E-03
rltpr.L	3.23	1,06E-04
ecel1.S	3.22	2,47E-02
insm1.S	3.22	6,55E-07
mmp11.L	3.22	5,56E-03
Xelaev18036111m.g	3.21	1,19E-07
shd.L	3.2	5,62E-03
aldh1b1.L	3.18	4,59E-03
LOC100495335.L	3.16	3,93E-04
zc3h12a.S	3.16	7,72E-03
tlr3.L	3.15	2,21E-02
LOC101733157.L	3.14	1,38E-03
foxa1.S	3.13	2,47E-10
tfe3.L	3.13	1,15E-02
rbm24.L	3.12	6,25E-17

hes9-2.L	3.09	7,34E-04
LOC100485259.L	3.09	2,97E-17
arhgef26.L	3.06	4,73E-06
neurod4.S	3.06	1,06E-03
Xelaev18019047m.g	3.06	2,20E-03
hmx3.L	3.05	1,44E-02
sp5.L	3.05	2,72E-06
rassf6.L	3.04	2,33E-02
slc3a2.L	3.02	1,15E-02
Xelaev18032400m.g	3.02	4,09E-02
snrk.S	3.01	3,94E-15
nptx2.L	3	3,50E-02
axin2.S	2.99	6,69E-03
ag1.S	2.97	3,67E-09
fgf16.L	2.97	1,52E-03
tn3.L	2.97	1,58E-02
muc1.L	2.96	2,99E-02
prr7.L	2.95	2,35E-05
emx1.L	2.94	4,10E-02
gfi1.S	2.94	1,02E-04
rab15.L	2.93	3,03E-10
p2ry4.L	2.91	1,71E-02
eln2.L	2.9	2,46E-04
axin2.L	2.88	6,17E-04
faxc.L	2.88	1,21E-24
Xetrov90002103m.L	2.87	3,20E-02
cfap70.L	2.85	7,65E-03
Xelaev18000619m.g	2.83	1,57E-03
prr18.L	2.82	1,95E-03
bhlhe22.L	2.81	1,15E-02
angptl4.L	2.79	9,30E-05
galnt12.L	2.78	3,56E-07
ccdc141.L	2.77	1,62E-03
pou2f3.L	2.77	2,81E-09
snai2.L	2.76	8,04E-05
irx3.L	2.75	3,20E-04
LOC100493614.S	2.74	8,14E-07
amotl2.S	2.72	4,42E-16

phlda1.L	2.72	1,50E-03
gch1.L	2.7	3,51E-13
tfap2b.S	2.69	2,89E-02
post.L	2.68	1,56E-07
LOC100494099.L	2.67	1,41E-02
mdk.S	2.66	1,27E-05
ncmap.S	2.64	8,17E-03
post.S	2.64	3,20E-07
bhlhe40.L	2.63	2,43E-03
Xelaev18005924m.g	2.63	2,41E-06
insm1.L	2.62	1,31E-05
frem2.S	2.6	1,02E-04
hes3.1.S	2.6	2,50E-09
rab15.S	2.57	3,20E-02
arhgap23.L	2.56	4,08E-05
eya1.S	2.56	2,54E-06
rnf165.L	2.56	4,03E-08
vtcn1.L	2.56	1,15E-03
hes5.2.S	2.55	2,87E-02
lypd6.L	2.55	4,38E-03
fjx1.S	2.54	1,68E-02
kremen2.S	2.53	2,85E-02
spo11.L	2.53	1,53E-02
Xetrov90025030m.L	2.53	4,37E-05
lmcd1.L	2.5	4,34E-02
gria1-like.1.S	2.49	4,75E-02
kctd12.L	2.49	1,18E-02
lrrc36.L	2.49	1,08E-05
meis1.L	2.48	4,50E-05
hes5_X2.L	2.47	3,78E-05
Xetrov90000859m.L	2.47	2,05E-02
LOC100497338-like.L	2.45	1,27E-05
vcan.L	2.44	7,74E-03
ctsk.L	2.43	1,68E-02
Xelaev18042455m.g	2.43	5,79E-03
pm20d1.L	2.42	1,88E-05
tfap2e.S	2.42	6,37E-03
elavl4.L	2.41	1,15E-02

lhx8.L	2.41	4,91E-06
prickle1.S	2.4	2,09E-11
bhlhe40.S	2.39	2,71E-03
tiparp.L	2.38	4,71E-16
slc1a1.L	2.37	3,03E-02
dbp.S	2.36	8,24E-05
irf1.L	2.35	1,83E-07
cidec.L	2.33	1,19E-16
glipr2.S	2.33	3,98E-05
Xelaev18026372m.g	2.32	7,78E-08
cdknx.L	2.31	2,71E-10
onecut1.2.L	2.31	3,39E-03
a2m.S	2.3	4,67E-16
amotl2.L	2.3	1,85E-15
aim1l.S	2.28	1,14E-02
syt16.L	2.28	1,23E-03
fam214a.S	2.27	2,20E-05
kcnc4.S	2.27	1,00E-02
Xelaev18013182m.g	2.27	6,39E-04
id4.L	2.25	5,22E-05
plk3.S	2.25	6,95E-05
atf6b.S	2.24	7,67E-04
rnf125.L	2.23	2,85E-02
znf238.2.L	2.21	6,04E-20
sept5.L	2.2	3,04E-04
sox9.L	2.19	7,42E-03
dll1.L	2.18	2,12E-07
sec24d-like.1.L	2.17	5,16E-03
serpinf1.L	2.17	4,44E-02
znf534.L	2.17	3,73E-04
pcdh18.L	2.15	4,14E-04
iqca1.S	2.14	2,11E-02
reep5.S	2.14	4,38E-05
znf238.2.S	2.13	6,45E-09
kdm7a.L	2.11	6,68E-04
c8orf4.L	2.1	1,21E-02
creb3l2.S	2.1	3,25E-03
rfk.S	2.1	4,10E-02

atp6v0d2.L	2.09	4,81E-02
dnase1l3.L	2.09	2,12E-02
eps8l2.L	2.08	3,64E-02
nes.L	2.08	2,37E-04
fam83e.S	2.06	6,05E-03
Xelaev18023501m.g	2.06	3,34E-07
ankrd65.L	2.05	3,80E-02
gse1.L	2.02	3,04E-05
rap1gap.S	2.01	1,47E-02
xk.L	2.01	2,82E-02

Table S17: Summary of differentially expressed genes activates after 12 h

ID	log2FC	p-value
prdm13.L	9.38	1,04E-37
prdm13.S	9.33	3,02E-45
neurod4.L	8.84	4,86E-27
scrt1.S	8.55	2,29E-31
aldh1b1.L	8.4	3,23E-28
ptf1a.L	8.38	5,09E-43
chst3.L	8.06	4,49E-28
ebf2.L	7.91	8,93E-34
ebf2.S	7.85	8,56E-27
neurod4.S	7.56	2,54E-20
dpysl3.L	7.44	3,18E-47
pck1.L	7.39	5,55E-22
Xetrov90027705m.L	7.24	4,51E-15
ppp1r9b.S	7.1	3,61E-22
tfap2b.S	7.06	1,27E-24
bgn.L	7.05	2,26E-31
mxra7.L	6.89	1,57E-24
shd.L	6.71	1,88E-19
slc18a3.S	6.53	4,21E-25
lbx1.S	6.52	5,90E-11
drgx.L	6.45	7,42E-13
pou3f1.L	6.34	8,84E-18
hesx1.S	6.33	4,28E-27

mmp28.L	6.28	6,27E-13
Xelaev18040877m.g	6.28	5,95E-16
npb.L	6.23	1,25E-09
LOC100490531-like.L	6.22	7,15E-10
igfbpl1.L	6.17	3,59E-11
prph.S	5.94	5,31E-37
LOC100487395.L	5.91	9,09E-22
tubb3.L	5.91	1,47E-11
igf2.L	5.82	9,07E-13
kirrel2.L	5.78	6,60E-41
pou3f1.S	5.77	2,20E-18
Xelaev18032183m.g	5.7	5,63E-08
dpysl4.L	5.63	3,67E-08
nr5a2.L	5.59	1,25E-08
cd247.S	5.55	3,82E-11
snap25.L	5.52	5,63E-12
kirrel2.S	5.5	2,41E-37
tfap2b.L	5.49	1,52E-07
map2.S	5.43	1,82E-22
onecut1.2.L	5.4	4,03E-40
nova1.L	5.17	7,10E-13
pyy.L	5.17	4,41E-06
elavl4.L	5.16	5,31E-15
LOC101733706-like.L	5.16	1,61E-09
myl1.L	5.14	1,00E-05
elavl3.S	5.12	2,58E-27
barhl2.L	5.09	6,54E-10
phlda1.L	5.08	8,25E-10
bmp3.L	5.02	5,90E-11
nhlh1.S	5.01	4,72E-06
tcf15.S	5.01	2,37E-06
tfap2e.S	5	3,53E-15
nhlh1.L	4.99	8,91E-07
scrt1.L	4.97	1,49E-06
gpr63.S	4.96	1,94E-18
tuba4a.L	4.9	1,52E-28
st18.L	4.82	1,45E-07
tlx3.S	4.8	5,65E-10

eln2.L	4.79	5,31E-11
tlx3.L	4.77	1,37E-14
tubb3.S	4.76	1,44E-16
dmrta2.L	4.72	4,72E-19
gch1.L	4.7	2,41E-37
map3k12.S	4.67	6,04E-09
pcmtd1.L	4.66	1,26E-05
ak3.S	4.64	1,34E-08
Xelaev18007508m.g	4.64	1,25E-04
LOC100490531-like.S	4.62	8,44E-05
fitm1.L	4.61	6,16E-05
tmem116.L	4.6	1,13E-20
adcyap1.S	4.56	2,19E-05
LOC100127750.S	4.56	9,24E-08
cuzd1.L	4.55	1,01E-04
slc3a2.L	4.53	8,31E-15
unc5a.L	4.52	2,30E-06
Xelaev18021728m.g	4.52	8,11E-05
tcf15.L	4.49	1,79E-10
Xetrov90027705m.S	4.49	1,15E-04
mmp17.L	4.48	9,72E-07
gria1-like.1.S	4.42	1,08E-07
skor1.S	4.42	1,32E-12
des.1.S	4.4	1,46E-04
tal1.L	4.39	1,74E-04
tespa1.S	4.39	6,16E-05
sparc.L	4.38	4,17E-07
aqp3.L	4.37	7,14E-05
rassf6.L	4.34	3,33E-05
ptger3.L	4.32	5,67E-08
mcf2l.S	4.31	7,41E-10
slc43a2.S	4.31	2,38E-22
lhx8.L	4.3	2,85E-18
prdm8.L	4.29	3,03E-04
cacnb1.S	4.28	2,58E-04
Xelaev18047032m.g	4.27	7,28E-05
cyp1c1.L	4.23	2,75E-04
six1.S	4.23	1,86E-05

gad1.1.L	4.2	2,45E-06
tfap2e.L	4.2	1,15E-06
emilin1.L	4.19	1,04E-10
bag2.L	4.16	3,76E-04
dpp10.S	4.15	5,57E-07
nat14.S	4.14	5,69E-05
evi5.L	4.13	2,58E-30
snai2.L	4.13	6,74E-13
zc3h12c.S	4.12	4,10E-15
Xelaev18007001m.g	4.11	2,37E-20
edn1.L	4.06	7,53E-07
LOC100487796-like.L	4.03	1,21E-09
mtcl1.S	4.02	1,14E-05
Xelaev18006418m.g	4.02	4,59E-04
kank2.L	4.01	1,06E-03
neurog2.S	3.99	4,04E-10
adamtsl1.L	3.9	1,11E-08
fezf1.L	3.89	3,74E-04
des.1.L	3.88	7,51E-05
kiaa1755.L	3.88	1,39E-04
LOC100496628-like.L	3.87	6,87E-06
LOC100271753.L	3.86	2,21E-06
barhl2.S	3.81	4,87E-04
runx1t1.S	3.77	5,46E-06
hmox1.L	3.76	3,23E-28
LOC100488523.L	3.76	6,38E-04
des.2.L	3.74	3,10E-03
serpinf1.L	3.74	1,45E-07
hmox1.S	3.73	1,48E-03
drgx.S	3.72	9,95E-07
reep5.S	3.72	1,34E-16
adcyap1.L	3.69	1,50E-03
arhgef26.S	3.69	4,63E-05
atg9b.L	3.69	2,25E-11
cacna2d2.L	3.68	6,27E-07
tmem35.L	3.68	7,24E-04
hes5.2.L	3.67	1,47E-06
kiaa1715.S	3.66	2,54E-03

pou3f2.L	3.66	1,45E-07
hdac7.S	3.64	4,16E-05
dlk2.L	3.63	5,60E-05
bhlhe22.L	3.59	2,83E-04
eva1b.S	3.59	8,10E-04
bcar1.S	3.58	2,98E-06
hoxc5.S	3.58	2,04E-03
lmo2.S	3.58	2,51E-03
samd7.L	3.58	3,35E-05
cbfa2t2.S	3.57	8,07E-21
runx1t1.L	3.57	3,27E-08
zc3h12c.L	3.56	5,45E-17
cbfa2t2.L	3.55	2,37E-20
ror2.S	3.55	8,28E-12
cbfa2t3.L	3.52	2,06E-03
six3.L	3.52	1,08E-08
lmcd1.S	3.51	8,02E-12
chat.S	3.49	4,76E-03
tapbp.L	3.49	3,16E-04
adam33.S	3.48	9,49E-06
zbtb16.S	3.47	7,30E-09
Xetrov90000859m.L	3.46	1,78E-05
ca14.S	3.41	4,67E-05
fdft1.L	3.39	1,01E-06
gas7.L	3.39	2,81E-07
clip2.S	3.38	2,09E-06
kank3.L	3.38	1,87E-08
mespa.S	3.36	7,44E-03
irx3.L	3.35	3,68E-05
rgmb.L	3.32	1,86E-11
skor1.L	3.32	2,52E-06
pak3.S	3.31	6,49E-23
rgs10.L	3.31	1,95E-03
Xelaev18024617m.g	3.31	2,73E-03
map2.L	3.3	8,94E-05
p2ry4.L	3.3	1,07E-08
Xetrov90010371m.L	3.3	7,61E-04
epb41l1.L	3.29	3,27E-04

foxc2.S	3.28	2,51E-03
sox11.L	3.28	2,79E-17
zcchc24.L	3.28	7,32E-03
adprh.S	3.27	2,26E-04
fam212a.L	3.26	3,93E-16
ppp1r14b.S	3.26	1,19E-05
Xetrov90016928m.L	3.25	9,10E-03
arhgap4.L	3.24	5,60E-05
c8orf46.S	3.24	1,18E-03
dennd2c.L	3.24	6,28E-11
otx2.L	3.24	1,03E-02
pip4k2b.L	3.24	2,08E-06
gfra1.S	3.2	2,29E-04
pmp22.L	3.19	7,49E-03
gfi1.L	3.16	2,45E-04
plekhg4.S	3.16	6,32E-10
celf2.L	3.15	2,67E-04
ncmap.S	3.15	3,65E-05
cdc42ep3.S	3.14	1,38E-04
dbn1.L	3.14	5,50E-34
nrp2.L	3.14	1,25E-08
sfrp2.L	3.14	1,53E-11
zbtb18.S	3.14	4,11E-09
rundc3a.L	3.13	7,20E-04
pkdcc.L	3.12	1,06E-03
sox11.S	3.1	7,43E-13
aldh1a2.S	3.09	1,74E-09
dlc.S	3.09	1,20E-04
nhs.S	3.09	4,17E-04
nox4.S	3.09	7,20E-03
faxc.L	3.08	4,03E-24
olig2.S	3.08	5,22E-03
ttc9.L	3.08	5,96E-26
cplx2.S	3.07	2,58E-02
Xelaev18020376m.g	3.07	3,13E-02
ptprt.L	3.06	1,68E-04
plekhg4.L	3.05	8,02E-12
vim.S	3.03	2,25E-07

zeb2.L	3.03	2,50E-05
dbn1.S	3.02	3,02E-15
dlx6.L	3.02	1,75E-07
clstn3.L	3.01	2,28E-02
dmbx1.S	3.01	2,53E-02
klf7.L	3.01	7,48E-04
LOC100125030.S	3.01	5,74E-03
pla2g12b.S	3.01	6,66E-03
rnf165.L	3.01	2,97E-11
Xelaev18021928m.g	3.01	1,96E-15
LOC100492460.L	2.99	1,91E-02
s1pr5.S	2.99	4,22E-11
slc38a8.L	2.99	1,08E-03
st8sia6.L	2.99	5,41E-07
aplnr.L	2.98	1,39E-06
aplnr.S	2.98	2,67E-05
cplx2.L	2.98	9,09E-04
crmp1.S	2.98	9,73E-04
sybu.L	2.98	8,46E-08
abtb2.S	2.97	2,39E-03
shox2.L	2.96	3,59E-02
neurog1.L	2.95	1,62E-02
Xelaev18041660m.g	2.95	1,58E-02
cpe.S	2.94	1,00E-02
emx1.L	2.94	1,30E-02
slc25a38.L	2.94	1,32E-08
zic3.L	2.94	1,31E-02
cables1.L	2.93	6,37E-03
Xelaev18003350m.g	2.93	2,93E-02
a2m.S	2.92	5,63E-27
slc8a2.S	2.91	1,83E-02
ulk1.L	2.91	7,25E-06
Xelaev18016582m.g	2.91	1,42E-04
Xelaev18047968m.g	2.91	2,16E-02
arid1b.L	2.9	4,23E-19
cacna2d1.L	2.9	2,18E-09
Xelaev18030957m.g	2.9	1,80E-02
il5ra.S	2.88	2,11E-04

LOC100487395.S	2.88	4,17E-04
LOC101733102.L	2.88	5,99E-04
st18.S	2.88	2,11E-02
zfhx4.S	2.88	1,32E-06
cep85l.S	2.87	5,02E-10
nova2.S	2.87	1,27E-03
plekhd1.L	2.87	3,27E-02
hlf.L	2.86	2,53E-03
pzp.L	2.86	2,17E-04
asb2.L	2.85	3,87E-02
bhlhe40.L	2.85	3,94E-04
pdia2.S	2.85	6,64E-03
Xelaev18039965m.g	2.85	2,18E-06
dbndd1.L	2.84	2,95E-02
LOC100494987-like.L	2.84	2,62E-02
ankrd6.L	2.83	5,04E-03
elavl3.L	2.82	4,21E-10
hoxd1.L	2.82	1,14E-05
limd2.L	2.82	2,04E-04
LOC100485834.L	2.82	1,75E-03
LOC100496678.L	2.81	4,38E-02
rap1gap.S	2.81	2,53E-05
slc26a9.S	2.81	9,22E-03
Xelaev18038420m.g	2.81	7,03E-09
afap1l1.L	2.8	3,50E-04
mdk.L	2.8	1,45E-19
plod2.S	2.8	7,29E-05
six1.L	2.8	3,80E-03
asb12.L	2.79	2,95E-03
lhx1.S	2.79	8,75E-05
fam102a.S	2.78	2,35E-04
mamdc2.L	2.78	2,18E-03
pcdh9.L	2.78	1,69E-04
plekhg1.L	2.78	6,74E-10
arhgef26.L	2.77	6,86E-05
btbd19.L	2.77	4,27E-02
gcnt1.S	2.77	7,64E-05
kcna1.S	2.77	8,53E-04

draxin.S	2.76	1,90E-02
nuak1.L	2.76	9,87E-06
cacnb3.L	2.75	3,23E-02
msx2.S	2.75	1,86E-08
hcar3.L	2.74	1,05E-03
hes5.2.S	2.74	4,75E-03
ag1.S	2.73	3,03E-08
cxcr2.L	2.73	4,90E-02
dnajc6.S	2.73	9,28E-03
hes6.2.L	2.71	3,04E-02
tmem169.L	2.7	4,11E-09
a2m.L	2.69	2,93E-04
cldn5.L	2.69	5,81E-03
map3k13.L	2.69	2,23E-02
sp5.L	2.68	2,48E-06
tet3.S	2.68	6,20E-04
glis2.S	2.67	1,07E-05
Xelaev18043580m.g	2.67	1,34E-08
insm1.L	2.66	4,72E-06
pcdh18.L	2.66	3,39E-05
tie1.S	2.66	1,77E-02
auts2.S	2.65	1,39E-11
cited2.L	2.65	7,77E-12
faxc.S	2.65	2,50E-02
agbl1.S	2.64	5,80E-08
agbl1.S	2.64	5,80E-08
agbl1.S	2.64	5,80E-08
agbl1.S	2.64	5,80E-08
LOC100495335.L	2.64	5,69E-03
limd2.S	2.63	5,21E-06
dmrta2.S	2.62	3,39E-05
fam89a.S	2.62	9,85E-06
grb14.L	2.62	2,91E-02
hes5_X2.L	2.59	3,16E-06
lrp4.S	2.59	2,09E-06
tdrp.L	2.58	3,01E-20
lrrn1-like.1.S	2.57	3,15E-11
nes.L	2.57	6,27E-07

cel-like.1.S	2.56	7,17E-03
ctsk.L	2.56	2,32E-03
irx4.L	2.56	2,60E-02
lhx5.L	2.55	9,53E-18
LOC100489305.S	2.55	9,69E-03
fstl1.L	2.54	3,73E-02
krt19.S	2.53	2,73E-12
LOC101733157.L	2.53	3,16E-04
Xelaev18016676m.g	2.53	5,12E-08
abtb2.L	2.52	2,05E-03
pcmtd1.S	2.52	8,75E-05
f2r.S	2.51	1,65E-02
st3gal2.1.L	2.51	4,22E-05
abcb9.L	2.5	2,97E-19
eya1.L	2.5	2,87E-04
fam102a.L	2.5	7,55E-05
frmd6.L	2.49	8,44E-18
gas1.L	2.49	2,19E-05
Xelaev18023424m.g	2.49	2,66E-02
Xelaev18039076m.g	2.49	4,64E-03
arhgap33.S	2.48	4,91E-05
hes5.3.S	2.48	9,01E-07
srrm4.L	2.48	1,50E-03
egr4.L	2.47	4,01E-02
fgf16.L	2.47	6,40E-03
hes2.L	2.47	1,34E-05
pnhd.S	2.47	2,56E-02
kansl1l.L	2.45	1,11E-02
rnf165.S	2.45	3,41E-07
Xelaev18024498m.g	2.45	3,42E-02
hand2.S	2.44	3,54E-04
stk40.L	2.44	2,95E-10
tox3.L	2.44	3,41E-12
f3.S	2.43	2,91E-03
rfk.S	2.43	2,03E-03
Xelaev18019210m.g	2.43	6,18E-03
prdm14.L	2.42	2,33E-05
rnd3.S	2.42	4,59E-05

tuba4a.S	2.41	8,16E-05
fgd1.S	2.4	5,75E-03
irx1.L	2.4	6,18E-03
zfhx4.L	2.4	7,52E-04
LOC100496628-like.S	2.39	4,59E-02
klhl25.S	2.38	2,12E-03
cemip.S	2.37	4,46E-04
mdk.S	2.37	5,63E-05
slc43a2.L	2.37	1,01E-03
myt1.L	2.36	6,16E-07
Xelaev18009525m.g	2.36	6,38E-04
eya2.S	2.35	4,76E-03
neurog2.L	2.35	4,08E-02
slit1.S	2.35	2,52E-03
znf329.S	2.35	5,74E-04
aldh1a2.L	2.34	1,17E-07
cep85l.L	2.33	5,64E-07
hoxd1.S	2.33	4,77E-02
lrig1.S	2.33	2,27E-02
myt1.S	2.33	1,74E-04
ndst1.S	2.33	7,54E-07
irf1.L	2.32	3,64E-06
pitx3.L	2.32	2,33E-02
spo11.L	2.32	3,16E-02
btg2.S	2.31	6,38E-04
mctp2.L	2.31	3,76E-03
LOC100492804.L	2.3	3,65E-05
manea.L	2.3	3,97E-03
mtcl1.L	2.3	1,47E-03
b4galnt1.S	2.29	2,87E-04
cldn6.1.L	2.29	2,17E-08
Xelaev18028850m.g	2.29	5,93E-05
cpe.L	2.28	6,64E-06
zeb2.S	2.28	6,74E-04
dennd2c.S	2.27	3,29E-05
hes5_X2.S	2.27	1,05E-03
smoc1.S	2.27	2,48E-02
arhgap36.L	2.26	9,88E-04

ephb3.S	2.26	1,11E-10
smim3.S	2.25	2,93E-03
Xelaev18033094m.g	2.25	3,86E-02
cdc42ep4.L	2.23	2,79E-03
tmem74b.S	2.23	8,06E-03
Xelaev18042973m.g	2.23	4,99E-02
meis1.L	2.22	6,77E-05
rufy3.L	2.22	4,54E-06
gtf2ird1.L	2.21	1,94E-02
rasal2-like.2.S	2.21	8,02E-12
antxr2.L	2.2	7,09E-04
rab3a.S	2.2	1,19E-12
mcc.S	2.19	2,69E-03
mybl1.S	2.19	1,07E-03
tuba1b.L	2.19	9,54E-07
cdyl2.S	2.18	1,74E-02
gfi1.S	2.18	9,57E-03
LOC100488626.L	2.18	1,96E-02
vim.L	2.18	1,13E-06
acy3.L	2.17	9,06E-07
numbl.L	2.17	3,10E-07
ppp1r1a.L	2.17	2,00E-04
rgma.L	2.17	7,29E-07
dgki.S	2.16	2,10E-02
insm2.L	2.15	4,46E-02
krt18.S	2.15	6,89E-07
cuedc1.S	2.14	1,06E-11
lhx1.L	2.14	4,68E-02
ptch2.S	2.14	2,65E-02
rph3al.S	2.14	2,13E-02
tuft1.L	2.14	3,29E-02
Xelaev18016674m.g	2.14	8,87E-04
dact1.L	2.13	9,63E-13
fsd1.L	2.13	2,13E-02
foxc1.S	2.12	3,99E-02
mcf2l.2.L	2.12	6,42E-03
pak3.L	2.11	1,84E-03
sall3.L	2.11	1,87E-08

aim1l.S	2.1	1,15E-02
dlk2.S	2.1	1,80E-02
hes8.L	2.1	8,78E-05
dnajc6.L	2.09	2,00E-02
cdc42se2-like.1.L	2.08	1,29E-05
dclk1.S	2.08	3,44E-02
insm1.S	2.08	3,83E-03
tmem170b.L	2.08	3,64E-03
kctd1.L	2.07	2,42E-03
map1lc3a.L	2.07	1,95E-03
nckap5l.L	2.06	3,82E-05
fbxo32.L	2.05	2,16E-02
pik3r3.L	2.05	2,54E-04
rbm38.L	2.05	1,74E-09
rexo1.S	2.05	4,59E-05
rnf130.S	2.05	2,99E-05
kiaa1468.L	2.04	1,08E-03
rasl10b.L	2.04	1,09E-06
Xelaev18044942m.g	2.04	1,75E-04
tes.L	2.03	4,43E-03
cttnbp2nl.L	2.02	7,68E-04
scamp4.S	2.02	4,56E-02
sfrp2.S	2.02	1,01E-14
stmn1.S	2.02	2,81E-08
hoxc4.S	2.01	2,06E-02
fstl1.S	2	1,39E-02
LOC100496433.1.L	2	1,68E-04
lrp4.L	2	4,06E-06
pmp22.S	2	1,78E-02

6.4.2 Candidate gene list for the RNA sequencing analysis of Brg1 knock-down experiment

Given are the genes which are differentially expressed between Ptf1a-GR + cMO or Ptf1a-GR + Brg1MO overexpressing animal caps over non-injected control caps in two individual replicates. Given are the gene ID, the log_2FC activation over CC and the p-value.

Table S18: Summary of differentially expressed genes by Ptf1a + cMO

ID	log2FC	P-value
Xelaev18007508m.g	14.26	9.14E-18
neurod4.L	12.86	4.40E-14
prdm13.L	12.29	4.88E-14
prph.S	12.22	6.31E-28
neurod4.S	11.98	1.88E-11
nhlh1.L	11.94	4.57E-13
pou3f1.L	11.65	1.21E-11
prdm13.S	11.46	7.21E-19
nhlh1.S	11.42	1.87E-11
scrt1.S	11.25	3.90E-12
igfbpl1.L	11.16	7.42E-11
dpysl4.L	10.93	6.15E-10
st18.L	10.78	2.33E-10
neurog1.L	10.75	1.53E-10
des.2.L	10.49	1.78E-08
hoxc3.L	10.43	4.64E-07
prdm8.L	10.31	2.43E-04
lmo2.S	10.28	4.37E-09
lbx1.S	10.14	1.36E-08
LOC100490531-like.L	9.95	3.31E-09
LOC100496628-like.L	9.89	1.83E-07
pyy.L	9.88	1.72E-07
hes5.2.L	9.75	7.77E-07
aqp3.L	9.69	1.68E-04
ebf2.L	9.65	6.74E-32
fezf1.L	9.64	1.12E-05
Xetrov90027705m.L	9.54	8.64E-15
nr5a2.L	9.43	1.86E-06
skor1.S	9.36	6.12E-12
Xelaev18047032m.g	9.35	8.25E-05
kiaa1755.L	9.26	4.74E-21
adcyap1.S	9.19	3.14E-06
aldh1b1.L	9.13	6.83E-06
Xelaev18032183m.g	9.06	1.65E-06
mllt11.S	9.01	2.31E-06
tfap2b.S	9.01	8.87E-36

skor2.S	8.94	6.35E-04
pcdh9.L	8.92	8.63E-06
map3k13.L	8.87	9.24E-05
Xelaev18002612m.g	8.83	1.62E-03
Xelaev18018357m.g	8.82	1.44E-05
Xelaev18004302m.g	8.81	1.49E-05
tespa1.S	8.77	1.14E-05
shox2.L	8.76	9.85E-06
prdm8.S	8.73	1.70E-04
igfbpl1.S	8.73	5.92E-05
tubb3.L	8.70	7.68E-07
shd.L	8.64	5.11E-12
hesx1.S	8.56	1.26E-09
des.1.L	8.52	2.53E-10
foxd2.L	8.48	7.82E-05
tfap2e.L	8.35	4.09E-06
ebf2.S	8.34	8.84E-31
dpysl3.L	8.27	5.82E-79
nova2.S	8.27	9.24E-05
nes.L	8.27	1.68E-19
pou3f1.S	8.20	8.52E-03
Xelaev18000445m.g	8.19	5.78E-05
tcf15.S	8.14	2.74E-04
Xetrov90027705m.S	8.14	8.38E-05
barhl2.S	8.03	7.62E-09
nts.L	8.03	1.67E-03
nkx3-2.S	8.01	5.50E-03
foxb1.S	7.99	2.18E-03
ptger3.L	7.99	1.32E-04
hmx1.1	7.97	5.85E-03
clstn3.L	7.93	2.51E-12
hes6.2.L	7.92	5.89E-03
LOC100490531-like.S	7.91	4.37E-04
sybu.L	7.89	6.70E-08
gad1.1.L	7.87	1.29E-16
ptf1a.L	7.83	6.09E-05
slc26a9.S	7.83	1.28E-04
spry4.S	7.74	1.96E-03

pnhd.S	7.72	1.88E-04
Xelaev18047333m.g	7.71	6.45E-05
eva1b.S	7.70	7.41E-05
bgn.L	7.68	3.14E-45
fam212b.L	7.66	6.98E-04
Xelaev18040877m.g	7.63	5.34E-18
Xelaev18045246m.g	7.62	7.76E-04
map2.S	7.58	8.87E-36
vsx1.S	7.56	6.56E-04
tal1.L	7.54	8.62E-08
stk32a.L	7.48	3.78E-04
map3k12.S	7.47	3.14E-07
Xelaev18036651m.g	7.46	1.23E-35
Xelaev18001525m.g	7.44	1.89E-02
nptx2.L	7.44	1.05E-02
mmp17.L	7.43	2.71E-04
chst15.L	7.41	3.38E-03
elavl3.S	7.41	2.06E-04
barhl2.L	7.40	4.55E-04
myl1.L	7.36	2.56E-04
LOC100489771.L	7.35	3.58E-03
tmem116.L	7.34	2.77E-17
slc1a2.S	7.33	4.01E-02
pdyn.S	7.33	1.24E-02
tubb3.S	7.33	6.66E-37
pcdh8.S	7.33	3.38E-04
neurod1.S	7.32	4.31E-03
kirrel2.L	7.24	2.18E-81
chat.S	7.23	3.03E-03
lrrn1-like.1.S	7.18	1.15E-45
kiaa1715.S	7.17	6.42E-03
foxd3.L	7.17	3.60E-05
dmrta2.L	7.14	1.77E-04
zeb2.L	7.14	1.44E-25
olig3.S	7.11	6.49E-03
plekhd1.L	7.11	7.85E-04
spns2.L	7.09	7.42E-04
dmrta1.L	7.05	5.53E-03

nat14.S	7.05	2.20E-03
dpp10.S	7.01	2.55E-28
ppp1r9b.S	6.97	2.20E-06
ppp1r9b.L	6.96	3.46E-11
myo3b.L	6.96	6.33E-03
nes.S	6.95	3.22E-24
cdh1.L	6.95	6.54E-12
Xelaev18042973m.g	6.94	1.05E-05
paqr9.L	6.94	1.23E-08
neurod1.L	6.93	1.11E-02
zeb2.S	6.93	8.19E-27
LOC101732256-like.L	6.92	4.00E-02
Xelaev18033867m.g	6.91	7.82E-03
cacnb1.S	6.89	7.51E-06
Xetrov90008914m.L	6.88	2.01E-02
Xelaev18004376m.g	6.87	4.33E-02
hes5.2.S	6.84	1.05E-02
chst3.L	6.84	2.61E-13
pnhd.L	6.83	2.05E-07
Xelaev18026149m.g	6.83	3.58E-03
shox2.S	6.75	1.51E-03
hoxd1.S	6.75	5.72E-03
myod1.S	6.74	1.51E-03
tal1.S	6.69	4.31E-06
ror2.S	6.67	2.53E-21
kirrel2.S	6.66	1.22E-64
mmp28.L	6.62	2.56E-02
slc18a3.S	6.61	1.19E-03
chrd.S	6.60	9.99E-04
Xelaev18022024m.g	6.59	2.08E-05
nova1.L	6.55	9.18E-18
lhx1.S	6.49	1.89E-02
LOC100127750.S	6.45	2.00E-02
slc24a2.L	6.41	1.93E-02
sp5.S	6.40	2.75E-02
mnx1.L	6.39	1.70E-02
olig2.S	6.34	1.49E-20
Xelaev18046363m.g	6.33	3.12E-02

Xelaev18020334m.g	6.31	3.76E-03
phlda1.L	6.29	5.18E-08
Xelaev18002611m.g	6.25	4.86E-05
LOC100487395.L	6.23	3.28E-34
LOC100487395.S	6.23	2.25E-12
tapbp.L	6.22	3.18E-03
faxc.S	6.21	7.27E-05
hes5_X2.L	6.21	9.17E-11
pax2.L	6.19	2.92E-07
elavl4.L	6.18	3.06E-10
dmbx1.L	6.17	9.20E-08
onecut1.2.L	6.16	1.74E-19
slc32a1.S	6.16	9.89E-03
LOC100490819.L	6.15	2.61E-02
mxra7.L	6.15	3.76E-23
tub.L	6.08	8.56E-03
LOC100496628-like.S	6.05	4.31E-15
sostdc1.S	6.04	2.05E-02
adcyap1.L	6.04	5.59E-05
Xelaev18044103m.g	6.01	4.81E-04
six1.S	6.01	4.12E-03
zic3.S	5.99	1.06E-03
mecom.L	5.99	4.08E-06
wnt8a.L	5.99	7.45E-04
slc3a2.L	5.96	7.20E-03
plod2.S	5.96	4.04E-02
sp5.L	5.95	9.89E-03
limd2.L	5.95	7.84E-23
bmp3.L	5.95	2.87E-02
pck1.L	5.93	3.80E-14
tfap2b.L	5.92	8.73E-21
scrt1.L	5.92	1.75E-05
tpbg.L	5.91	3.02E-03
dkk1.L	5.91	3.92E-02
gria1-like.1.S	5.91	1.48E-12
slc1a3.L	5.91	1.60E-02
myct1.L	5.90	1.04E-03
Xetrov90000859m.L	5.89	1.72E-10

cldn3.L	5.89	5.43E-03
skor1.L	5.83	1.02E-05
kif26a.S	5.83	1.39E-17
gad1.1.S	5.83	1.72E-05
hcrtr2.L	5.79	1.66E-02
LOC100495096.1	5.77	1.43E-02
tmem35.L	5.75	1.33E-12
Xelaev18024653m.g	5.75	1.40E-06
Xelaev18025499m.g	5.74	3.60E-05
cyp1a1.S	5.73	3.42E-02
neurog2.S	5.72	1.55E-03
kcnj2.S	5.70	1.08E-02
bhlhe22.L	5.68	3.35E-02
nkx6-2.L	5.67	7.65E-04
neurog2.L	5.67	3.40E-02
sall3.L	5.66	2.74E-10
snap25.L	5.63	3.22E-24
drgx.L	5.62	2.70E-04
cplx2.L	5.57	1.26E-15
mamdc2.L	5.55	6.26E-05
tubb2b.S	5.55	1.31E-07
kiaa0408.L	5.55	4.64E-02
tox2.S	5.55	6.62E-25
stxbp1.S	5.53	6.87E-03
pax8.L	5.52	2.82E-09
LOC100487796-like.L	5.50	1.23E-25
Xelaev18026630m.g	5.49	5.46E-06
pla2g12b.S	5.48	3.04E-02
st18.S	5.47	1.39E-06
kank2.L	5.47	4.16E-02
homer3.L	5.46	2.63E-02
Xelaev18015119m.g	5.44	1.65E-06
c8orf46.S	5.41	5.50E-05
Xelaev18039076m.g	5.41	5.02E-26
Xetrov90016928m.L	5.39	5.16E-04
Xelaev18007001m.g	5.39	2.00E-14
hapln3.S	5.37	3.19E-08
c8orf46.L	5.37	7.03E-03

igf2.L	5.36	2.49E-03
st8sia1.S	5.36	1.61E-02
cbfa2t3.L	5.36	2.32E-06
pax8.S	5.35	7.94E-03
six1.L	5.35	2.54E-02
rph3al.S	5.33	1.10E-03
Xelaev18024617m.g	5.33	7.28E-12
Xelaev18047557m.g	5.32	2.01E-02
gpx3.S	5.31	2.55E-03
slc43a2.S	5.28	1.82E-28
tfap2e.S	5.24	6.45E-14
Xetrov90008930m.S	5.24	1.45E-03
sox9.L	5.24	2.40E-02
adora2a.L	5.24	7.28E-03
aldh1a2.L	5.24	2.27E-09
LOC100496446.L	5.22	1.57E-02
celf2.L	5.22	4.54E-13
hoxc3.S	5.21	1.16E-02
pmp22.L	5.21	1.74E-12
Xelaev18021728m.g	5.17	1.53E-12
mcf2l.S	5.16	2.81E-09
gpr63.S	5.15	2.37E-07
kremen2.S	5.10	9.50E-07
hes5_X2.S	5.09	4.52E-04
Xelaev18015305m.g	5.09	1.40E-02
dbn1.L	5.08	3.22E-27
Xelaev18018196m.g	5.08	1.63E-06
dlx6.L	5.07	1.68E-19
Xelaev18016582m.g	5.07	5.34E-19
sacs.L	5.07	1.16E-05
dbn1.S	5.06	2.56E-20
dnajc6.S	5.05	1.83E-08
nrp1.L	5.05	5.16E-12
nrp2.L	5.04	1.64E-16
abcd2.S	5.04	4.17E-02
Xelaev18005831m.g	5.04	3.34E-05
Xetrov90016831m.L	5.03	5.99E-05
jam3.S	5.03	1.25E-05

tmeff1.S	5.02	1.14E-09
insm1.L	4.99	8.73E-03
gli2.S	4.98	6.18E-11
kif26a.L	4.95	5.42E-09
fam198b.L	4.94	8.39E-03
runx1t1.S	4.94	9.66E-09
crabp2.S	4.90	1.25E-10
syt2-like.S	4.90	1.96E-03
clip2.S	4.89	1.16E-04
npr3.L	4.88	1.55E-02
LOC101734468.L	4.87	4.56E-02
arhgap4.L	4.87	1.42E-18
rab3b.S	4.87	4.16E-04
pax2.S	4.86	1.83E-09
tbx22.S	4.85	4.31E-02
tuba4a.L	4.85	3.70E-23
slc38a8.L	4.83	5.61E-03
ube2ql1.S	4.82	2.40E-02
arx.L	4.80	4.96E-02
asb2.L	4.80	2.07E-03
dmbx1.S	4.78	1.40E-04
flnc.S	4.78	1.77E-08
plekhg4.S	4.77	6.24E-07
Xelaev18044320m.g	4.77	3.66E-05
nr2f2.L	4.73	1.76E-03
hdac7.S	4.73	2.27E-05
cacnb3.L	4.72	3.97E-02
LOC100488523.L	4.72	1.99E-03
nkx2-6.S	4.70	1.97E-04
pak3.S	4.70	5.13E-21
Xelaev18043580m.g	4.69	3.76E-24
sox11.L	4.66	3.76E-04
hes5.3.S	4.66	5.74E-04
fstl1.S	4.66	6.57E-08
Xelaev18013307m.g	4.64	4.51E-02
Xelaev18042154m.g	4.64	1.28E-08
kif5a.L	4.63	6.32E-03
faxc.L	4.63	3.01E-12

bcam.S	4.62	9.73E-06
emilin1.L	4.62	5.88E-13
zic3.L	4.61	3.97E-04
six3.S	4.60	5.50E-09
bmpr1b.L	4.58	2.91E-02
st6galnac6.L	4.57	3.88E-03
Xelaev18025917m.g	4.56	3.15E-06
adamtsl1.L	4.55	1.80E-11
scg3.L	4.55	1.71E-02
lef1.S	4.55	1.18E-05
LOC100489483-like.S	4.55	1.64E-02
pak3.L	4.55	7.82E-05
rgs9bp.S	4.53	6.82E-05
runx1t1.L	4.53	1.12E-05
aldh1a2.S	4.53	8.36E-17
slco5a1.S	4.52	4.40E-07
limd2.S	4.51	5.67E-05
b4galnt1.S	4.49	1.10E-08
gfra1.S	4.46	2.12E-11
plekho1.L	4.46	4.33E-05
nckap5l.L	4.45	1.46E-19
prph.L	4.45	4.92E-14
hdac9.S	4.44	4.00E-02
cited2.L	4.43	7.42E-14
ebf3.L	4.42	3.97E-03
pitx2.L	4.39	4.02E-03
otx2.L	4.38	2.27E-09
unc5a.L	4.37	4.99E-03
ssbp4.S	4.37	4.02E-03
Xelaev18019210m.g	4.37	2.19E-13
unc45b.S	4.36	2.60E-12
tmem116.S	4.36	6.02E-09
cpe.S	4.35	2.85E-07
auts2.S	4.34	4.42E-07
cxcr2.L	4.34	1.08E-02
insm2.L	4.33	2.09E-06
fgf16.L	4.32	3.10E-07
des.1.S	4.31	9.24E-06

six3.L	4.30	1.56E-29
srrm4.L	4.29	6.76E-05
tcf15.L	4.29	5.39E-04
pip4k2b.L	4.25	1.77E-16
pou3f2.S	4.25	9.24E-05
cacna2d1.L	4.25	7.42E-04
bag2.L	4.23	7.74E-04
cacna2d2.L	4.21	1.41E-04
itga8.L	4.21	2.60E-03
sfrp2.L	4.20	1.67E-20
skor2.L	4.19	7.95E-03
itgb8.L	4.18	1.98E-02
ppp1r9a.S	4.17	2.84E-02
nkx6-1.L	4.16	9.80E-04
Xelaev18024654m.g	4.16	7.21E-08
cep85l.L	4.15	6.18E-08
lrat.S	4.15	5.56E-03
pax6.S	4.14	5.29E-09
zfhx4.S	4.12	1.85E-14
pmp22.S	4.11	4.06E-13
zcchc24.L	4.10	9.16E-03
cbfa2t2.L	4.10	9.62E-12
eln2.L	4.09	9.78E-03
tlx3.L	4.09	1.74E-02
evi5.L	4.08	4.52E-26
rgmb.L	4.08	7.61E-05
lhx5.L	4.08	2.25E-02
cyp26c1.L	4.07	9.77E-04
dnajc6.L	4.05	1.12E-07
hes2.L	4.04	1.27E-04
dpysl3.S	4.03	1.68E-19
klf7.L	4.02	1.40E-02
pde11a.S	4.02	1.22E-02
pde11a.S	4.02	1.22E-02
crmp1.L	4.01	1.00E-02
mctp2.L	4.01	4.11E-05
vim.S	4.00	5.77E-03
fam212a.L	3.99	4.79E-08

Xelaev18004886m.g	3.99	2.16E-08
nuak1.L	3.98	3.50E-07
sncb.L	3.98	8.27E-10
tdrp.L	3.98	3.22E-24
pcdh8.L	3.98	1.45E-03
serpinf1.L	3.97	1.35E-04
ror2.L	3.94	1.25E-10
map3k13.S	3.94	2.90E-02
Xelaev18008189m.g	3.93	4.58E-05
cbfa2t2.S	3.92	7.07E-13
mex3b.L	3.92	1.10E-09
gngt2.1.S	3.92	3.68E-02
cdc42ep3.S	3.90	3.95E-07
arl8a.S	3.89	1.72E-04
Xelaev18003346m.g	3.89	3.48E-03
prr5l.S	3.88	6.16E-03
scn8a.L	3.88	2.89E-02
elavl3.L	3.88	5.43E-18
fam110b.L	3.87	1.11E-06
foxg1.L	3.86	7.65E-08
Xelaev18023457m.g	3.86	1.01E-03
mef2d.S	3.86	1.73E-08
zc3h12c.L	3.85	8.45E-15
slc6a5.L	3.84	4.72E-02
LOC100494817.L	3.82	9.87E-06
dpysl4.S	3.82	4.34E-02
hes8.L	3.82	1.74E-12
dbndd1.L	3.80	2.05E-05
lhx5.S	3.78	1.52E-06
dennd2c.L	3.78	9.03E-11
hes10.L	3.77	1.18E-06
gcnt1.S	3.75	1.18E-05
hes5.1.L	3.74	4.31E-06
mdk.L	3.73	3.40E-17
tox.L	3.73	1.04E-05
spon1.S	3.72	5.18E-04
cdc42bpa.S	3.71	1.04E-13
adamdec1.L	3.71	1.10E-02

fn1.S	3.70	1.47E-19
Xelaev18037602m.g	3.69	7.76E-10
map2.L	3.69	5.12E-05
sox9.S	3.68	1.89E-05
edn1.L	3.67	2.50E-03
hnrnpll.S	3.67	2.69E-13
mtcl1.L	3.67	1.81E-04
mycl.S	3.67	3.02E-08
nr5a2.S	3.66	1.22E-08
nox4.S	3.64	6.16E-03
dll1.L	3.62	9.68E-07
Xelaev18044758m.g	3.61	4.33E-02
sgip1.L	3.60	1.23E-06
Xelaev18020376m.g	3.60	1.01E-02
klhl35.S	3.60	1.38E-03
st3gal2.2.L	3.60	3.57E-02
sox11.S	3.58	1.43E-02
nceh1.L	3.57	2.09E-05
manea.S	3.57	3.67E-03
ulk1.L	3.56	2.07E-08
spon1.L	3.56	9.47E-06
rnf165.L	3.56	1.22E-03
cplx2.S	3.55	2.37E-02
dst.L	3.54	8.87E-05
slc43a2.L	3.54	2.77E-07
mxi1.S	3.54	5.02E-05
gsta1.L	3.53	5.27E-03
cdc42ep4.L	3.53	3.79E-04
kcnq3.S	3.52	2.77E-07
ncam1.S	3.52	6.76E-11
creb3l1.S	3.51	1.03E-07
aplnr.S	3.51	4.93E-04
xkr4.L	3.49	1.39E-06
lrch2.L	3.48	9.72E-08
sp5l.S	3.48	2.17E-03
gfi1.L	3.47	1.85E-02
dennd2c.S	3.46	1.83E-07
zic2.L	3.44	2.27E-04

rassf6.L	3.44	2.51E-03
hes9-1.L	3.44	6.62E-04
dact1.L	3.43	2.38E-06
st8sia1.L	3.43	3.02E-05
wipf1.L	3.42	1.64E-02
eya1.S	3.42	4.20E-07
slco5a1.L	3.41	3.63E-09
fbxo10.L	3.41	1.35E-10
sox4.S	3.41	5.45E-05
LOC105946937.L	3.41	2.26E-05
dusp4.S	3.40	9.50E-07
zbtb16.S	3.40	7.24E-05
LOC100490436.L	3.39	2.57E-02
cdc42se2-like.1.L	3.39	1.64E-09
LOC100494502.L	3.38	1.14E-02
ap3b2.L	3.38	2.70E-04
bmpr1b.S	3.37	1.95E-03
asb1.L	3.37	2.15E-07
flrt3.L	3.37	7.45E-04
fam134b.S	3.37	1.29E-02
dlc.S	3.35	8.87E-05
crabp2.L	3.34	1.08E-05
lmcd1.S	3.34	2.63E-02
gch1.L	3.34	6.12E-05
gli2.L	3.34	4.31E-11
ell3.L	3.32	4.08E-02
ag1.S	3.32	1.31E-10
tmod4.S	3.32	2.31E-02
Xelaev18030284m.g	3.31	4.39E-03
hes9-1.S	3.31	7.49E-14
sesn1.L	3.31	4.16E-06
sulf1.S	3.31	3.55E-03
mcf2l.2.L	3.30	2.56E-05
rundc3a.L	3.30	2.58E-04
LOC101732576.S	3.30	4.01E-02
ppp1r14b.S	3.29	3.10E-07
tmem169.S	3.29	3.01E-04
arid1b.L	3.28	1.99E-13

reep5.S	3.28	2.29E-24
cd82.L	3.26	4.77E-07
fam43a.S	3.25	1.79E-03
cttnbp2nl.L	3.25	4.11E-04
arhgef26.S	3.25	1.08E-02
sfrp2.S	3.24	3.87E-39
sparc.L	3.24	7.18E-04
tmem169.L	3.22	4.37E-04
fyn-like.L	3.22	6.87E-03
Xelaev18027950m.g	3.21	4.03E-10
plekhg1.L	3.21	6.37E-06
Xelaev18044942m.g	3.19	3.18E-02
ak3.S	3.19	3.89E-10
lrpprc.S	3.19	5.15E-04
dclk1.S	3.19	9.03E-03
tmem158.L	3.19	1.36E-05
lrp4.L	3.17	1.12E-05
irx1.L	3.17	1.23E-06
st6galnac1.S	3.17	2.50E-03
bcar1.S	3.15	1.41E-04
LOC100498409-like.S	3.15	2.72E-03
LOC100170576.L	3.15	7.02E-10
otx1.S	3.14	9.33E-06
MGC147600.S	3.13	3.85E-02
eya2.S	3.12	6.03E-04
fmnl2-like.S	3.12	3.61E-02
pkdcc.L	3.11	2.80E-15
mybl1.S	3.11	2.22E-02
nr2e1.S	3.11	4.31E-03
Xelaev18024436m.g	3.11	1.94E-06
fgfr1.S	3.10	8.39E-13
LOC100487080-like.L	3.10	1.46E-02
cdk5r1.S	3.10	5.85E-06
arhgef40.S	3.10	1.34E-02
LOC101730599.S	3.10	1.29E-03
egln2.L	3.09	9.62E-04
emx2.S	3.09	4.41E-02
pag1.S	3.08	2.06E-05

psat1.L	3.07	2.34E-05
sulf1.L	3.07	2.74E-10
cel-like.1.S	3.06	2.21E-02
zfhx4.L	3.06	2.63E-09
Xelaev18029662m.g	3.05	2.77E-02
znf219.L	3.04	3.06E-03
plekhg4.L	3.04	1.80E-07
abcb9.L	3.03	1.48E-05
tnni1.2.L	3.02	4.82E-02
tuba4a.S	3.02	1.22E-03
pdia2.S	3.01	2.87E-02
rnf165.S	3.00	4.61E-12
trabd2a.L	3.00	7.06E-07
ptch2.S	2.99	2.26E-02
ngfr.L	2.98	1.43E-06
manea.L	2.98	1.62E-03
ptprt.L	2.97	4.02E-03
tpbg.S	2.97	1.17E-04
pik3r3.L	2.97	1.18E-04
afap1.S	2.96	3.94E-03
cblb.L	2.94	3.52E-06
plxnb1.L	2.94	5.45E-09
ptch1.L	2.93	8.95E-06
Xelaev18016487m.g	2.93	2.37E-02
fdft1.L	2.93	1.02E-03
fgfr4.L	2.93	1.34E-11
prickle1.S	2.92	7.63E-09
spsb4-like.L	2.92	1.33E-03
pitx2.S	2.92	2.76E-02
dclk1.L	2.91	2.70E-02
rgma.L	2.91	1.09E-06
LOC100498368-like.L	2.90	2.04E-02
smim3.S	2.90	7.08E-04
amotl2.L	2.90	1.15E-08
gas7.L	2.89	5.18E-03
mgc69520.S	2.88	2.15E-07
slit1.S	2.88	2.77E-02
sox4.L	2.88	8.44E-04

myh6.L	2.88	1.72E-02
ncam1.L	2.88	9.12E-06
Xelaev18044438m.g	2.87	9.51E-03
znf608.S	2.87	6.99E-16
Xelaev18003796m.g	2.86	1.67E-02
homer1.S	2.85	7.12E-03
tmem132a.L	2.85	5.71E-04
il17rd.S	2.85	2.47E-04
Xetrov90002103m.L	2.85	3.27E-03
lmx1b.1.L	2.85	6.18E-03
ankrd65.L	2.85	2.70E-03
akap12.L	2.83	1.65E-06
rfk.S	2.82	8.23E-04
lfng.L	2.82	4.22E-10
mtcl1.S	2.82	1.19E-02
mex3a.S	2.81	7.45E-04
Xelaev18015889m.g	2.81	4.70E-03
hes3.3.L	2.80	1.04E-06
calb1.S	2.80	2.20E-02
kank3.L	2.80	1.07E-03
Xetrov90009914m.S	2.79	1.24E-04
arhgap36.L	2.79	1.70E-11
scamp4.S	2.79	4.96E-04
gmnn.L	2.79	4.12E-20
rai2.S	2.79	2.04E-03
st3gal6.L	2.78	1.42E-04
mamld1.L	2.77	2.18E-02
afap1l1.L	2.77	2.27E-19
dsc3.S	2.77	8.95E-03
ndst1.S	2.77	2.95E-07
Xelaev18010427m.g	2.76	2.53E-04
rbm38.S	2.76	6.82E-10
LOC100492579.S	2.76	2.49E-03
rnf130.S	2.75	4.50E-02
lrrn1-like.1.L	2.75	8.62E-08
plxnb1.S	2.75	1.71E-04
spry2.L	2.74	7.60E-03
vcan.L	2.74	4.26E-04

auts2.L	2.73	8.62E-08
ulk1.S	2.73	7.06E-06
pros1.S	2.73	2.05E-04
prtg.L	2.73	1.55E-02
crmp1.S	2.73	1.27E-02
Xelaev18004582m.g	2.73	2.35E-02
Xelaev18030439m.g	2.72	1.19E-02
scn1b.L	2.70	3.97E-02
magi1.S	2.70	8.65E-06
LOC100489386-like.L	2.70	8.48E-04
pcmtd1.S	2.69	1.64E-05
Xelaev18038420m.g	2.69	4.79E-06
myt1.L	2.69	1.66E-04
tmem198.S	2.68	2.15E-07
ptpru.L	2.68	4.99E-05
fam102b.S	2.67	3.56E-02
pkdcc.S	2.67	1.48E-02
fam222a.L	2.67	1.13E-07
rtn2.L	2.67	2.59E-09
irf1.L	2.66	1.05E-02
fgf8.L	2.66	1.69E-02
tmem55a.S	2.65	1.69E-02
atp8a1.L	2.65	2.15E-03
sst.S	2.64	1.71E-02
twist1.L	2.64	1.31E-05
cables1.L	2.64	4.43E-02
fmn2.L	2.64	1.95E-02
LOC100492639-like.L	2.63	1.93E-09
Xelaev18027769m.g	2.63	3.42E-03
fgd1.S	2.63	1.24E-04
epn1.S	2.62	4.49E-06
slc27a3.L	2.61	1.57E-18
acer2.L	2.61	8.32E-06
btbd11.L	2.61	2.90E-02
hes8.S	2.60	7.63E-09
lrp4.S	2.60	3.56E-05
rcor2.L	2.60	1.35E-10
LOC496795.L	2.60	1.54E-03

tet3.S	2.59	5.99E-05
cdc42se2-like.1.S	2.58	1.73E-04
gdpd5.S	2.57	4.02E-05
rnf125.S	2.57	7.33E-03
spry2.S	2.57	3.58E-03
gnao1.S	2.56	2.07E-06
skida1.S	2.56	5.20E-11
sh2b2.L	2.56	8.47E-03
nkx3-1.L	2.56	2.87E-02
rassf2.L	2.56	1.11E-04
gse1.L	2.56	2.46E-07
psat1.S	2.55	4.53E-02
mospd1.L	2.55	2.27E-09
Xetrov90023254m.S	2.55	3.36E-03
enpp2.L	2.54	1.37E-03
pcbp2.S	2.54	8.59E-05
cpe.L	2.54	3.04E-04
zc4h2.L	2.54	6.02E-07
ano8.L	2.53	9.38E-03
fam222a.S	2.53	3.37E-03
lrrn1-like.2.L	2.53	2.28E-03
cuedc1.L	2.51	1.57E-04
map1lc3a.L	2.51	1.13E-03
rufy3.L	2.50	8.24E-10
gramd1a.L	2.49	3.43E-03
sh3glb2.S	2.49	1.57E-02
Xelaev18000699m.g	2.48	2.95E-03
onecut2.L	2.48	4.86E-03
chst8.S	2.48	1.78E-02
cass4.L	2.48	2.33E-06
krt19.S	2.48	2.70E-04
a2m.S	2.47	5.92E-06
rnd3.S	2.45	1.40E-02
best2.S	2.45	1.15E-02
epb41l1.L	2.45	5.25E-05
Xelaev18031949m.g	2.44	9.04E-03
lpar4.S	2.43	7.38E-07
Xelaev18021928m.g	2.43	8.13E-05

Xelaev18039965m.g	2.43	4.09E-11
myt1.S	2.43	1.28E-05
hnrnpll.L	2.43	1.39E-04
mob3b.L	2.42	3.12E-02
tox3.L	2.42	3.79E-03
nxpe3.L	2.42	3.24E-02
pik3r3.S	2.41	9.24E-05
efnb2.S	2.41	1.40E-03
rnf125.L	2.40	9.26E-05
lrrc8b.S	2.40	1.44E-03
Xelaev18009525m.g	2.40	1.63E-03
mex3b.S	2.40	2.55E-04
hdac4.L	2.40	2.77E-02
atg9b.L	2.40	1.21E-02
dlx6.S	2.40	2.95E-03
lrig3.L	2.39	2.38E-06
clic5.S	2.38	1.18E-03
tet3.L	2.38	3.74E-04
cybrd1.L	2.38	3.13E-08
st3gal2.1.S	2.38	4.18E-04
fyn-like.S	2.38	4.42E-03
stx2.L	2.37	5.27E-05
fam102a.L	2.37	3.27E-05
dock6-like.L	2.37	1.11E-06
cyp27c1.S	2.37	3.82E-04
LOC100145446.S	2.37	2.84E-02
mmp14.L	2.36	3.18E-05
rgs10.L	2.36	3.31E-02
slc23a2.L	2.36	5.63E-05
myh6.S	2.36	2.75E-02
pknox2.L	2.36	4.31E-06
srrm4.S	2.35	3.69E-02
rimbp2.L	2.34	2.61E-02
tuba1b.L	2.33	7.24E-09
Xetrov90025030m.L	2.33	3.88E-03
map1lc3b.S	2.32	2.45E-02
jag1.L	2.32	9.73E-04
hectd4.L	2.32	1.18E-04

cyyr1.L	2.31	1.02E-02
aplnr.L	2.31	5.80E-07
rufy3.S	2.30	4.99E-02
fam211b.S	2.30	2.37E-02
vim.L	2.30	9.84E-07
rnf130.L	2.30	5.49E-03
kctd1.S	2.29	8.02E-08
epha4.L	2.28	4.47E-03
nkain1.L	2.28	2.36E-02
ephb3.S	2.27	3.76E-09
onecut1.2.S	2.27	3.26E-05
b4galt4.S	2.26	3.90E-04
sept5.L	2.26	8.33E-08
rtbdn.S	2.26	2.34E-04
LOC100489897.L	2.26	4.67E-02
gas1.S	2.26	5.39E-04
cdc25b.L	2.25	2.47E-04
LOC100492859.L	2.25	3.77E-02
fnbp1.S	2.25	3.58E-03
smarcc2.S	2.24	2.89E-02
fam43a.L	2.24	1.45E-02
cep85l.S	2.24	2.37E-02
nrarp.L	2.24	2.27E-04
Xelaev18019689m.g	2.24	3.48E-02
Xelaev18016676m.g	2.24	8.81E-05
kctd1.L	2.24	6.53E-03
fam189a1.L	2.24	1.51E-02
map4k4-like.L	2.23	5.45E-09
hmox1.L	2.23	1.01E-09
pcsk5.S	2.23	1.67E-03
sox2.S	2.22	3.18E-02
notch1.L	2.22	1.06E-04
Xelaev18044381m.g	2.22	2.39E-06
Xelaev18016675m.g	2.20	2.30E-06
tubb2b.L	2.19	8.41E-04
bhlhe40.L	2.19	7.01E-04
hes9-2.L	2.19	3.96E-02
bcr.L	2.18	1.90E-06

mylip.S	2.18	1.56E-02
frmd4a.S	2.18	4.40E-07
spire2.S	2.17	2.38E-02
tacc1.L	2.17	3.48E-02
prnp.S	2.17	3.11E-03
dact1.S	2.17	7.08E-03
acy3.L	2.16	7.06E-06
znf850.L	2.16	2.41E-03
cdc42ep4.S	2.16	4.57E-03
hes6.1.S	2.16	3.75E-03
zbtb18.S	2.15	4.19E-02
Xelaev18024012m.g	2.15	8.14E-03
dkk1.S	2.15	3.07E-02
lrig3.S	2.14	2.16E-02
tes.L	2.14	1.42E-02
Xelaev18044325m.g	2.13	2.32E-05
p2ry4.L	2.13	4.23E-07
arid1b.S	2.12	4.50E-03
numbl.L	2.12	1.35E-02
gatm.S	2.12	3.17E-02
fgfr1.L	2.12	7.61E-09
marcks.S	2.12	8.29E-10
lhx2.L	2.11	3.88E-02
Xelaev18028757m.g	2.11	3.94E-02
ppm1e.S	2.11	7.40E-03
cbfb.S	2.11	9.12E-06
mprip.L	2.11	2.06E-02
meis2.L	2.11	2.45E-02
cuedc1.S	2.10	4.17E-07
tmem2.L	2.10	9.24E-05
Xelaev18043719m.g	2.10	1.22E-02
smtn.L	2.09	1.43E-03
msi1.L	2.09	9.71E-04
bach2.S	2.09	2.18E-02
sh3rf1.S	2.09	1.44E-04
rbms1.S	2.08	3.39E-04
atat1.L	2.08	9.96E-06
LOC100493716.S	2.07	1.04E-06

stk40.L	2.07	1.27E-03
lppr3.S	2.07	3.82E-02
fzd2.L	2.07	2.05E-05
grm7.S	2.07	3.31E-02
lace1.L	2.06	2.47E-03
rftn1.L	2.05	3.27E-02
vegfa.L	2.05	1.38E-02
Xetrov90024734m.L	2.05	2.64E-05
rab11fip4l.S	2.05	2.78E-02
vav2.S	2.05	3.75E-04
Xelaev18010400m.g	2.05	1.85E-02
tspan17.S	2.05	2.51E-06
sesn1.S	2.04	8.95E-07
tiparp.L	2.04	1.35E-04
LOC100489393.L	2.04	4.10E-03
hes5.1.S	2.03	5.25E-03
fsd1.L	2.03	8.36E-04
ankrd10.L	2.02	4.16E-04
paqr4-like.S	2.02	3.36E-02
irx2.L	2.01	4.57E-05
draxin.S	2.01	2.68E-02
fgfr4.S	2.00	6.94E-10
dock4.L	2.00	5.02E-03
amotl2.S	2.00	4.42E-03

Table S19: Summary of differentially expressed genes by Ptf1a + Brg1MO

ID	log2FC	P-value
Xelaev18007508m.g	12.92	2.82E-14
neurod4.L	11.64	2.14E-11
prdm13.L	10.92	5.72E-11
pnhd.S	10.65	3.20E-08
prph.S	10.55	2.20E-20
neurod4.S	10.49	1.02E-08
prdm13.S	10.45	2.57E-15
scrt1.S	9.99	1.73E-09
pou3f1.L	9.59	7.06E-08

prdm8.L	9.58	6.76E-04
neurog1.L	9.55	2.85E-08
igfbpl1.L	9.37	1.21E-07
dpysl4.L	9.08	7.21E-07
fezf1.L	9.05	4.24E-05
eva1b.S	9.00	1.57E-06
st18.L	8.95	3.86E-07
LOC100490531-like.L	8.84	2.66E-07
Xetrov90027705m.L	8.63	6.53E-12
des.2.L	8.59	9.57E-06
foxd2.L	8.58	5.57E-05
shd.L	8.43	2.83E-11
ebf2.L	8.41	1.15E-23
slc26a9.S	8.36	2.91E-05
hes5.2.L	8.30	4.58E-05
pyy.L	8.25	2.52E-05
aldh1b1.L	8.16	8.16E-05
tfap2b.S	8.14	1.39E-28
LOC100496628-like.L	8.06	4.50E-05
slc18a3.S	8.05	3.01E-05
tespa1.S	8.02	7.93E-05
olig3.S	8.01	1.22E-03
Xelaev18032183m.g	7.98	3.98E-05
tubb3.L	7.94	8.95E-06
shox2.L	7.91	9.14E-05
skor1.S	7.86	2.10E-08
Xelaev18047032m.g	7.84	1.42E-03
adcyap1.S	7.81	1.29E-04
sp9.L	7.79	1.47E-02
tfap2e.L	7.68	2.89E-05
des.1.L	7.63	3.06E-08
chat.S	7.58	1.39E-03
sag.S	7.58	2.40E-03
admp.L	7.57	1.65E-02
fam212b.L	7.55	7.85E-04
ptf1a.L	7.55	1.07E-04
nhlh1.L	7.51	3.24E-05
Xelaev18000445m.g	7.51	2.94E-04

Xelaev18018357m.g	7.49	3.84E-04
slc46a2.L	7.45	1.51E-02
kirrel2.L	7.44	5.77E-86
hoxd1.S	7.44	1.44E-03
egr4.L	7.43	3.14E-03
dpysl3.L	7.36	5.79E-62
mllt11.S	7.31	2.71E-04
pnhd.L	7.15	4.38E-08
bgn.L	7.10	4.49E-38
aqp3.L	7.07	9.68E-03
nr5a2.L	7.06	7.56E-04
ebf2.S	7.05	2.59E-21
lbx1.S	7.04	3.03E-04
barhl2.L	6.99	9.12E-04
hesx1.S	6.97	1.83E-06
sybu.L	6.97	3.28E-06
Xelaev18040877m.g	6.96	1.47E-14
prdm8.S	6.95	4.51E-03
vsx1.S	6.93	2.12E-03
pcdh9.L	6.89	1.08E-03
elavl3.S	6.86	6.30E-04
nptx2.L	6.84	1.89E-02
clstn3.L	6.84	4.64E-09
shox2.S	6.84	1.07E-03
Xetrov90027705m.S	6.83	1.41E-03
kiaa1755.L	6.82	3.89E-11
Xelaev18046363m.g	6.82	1.42E-02
map2.S	6.80	4.04E-28
tapbp.L	6.79	8.13E-04
ptger3.L	6.74	1.78E-03
LOC100490531-like.S	6.74	3.97E-03
hspb8.L	6.73	2.82E-02
nhlh1.S	6.71	4.78E-04
barhl2.S	6.70	3.51E-06
mnx1.L	6.69	9.01E-03
tcf15.S	6.65	4.71E-03
gad1.1.L	6.63	1.47E-11
nkx3-2.S	6.63	2.69E-02

spry4.S	6.60	1.06E-02
Xelaev18045246m.g	6.60	4.97E-03
admp.S	6.60	4.95E-02
skor2.S	6.59	1.96E-02
myod1.S	6.57	1.83E-03
kirrel2.S	6.54	5.79E-62
hmx1.1	6.50	3.13E-02
sox17a.L	6.49	1.35E-03
Xelaev18033867m.g	6.42	1.40E-02
Xelaev18020334m.g	6.39	2.71E-03
Xelaev18036651m.g	6.28	2.51E-24
myo3b.L	6.23	1.67E-02
tmem116.L	6.22	4.53E-12
mmp17.L	6.21	3.34E-03
hes6.2.L	6.21	4.19E-02
nova2.S	6.18	6.24E-03
nes.L	6.16	1.76E-10
sostdc1.S	6.15	1.45E-02
mmp28.L	6.12	3.62E-02
neurod1.L	6.11	2.89E-02
ror2.S	6.09	2.63E-17
lmo2.S	6.08	1.91E-03
Xelaev18034787m.g	6.08	1.57E-02
pla2g12b.S	6.07	1.06E-02
lrrn1-like.1.S	6.06	9.05E-32
Xelaev18042973m.g	6.01	2.14E-04
chst3.L	5.96	5.95E-10
cdh1.L	5.94	1.53E-08
tmem47.L	5.93	2.47E-02
Xelaev18026532m.g	5.90	1.35E-02
sp5.L	5.88	8.84E-03
matn4.S	5.88	2.25E-02
LOC100495096.1	5.87	1.01E-02
chrd.S	5.85	4.11E-03
bmp3.L	5.82	2.82E-02
igf2.L	5.78	7.57E-04
Xelaev18035158m.g	5.76	4.19E-02
olig2.S	5.74	2.57E-16

usp13.S	5.71	1.90E-03
LOC100489771.L	5.70	3.60E-02
limd2.L	5.67	3.98E-20
tubb3.S	5.67	2.86E-21
mxra7.L	5.67	4.50E-19
Xelaev18004302m.g	5.65	1.53E-02
map3k13.L	5.63	3.05E-02
fam198b.L	5.62	1.56E-03
plekhd1.L	5.61	1.23E-02
neurog2.S	5.54	1.93E-03
neurod1.S	5.50	4.96E-02
neurog2.L	5.50	3.42E-02
dmrta2.L	5.49	6.01E-03
hoxc3.L	5.49	2.77E-02
lhx8.L	5.47	1.51E-02
hcrtr2.L	5.42	2.46E-02
nova1.L	5.41	1.10E-11
wnt8a.L	5.40	2.82E-03
hes5_X2.L	5.40	5.35E-08
Xelaev18025499m.g	5.39	1.32E-04
nkx2-6.S	5.36	1.14E-05
dpp10.S	5.35	8.39E-16
Xelaev18015119m.g	5.33	3.04E-06
tlx3.L	5.31	6.78E-04
zeb2.L	5.28	2.34E-13
LOC101730771-like.L	5.28	4.13E-04
sez6.S	5.26	9.88E-05
zeb2.S	5.25	1.47E-14
LOC100487395.L	5.25	1.90E-23
six1.S	5.24	1.33E-02
bhlhe22.L	5.23	4.68E-02
elavl4.L	5.22	2.73E-07
fam212a.L	5.22	1.47E-13
tub.L	5.22	2.88E-02
spns2.L	5.20	2.31E-02
Xelaev18026630m.g	5.20	1.88E-05
gpr63.S	5.19	1.81E-07
nmb.S	5.17	1.55E-03

tal1.L	5.14	7.85E-04
faxc.S	5.11	1.85E-03
skor2.L	5.10	5.37E-04
npr3.L	5.09	8.67E-03
onecut1.2.L	5.08	5.74E-13
stk32a.L	5.06	3.08E-02
pax2.L	5.06	6.42E-05
ppp1r9b.S	5.03	1.33E-03
nes.S	5.00	6.41E-12
slc32a1.S	4.94	4.98E-02
hes5_X1.L	4.92	4.89E-02
cplx2.L	4.92	8.77E-12
phlda1.L	4.91	6.03E-05
LOC100492420.L	4.91	3.43E-02
sox9.L	4.88	3.30E-02
sall3.L	4.87	1.51E-07
adcyap1.L	4.86	1.90E-03
tal1.S	4.86	1.96E-03
Xelaev18003346m.g	4.85	9.53E-05
map3k12.S	4.85	2.66E-03
tfap2b.L	4.85	2.40E-13
map3k12.L	4.85	2.42E-05
dmbx1.L	4.82	8.47E-05
eda2r.L	4.79	2.63E-17
crabp2.S	4.78	5.95E-10
mcf2l.S	4.78	6.86E-08
nt5e.S	4.76	4.56E-02
cacna2d1.L	4.74	1.02E-04
Xelaev18007001m.g	4.74	5.35E-11
LOC100494774.L	4.74	2.75E-02
des.1.S	4.72	7.11E-07
Xelaev18005831m.g	4.72	1.18E-04
Xetrov90000859m.L	4.72	1.36E-06
mycl.S	4.71	2.08E-13
vegt.S	4.70	4.58E-03
arx.L	4.70	4.66E-02
stxbp1.S	4.69	2.67E-02
gcnt1.S	4.69	1.18E-08

Xelaev18016582m.g	4.68	1.07E-15
zic3.S	4.68	1.65E-02
hdac9.S	4.68	2.34E-02
LOC100487395.S	4.65	8.27E-07
slc38a8.L	4.65	7.49E-03
LOC100492804.S	4.64	9.94E-03
bhlhe22.S	4.64	1.30E-02
plekhg4.S	4.64	1.50E-06
ankrd65.L	4.62	4.21E-08
pax2.S	4.62	2.21E-08
efemp2.L	4.60	4.15E-02
myl1.L	4.59	4.76E-02
wipf1.L	4.55	4.09E-04
rufy2.L	4.53	8.98E-04
skor1.L	4.53	1.04E-03
insm1.L	4.51	1.76E-02
hes5_X2.S	4.48	2.79E-03
runx1t1.S	4.48	3.74E-07
mtmr7-like.L	4.47	2.51E-04
LOC100487796-like.L	4.46	6.78E-16
faxc.L	4.46	3.63E-11
lef1.S	4.43	2.07E-05
celf2.L	4.43	4.34E-09
asb2.L	4.42	5.32E-03
pck1.L	4.42	8.35E-08
dlx6.L	4.41	2.44E-14
Xelaev18038044m.g	4.39	5.84E-03
gfra1.S	4.39	7.78E-11
adora2a.L	4.36	3.28E-02
nyx.S	4.35	1.84E-02
cxcr2.L	4.35	9.45E-03
Xetrov90016928m.L	4.34	8.02E-03
klf7.L	4.32	5.92E-03
cfd.L	4.32	2.60E-02
foxd3.L	4.31	2.92E-02
sema3d.L	4.31	1.04E-04
kif26a.S	4.29	4.64E-09
Xelaev18030284m.g	4.28	7.28E-05

serpinf1.L	4.27	2.74E-05
pitx2.L	4.27	5.05E-03
Xetrov90008930m.S	4.23	1.51E-02
dbn1.S	4.22	7.23E-14
spon1.S	4.21	5.16E-05
gad1.1.S	4.21	4.56E-03
Xelaev18042154m.g	4.20	4.48E-07
Xelaev18002611m.g	4.20	1.23E-02
snap25.L	4.20	5.96E-13
Xelaev18024617m.g	4.19	3.74E-07
cbfa2t2.L	4.18	5.24E-12
lhx5.L	4.16	1.53E-02
tmeff1.S	4.14	1.50E-06
hes5.3.S	4.14	2.78E-03
sncb.L	4.14	2.09E-10
dbn1.L	4.12	1.96E-17
itga2b.1-like.S	4.12	2.10E-06
c8orf46.S	4.12	4.41E-03
st8sia6.L	4.11	1.94E-02
Xelaev18021728m.g	4.10	1.23E-07
gngt2.1.S	4.09	2.28E-02
aldh1a2.L	4.08	9.73E-06
bcam.S	4.08	1.60E-04
dnajc6.S	4.06	1.66E-05
Xelaev18018196m.g	4.06	3.16E-04
LOC100489305.S	4.06	4.89E-02
kremen2.S	4.06	2.14E-04
plekho1.L	4.05	3.03E-04
hes7.L	4.04	1.21E-02
tbx6.L	4.04	1.04E-03
crabp2.L	4.04	3.56E-08
hes8.L	4.03	1.15E-13
hoxd1.L	4.03	2.83E-03
Xelaev18025917m.g	4.02	7.63E-05
dmbx1.S	4.01	1.99E-03
gfi1.L	4.00	3.73E-03
crybb3.L	4.00	5.61E-03
mamdc2.L	3.99	9.01E-03

asb1.L	3.98	3.36E-10
Xelaev18039076m.g	3.98	1.89E-13
hdac7.S	3.97	5.99E-04
nrp2.L	3.97	6.14E-10
rab3b.S	3.95	6.48E-03
sacs.L	3.95	1.33E-03
mecom.L	3.92	6.80E-03
nox4.S	3.92	2.27E-03
st6galnac6.L	3.87	1.87E-02
gli2.S	3.87	1.29E-06
cpe.S	3.84	9.43E-06
pde10a.L	3.84	9.58E-03
fn1.S	3.83	1.41E-20
zc3h12c.L	3.82	2.44E-14
gipr.L	3.82	4.09E-02
tmcc2.S	3.81	3.08E-02
zcchc24.L	3.80	1.62E-02
crmp1.L	3.80	1.49E-02
fstl1.S	3.79	3.13E-05
dennd2c.L	3.78	1.18E-10
st3gal2.2.L	3.78	2.08E-02
clip2.S	3.77	5.35E-03
manea.L	3.77	2.06E-05
ssbp4.S	3.75	1.62E-02
plekhg4.L	3.73	4.11E-11
sox11.L	3.72	6.24E-03
ulk1.L	3.72	5.04E-09
lhx5.S	3.71	2.72E-06
pmp22.L	3.70	2.41E-06
st18.S	3.69	3.58E-03
tuba4a.L	3.67	1.47E-12
Xelaev18008189m.g	3.67	1.77E-04
ror2.L	3.66	4.64E-09
srrm4.L	3.65	9.79E-04
insm2.L	3.65	1.19E-04
cd82.L	3.64	1.10E-08
jam3.S	3.64	3.63E-03
nr2f2.L	3.63	2.48E-02

dennd2c.S	3.63	4.25E-08
cyp1c1.L	3.62	3.99E-02
cbfa2t2.S	3.62	7.57E-11
ppp1r9b.L	3.61	3.61E-03
LOC101734175.L	3.60	4.55E-02
cacna2d2.L	3.59	1.83E-03
artn.S	3.58	2.02E-02
dnajc6.L	3.55	6.61E-06
lrp4.L	3.54	4.79E-07
elavl3.L	3.54	1.80E-14
runx1t1.L	3.53	1.09E-03
Xelaev18043580m.g	3.53	6.95E-13
hes10.L	3.53	8.68E-06
limd2.S	3.52	3.03E-03
tox.L	3.52	4.70E-05
eln2.L	3.51	2.99E-02
cdk5r2.L	3.51	3.35E-02
mdk.L	3.51	7.13E-15
vim.S	3.50	1.66E-02
hes2.L	3.49	1.27E-03
mtcl1.L	3.48	4.41E-04
Xelaev18044438m.g	3.45	9.17E-04
tmem35.L	3.44	1.84E-04
sp5l.S	3.43	2.26E-03
LOC100498368-like.L	3.43	3.42E-03
zfhx4.S	3.42	9.24E-10
lrrn1-like.1.L	3.41	9.20E-12
cyyr1.L	3.40	2.37E-05
myh6.L	3.39	2.66E-03
adamtsl1.L	3.38	4.08E-06
aldh1a2.S	3.37	4.12E-09
mcf2l.2.L	3.36	1.60E-05
rgmb.L	3.36	1.63E-03
abcb9.L	3.36	9.36E-07
cttnbp2nl.L	3.36	2.25E-04
lppr3.S	3.36	8.24E-05
Xelaev18029662m.g	3.35	1.06E-02
slco5a1.S	3.35	4.80E-04

lrfn1.S	3.33	3.98E-02
LOC101732555.L	3.33	2.16E-02
arl8a.S	3.32	1.99E-03
pak3.L	3.32	8.96E-03
gli2.L	3.31	1.45E-10
LOC105946937.L	3.31	4.75E-05
tfap2e.S	3.31	1.50E-05
gria1-like.1.S	3.30	6.72E-04
Xelaev18012713m.g	3.29	1.15E-02
Xelaev18007062m.g	3.29	5.12E-07
evi5.L	3.27	3.05E-16
zic3.L	3.27	2.06E-02
LOC100490436.L	3.27	3.08E-02
Xelaev18047968m.g	3.26	3.83E-02
Xelaev18004582m.g	3.26	3.55E-03
rassf6.L	3.26	4.08E-03
rgs3.L	3.26	6.20E-03
Xelaev18032990m.g	3.24	3.80E-02
mxi1.S	3.24	2.94E-04
Xelaev18001443m.g	3.24	1.66E-03
ulk1.S	3.24	4.05E-08
sgip1.L	3.23	2.68E-05
Xelaev18027950m.g	3.23	6.77E-10
sox11.S	3.22	2.70E-02
sesn1.L	3.21	9.96E-06
hapln3.S	3.20	4.31E-03
btbd19.S	3.20	1.19E-02
arid1b.L	3.18	2.21E-12
Xelaev18028200m.g	3.17	4.85E-02
pax8.L	3.17	2.84E-03
cmtm4.S	3.17	2.33E-02
unc45b.S	3.16	2.15E-06
eya1.S	3.16	3.86E-06
kif26a.L	3.15	8.12E-04
lrpprc.S	3.15	5.54E-04
rnf165.L	3.15	4.89E-03
LOC100496628-like.S	3.13	5.26E-04
xkr4.L	3.12	3.03E-05

pip4k2b.L	3.12	1.35E-08
foxf1.L	3.11	2.18E-02
cdc42ep3.S	3.11	1.25E-04
dll1.L	3.11	4.08E-05
pak3.S	3.10	1.74E-08
pole3.S	3.09	2.23E-02
auts2.S	3.09	8.08E-04
st3gal5.S	3.09	2.49E-02
b4galnt1.S	3.07	3.39E-04
pik3r3.S	3.06	1.94E-07
tdrp.L	3.06	1.05E-13
Xelaev18044942m.g	3.06	3.49E-02
slc43a2.S	3.05	6.22E-09
Xelaev18016487m.g	3.04	1.56E-02
tars2.L	3.04	6.88E-04
dlx6.S	3.03	5.56E-05
Xelaev18037602m.g	3.02	1.61E-06
nrp1.L	3.02	2.34E-04
prr5l.S	3.01	4.80E-02
creb3l1.S	3.01	9.56E-06
dkk1.S	3.00	6.83E-04
dact1.L	3.00	5.75E-05
hes3.3.L	2.99	1.44E-07
dpysl3.S	2.99	3.05E-10
nkx6-1.L	2.98	3.08E-02
Xelaev18027769m.g	2.97	5.10E-04
larp6-like.1.S	2.97	3.56E-04
fam222a.L	2.97	2.38E-09
ptch2.S	2.96	2.16E-02
sulf1.L	2.96	1.63E-09
vim.L	2.96	5.23E-11
plekhg1.L	2.96	3.84E-05
cdc42ep4.S	2.95	2.20E-05
aplnr.L	2.95	3.63E-11
enpp1.L	2.95	3.54E-02
mex3a.S	2.95	3.58E-04
epn1.S	2.94	1.66E-07
ap3b2.L	2.94	2.21E-03

LOC100498215-like.L	2.94	2.65E-10
reep5.S	2.93	5.80E-19
tmem169.S	2.93	1.72E-03
fgfr4.L	2.91	3.07E-11
rev1.L	2.88	1.01E-04
tox2.S	2.88	3.84E-06
rundc3a.L	2.87	2.03E-03
st3gal6.L	2.87	8.07E-05
spsb4-like.L	2.87	1.41E-03
six3.L	2.87	1.33E-12
map2.L	2.86	3.50E-03
ag1.S	2.86	6.90E-08
rgs9bp.S	2.86	2.73E-02
cited2.L	2.85	1.64E-05
slco5a1.L	2.85	2.67E-06
tmem116.S	2.82	7.76E-04
cemip.S	2.82	2.31E-02
numbl.L	2.80	3.53E-04
Xelaev18003796m.g	2.79	1.70E-02
Xelaev18019210m.g	2.79	2.68E-05
gsta1.L	2.78	3.66E-02
akap12.L	2.78	3.13E-06
fam222a.S	2.77	8.29E-04
znf219.L	2.76	7.32E-03
sparc.L	2.76	5.09E-03
slc27a3.L	2.76	4.21E-20
psat1.S	2.75	2.26E-02
mex3b.L	2.75	6.51E-05
sox4.S	2.75	1.74E-03
rnf165.S	2.74	6.87E-10
plxnb1.S	2.74	1.54E-04
hes9-1.S	2.74	4.64E-09
cep85l.S	2.73	2.78E-03
LOC100145446.S	2.73	7.33E-03
nipa1.L	2.72	2.37E-04
rpa2.S	2.72	1.23E-02
dgki.S	2.72	4.10E-02
twist1.L	2.72	7.98E-06

hes5.1.L	2.72	1.79E-03
sox21-like.S	2.71	9.94E-03
otx2.L	2.71	7.06E-04
LOC733561.S	2.71	6.98E-08
LOC100485511-like.S	2.71	1.36E-02
znf608.S	2.70	1.28E-13
vcan.L	2.69	6.14E-04
irf1.L	2.69	8.14E-03
ptpdc1.L	2.68	4.18E-04
crmp1.S	2.68	1.24E-02
enpp2.L	2.67	5.83E-04
lrp4.S	2.67	1.77E-05
smarcc2.S	2.67	4.94E-03
rgma.L	2.65	1.14E-05
LOC100492639-like.L	2.65	2.79E-09
lrwd1.L	2.64	3.33E-14
edn1.L	2.63	4.61E-02
fgf16.L	2.63	6.52E-03
lmx1b.1.L	2.63	1.33E-02
sulf1.S	2.62	2.77E-02
pik3r3.L	2.62	8.73E-04
tox3.L	2.61	1.09E-03
nckap5l.L	2.61	1.69E-06
nkd1.S	2.60	1.09E-02
spry2.S	2.60	2.61E-03
ak3.S	2.59	1.76E-06
Xelaev18032779m.g	2.59	2.10E-02
gse1.L	2.59	1.66E-07
efnb2.S	2.58	3.96E-04
kcnq3.S	2.58	5.85E-04
lrch2.L	2.58	2.50E-04
ncam1.S	2.58	8.07E-06
fam43a.S	2.57	2.05E-02
ckap2.S	2.57	2.08E-03
nxpe3.L	2.56	1.79E-02
s1pr5.L	2.56	2.62E-03
zic2.L	2.56	1.01E-02
ppp1r14b.S	2.55	2.15E-04

Xelaev18010427m.g	2.55	8.48E-04
tacc1.L	2.55	7.07E-03
Xelaev18021928m.g	2.55	2.97E-05
fbxo10.L	2.54	9.01E-06
cdk5r1.S	2.54	3.59E-04
hnrnpll.S	2.54	3.81E-06
hes8.S	2.53	3.04E-08
sox9.S	2.53	6.34E-03
LOC100489393.L	2.53	1.41E-04
magi1.S	2.53	3.94E-05
fgfr1.S	2.51	2.81E-08
cdc42bpa.S	2.51	3.10E-06
hes9-1.L	2.51	2.37E-02
pou5f3.2.S	2.51	4.97E-03
homer3.S	2.51	3.75E-02
aim1l.S	2.50	1.03E-11
jag1.L	2.50	2.69E-04
fdft1.L	2.49	6.78E-03
pkdcc.L	2.48	2.05E-09
ttc9.L	2.48	4.45E-08
cbfb.S	2.48	7.74E-08
irx2.L	2.47	1.70E-07
fndc3b.S	2.47	2.10E-02
cyp27c1.S	2.47	1.67E-04
cdc42ep4.L	2.46	2.28E-02
sh2b2.L	2.46	1.19E-02
riok3.S	2.46	3.63E-11
dnajc11.S	2.45	2.92E-06
Xelaev18015889m.g	2.45	1.80E-02
stx2.L	2.45	3.15E-05
krt19.S	2.44	2.85E-04
aplnr.S	2.44	2.78E-02
scamp4.S	2.44	3.30E-03
tmem169.L	2.44	1.41E-02
pdgfb.L	2.44	7.32E-03
hn1.S	2.43	8.06E-10
Xetrov90002103m.L	2.43	1.50E-02
lmx1b.1.S	2.42	3.86E-02

sfrp2.L	2.42	9.20E-07
Xelaev18028757m.g	2.42	1.18E-02
tpbg.S	2.42	2.75E-03
sesn1.S	2.41	3.77E-09
egln2.L	2.41	1.49E-02
pmp22.S	2.40	1.59E-04
Xetrov90025030m.L	2.40	2.27E-03
slit1.L	2.40	3.43E-02
plxnb1.L	2.40	4.79E-06
zbtb16.S	2.39	1.09E-02
lims1.L	2.39	8.02E-03
Xelaev18029838m.g	2.38	8.02E-03
ngfr.L	2.37	3.17E-04
rbm38.L	2.37	2.10E-08
hdac4.L	2.37	2.58E-02
trmt6.S	2.36	1.79E-05
spon1.L	2.36	8.84E-03
gas7.L	2.35	3.15E-02
fmn2.L	2.34	4.16E-02
dbndd1.L	2.34	2.41E-02
mprip.L	2.33	6.68E-03
nuak1.L	2.33	8.38E-03
pag1.S	2.33	2.63E-03
rcan1.S	2.33	2.27E-03
lysmd2.S	2.32	2.68E-02
hunk.S	2.32	8.85E-03
stk40.L	2.31	2.15E-04
draxin.S	2.31	7.33E-03
mycn.L	2.30	8.31E-03
prph.L	2.30	5.18E-04
hmox1.L	2.30	3.86E-10
notch1.L	2.30	4.59E-05
rcor2.L	2.30	5.43E-08
bach2.S	2.30	8.17E-03
bcar1.S	2.29	1.01E-02
smarca5.L	2.29	1.03E-06
ephb3.S	2.29	3.37E-09
cybrd1.L	2.29	1.34E-07

rassf2.L	2.29	7.91E-04
irx1.L	2.28	1.01E-03
zc4h2.L	2.28	1.18E-05
zfhx4.L	2.28	2.81E-05
Xetrov90018501m.S	2.28	2.68E-02
psat1.L	2.28	3.50E-03
lhfpl2.L	2.27	1.01E-02
fam69a.L	2.27	6.59E-03
dock6-like.L	2.27	4.41E-06
fam43a.L	2.27	1.16E-02
LOC100492804.L	2.27	4.29E-03
gatm.S	2.26	1.60E-02
Xelaev18024436m.g	2.25	1.27E-03
ubac1.S	2.25	1.21E-02
smim3.S	2.25	1.28E-02
Xelaev18030439m.g	2.24	4.68E-02
ptprt.L	2.24	4.46E-02
Xelaev18015058m.g	2.24	1.53E-12
fat1.S	2.23	3.77E-09
fzd2.L	2.23	3.70E-06
tfap2a.S	2.22	1.16E-05
spry2.L	2.21	4.27E-02
hyal2.S	2.20	7.57E-03
hes6.1.S	2.20	2.43E-03
rcor1.L	2.19	4.65E-08
hand2.S	2.19	5.45E-04
dicer1.S	2.18	2.09E-06
Xetrov90009914m.S	2.18	5.28E-03
rai2.S	2.18	2.28E-02
calb2.S	2.17	1.57E-02
LOC100144919.L	2.17	2.33E-05
t.S	2.17	4.49E-02
rfk.S	2.16	1.49E-02
ndst1.S	2.16	1.31E-04
rasgef1b.L	2.16	1.57E-06
nkain1.L	2.16	3.02E-02
cdc25b.L	2.15	4.39E-04
hes3.3.S	2.15	1.06E-03

ano8.L	2.14	3.71E-02
lfng.L	2.14	6.97E-06
afap1l1.L	2.14	3.54E-11
cdc25b.S	2.14	3.12E-04
nrarp.L	2.14	4.87E-04
cdc42se2-like.1.S	2.13	3.42E-03
cdc42se2-like.1.L	2.12	6.47E-04
cmip.L	2.12	4.41E-03
fgd1.S	2.12	3.11E-03
nceh1.L	2.11	2.82E-02
sox4.L	2.11	2.23E-02
acer2.L	2.11	6.78E-04
LOC733709.S	2.11	4.71E-02
sh3glb2.S	2.11	4.86E-02
ets2.S	2.10	4.15E-02
srgap2.S	2.10	2.81E-05
dusp4.S	2.10	7.46E-03
st3gal2.1.L	2.10	8.50E-04
lifr.L	2.09	1.46E-03
ccnt2.S	2.09	6.53E-09
atg9b.L	2.09	3.05E-02
fgfr4.S	2.09	1.32E-10
wasf3.L	2.09	1.22E-02
snx7.S	2.07	7.40E-03
sox2.S	2.07	4.30E-02
LOC100145450.S	2.07	4.11E-03
tfap2a.L	2.06	2.57E-08
Xelaev18041479m.g	2.06	2.14E-02
slc23a2.S	2.06	2.58E-02
prickle1.S	2.05	1.83E-04
plekha3.L	2.05	1.99E-02
myt1.S	2.05	3.35E-04
cuedc1.L	2.05	3.61E-03
rap2b.S	2.05	5.86E-14
clic5.S	2.04	7.53E-03
lpar4.S	2.04	8.07E-05
gpatch11.L	2.04	3.76E-05
memo1.L	2.03	2.34E-03

Xetrov90025030m.S	2.03	6.19E-03
aen.L	2.03	1.82E-03
eya2.S	2.02	4.82E-02
myt1.L	2.02	7.32E-03
auts2.L	2.02	2.25E-04
il5ra.S	2.02	4.44E-02
gas1.S	2.01	2.52E-03
arhgap4.L	2.01	2.86E-03
kiaa1755-like.S	2.01	1.37E-02
dynll2.L	2.00	3.27E-03
mex3b.S	2.00	3.12E-03
mapkapk5.L	2.00	6.71E-06
amotl2.L	2.00	2.50E-04

6.4.3 Candidate gene list for the RNA sequencing analysis of Brg1 knock-down affected genes

Given are the genes which are differentially expressed between Ptf1a-GR + cMO overexpressing animal caps over Ptf1a-GR + Brg1MO overexpressing caps in two individual replicates. Given are the gene ID, the log_2FC activation over CC and the p-value.

Table S20: Summary of genes Ptf1a + cMO vs. Ptf1a + Brg1MO (downregulated by Brg1 knock-down)

ID	log2FC	P-value
cacnb1.S	5.02	2.69E-03
paqr9.L	4.94	4.11E-05
hoxc3.L	4.94	7.45E-03
nhlh1.S	4.72	2.24E-10
nhlh1.L	4.43	9.66E-16
scrt1.L	4.28	1.51E-02
tubb2b.S	4.20	2.13E-03
lmo2.S	4.19	3.31E-06
Xetrov90016831m.L	4.06	1.94E-02
dnajc18.L	3.94	2.43E-02
Xelaev18024654m.g	3.94	3.29E-05
Xelaev18024653m.g	3.87	1.22E-02
tvp23a.S	3.84	1.93E-02
Xelaev18044320m.g	3.78	1.77E-02

Xelaev18047333m.g	3.74	1.22E-02
ppp1r9b.L	3.35	2.35E-03
six3.S	3.25	1.60E-03
emilin1.L	3.17	4.11E-05
lbx1.S	3.11	3.27E-03
LOC100496628-like.S	2.92	7.87E-04
arhgap4.L	2.86	9.77E-06
pax6.S	2.86	2.27E-03
flnc.S	2.80	1.26E-02
manbal.S	2.75	1.61E-02
tox2.S	2.67	1.09E-06
gria1-like.1.S	2.61	6.01E-03
Xelaev18011187m.g	2.53	7.05E-03
mef2d.S	2.53	6.95E-03
gch1.L	2.51	3.91E-02
trabd2a.L	2.46	2.27E-03
kiaa1755.L	2.44	8.21E-03
Xelaev18004886m.g	2.41	1.74E-02
cep85l.L	2.39	3.87E-02
tmem35.L	2.32	2.50E-02
traf4.S	2.27	2.56E-02
slc43a2.L	2.25	2.33E-02
slc43a2.S	2.23	6.30E-05
ptch1.L	2.21	1.81E-02
ypel1.S	2.15	2.90E-03
prph.L	2.14	1.37E-02
guca1a.S	2.11	2.87E-02
nes.L	2.11	4.42E-03
rufy3.L	1.98	7.73E-05
plxna3.L	1.97	1.18E-02
nr5a2.S	1.96	4.78E-02
nes.S	1.95	8.62E-03
dpy19l4.L	1.93	1.97E-02
pgs1.S	1.93	2.13E-03
zeb2.L	1.85	2.76E-03
st18.L	1.84	4.09E-02
nckap5l.L	1.83	6.95E-03
nfe2l3.L	1.80	8.97E-03

acy3.L	1.79	4.42E-03
sfrp2.S	1.78	3.34E-10
sfrp2.L	1.77	6.49E-03
fbrsl1.S	1.73	1.26E-03
slc25a28.L	1.71	2.47E-04
zeb2.S	1.68	5.64E-03
prph.S	1.66	3.23E-06
tubb3.S	1.66	1.90E-02
slc7a7.L	1.62	4.11E-03
pak3.S	1.60	1.58E-02
lrrc45.L	1.54	1.26E-02
plk3.L	1.54	2.35E-03
c1orf194.L	1.54	2.92E-02
ak2.S	1.51	1.97E-02
klhdc7a.S	1.47	2.92E-02
bcr.L	1.45	3.51E-02
six3.L	1.44	1.05E-02
slc7a8.S	1.42	4.44E-02
sp8.S	1.41	2.50E-02
ifitm10-like.L	1.40	3.63E-02
nrm.L	1.34	4.87E-04
spata18-like.S	1.34	2.50E-02
skida1.S	1.31	2.70E-02
tuba1b.L	1.30	3.73E-02
fbrsl1.L	1.22	1.34E-02
sp7.L	1.20	3.37E-02
ypel1.L	1.19	1.51E-02
asna1.S	1.19	2.11E-02
c19orf43.S	1.14	1.17E-02
pxmp4.L	1.10	6.33E-03
slc7a6.L	1.08	4.92E-02
ube2r2.L	1.08	2.29E-02
ubap2.S	1.05	3.20E-02
gmnn.L	1.04	3.08E-02
mfsd9.L	1.02	4.43E-02

Table S21: Summary of genes Ptf1a + cMO vs. Ptf1a + Brg1MO (upregulated by Brg1 knock-down)

ID	log2FC	P-value
LOC101730771-like.L	-4.84	8.60E-03
larp6-like.1.S	-3.74	7.21E-05
LOC100485511-like.S	-3.55	1.06E-02
eda2r.L	-3.12	8.29E-07
pou5f3.2.L	-3.07	6.55E-06
itga2b.1-like.S	-3.00	7.74E-03
tars2.L	-2.97	1.04E-02
LOC733561.S	-2.67	2.54E-06
LOC100495756-like.S	-2.61	2.54E-06
pou5f3.2.S	-2.57	3.49E-02
nipa1.L	-2.37	1.58E-02
rev1.L	-2.28	2.96E-02
hand2.S	-2.19	6.95E-03
riok3.S	-2.14	3.32E-07
lrwd1.L	-2.12	6.11E-08
nudt22.L	-1.82	1.31E-03
ctnnal1.S	-1.79	1.18E-02
dicer1.S	-1.79	2.27E-03
LOC100144919.L	-1.76	9.06E-03
tinf2.L	-1.71	3.27E-03
Xelaev18043774m.g	-1.70	2.40E-02
Xelaev18034615m.g	-1.68	2.40E-03
Xelaev18043947m.g	-1.66	3.75E-02
tex2.2.L	-1.63	7.05E-03
itpr1.S	-1.58	4.47E-05
skil.S	-1.56	2.41E-02
cog5.L	-1.51	1.51E-02
cdo1.S	-1.50	1.51E-02
Xelaev18034617m.g	-1.49	1.31E-02
srsf5.S	-1.45	3.35E-02
kitlg.S	-1.44	6.33E-03
ska3.L	-1.43	7.49E-03
rest.S	-1.43	2.76E-03
pou5f3.1.S	-1.39	1.93E-02
pawr.S	-1.37	9.92E-03

plekhn1.S	-1.35	2.57E-03
ccdc30.L	-1.35	2.35E-03
pdgfa.S	-1.32	3.44E-02
rnf168.L	-1.26	1.56E-02
gata2.L	-1.25	1.41E-04
cdkn2aip.L	-1.22	3.51E-02
Xelaev18036901m.g	-1.20	1.04E-03
marveld3.L	-1.19	2.92E-02
ccnt2.S	-1.17	3.19E-02
tob1.S	-1.17	3.91E-03
snrpb2.S	-1.17	2.13E-03
bambi.S	-1.15	7.73E-05
ccna2.S	-1.15	3.05E-03
znf654.L	-1.14	2.02E-02
hal.1.L	-1.13	6.72E-03
Xelaev18024066m.g	-1.13	4.66E-02
Xelaev18023103m.g	-1.12	4.09E-03
tp53.L	-1.12	2.67E-02
tacc2.L	-1.10	1.99E-02
ptpn2.S	-1.02	1.58E-02
bambi.L	-1.00	3.97E-02

6.5 Quantification of the BiFC assay

Given are the corresponding N- and C-terminal Venus-constructs used for the BiFC analysis, the relative amount of EYFP positive cells compared to the total number of mRFP positive cells, the total number of mRFP positive cells, and the SEM value

TableS22: Quantification of the BiFC

Vc-construct	Vn-construct	EYFP pos cells (in %)	total number of cells	SEM
Ptf1a-Vn	E12-Vc	80%	165	20%
	Rbpj-Vc	84%	1118	9%
	Prdm13-Vc	3%	657	2%

Ptf1aW224A/W242A-Vn	E12-Vc	71%	196	20%
	Rbpj-Vc	0%	659	0%
	Prdm13-Vc	3%	494	3%
Ptf1aT243A-Vn	E12-Vc	73%	59	20%
	Rbpj-Vc	84%	1182	16%
	Prdm13-Vc	49%	697	2%
Ptf1aT243E-Vn	E12-Vc	100%	57	0%
	Rbpj-Vc	88%	336	2%
	Prdm13-Vc	40%	777	24%

Curriculum vitae

Name:	Sven Richts
Date of birth:	29.01.1988
Place of birth:	Werl, Germany
Address:	Stumpfe Eiche 1, 37077, Göttingen
Nationality:	German
E-Mail:	sven.richts@med.uni-goettingen.de

Since 2014

PhD studies: “Mechanisms underlying the temporal and selective induction of Ptf1a target genes”
Georg-August Universität Göttingen, Göttingen, Germany
PhD. candidate in GGNB program Genes and Development

2010-2013

Master studies: “Characterization of Ptf1a protein domains during neurogenesis”
Georg-August Universität Göttingen, Göttingen, Germany
Master of Science in Developmental, Neural and Behavioral Biology (DNB)
Area of specialization: Developmental and Cellular Biology

2007-2010

Bachelor studies: “Untersuchungen zur Funktion von Dachshund im Mehlkäfer *Tribolium Castaneum*“
Georg-August Universität Göttingen, Göttingen, Germany
Bachelor of Science in Biology

1998-2007

Abitur: Städtisches Marien-Gymnasium Werl, Werl, Germany